WOODHEAD PUBLISHING IN MATERIALS

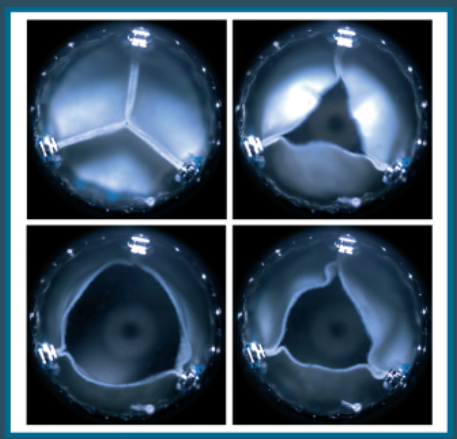

Biomaterials for artificial organs

Edited by Michael Lysaght and Thomas Webster

WP
WOODHEAD PUBLISHING

Biomaterials for artificial organs

Related titles:

Biomaterials, artificial organs and tissue engineering
(ISBN 978-1-85573-737-2)
Biomaterials are materials and devices that are used to repair, replace or augment the living tissues and organs of the human body. The purpose of this wide-ranging introductory textbook is to provide an understanding of the needs, uses and limitations of materials used in the human body and to explain the biomechanical principles and biological factors involved in achieving the long-term stability of replacement parts in the body. This book examines the industrial, governmental and ethical factors involved in the use of artificial materials in humans and discusses the principles and applications of engineering of tissues to replace body parts. The approach necessarily incorporates a wide range of reference material because of the complex multidisciplinary nature of the fields of biomedical materials, biomechanics, artificial organs and tissue engineering. There is an accompanying CD-ROM providing supplementary information and illustrations to support the book.

Surfaces and interfaces for biomaterials
(ISBN 978-1-85573-930-7)
This book presents our current level of understanding on the nature of a biomaterial surface, the adaptive response of the biomatrix to that surface, techniques used to modify biocompatibility, and state-of-the-art characterisation techniques to follow the interfacial events at that surface.

Shape memory alloys for biomedical applications
(ISBN 978-1-84569-344-2)
Shape memory metals are suitable for a wide range of biomedical devices including applications in dentistry, bone repair, urology and cardiology. This book provides a thorough review of shape memory metals and devices for medical applications. The first part of the book discusses the materials, primarily Ti–Ni based alloys; chapters cover the mechanical properties, thermodynamics, composition, fabrication of parts, chemical reactivity, surface modification and biocompatibility. Medical and dental devices using shape memory metals are reviewed in the following section; chapters cover stents, orthodontic devices and endodontic instruments. Finally, future developments in this area are discussed including alternatives to Ti–Ni based shape memory alloys.

Details of these and other Woodhead Publishing materials books can be obtained by:

- visiting our web site at www.woodheadpublishing.com
- contacting Customer Services (e-mail: sales@woodheadpublishing.com; fax: +44 (0) 1223 893694; tel.: +44 (0) 1223 891358 ext. 130; address: Woodhead Publishing Limited, Abington Hall, Granta Park, Great Abington, Cambridge CB21 6AH, UK)

If you would like to receive information on forthcoming titles, please send your address details to: Francis Dodds (address, tel. and fax as above; e-mail: francis.dodds@woodhead publishing.com). Please confirm which subject areas you are interested in.

Biomaterials for artificial organs

Edited by
Michael Lysaght and Thomas J. Webster

Oxford Cambridge Philadelphia New Delhi

Published by Woodhead Publishing Limited, Abington Hall, Granta Park,
Great Abington, Cambridge CB21 6AH, UK
www.woodheadpublishing.com

Woodhead Publishing, 525 South 4th Street #241, Philadelphia, PA 19147, USA

Woodhead Publishing India Private Limited, G-2, Vardaan House, 7/28 Ansari Road,
Daryaganj, New Delhi – 110002, India
www.woodheadpublishingindia.com

First published 2011, Woodhead Publishing Limited

British Library Cataloguing in Publication Data
A catalogue record for this book is available from the British Library.

ISBN 978-1-84569-653-5 (print)
ISBN 978-0-85709-084-3 (online)

The publisher's policy is to use permanent paper from mills that operate a sustainable forestry policy, and which has been manufactured from pulp which is processed using acid-free and elemental chlorine-free practices. Furthermore, the publisher ensures that the text paper and cover board used have met acceptable environmental accreditation standards.

Typeset by Godiva Publishing Services Limited, Coventry, West Midlands, UK
Printed by TJI Digital, Padstow, Cornwall, UK

Cover image: series of still photographs of the Sadra Lotus™ valve when tested in an accelerated wear tester. Photos reprinted with permission from Sadra Medical. Lotus™ is a trademark of Sadra Medical. All right reserved.

Contents

Contributor contact details

(* = main contact)

Editors

Dr Michael Lysaght and
Dr Thomas Webster
Division of Engineering and
Department of Orthopaedics
Brown University
182 Hope Street
Providence, RI 02912
USA

E-mail: Thomas_Webster@brown.edu

Chapter 1

Dr Stefan Breiter
Membrana GmbH
Öhder Straße 28
42289 Wuppertal
Germany

E-mail: stefan.breiter@membrana.de

Chapter 2

Dr Chang Yao*
Nanovis LLC
3000 Kent Ave
West Lafayette, IN 47906
USA

E-mail: chang.yao@nanovisinc.com

Jing Lu and Dr Thomas J. Webster
Division of Engineering and
Department of Orthopaedics
Brown University
182 Hope Street
Providence, RI 02912
USA

E-mail: Thomas_Webster@brown.edu

Chapter 3

Dr Ebru Oral
Massachusetts General Hospital/
Harvard Medical School
55 Fruit Street
GRJ 1206
Boston, MA 02114
USA

E-mail: eoral@partners.org

Chapter 4

Michael J. Ebert
Medtronic Cardiac Rhythm Disease
Management
Coral Sea ST NE
Mounds View, MN 55112
USA

E-mail:
michael.ebert@medtronic.com

SuPing Lyu* and Michael F. Wolf
Medtronic Strategy and Scientific Operations
710 Medtronic Parkway
Minneapolis, MN 55432
USA

E-mail: suping.lyu@medtronic.com
michael.wolf@medtronic.com

Mark T. Rise
Medtronic Neuromodulation
7745 Aetna Ave NE
Monticello, MN 55362
USA

E-mail: mtrise@tds.net

Chapter 5

Michael N. Helmus
Worcester, MA
USA

E-mail: mnhelmus@msn.com

Crystal M. Cunanan*
Cunanan Consulting
Mission Viejo, CA
USA

E-mail: crystalc@cox.net

Chapter 6

Dr Michael Hiles* and Jason Hodde
Cook Biotech Incorporated
1425 Innovation Place
West Lafayette, IN 47906
USA

E-mail: hiles@cookbiotech.com

Chapter 7

Professor Mohamed N. Rahaman*
Department of Materials Science and Engineering and Center for Bone and Tissue Repair and Regeneration
Missouri University of Science and Technology
Rolla, MO 65409-0340
USA

E-mail: rahaman@mst.edu

B. Sonny Bal
Department of Orthopaedic Surgery
University of Missouri–Columbia
Columbia, MO 65212
USA

Chapter 8

Dr Deniz Ufuk Erbulut and Associate Professor Ismail Lazoglu*
Department of Mechanical Engineering
Koc University
Rumeli Feneri Yolu
Sariyer, 34450
Istanbul
Turkey

E-mail: ilazoglu@ku.edu.tr

Chapter 9

Yupeng Chen
Department of Chemistry and Division of Engineering
Brown University
Providence, RI 02912
USA

Dr Thomas J. Webster*
Division of Engineering and
Department of Orthopaedics
Brown University
182 Hope Street
Providence, RI 02912
USA

E-mail:
Thomas_Webster@brown.edu

Chapter 10

Deb Gorth* and Dr Thomas J.
Webster
School of Engineering and
Department of Orthopaedics
Brown University
182 Hope Street
Providence, RI 02912
USA

E-mail: deborah_gorth@brown.edu
Thomas_Webster@brown.edu

Michael Lysaght: A great educator, researcher, and friend

Last year, in the midst of soliciting and compiling chapters for this textbook (and countless other activities), Michael J. Lysaght passed away. Although it is impossible for anyone to fill the shoes of Michael Lysaght, it was my honor in remembrance of him to complete this project and dedicate this book to him. For anyone who knew Michael and interacted with him, you know why he was so respected in the field of biomedical engineering. For those of us representing the 'younger generation' of biomedical engineering, we often take for granted how prominent this field is today, but we would be nowhere without the pioneering work of people like Michael Lysaght, who got this field off the ground and molded it into what it is today.

His accomplishments forming biomedical engineering and tissue engineering into what it is today are too numerous to list here, and I believe he would be embarrassed if, in this dedication, I emphasized such accomplishments. Rather, it is my opinion that Michael would have wanted to be remembered for his interactions with people, particularly students. As he mentioned to me on many occasions, we have the unique opportunity in all of our professions to touch the lives of many young people, helping and assisting them to figure out their place in this world and how best to actively contribute to the world. Of course, Michael's life's work developing the biomedical engineering, tissue engineering, commercialization, and medical device fields when many were not even thinking of such disciplines, gave him lots to talk about with students – and students loved him for the time he took to talk to them and the advice he gave. The courses he taught at Brown University were revolutionary, and the fact that he averaged an aggregate annual enrollment in the elective courses he taught of 150 to 200 emphasizes how much students appreciated his efforts.

On a personal note, I could tell why students loved him: he deeply, deeply cared about them (and all of us). I first interacted closely with Michael when I came to Brown University, trying to figure out the 'inner workings' of the

university. Without hesitation, he spent numerous hours with me explaining history, his experiences, and most importantly providing poignant advice. However, what made conversations with Michael so unique and unlike many of the typical conversations held today, is that conversations with him were not 'professorial'. Instead, conversations with Michael were insightful, empowering, and thought provoking. This is because he took the time needed to help people, he never rushed a conversation or thought. I am convinced that Michael's ability to have conversations like this with me (and students and others) was his gift to this world. A gift that helped him develop several start-up companies, bio-medical engineering programs, state-of-the-art research, popular courses, and a worldwide network of former students, colleagues, and collaborations that will take his gift and spread it to future generations. Michael will be missed, but by taking his special gift of spending quality time with the next generation of educators, researchers, and friends, he will always live on to me.

Thomas J. Webster

1

Membranes for oxygenators and plasma filters

S. BREITER, Membrana GmbH, Germany

Abstract: Membranes used for blood oxygenation and blood plasma separation represent well-proven applications as artificial organs. Although the absolute consumption is much less compared with dialysis membranes, their relevance for medical devices and healthcare around the world does not hide behind the big brother. This chapter illustrates the cornerstones for production and application of these products. Blood oxygenation membranes produced by different methods, both symmetrical and asymmetrical, are discussed first. The second part describes hydrophobic and hydrophilic synthetic blood plasma separation membranes. For both types of membranes, membrane make-up and medical device implications are considered.

Key words: blood oxygenation, plasma separation, TIPS, SIPS, membrane structure, membrane manufacture, artificial lung, apheresis.

1.1 Introduction

Over one million patients per year undergo cardiac surgery with the aid of the heart–lung machine. This life-saving procedure on the organ, which is said to be the centre of life, love and desire, often takes less than an hour, although difficult cases may extend to six or even ten hours. While the cardiac surgeon performs the operation, a pump keeps the blood flowing and membranes inside an oxygenator take over from the lungs in that they add oxygen and remove carbon dioxide from the blood.

In tens of thousands of cases of sepsis or severe lung trauma, the lung needs assistance or rest for a few days. A similar setting as for cardiac surgery may then release the stressed organs for several days. In such cases, membrane lungs have worked in clinics for more than four weeks.

A great number of diseases can be alleviated by removing the harmful substances from blood that cause clogging of arteries, recurring or even persisting inflammation or overshooting immune response. Often the removal of these substances would damage blood cells; therefore cells and blood plasma are separated and the plasma is then cleaned vigorously. The procedure that does this separation with the least stress for the blood cells is plasma separation with membranes.

Over the years, tens of millions of lives have been saved and many more have been eased with the help of membranes for blood oxygenation and plasma

separation. While cardiac surgery today is an established procedure, where improvements over generations have built a gold standard, long-term lung assistance and plasma separation and plasma treatment are rather in their infancy. It is still a matter of debate how to achieve the best results, who should perform the procedures, which patients can effectively and efficiently be treated and last, but not least, who will pay for these procedures.

Membranes as biomaterials form the basis for the procedures of lung substitution and plasma separation. These membranes are readily available and look very simple: white capillaries, wound to bundles or finished with rather basic textile technologies. But it is not as simple as that: they represent the highest standards of biomedical technology.

1.2 Membranes for blood oxygenation

1.2.1 History

To perform delicate surgery on the human heart, for many interventions it is essential to stop the heart beating (e.g. for any surgery on the heart valves), and for all procedures the stoppage greatly facilitates the work of the surgeon. The heart with its four chambers pumps the blood through body and brain, which consume oxygen and produce carbon dioxide, and through the lungs simultaneously, where carbon dioxide is exhaled and oxygen taken up. If during a cardiac surgery procedure the heart is still then the lungs are also at rest. This means that the blood not only needs to be pumped through body and brain to continue their supply, but also needs to be oxygenated artificially. Therefore, for any cardiac surgery procedure where the heart is stopped, a device to oxygenate the blood and to remove the carbon dioxide is also needed.

A good overview of the development of the blood oxygenator is given by Leonard.[1] The first heart–lung machines have worked with film or bubble oxygenators.[2,3] In film oxygenators, blood was passed over sieves, plates or discs in pure oxygen or an oxygen-rich atmosphere. Oxygen and carbon dioxide were exchanged on this large surface. The second generation of oxygenators, bubble oxygenators, simply consisted of a bubble chamber where oxygen was dispersed into the patient's blood and a defoamer which removed the majority of gaseous residuals from the blood. Both procedures were a major insult to the patient and their blood, and therefore a more gentle procedure had to be found.

In the 1940s, Kolff observed that the blood in his rotating drum kidneys turned to a brighter red during treatment. This was simply due to take up of oxygen through the cellophane membrane he used to separate the blood from the dialysis solution, which was exposed not only to the dialysate, but also to the open air. In a way, the first clinical application of an artificial kidney also was the first application of a membrane artificial lung. From this starting point, Kolff

et al. developed a membrane oxygenator, the first clinical application of which was described in 1956.[4]

The first membrane oxygenators incorporated various membrane materials, among them cellophane, polyethylene (PE) and Teflon, all of which were comparatively impermeable to oxygen. In the 1960s, the first oxygenators with silicone membranes were developed.[5] For these, thin films of polysiloxane (silicone) were supported by meshes or sieves, then wrapped to a roll or stacked to a pile to incorporate sufficient surface in a volume that could still be handled. Those oxygenators had large priming volumes and large surfaces and consequently resulted in considerable blood dilution and blood damage.

In the 1980s, the first oxygenators with microporous membrane sheets were produced. The preferred material for microporous membranes in blood oxygenation was and remains polypropylene (PP).[6] Owing to the presence of pores, the permeability of these membranes to oxygen was much higher than that of any other material before, so that the limiting factor for gas transfer was no longer the membrane, but the gas transport within the blood films directly adjacent to the membrane (see also page 10).

The next breakthrough in oxygenator performance was the introduction of capillary membranes. Those had the same pore size and same polymer (PP) as the flat sheet microporous membranes introduced. Similar to the development with haemodialysers, the introduction of capillary membranes reduced the priming volume of the oxygenator and turned a bulky space consumer into a handy device. The first capillary membrane oxygenators worked with blood flow inside the capillaries, but soon the trend to blood flow outside the capillaries prevailed: blood side pressure drop always used to be a limiting factor for 'blood inside' oxygenators, and the 'blood outside' models were smaller and more handy, and demanded less priming and thus less haemodilution. Finally, this was also welcomed from the manufacturer's perspective, as it saves about half the amount of membrane.

These microporous membranes provide excellent performance, but compared with the older silicone membranes are more prone to plasma breakthrough. Around the year 2000, the first oxygenators with a membrane from polymethylpentene (PMP) with a very thin dense outer skin on a microporous body were introduced. These provide performance on the same level as the microporous PP membranes, but do not show the phenomenon of plasma breakthrough.

Today, almost all commercially available blood oxygenators incorporate capillary membranes and have the blood flow outside and the gas flow inside the capillaries. Most of the oxygenators have microporous membranes of PP, and a growing share is equipped with the dense PMP membrane type. Only one silicone membrane oxygenator is still commercially available.

1.2.2 Material, polymer and technical requirements

Gas transfer

Membranes for blood oxygenation need to provide sufficient gas exchange and at the same time prevent any mixing of blood and gas (oxygen or oxygen-enriched air). The driving force for the gas transport across the membrane wall is the difference in chemical potential of the gas on both sides of the membrane, i.e. the different partial pressures or concentrations in the blood and on the gas side. Transport of the gas will always occur into the direction of the lower concentration or pressure.

The exchanged amount of gas on a given contact surface follows Fick's law:

$$V = \frac{(a_1 - a_2)}{d} K_\mathrm{d} A t$$

where V is the amount of gas exchanged; a_1 and a_2 are activities (pressures) of gas on either side; d is the diffusion distance; K_d is the diffusion constant, A is the surface area; and t is time.

In the human lung, gas exchange occurs on a surface (A) of 50–200 m^2, at blood film thicknesses of 6–15 μm, and with contact times (t) in the sub-second level.[7] Most of all, there is no direct contact of blood and air, but both media are always separated by the alveolar capillary membrane with a diffusion distance (d) of only 1–2 μm. The important point in this is that blood only 'sees' endothelial cells, thus no foreign surface. Blood is oxygen enriched and carbon dioxide deprived without any unphysiological interference.

In air, oxygen has a volume share of 21%, which corresponds to a partial pressure of oxygen of 160 mmHg. In the human lungs, due to mixing with dead space air and the increased water vapour pressure, in the alveoli this is reduced to slightly more than 100 mmHg at the alveolar capillary interface. As venous blood has an oxygen partial pressure of only 40 mmHg, oxygen is easily taken up and the oxygen partial pressure for arterial blood goes up to 100 mmHg, which means that equilibrium with the breathed air is almost reached. For carbon dioxide, the gradients are exactly opposite: the partial pressure of carbon dioxide in air is close to zero. The partial pressure in the blood that enters the lungs is about 46 mmHg, and thus carbon dioxide diffuses through the alveoli capillary membrane, so that in the alveoli the carbon dioxide partial pressure rises to about 40 mmHg. Although the driving force is smaller than for oxygen, the exchange of carbon dioxide takes place readily, so that arterial blood has a partial pressure of carbon dioxide of 35–45 mmHg.

The main difficulty in the construction of any blood contacting biomedical device is that no foreign material can be as gentle to blood as the endothelium. Whenever blood touches a surface that is not endothelium, this means to the body defence system that there is an injury that needs to be counteracted and treated. The larger the foreign surface the blood touches and

the longer time of exposure to this foreign surface, the stronger the reaction of the body must be.

From this it is obvious that an artificial lung, like other similar biomedical devices, must find a difficult compromise: to reduce insult to the blood, both surface and contact time should be minimised. Today's oxygenators have exchange surfaces of 0.25 m^2 (devices for neonates) to 2.5 m^2 (for large adults). In order to make up for this lack of exchange surface, according to Fick's law, one must thus use high activity gradients, longer contact times, low diffusion distances and materials with high diffusion constants (high permeabilities to the relevant gases).

Interfaces

The interface of blood and gas in an artificial lung consists of (at least) five phases (Fig. 1.1). In the example of oxygen, oxygen is first transported towards the membrane from the bulk gas by convection. On the gas side of the membrane, there is a diffusion layer, where oxygen is no longer transported by convection, but can only diffuse. Then follows the membrane as one or possibly more distinct phase(s) (more on that below). Next follows a diffusion layer on the blood side of the membrane, before the oxygen finally reaches the bulk of the blood flow and can be transported to the organ of the patient, again by convection. The overall permeability of a given gas from the gas side to the blood side of an artificial lung is thus a combination of different permeabilities. In the end, the overall permeability can only be as high as the permeability with the lowest single value.

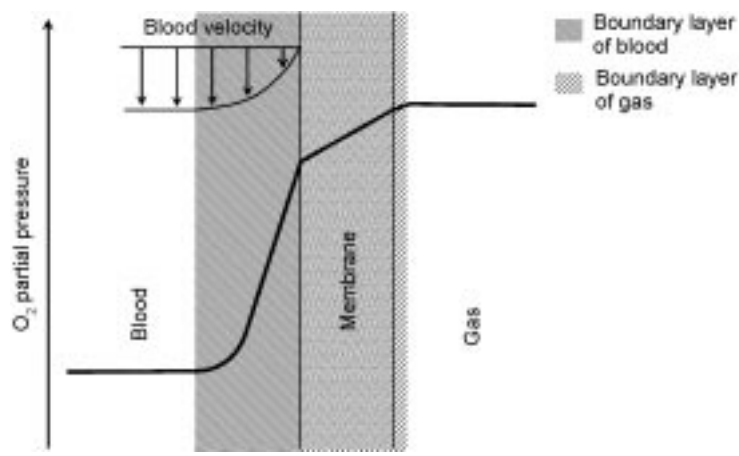

1.1 Blood–membrane–gas interface.

Membrane transport

In a closer view on the transport of gases through the membrane in an artificial lung, two mechanisms can apply: diffusion through pores or solution diffusion through a dense, solid material. Federspiel *et al.*[7] give a good overview of the mechanisms involved.

In a non-porous membrane where solution diffusion is the only transport mechanism, two basic values determine the permeability: the solubility of the gas in the membrane material and the diffusion through the material as such, with the permeability as the product of solubility and diffusivity. Here, the solubility is a function of the polarity of the gas and membrane material, and for the diffusivity as a rule of thumb smaller molecules tend to have high diffusion coefficients, as they can move more freely and faster. The transport of gases by solution diffusion always has a certain hysteresis: when concentrations on the gas side are changed, this higher concentration needs to dissolve in the membrane material and migrate through the membrane wall and only then will the gases reach the blood side of the device. Depending on the thickness of the membrane and the diffusion coefficient of the gas in the membrane material, this hysteresis can take some minutes. This delay in concentration changes makes the conduct of a clinical application of an artificial lung, in particular a cardiopulmonary bypass, more difficult and contributed to the displacement of silicone oxygenators in cardiac surgery.

In porous membranes, the diffusion of gas molecules through the pores is not entirely clarified in detail. Commonly, only an overall permeability of a given gas through the membrane is defined. This is a function of pore size, pore tortuosity, wall thickness/gas path length and, of course, the size and mass of the gas molecule, temperature and pressure gradient. This permeability is a composite of the three contributing mechanisms:

- free diffusion comparable to that in a gas phase;
- Knudsen diffusion;
- solution diffusion.

(Formally, also convection can contribute to the permeance, but pressure gradients in blood oxygenators need to be kept at a minimum to prevent the build-up of gas bubbles on the blood side; therefore convection in this case can be neglected.)

In large pores, the transport will take place according to the diffusion laws as they are valid for a gas-in-a-gas model (Fick's model, see above): all molecules move randomly with the speed as a function of temperature and pressure. This leads to a concentration equilibration and thus net transport from areas of high concentration to areas of low concentration. The narrower the pores get, the more molecules will not only collide with other gas molecules, but increasingly also with the pore walls, which decreases speed of exchange.

At ambient pressure and temperature, the mean free path of a gas molecule such as oxygen, nitrogen or carbon dioxide is about 70 nm (before it collides with other gas molecules). The so-called Knudsen number, $K = \Lambda/d_p$ (where Λ = mean free path and d_p = pore diameter) is thus small. Considering the pore sizes quoted by the manufacturers[8] in the region of $0.1\,\mu m = 100\,nm$ the Knudsen number is close to 1 or somewhat lower. Below $K = 1$, one assumes increasing so-called Knudsen diffusion, where the interaction and collisions with the borders (here the walls of the pores) gain importance over the bare diffusion. These collisions are determined by the pore size, the tortuosity (τ) of the pores and the porosity of the medium. Since the walls between the pores of a highly porous medium are very thin and many pores will have dead ends, the solution diffusion through the polymer medium also plays a role.

A method to determine how much of the gas transport occurs by diffusion and how much by convection[9] analyses the transport through the membrane at different pressure gradients and extrapolates the data to a pressure difference of zero. This value at zero pressure difference represents the bare diffusion part, whereas the slope of the curve gives the convection part. As the pressure difference across a membrane for blood oxygenation must be kept low, this represents an interesting method to characterise the membranes and to illustrate the flow conditions, but has no direct meaning for the process of blood oxygenation itself.

In composite membranes with both a microporous backbone and a non-porous skin, the membrane forms two phases with two permeabilities. The overall permeability of the composite membrane cannot be larger than the permeability of the layer with the lower permeability, which is almost always the non-porous layer. Composite membranes therefore have a very thin non-porous layer on a (micro)porous backbone, which serves as a scaffold for the skin and is only needed for sufficient mechanical stability. If the skin is sufficiently thin, the composite membrane can reach the permeability and performance of a microporous membrane.[10]

Table 1.1 shows the permeabilities of different polymers for oxygen and carbon dioxide. Blood oxygenation membranes from PP are microporous; their permeability therefore mostly depends on the pore geometry. Membranes for longer-term use as artificial lungs should have a non-porous outer surface to

Table 1.1 Permeability of different polymers for breathing gases (in Barrer = $10^{-10}\,cm^3\,cm/(s\,cm^2\,cmHg)$)[11,12]

	Oxygen	Carbon dioxide
Silicone (polysiloxane)	~600	~3200
PP (polypropylene)	2.2	9.2
PMP (polymethylpentene)	32.2	92.6

prevent blood plasma and plasma water from entering the pores (wet lung phenomenon). Membranes from silicone are non-porous over their entire thickness of 100–200 μm. The most recent development is a membrane made from PMP with a microporous wall with only a very thin (<1 μm) outer skin (OXYPLUS®, by Membrana GmbH, Wuppertal, Germany). As the permeability of PMP for oxygen and carbon dioxide is high compared with PP and the skin is very thin, this skin does not impair the performance of the membrane.[13]

Boundary layers

The most important limiting factor for the performance of blood oxygenators with microporous membranes today is the blood side diffusion layer.[7] Although flow conditions in a bundle of capillary bundles are much more complex, the simple model of a boundary layer of laminar flow on a flat surface can serve to illustrate the phenomenon. On the surface, a boundary layer will develop, in which the volume increments directly adjacent to the surface have a velocity that approximates zero. The boundary layer thickness is a function of the square root of the bulk fluid velocity. Through the thickness of this boundary layer, the velocity of the fluid will increase to reach the bulk velocity. Within this layer, the main transport mechanism will be diffusion (see Fig. 1.1).

To reach a high performance of the final device, a primary goal is to achieve a thin blood side diffusion layer and good blood mixing (see Section 1.2.8). In a medical device with blood as the fluid, the adsorption of blood components, mainly proteins, to the surface also needs to be accounted for. A hydrophobic surface like a microporous PP membrane will soon be covered by a layer of blood proteins. Here, one can expect the surface to be covered first by those proteins that have the highest concentrations in blood (albumin). In due course, albumin can then be replaced by other proteins with higher binding forces to the particular polymer. This protein layer ('protein cake') forms an additional layer and influences the permeability of the membrane. As the blood of every patient is individual, and additionally haemodilution and medication have an influence on the build-up of this additional protein layer, it is very difficult to quantify these factors and predict their effects in the individual clinical case. Furthermore, most oxygenators today are coated with proprietary coatings of individual manufacturers, which have great impact on the adsorption of proteins and primarily cells on the membrane.[14] Further information on protein adsorption to biomaterials can be found in Goldstein *et al.*[15]

1.2.3 Membrane manufacture and resulting structures

Thermally induced phase separation (TIPS)

For the manufacture of current capillary membranes, the thermally induced phase separation (TIPS) process is one preferred method (Fig. 1.2). For this, the

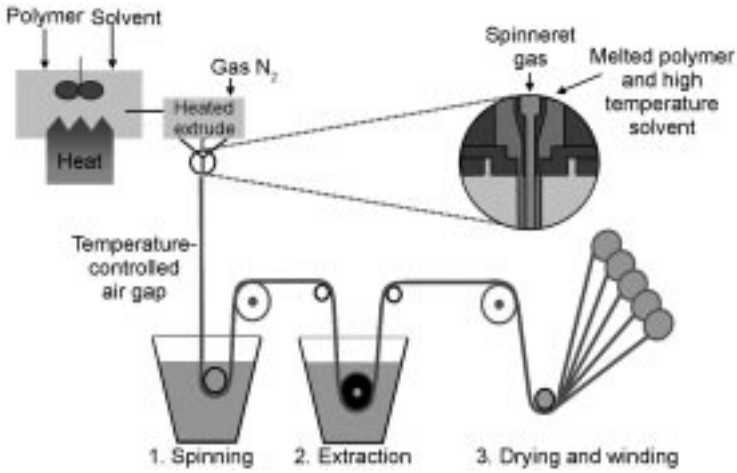

1.2 Thermally induced phase separation (TIPS) process for manufacture of hollow fibre blood oxygenation membranes.

polymer (PP or PMP) is dissolved in a hot mixture of solvents (mostly natural oils) and then pumped through a ring-shaped spinneret, with gas being blown through a circular opening in the centre of the spinneret, concentric with the ring, to keep the lumen of the capillary open. The solvent system needs to be composed so that the polymer is soluble in a hot mixture of the solvents, but not in a cold mixture: when the hot solution exits the heated spinneret, it is cooled down and the polymer is thermally induced to precipitate (recrystallise) to form the membrane wall. This crystallisation process needs to start in many nucleation centres homogeneously distributed through the polymer solution and to proceed quickly, so that the solvent mixture is trapped in many tiny droplets throughout the membrane wall that is created. These droplets need to be connected with each other: after the cooling step, the membrane is extracted with a suitable solvent such as alcohol to wash out all oil and oil residues. A fine network of pores penetrates the membrane wall where the oil has been. The membrane exhibits a sponge-like structure (Fig. 1.3).

Depending on the exact conditions (composition of the solvent system, temperature, temperature gradients, cooling from outside only or inside and outside, spinning speed, pressures, etc.), the membrane structure can be influenced to yield membranes with larger or smaller pores, with symmetrical structures (i.e. constant pore size throughout the whole wall thickness) or asymmetrical structures, development of an outer or inner skin, tortuosity of the pores, etc. After the washing step, the membrane is dried and wound on spools for further processing.

This process yields a membrane that can be produced with very high porosities (exceeding 50% by volume) and at the same time very high tortuosity of the pores, so that the membrane is very resistant to blood plasma breakthrough.

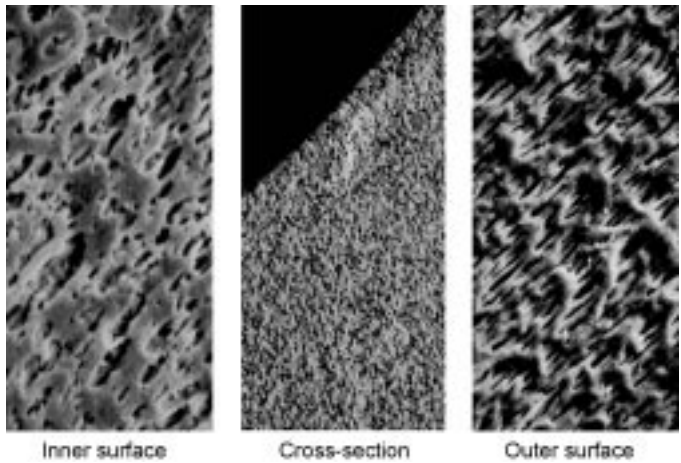

1.3 Scanning electron micrograph (SEM) of oxygenation membranes produced by TIPS.

Generally, the process is also capable of producing flat sheet membranes. One then casts the hot polymer solution on a chill roll. The principle of membrane formation remains the same. However, such membranes have never played a significant role in blood oxygenation. An overview of membrane pore sizes and dimensions is given in Table 1.2.

Dry stretch

Alternatively, the capillary membrane can be produced without the use of solvents directly from a solid capillary. For this, a capillary from PP is produced by extrusion. The exact polymer and the extrusion conditions need to be chosen carefully to enable the membrane production in the next steps. This capillary is then subjected to a series of annealing and stretching and relaxation procedures at different temperatures. Preferably, an annealing step is followed by a cold and then a hot stretch procedure (Fig. 1.4).

Table 1.2 Dimensions and pore sizes of current blood oxygenation membranes[8,16]

	Inner diameter (μm)	Outer diameter (μm)	Wall thickness (μm)	Pore size (μm)
OXYPHAN®	200, 280	300, 380	50	$\leq$0.2
OXYPLUS®	200	380	90	n/a
CELGARD®	150, 240	200, 300	25, 40	0.04×0.1
Terumo	280	380	50	0.05

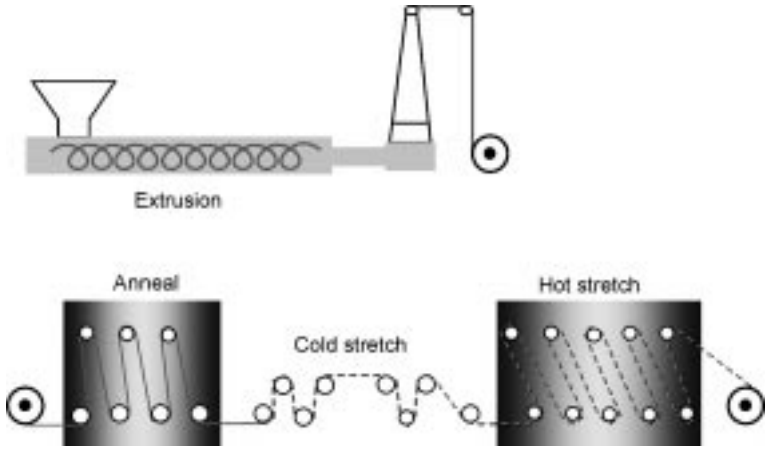

1.4 Dry stretch process for manufacture of hollow fibre blood oxygenation membranes.

By this annealing and stretching process, the tight capillary wall is ruptured to build pores. Of course the properties of the raw capillary and the conditions of the various stretching and annealing steps need to be adjusted very carefully to yield pores of the desired shape and in the target range of pore size. In the scanning electron micrographs (SEMs) in Fig. 1.5 the direction of the stretching process is in the vertical direction: the pores exhibit a lengthy shape into the direction of the stretch.

This process yields a membrane that has good mechanical stability and is ideal for demanding textile make-up such as winding at elevated speed. By adjusting the temperatures and forces, the pores can be generated in a way that means plasma breakthrough is not an issue.

The same technology can of course also be applied to films of PP, so that flat sheet membranes can be produced according to the same scheme. Such mem-

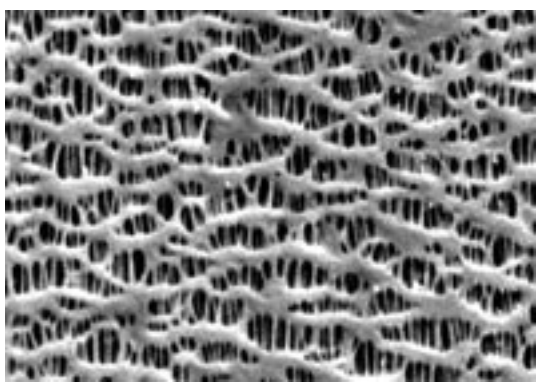

1.5 SEM of oxygenation membranes produced by dry stretch.

branes were used in blood oxygenators until about 2004 but are no longer in large-scale use.

Other

A minor share of the oxygenators available today contain flat sheet silicone membranes. To ensure the wall is thin for increased transport performance, these membranes are composite membranes with a very thin silicone deposit on a support mesh. Other membrane production technologies such as casting or etching do not play a role in commercially available oxygenators.

1.2.4 Membrane structural implications for use

The different production schemes of course produce membranes with different structures. A closer look into the pore structures reveals the differences (Fig. 1.6). Membranes produced by TIPS exhibit pores with very high tortuosity and extremely long pore paths. From this they are very resistant against plasma breakthrough, as the hydrophilic and amphoteric components of blood plasma will hardly ever make it through the long hydrophobic pore. Membranes produced by dry stretch have a very solid backbone as can be seen in the figure. This backbone makes them resistant against mechanical stress and thus easy to handle and process.

In the 1980s, plasma breakthrough was a problem in blood oxygenation. However, owing to improvements in the production process and consecutive narrowing of the pore size range, plasma breakthrough today is no longer an issue for blood oxygenator applications in cardiac surgery, where oxygenators are used for no more than six hours.

If an oxygenator is to be used for a prolonged time, wetting of the membranes may also occur with the improved microporous membrane types used today. A wetting phenomenon after ten or more hours commonly is not a plasma breakthrough in the classical sense, in that plasma starts to creep through the pores, facilitated by the blood proteins, but is often a mixture of a condensation process with such plasma creeping. Usually, the blood will have a temperature clearly above room temperature. Therefore, water vapour from the blood may enter the hydrophobic pores and then condense in the capillary lumen, where colder gas flows. Partial condensation may also occur in the pores and help plasma breakthrough.

To prevent this wetting for periods of many hours and even days or weeks, one needs to go back to fully diffusive membranes, with additional safety against the entry and penetration of water or plasma. With a TIPS process, a membrane with a microporous backbone and a thin outer skin can be produced. As mentioned on pages 8–10, the polymer for this membrane must be permeable to carbon dioxide and oxygen. SEMs of such a membrane (trade name

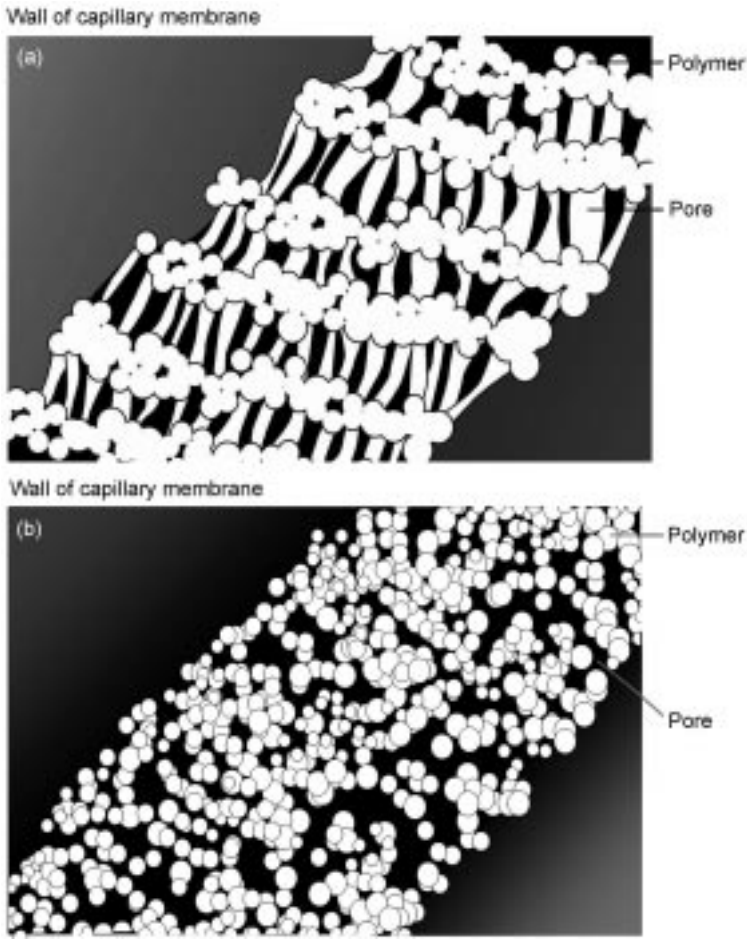

1.6 Comparison of pore structures of membranes produced by TIPS (a) and dry stretch (b).

OXYPLUS®, Membrana GmbH, Germany, Fig. 1.7) show the microporous wall, which provides mechanical stability and the thin outer skin, which prevents water or plasma from entering the pores.

This particular type of membrane has been used as an artificial lung for up to four weeks with no sign of plasma breakthrough.[17,18]

1.2.5 Membrane geometry

Today, only capillary membranes play a role in commercially available blood oxygenators. Those have outer diameters ranging from 200 to about 400 μm with the majority at 300 and 380 μm and inner diameters ranging from 150 to

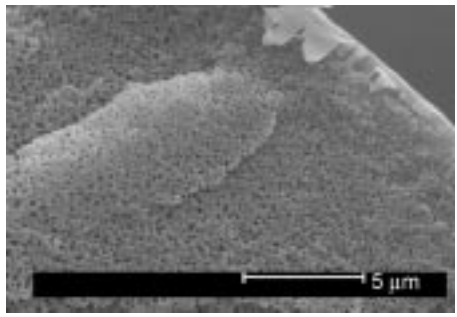

1.7 SEM of PMP membrane with outer skin.

300 μm.[8,16,19] Most of these diameters are a relict from times where oxygenators were constructed with blood flowing inside the capillaries. To ensure a proper flow of blood through the tiny capillaries at the haematocrit of around 30% that is commonly employed during cardiac surgery, an inner diameter (i.d.) of 200–280 μm became the preferred dimension. Many oxygenators were then developed and approved with capillaries with i.d. of 200–280 μm and outer diameter (o.d.) of 300–380 μm. With the trend to blood flow outside the capillaries, these dimensions were not changed. As new developments and new approvals in the medical device industry are time consuming and costly, the 'standard' dimensions have remained the same.

Of course, priming volume can be reduced with smaller membranes, and therefore small membranes are the preferred choice for baby and infant oxygenators to reduce the use of foreign blood products. However, with small dimension membranes manufacturers need more kilometres of membrane for the same active exchange surface, so that for the more cost-sensitive products such as adult oxygenators for cardiac surgery the standard dimensions with o.d. of 300 or 380 μm are the best compromise.

1.2.6 Membrane make-up

For devices with blood flow outside the capillaries, the make-up (arrangement) of the capillaries is of great importance. The simplest construction of a capillary membrane device would be a bundle of parallel capillaries in a cylindrical housing, as has been produced by Terumo (Japan) in the SX series. With such a construction, the fluid around the capillaries is prone to create shunt flows in some parts of the bundle and stagnant regions in other parts. Therefore, the membranes need to be properly arranged to yield a uniform flow around the capillaries and good mixing of the blood.

This can be achieved by winding the capillaries on a core in a symmetrical fashion, similar to a spool of thread. By using a defined angle between the layers and a suitable blood inlet and distribution, good mixing and thus high per-

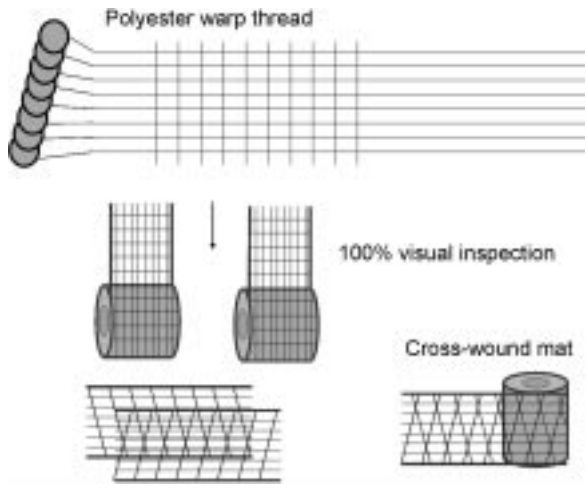

1.8 Membrane makeup to a cross-wound knitted mat.

formance can be achieved. Examples for such a technique today are the RX series oxygenators by Terumo or the Affinity® model by Medtronic. For such a technique, quite large amounts of membrane are lost at the edges of the wound body, where the capillaries change their direction. These are embedded in the potting material and cut away.

Another method is to make up the membranes on a knitting machine according to Fig. 1.8, a unique technology by Membrana GmbH, Germany. For this, the capillaries are knitted to a mat with the parallel capillaries being fixed with warp threads that are fixed with a knot to the capillary. These mats are cut to customer-specified widths and then angled, so that warp thread and capillaries are no longer perpendicular to each other. Two such mats are then superimposed on each other, so that the capillaries lie X-shaped over each other. This double layer mat roll can then easily be incorporated into the final device by the manufacturer. The high packing density and well-defined distances and angles and the arrangement of the warp threads ensure an ideal mixing of blood around the capillaries and thus full utilisation of the incorporated surface with consecutive maximum performance. Oxygenators available with this make-up technique include those from Sorin, Nipro and the Medos Group.

A similar method is employed by Maquet for their Quadrox® oxygenators: these incorporate mat segments that are stacked to a pile in which the mats lie rectangular to their adjacent layers.

1.2.7 Biocompatibility

For oxygenators used in cardiac surgery, biocompatibility is not as much of an issue as it is, for example, in haemodialysis: a patient will use an oxygenator

commonly only once in their lifetime and in most cases for only an hour or two. This is often done in the case of an immediately life-threatening condition, or at least this comparatively short one-off treatment is performed to cure a probably fatal disease. Additionally, the major surgical insult of a coronary artery bypass operation or valve replacement with opening of the chest and exposition of the heart undoubtedly is bio-incompatible to a degree that the biocompatibility of the membrane becomes unimportant.

Microporous membranes that are capable of providing a sufficient gas exchange performance need to be hydrophobic enough not to allow any plasma entrance into the pores and plasma breakthrough to the gas side. This hydrophobicity inevitably brings about contact phase activation and will lead to cell adhesion to the membrane. This has been shown in numerous investigations:[20,21] main concerns with the use of oxygenators are the activation of the coagulation cascade, thrombus formation and drops in cell counts. Manufacturers deal with this problem by coating the whole circuit tip-to-tip with biocompatible coatings such as heparin. Manufacturers have their own proprietary technologies. None of them has yet shown a significant clinical benefit, e.g. in terms of morbidity or mortality, but all coatings provide reduced cell adhesion, reduced coagulation and contact phase activation, many studies show reduced use of donor blood and some show reduced length of stay in the ICU and/or in the hospital. The drawback in most of the studies are the many confounders like the surgical insult as such, the return of suction blood, a great number of comorbidities, the exact conduct of the extracorporeal circulation (temperature, anticoagulation, blood dilution and haematocrit, blood flows, cannulation sites, antegrade or retrograde brain perfusion, unphysiological flows in the whole extracorporeal circuit, non-pulsatility of flow, etc.).

Numerous studies have compared microporous membrane oxygenators of different builds and with different coatings. Most of them have been done on a very small number of patients and none could show a significant superiority of one product over the other. Although it needs to be acknowledged that a hydrophobic microporous membrane is undoubtedly not biocompatible, the other contributors to cell and immune activation obviously significantly override the membrane and oxygenator build effects.

Silicone membranes by nature are more biocompatible than, for example, membranes made from PP because they are less hydrophobic. The downside is that owing to the lower gas exchange performance much higher surfaces are needed, which means higher priming volume, greater blood dilution and a larger foreign surface contact that triggers immune response. An additional advantage over microporous membranes is that blood does not come into direct contact with oxygen or air in the oxygenator. However, the blood–air contact at the direct surgical site seems to override this benefit. Owing to the large priming volume and inferior performance of silicone oxygenators, these do not play a significant role in the cardiac surgery market, anyway.

Biocompatibility is more of a concern for extracorporeal circuits used for longer term lung assist.[22] The survival of extracorporeal membrane oxygenation (ECMO) as the last resort treatment for severe lung failure continue to be poor at clearly less than 50% for adults and not too much above 50% for infants. Most of this may be attributed to the extreme morbidity of the patients treated with ECMO, but nevertheless this mirrors the extreme bio-incompatibility of a prolonged cardiopulmonary extracorporeal support with the large setting as in ECMO. Better perspectives exist for patients with arterio-venous carbon dioxide removal, such as with the new Novalung® device of Novalung GmbH, Germany. These devices have been used for periods of some weeks.[23] However, here the main clinical concerns do not focus on biocompatibility (such as cell adhesion, complement activation) but rather on the performance of the device, anticoagulation, general inflammation and the prevention of organ failure.

1.2.8 Medical device considerations

To create an artificial lung of capillary membranes, the membranes need to be arranged in a repeating, symmetrical manner by either winding capillaries on a core, by winding capillary membrane mats on a core or by piling capillary membrane mats to a stack (see Section 1.2.6). When mats are used, the capillary ends need to be sealed to prevent potting agent from entering the capillary lumen. These membrane bodies are then inserted into a housing and potted: a liquid potting agent such as freshly mixed but not yet polymerised polyurethane (PUR) or silicone is used to glue the body into the housing. After hardening of the potting agent, the ends of the potting are cut with a saw or sharp blades, so that the very end of the capillaries is cut away. The capillaries are thus open; in the device oxygen or oxygen-enriched air will flow into the capillary lumina. The outside of the capillaries is sealed to the housing; blood will enter the housing through a blood inlet port and flow around the capillaries.

Blood film thickness and thus the oxygenator gas exchange performance depend on blood velocity, and hence the packing density: the lower the void volume, the higher the blood velocity will be, the better the gas exchange capacity will become and low surface areas can be employed. The downside of high packing density is the high blood side pressure drop, which indicates pressure and shear stress to the cells.

Flow through the bundle can be either longitudinal (i.e. in the same direction as the capillaries), across (i.e. perpendicular to the capillaries) or anything in between. Most oxygenators have manifolds that distribute the blood into and through the wound body. All types of flow can be found.

Blood oxygenators additionally incorporate a heat exchanger to adjust the patient's blood temperature. Blood commonly flows through the heat exchanger first and then through the gas exchanger. Heat exchanger material can be metal or polymeric material. Metal heat exchangers provide superior heat exchange

capacity due to better thermal conductivity of metal over polymer materials. The latter are easier to process and provide better biocompatibility.

A recent development is to include an arterial filter into the oxygenator, as thrombus formation or introduction of other particulates or gaseous emboli is of concern.

The final device will need to be sterilised before use. As the most widespread membrane material, PP, is not gamma stable, oxygenators are sterilised with ethylene oxide (ETO) gas. An oxygenation membrane from PE ('OXYRAY', Membrana GmbH, Germany), which can be sterilised by gamma irradiation, gained little market share in the 1980s and is no longer commercially available.

1.2.9 Alternative technologies

Cardiac surgery can also be performed without the aid of extracorporeal circulation and thus without an oxygenator. This means that during the procedure the heart needs to keep beating and supplying blood to the body and brain. This of course is only possible for surgery on the outside of the heart such as coronary artery bypass surgery. The site of the intervention is stabilised with a suction device, so that the surgeon can perform the bypass operation on the otherwise beating heart. Recent studies indicate that results of this form of surgery are somewhat inferior to the classical stopped heart surgery.[24] In the late 1990s this kind of procedures were reinvented and reintroduced to the surgical community and rapidly gained acceptance. But since operating on a beating heart is more stressful and demanding to the whole surgical team, the off-pump procedures ceased their growth some years later and since about 2002/2003 account for about 20% of all bypass procedures.[25]

Other options for interventions on the coronary arteries include balloon angioplasty and stenting, where a tiny balloon is forwarded to the narrowing of the artery and then inflated to reopen the clogged section. This can also be combined with a stent, a tiny metal wire mesh around the balloon, which is left in place in the artery to prevent a re-narrowing. Most recent products are coated with growth inhibitors, so that the lumen of the artery stays open for prolonged time. This intervention is of course less invasive, as it is done through a simple cannulation of the arteries, whereas the surgical intervention includes opening the chest. The downside is that through the tortuous arteries not every part of the coronary system can be reached and reopened equally well with a balloon or stent. Additionally, the reintervention rate is higher for the latter approaches, as despite most recent developments the re-narrowing (restenosis) of the arteries still is significantly higher with angioplasty and stenting than with coronary artery surgery.[26]

There currently is no real alternative for long-term lung support. Mechanical ventilation may assist or even replace spontaneous breathing for some time. This can be done with negative pressure (sucking air into the lungs) or positive

pressure (pushing air into the trachea). More elaborate techniques employ pressure curves during each cycle and have their rhythm triggered by the natural breathing of the patient. However, the problem remains that when a lung needs such support, it is already highly stressed and needs time to heal and rest. All artificial addition of oxygen or gas into the lungs necessarily means stress to the lungs, so that the condition is bound to become aggravated. Relief of the stressed lung is possible only with extracorporeal carbon dioxide removal and oxygenation. This again means stress to the whole body due to the exposition of blood to a large foreign surface, the anticoagulation regime and the unphysiological flow. It is supposed, that extracorporeal lung support could yield better clinical results, if it were instituted earlier.

1.3 Membranes for plasma separation

1.3.1 Introduction

In the literature, the terms 'plasmapheresis', 'plasma separation' and 'apheresis' are used. 'Apheresis' is the broadest term, in that it describes any process that removes/eliminates (Greek: *aphairesis*) harmful substances from blood. In this sense, also (haemo)dialysis falls under the term 'apheresis'. The terms 'plasmapheresis' and 'plasma separation' are synonymous and will both be used in this chapter to describe the same process: to separate blood plasma from blood cells.

The idea behind membrane plasma separation is to eliminate harmful substances from a patient's blood. Smaller molecules, i.e. water-soluble toxins such as urea or creatinine or low molecular weight protein toxins such as beta-2-microglobulin can effectively be removed by dialysis. For larger molecules plasma separation is the method of choice. Blood plasma together with the toxins is separated from the blood cells (white cells, red cells, platelets), which are returned to the patient. The plasma can then be treated to remove the toxins or be discarded and replaced by healthy donor plasma. The treatment of the plasma can either be a fractionation (by cascade filtration with a plasma fractionation membrane) or adsorption of the toxins to be removed.

Over the years, a great number of treatment variants that include plasma separation have been developed. Those aim at removing harmful substances that cannot be removed by haemodialysis, such as immunoglobulins (IgM, IgG), immune complexes, low density lipoproteins (LDL), fibrinogen, light and heavy chains, etc. Those cannot be removed by haemodialysis, as these molecules are larger than the smallest essential blood components that are to be preserved and not removed, namely the smaller proteins, the prominent example of which is albumin. As long as albumin is to be retained, it is not possible to remove the larger toxins by a one stage membrane separation process such as haemodialysis, which functions on the basis of size exclusion.

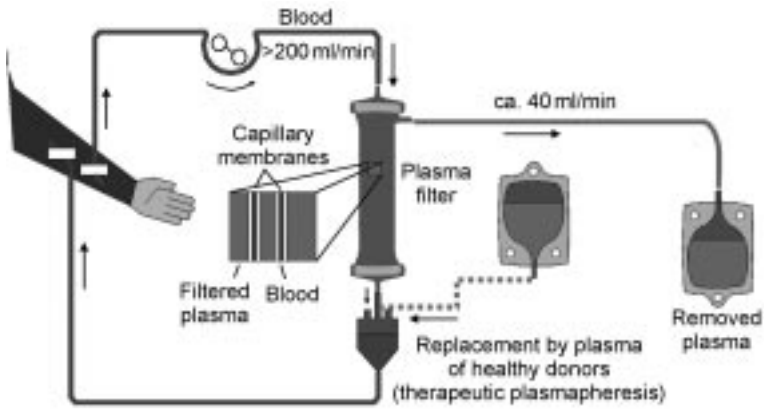

1.9 Principle of membrane plasma separation.

For plasma separation, the blood plasma is separated from the cells by either centrifugation or membrane filtration (Fig. 1.9). The pore size of the separation membranes is in the range of less than 0.5 μm, thus small enough to hold back the smallest blood cells: platelets.

Blood plasma is pumped through a filter very similar to a dialyser and plasma migrates through the pores driven by an excess pressure on the blood side. This excess pressure can be achieved by a pump or through gravity. The plasma can then be discarded and replaced by saline or protein solutions or treated further. The consecutive steps can be additional filtration steps as in cascade filtration or adsorption processes. The blood cells are dispersed in saline or a protein solution and returned to the patient.

1.3.2 Manufacture and resulting structure

Hydrophobic synthetic membranes

The production of hydrophobic synthetic plasma separation membranes is done through a TIPS process and is very similar to that of blood oxygenation membranes (see pages 10–12): the basic polymer (PE or PP) is dissolved in a hot mixture of solvents. This solution is forced through a ring-shaped spinneret. After exiting the spinneret, the solution is cooled, so that the polymer recrystallises. The solvent aggregates to droplets, which are trapped in the polymer matrix. After extraction of the solvent, the space where the solvent has been constitutes the pores. These pores need to be larger than those for the blood oxygenation membranes to allow a sufficient transport of plasma through the membrane wall.

The structure of these membranes consequently is very similar to that of TIPS-produced blood oxygenation membranes (Fig. 1.10). The membrane has a homogeneous, sponge-like structure with a constant pore size throughout the whole membrane wall.

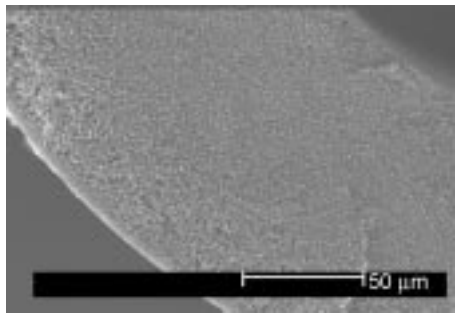

1.10 SEMs of a TIPS produced hydrophobic plasma separation membrane.

To be applicable for plasma separation, a hydrophobic membrane needs to be hydrophilised before use, so that blood plasma can enter and penetrate the pores. This is either done in the place of use or the plasma filter comes ready hydrophilised. Such hydrophilisation can be achieved, for example, by rinsing the membrane with a liquid such as alcohol, that completely penetrates the pores easily. This liquid is then replaced by water or saline and completely washed out of the pores. Alternatively, solutions containing surfactants can be used instead of the alcohol. The plasma separator must not be dried completely after this hydrophilisation step, so that the pores keep being wetted by the water or saline. Once dried completely, the membrane regains its hydrophobic properties and needs to be re-hydrophilised. To prevent complete drying, some low volatile hydrophilic components can be added, such as glycerol.

Hydrophobic synthetic membranes dominated membrane plasma separation for many years, but have today increasingly been replaced by hydrophilic synthetic membranes more and more.

Synthetic hydrophilic membranes

Synthetic hydrophilic plasma separation membranes are very similar in composition and production to dialysis membranes. The majority consist of a blend of polysulphone (PSu) or polyethersulphone (PES) and polyvinylpyrrolidone (PVP) and are produced according to the same schemes as synthetic dialysis membranes (reference to dialysis chapter). Other materials include polyvinylchloride (PVC), polymethylmethacrylate (PMMA) and polyvinylalcohol (PVA). As the polymers PSu and PES have the largest industrial meaning, the following will focus on these two materials. The membrane formation as such is achieved by a solvent-induced phase separation process (SIPS) (Fig. 1.11).

For this, the basic polymers PSu + PVP or PES + PVP are dissolved in a mixture of solvents. Various solvent systems are used by the different manufacturers. As for all productions of capillaries, this polymer solution is pumped through a ring-shaped spinneret, at the same time a core liquid is pumped

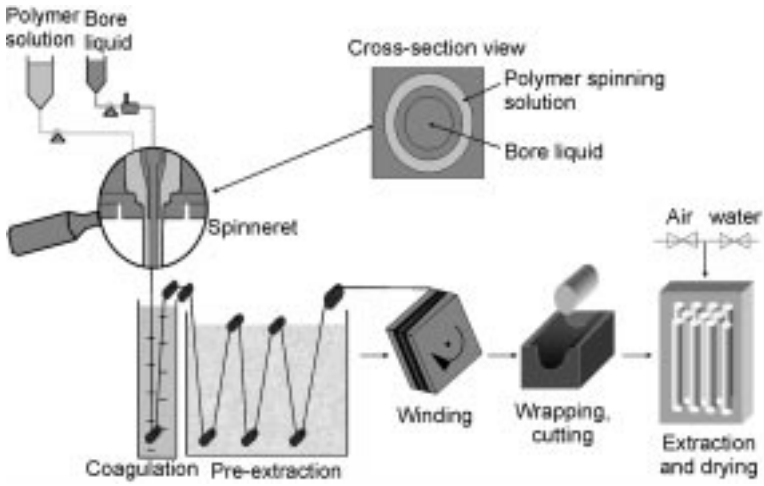

1.11 Production scheme for synthetic hydrophilic plasma separation membranes by solvent-induced phase separation (SIPS).

through an opening in the centre of the ring spinneret to prevent the capillary from collapsing to a simple thread. This core liquid is a non-solvent to the polymer mix, and is commonly a water-based mixture. When the polymer solution comes into contact with the non-solvent, the polymer precipitates from the solution and forms the membrane wall. This process is also called diffusion-induced phase separation (DIPS) process, because the initiation of the precipitation of the polymer takes place due to diffusion of the solvent and non-solvent into each other.

In this technique it is important to achieve a fast precipitation rather than a small, controlled recrystallisation (Fig. 1.12) and for it to come directly from a stable solution (which consists of polymer and solvent and virtually no non-solvent) to a non-stable system, in which the polymer then precipitates.[27] The faster the precipitation occurs, the more nucleation centres will build, which will quickly aggregate in all three dimensions, produce a somewhat random structure and thus trap the solvent and non-solvent as tiny droplets in a scaffold of polymer (path B). If a path is chosen that leads to a meta-stable system, then nucleation and growth will occur slowly and result in larger chunks of polymer, so that solvent and non-solvent can run off, yielding a capillary with almost no pores (path A).

This precipitation occurs from the lumen to the outside of the wall, because it is initiated by the core liquid. Therefore, membranes produced with SIPS often display a non-homogeneous pore structure, with the pores on the lumen side having different diameters from those on the outside. After this (first) precipitation, the membrane is spun into a bath of non-solvent (again mostly water). This completes the precipitation of the polymer and serves as a first washing step of the pore structure to wash out the solvent.

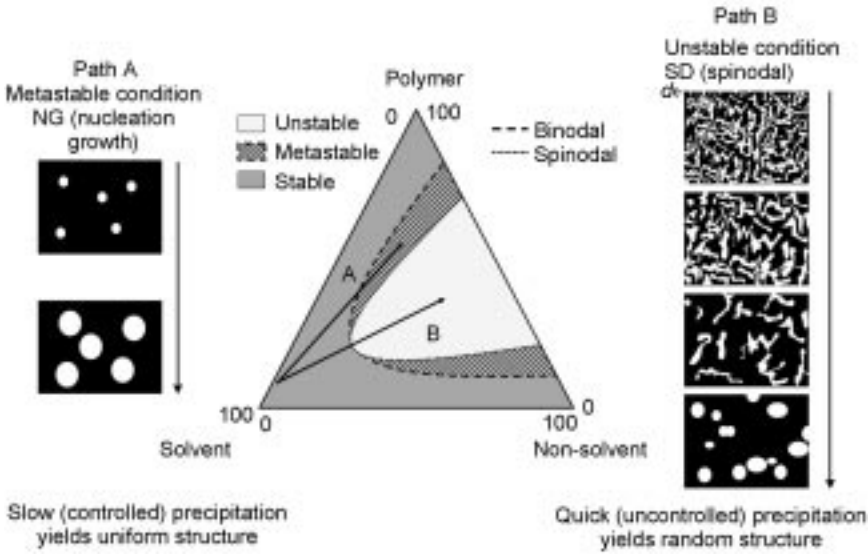

1.12 Precipitation paths in SIPS. Adapted from *Membranen: Grundlagen, Verfafen und ind. Anwendung*, K. Ohlrogge and K. Ebert, Wiley, 2006.

The resulting capillary is then washed. This can either be done online, i.e. by passing the capillaries through water baths of increasing purity, or by winding the capillaries to bundles and then extracting the bundles with water.

Cellulosic hydrophilic membranes

Cellulosic membranes for plasma separation still play a certain role in the medical device market, but similar to dialysis membranes their significance in the market has decreased (Fig. 1.13). They are produced in a similar way to the

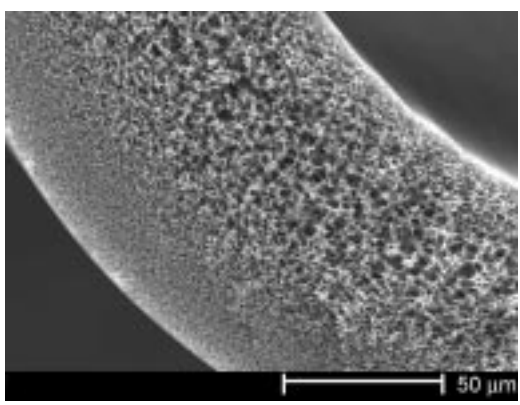

1.13 SEM of a synthetic hydrophilic plasma separation membrane.

schemes for cellulosic dialysis membranes. Membranes for plasma separation are produced from cellulose acetate. For this, cellulose acetate is dissolved, e.g. in an acetic acid solution, and spun through a ring nozzle into a precipitation bath that can have only a low concentration of acetic acid. To keep the capillary open, a bore liquid is injected through an opening in the centre of the ring nozzle into the lumen of the capillary. The capillary is washed in several steps with water: ideally the final washing step brings the membrane into contact with a pore stabilising agent such as glycerol. It is finally wound to bundles and then dried.

1.3.3 Characterisation of plasma separation membranes

Plasma separation membranes are much more open than dialysis membranes. Table 1.3 gives an overview of plasma separation and plasma fractionation membrane classification according to their sieving coefficients. The sieving coefficient SC is the fraction of a given molecule that can pass the membrane:

$$\mathrm{SC} = \frac{2C_\mathrm{f}}{C_\mathrm{o} + C_\mathrm{i}}$$

where SC is the sieving coefficient; C_f is the concentration in the filtered plasma; C_o is the concentration in the blood at outlet; and C_i is the concentration in the blood at inlet.

Sieving coefficients of a plasma separation membrane for virtually all plasma proteins (e.g. albumin, 66 kDa; IgG, 150 kDa; IgM, 970 kDa; β-lipoprotein, 2400 kDa) should be in the range of 0.95 to 1.00 to allow for an efficient removal in particular of the larger proteins. A plasma fractionation membrane should hold back these larger molecules to a considerable portion, e.g. with an SC for IgM of 0.2 or similar. The IgM-containing fraction can then be discarded, and the smaller proteins like albumin returned to the patient.

Another important value to characterise a plasma separation membrane is the transmembrane pressure (TMP) during operation:

$$\mathrm{TMP} = \frac{p_\mathrm{i} + p_\mathrm{o}}{2} - p_\mathrm{f}$$

Table 1.3 Typical sieving coefficients of separation membranes

	Beta-2 microglobulin	Albumin	IgM
Low flux dialysis membrane	0.00		
High flux dialysis membrane	0.60	0.01	
Super-flux dialysis membrane	0.9	0.02–0.05	0
Plasma fractionation membrane	1.0	0.8	0.2
Plasma separation membrane		1.0	1.0

where TMP is the transmembrane pressure; p_i is the blood pressure at inlet; p_o is the blood pressure at outlet; and p_f is the pressure of filtrate.

Too high a transmembrane pressure may result in blood stress and damage and thus pressure must be monitored closely and kept at (ideally) about 50 mmHg, but not higher than 150 mmHg, where haemolysis may occur. This haemolysis is caused by damage to the red blood cells in the rather large pores. At high pressure, the red cells are pressed into the pores and rupture. It is therefore advisable to start a plasma separation procedure at zero plasma flow, to allow a certain protein deposition on the membrane walls (see Section 1.3.5) to protect the blood cells.

1.3.4 Membrane make-up

Plasma separators are produced from membrane bundles. As the separation principle is simply to press the plasma out through the capillary wall, the separator architecture and thus bundle makeup can be rather basic. Blood is flowing inside the lumen of the membranes and the plasma simply runs off on the outside of the capillaries. The packing density of the bundle must thus not be too high to allow for an unhindered flow of plasma. Further flow optimisation on the outside of the capillaries, such as that employed, for example, by undulation or spacer yarns for dialysers, is unnecessary and even counterproductive.

In the manufacture of the membrane bundles, the bundles are therefore simply collected to multifilament strands. This can be achieved by winding the capillaries on a large wheel or by laying them on a table in parallel fashion. These strands are then cut to the length needed for the final device and wrapped into a foil to aid the insertion of the bundle into the housing of the plasma separator.

1.3.5 Medical device considerations

To ensure a proper functioning of the final separator, several issues need to be addressed:

- high porosity (both surface and volume) for sufficient plasma flow;
- low fouling (i.e. protein adsorption and blocking of the capillary);
- biocompatibility (low complement activation, no haemolysis);
- sterilisation possible by ETO, gamma irradiation, steam.

A finished plasma separator contains about 0.2–0.9 m^2 of membrane surface and is operated at blood flows of 50–200 ml/min. The transmembrane pressure is kept low at typically less than 50 mmHg and, depending on the device, does not exceed 150 mmHg.

During the plasma separation, blood cells and larger proteins will accumulate by the membrane wall, as the plasma exits through the wall and the larger components of blood are retained. This so-called cell concentration polarisation will hinder the plasma flow across the membrane wall. An increasing blood flow

will tend to remove the cells from the membrane wall and support flow through the wall. In particular towards the exit of the plasma separator, where a considerable fraction of plasma has already been removed and the haematocrit rises to up to 70%, parts of the membrane surface may be lost to removal of plasma due to increased blocking.

Most plasma separators have active lengths between 200 and 250 mm, which seems to be the optimum. A longer device will need higher operating pressures, in particular due to the concentration of blood cells and the rising viscosity of the blood over the length of the separator. Higher operating pressures will also mean higher transmembrane pressures at least by the blood inflow into the device and can result in a higher tendency towards haemolysis. Shorter devices may result in too low a pressure gradient, which means that fewer plasma can be pressed off.

1.3.6 Alternative technologies

A direct alternative to plasma separation with membranes is the centrifugation of blood. This method is currently far more popular than plasma separation with membranes. It is used widely in blood and plasma donation centres. The patient's or donator's blood is pumped into a centrifuge, where the plasma is simply centrifuged off. Both fractions can be handled as after a membrane separation: cells are returned to the patient or donor and the plasma is treated further.

This process is technically established almost everywhere in the world. It is a proven technology and fairly simple to operate. However, it needs to rely on an elaborate infrastructure with energy supply to the centrifuge and sterilisation of the reusable parts of the machine. A membrane plasma separation is independent of such infrastructure and can also be operated in any country. Another downside of centrifuged plasma is that it may contain cell debris generated during the procedure. Such debris is rarely generated during membrane plasma separation, and additionally any particulates would be completely retained by any plasma separation membrane.

Another option would be removal of the target molecules from whole blood, without separation into cells and plasma.[28] This, however, is a very difficult task. It demands highly selective adsorbents to the target molecule to be removed, which needs to avoid any triggering of immune response or other bioincompatibilities. Today, only a few methods for direct removal from whole blood exist, such as DALI or Liposorber for removal of lipoproteins.

1.4 Economic considerations

1.4.1 Blood oxygenation

In the era of ever-growing economic pressure, including in the healthcare sector, any treatment and component must be put under scrutiny for its economy.

Economic considerations for blood oxygenation membranes are of course a concern to the medical device manufacturers, but do not impact the overall procedure cost.

The oxygenator represents about a hundredth of the cost of a cardiac surgery intervention,[29] including all costs for medical care, hospital stay and all consumables. The membrane inside the oxygenator contributes only a minor fraction of the cost of the oxygenator.

The major economic aspect is therefore in the decision for either a cardiac surgery procedure with blood oxygenator or an alternative treatment, such as an operation on the beating heart, a catheter intervention or a drug therapy.[30] Different data evaluations have yielded different results. Some argue that an operation on a beating heart is cheaper than an operation with oxygenator, as the expenses for the heart–lung machine can be saved, while others find that the disposables for a beating-heart operation are rather more expensive than those for a procedure with extracorporeal circulation. Additionally, there is no conclusion yet as to whether any short-term savings may be overcompensated by long-term effects, e.g. in that a catheter procedure, which is less costly up-front, may generate higher cost in the years following the procedure due to a higher rate of reintervention.

From the oxygenator manufacturing perspective, the main aspect is that in emerging countries with growing healthcare budgets more and more cardiac surgery can be afforded and by this growing number the decrease in the developed countries due to upcoming alternatives such as interventional cardiology is roughly compensated for. In some developing countries, in particular in China, bubble oxygenators are still used, which are far simpler than membrane oxygenators and thus sell at less than half the price of a membrane device. Owing to the imminent medical advantages, bubble oxygenators will vanish from the market within the next few years and be replaced by membrane oxygenators. Therefore, the worldwide overall number of cardiac surgery procedures with the aid of a blood oxygenator is roughly flat.[31,32]

One growing segment is the replacement of the lung in intensive care. If in systemic inflammation, severe lung trauma or (multi) organ failure a patient's lung needs support, the underlying diseases are characterised by very high mortalities. Where available, measures to help save the patient's life by lung support therefore are mostly not economically restricted. The reason for a rather slow adoption of this treatment variant is in the complexity of the treatment: although routine in cardiac surgery, there are hardly any trained personnel in an intensive care unit to conduct an extracorporeal blood oxygenation. So, one may well be able to see this segment growing within the next years, but the bottleneck will be the education of the medical professionals in the task of facilitating the procedure and devices.

1.4.2 Plasma separation

Although successful treatment of, for example, Goodpastures syndrome with plasma separation had been reported in the 1970s and plasma separation for removal of larger toxins from human blood has been practised since at least the 1980s, it is still not a widespread and widely accepted treatment method. This is mainly due to the absence of large controlled, randomised studies that prove the effectiveness of plasma separation procedures. Although there are many smaller studies and case reports that suggest that plasma separation can be an effective treatment for a variety of diseases, there is still a lack of evidence.[33] Without such evidence, reimbursement for these therapies can be achieved only in rare cases, which limits plasma separation to a last resort treatment when all other options have failed.

The potential cost for the payers, if plasma separation and treatment were more widespread, is considerable. A bare plasma separation process was reimbursed in 2007 in the USA at US$720, therapies involving further separation steps at more than US$1500.[34] Healthcare providers and payers are therefore in a chicken-and-egg situation: as there is hardly any reimbursement, it is virtually impossible to collect the evidence needed to support more widespread application of blood plasma treatment. Without evidence-based recommendations and good practice guidelines an approval for more liberal reimbursement cannot be achieved, even if therapies based on plasma separation may in the end save money due to their selectivity and efficiency. Without rising numbers of treatments, the cost per procedure will remain high, which will again make payers cautious to more liberally grant reimbursement. The reports about successful treatments are increasing and medical societies and healthcare authorities around the world are discussing plasma separation treatments more often. Before systematic approvals can be given, however, medical professionals, societies and providers have a long way to go.

1.5 Future trends

Perspectives for blood oxygenation membranes in cardiac surgery are rather flat: cardiac surgery with the aid of an oxygenator is established as the gold standard with excellent outcomes. Major changes to the procedure as such, to the oxygenator or the oxygenation membrane, are not expected. Devices will continue to become smaller with less priming volume and less surface area, improved blood flows and better biocompatibility through optimised shear rates and haemocompatible coatings. The basic principle of a microporous hydrophobic membrane in plastic housing is no matter of debate. Alternative treatment methods have been established, such as off-pump cardiac surgery or developments such as catheter interventions for heart valve replacement. The decrease due to this competition has for some years already been compensated

by the growth due to increasing civilisation diseases in developed countries and by the expansion of demanding and costly cardiac surgery in developing countries.

The application of a long(er) term artificial lung is much more lively. Here a device is needed that can oxygenate blood and remove carbon dioxide with as reduced blood trauma as possible for many consecutive days. Such devices have entered the market in the recent past years. Membranes with a dense outer skin, such as the OXYPLUS® membrane from PMP, function for several weeks with no breakdown, like the Novalung device.[35] The obstacles to overcome here are rather in the prevention haemolysis and that of clotting and deposition of, for example, fibrin, then on the side of the membrane.

In the 1980s and 1990s, several mathematical models have been established to describe mass transfer in oxygenators, e.g. by Mockros.[36] With today's tools, mathematical modelling of oxygenators is possible. Theoretically, today we can calculate the ideal form of an oxygenator at the given parameters of volume, shear stress, surface area, etc. However, although several such models are being developed,[37] differences between theory and experiment seem to prohibit the widespread use of these approaches.

Alternative technologies such as bioartificial lungs with live cells are today nothing but a dream. Research with live endothelial and alveolar cells is going on, but it will take years, if not generations, of research to develop a live alternative to the current artificial lungs.

The outlook for plasmapheresis similarly does not focus on the membranes, as these are readily available. The technology to produce plasma separation membranes is there, as is the technology to manufacture plasma separators out of these. The field where we will see developments in the next few years is that of clinical application. Evidence for the effectiveness and efficiency of plasmapheresis for various diseases will have to be collected and documented. In this course, the consecutive steps after the separation of blood plasma and blood cells will have to be improved. This will involve affinity and adsorption techniques for the selective removal of pathogens from plasma. With this evidence, plasma separation therapies can become more widespread.

1.6 Abbreviations

A	surface area
a_1, a_2	activities
C	concentration
d	distance (of diffusion)
d_p	diameter of pore
EMO	extracorporeal membrane oxygenation
ETO	ethylene oxide
i.d.	inner diameter

K	Knudsen number
K_d	diffusion constant
mmHg	millimetres of mercury (torr)
o.d.	outer diameter
p	pressure
PE	polyethylene
PES	polyethersulphone
PMP	polymethylpentene
PP	polypropylene
PSu	polysulphone
PVP	polyvinylpyrrolidone
SC	sieving coefficient
SIPS	solvent-induced phase separation
t	time
TIPS	thermally induced phase separation
TMP	transmembrane pressure
V	amount of gas exchanged
Λ	mean free path

1.7 References

1. Leonard RJ, *Perfusion*, 2003, **18**, 179–183.
2. Weitkemper HH *et al.*, in: Tschaut RJ (Ed.): *Extrakorporale Zirkulation in Theorie und Praxis*, Pabst Science Publishers, Lengerich, 1999.
3. Lillehei CW, in: Gravelee GP (Ed.): *Cardiopulmonary Bypass*, 3rd Edition, Wolters Kluwer, Philadelphia, 2008.
4. Kolff WJ *et al.*, *Cleve Clin O*, 1956, **23**, 69–97.
5. Kolobow T *et al.*, *Trans Am Soc Artif Intern Organs*, 1963, **9**, 238–243.
6. Wodetzki A *et al.*, *Membrane*, 2000, **25**(3), 102–106.
7. Federspiel WJ *et al.*, Artificial lung: basic principle and current applications, in: Wnek B: *Encyclopedia of Biomaterials and Biomedical Engineering*, 2nd Edition, Vol 3, Informa.
8. Data sheets OXYPHAN®, OXYPLUS® and CELGARD®, Membrana GmbH, Wuppertal, 2010.
9. Yasuda H *et al.*, *J Appl Polymer Sci*, 1974, **18**, 805–819.
10. Breiter SM *et al.*, *ASAIO J*, 2004, **50**(2), 153.
11. Allen SM *et al.*, *J Membr Sci*, 1977, **2**, 153.
12. Robb WL, *NY Acad Sci*, 1968, **146**, 119.
13. Agati S *et al.*, *ASAIO J*, 2006, **52**, 509–512.
14. Wendel HP *et al.*, *Eur J Cardio-Thoracic Surg*, 1999, **16**, 342–350.
15. Goldstein AH *et al.*, in: Gravelee GP (Ed.): *Cardiopulmonary Bypass*, 3rd Edition, Wolters Kluwer, Philadelphia, 2008.
16. Dramburg WE *et al.*, in: Tschaut RJ (Ed.): *Extrakorporale Zirkulation in Theorie und Praxis*, Pabst Science Publishers, Lengerich, 1999.
17. Philipp A *et al.*, *Kardiotechnik* 01/2003, 7–13.
18. Horton S *et al.*, *Perfusion*, 2004, **19**, 17–23.

19. Data sheet Terumo Capiox, Terumo Corp., 2010.
20. Hsu LC, *J Cardiothorac Vasc Anaesth*, 1997, **11**(3), 376–382.
21. Janiver G *et al.*, *Ann Thorac Surg*, 1996, **62**, 1923–1934.
22. Marasco S *et al.*, *Heart, Lung and Circulation*, 2008, **17**, S41–S47.
23. Flörchinger B *et al.*, *Ann Thorac Surg*, 2008, **86**, 410–417.
24. Shroyer AL *et al.*, *New England J Med*, 2009, **361**(19), 1827–1837.
25. Rechenschaftsbericht der Deutschen Gesellschaft für Thorax-, Herz- und Gefäßchirurgie, Annual Conference 2010, Feb 2010, Stuttgart.
26. Serruys PW *et al.*, *New England J Med*, 2009, **360**(10), 961–972.
27. Peinemann KV *et al.*, in: Ohlrogge K *et al.* (Eds): *Membranen*, Wiley, Weinheim, 2006.
28. Stegmayr BG, *Blood Purification*, 2000, **18**, 149–155.
29. Yock CA *et al.*, *Am J Med*, 2003, **115**, 382–389.
30. Yock CA *et al.*, *Am Heart J*, 2000, **14**(4), 556–564.
31. Theta report No 924, 2000, PJB Medical Publications, New York.
32. Research and Markets report 'U.S. Market for cardiac surgery devices', 2009, Research and Markets, Dublin.
33. Szczepiorkowski CM *et al.*, *J Clin Apher*, 2007, **22**(3), 106–175.
34. ASFA Reimbursement guide 2006, American Society for Aphersis, Vancouver, BC, Canada.
35. www.novalung.com/en/publications
36. Mockros LF *et al.*, *Trans Am Soc Artif Intern Org*, 1985, **31**, 628–633.
37. Hormes M, thesis, University of Aachen, in preparation.

2

Titanium and cobalt–chromium alloys for hips and knees

C. YAO, Nanovis LLC, USA and J. LU and T. J. WEBSTER, Brown University, USA

Abstract: As dominant materials used in today's joint prostheses, titanium and cobalt–chromium alloys frequently suffer from failure due to wear particles, mismatch of modulus, lack of sufficient osseointegration for cementless implants, etc. From this point of view, this chapter will first review material science fundamentals of titanium and cobalt–chromium alloys currently used in hip and knee replacement as well as pointing out their shortcomings in some specific areas. Then, advances in this field will be discussed. Lastly, this chapter will focus on discussing one of the promising metal surface modification methods, called anodization, which has increased implant osseointegration. Some additional surface treatments to increase wear resistance and biocompatibility of titanium and cobalt–chromium alloys surfaces will also be discussed at the end of the chapter.

Key words: titanium, cobalt–chromium, hip replacement, knee replacement, surface modification, osseointegration.

2.1 Hip and knee joint replacement

The use of modern hip replacements can be traced back to the 1960s when Charnley (1961) performed the first modern total hip replacement with low friction arthroplasty (shown in Fig. 2.1). Following Charnley's success, numerous attempts have been made to design knee replacements. Since then, continued innovations in hip and knee replacements have been made and they have become one of the most successful and revolutionized surgeries in the orthopedic field. Total hip replacements as well as knee replacements enable hundreds of thousands of elderly patients to fight against arthritis and restore their quality of life. Today, younger patients can even expect physically demanding activities after implantation of highly functional and long-lasting joint prostheses.

2.1.1 Hip implant design and construction

Physiologically, the hip joint is called a ball-and-socket structure because the spherical head of the thighbone (femur) moves inside the cup-shaped hollow

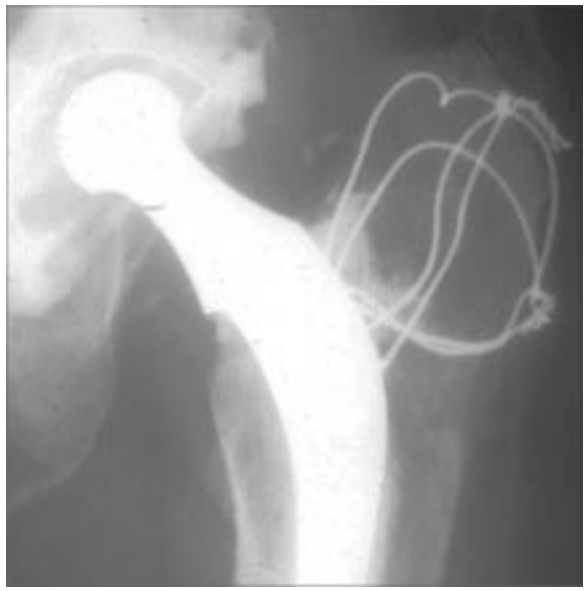

2.1 Radiograph of 26-year follow-up of first-generation Charnley low friction arthroplasty composed of a stainless steel femoral head and high density polyethylene cup.

socket (acetabulum) of the pelvis. Thus, to mimic this structure, a total hip replacement usually has three parts: (i) the stem that fits into the femur; (ii) the ball that replaces the spherical head of the femur; and (iii) the cup that fits into the worn out acetabulum. As shown in Fig. 2.1, the stem and ball can be one piece but they can also be modular for additional customization.

Today's hip implants are composed of high performance metal alloys, ceramics, and polymers (Table 2.1). Specifically, the stem is usually made of titanium or cobalt–chromium alloys. These metal alloys are designed to possess good mechanical strength and corrosion resistance. Certain kinds of surface treatments (such as bioactive coatings, porous structures) are often used to enhance bone ingrowth onto the hip implant. The ball is commonly made of cobalt–chromium alloys or ceramic materials (e.g., aluminum oxide and zirconium oxide) due to their good wear resistance properties. The ball surface is smooth in order to minimize rotation resistance against the socket. The acetabular socket can be composed of metal or ultrahigh molecular weight polyethylene (UHMWPE).

Although new materials, such as polyetheretherketone (PEEK), are being investigated for hip stems (Kurtz and Devine, 2007), titanium and cobalt–chromium alloys are still dominant. This chapter is thus focusing on reviewing the fundamentals of these alloys summarizing some of the new advances in developing more efficient metal hip and knee implants.

Table 2.1 Materials for hip and knee joint replacement

Material	Hip replacement				Knee replacement			
	Hip stem (uncemented)	Femoral head	Cup/ insert	Metal back shell	Femoral component	Tibial plate	Tibial cushion	Patella
CP Ti	–	–	–	X	–	–	–	–
Ti alloys	X	–	–	X	X	X	–	–
CoCr alloys	X	X	X(M)	X	X	X	–	–
Stainless steel	–	X	–	–	–	–	–	–
Alumina	–	X	X(C)	–	–	–	–	–
Zirconia	–	X	–	–	–	–	–	–
UHMWPE	–	–	X	–	–	–	X	X

CP Ti: commercially pure titanium; UHMWPE: ultrahigh molecular weight polyethylene.
X: clinically used. –: clinically not used or not successful; M: metal-on-metal bearing; C: ceramic-on-ceramic bearing.

2.1.2 Cemented and cementless hip replacements

Hip replacements can be cemented, cementless, or hybrids. For cemented hip replacements, the clinically used stem materials include stainless steel and cobalt–chromium alloys. The most often used bone cement is polymethylmethacrylate (PMMA). The success of a cemented hip implant depends on both a strong bone–cement bonding and a stable cement–prosthesis interface. Though cemented hip replacements have been generally considered as a good fixation option, there is concern about implant loosening. This could occur when surrounding cemented fractures over time lead to wear debris particle generation (from both the cement itself and polyethylene socket); such events cause inflammation which further causes osteolysis (bone destruction and resorption) and instability of the implant (loosening).

Because of this, cementless hip replacements have been developed to eliminate PMMA-related mechanism of failure. Both titanium and cobalt–chromium alloys are used in cementless hip stems. Initial stability and fixation of cementless hip implants can be achieved by press-fitting the component and using screws, spikes, and pegs. However, the long-term stability and fixation of cementless femoral and acetabular components rely on adequate osseointegration onto and into the implant. For this purpose, stem surfaces are mostly textured or roughened to allow intimate bony apposition and provide long-term implant anchorage. They can also be made porous or coated with bioactive ingredients to enhance bone ingrowth. Metal-backed shells of acetabular cups in cementless hip replacements also have a porous or coated surface to promote bone ingrowth.

Although some cementless stem designs have good long-term outcomes, cementless stems can still loosen if a strong bond between bone and the stem is not achieved. Additionally, the acetabular component survival is relatively poor (Capello *et al.*, 2003; Kearns *et al.*, 2006). This is mainly because cementless hip replacements still suffer from polyethylene wear debris and osteolysis. Therefore, a second-generation of metal-on-metal bearing systems for total hip replacements have received a lot of attention since the 1980s (Dumbleton and Manley, 2005). However, this design raises questions on the release of metal ions and puts higher criteria for the wear resistance of metal components (mainly cobalt–chromium alloys).

In summary, cemented hip replacements are usually recommended for older patients while cementless hip replacements are more suitable for younger patients who can achieve bone ingrowth onto the prosthesis more easily.

2.1.3 Knee implant design and construction

The knee can be simply considered as a hinge joint. In reality, it includes more complicated motions like rolling and gliding. There are over 150 knee implant designs in the market today but, generally, all of them are composed of three parts: a curved femoral component to replace the lower end of the thighbone, a flat tibial component to replace the top surface of the shinbone, and a dome-shaped patella component to replace the kneecap.

To provide smooth motion and minimize wear, all articulating interfaces are between metals and plastics (Table 2.1). Specifically, the femoral component is usually made of cobalt–chromium alloys. The tibial component has a metal platform and an ultrahigh density polyethylene cushion. The patella component is also made of ultrahigh density polyethylene. Titanium and titanium alloys tend to have a subordinate role in knee replacements due to their less superior wear properties than cobalt–chromium alloys. To date, wear is still the major reason for a knee revision.

2.2 Challenges for current metal hip and knee implants

Over a million patients undergo hip and knee replacement surgeries every year in the US (Table 2.2), and a significant percentage of these surgeries are revision surgeries. Recent statistics pointed out that the chance of a hip replacement lasting 20 years is approximately 80% (AAOS, 2007a) and the chance of a knee replacement lasting 20 to 25 years is about 95% (AAOS, 2007b). Although this is generally acceptable for older patients who may not live longer than this, it is not acceptable for younger and more active patients receiving hip and knee replacement. Thus, novel hip and knee prosthesis with improved efficacy are in high demand and are now under investigation by many researchers.

Table 2.2 Primary/revision hip and knee replacements performed in the US during 2001 to 2005

Description	2001	2002	2003	2004	2005
Total hip replacement	165 000	193 000	220 000	234 000	235 000
Partial hip replacement	119 000	109 000	108 000	240 000	234 000
Revision of a hip replacement	109 000	43 000	36 000	46 000	35 000
Total knee replacement	326 000	381 000	418 000	478 000	534 000
Revision of a knee replacement	29 000	25 000	33 000	40 000	37 000

As discussed above, the main challenges for current titanium/cobalt–chromium based components (such as the femur, ball, and metal back of acetabular cups in hip replacement; femoral shells and tibial trays in knee replacements) lie in the following three areas:

- Provide mechanical stability for the system; avoid stress shielding and bone resorption resulting from a mechanical mismatch with bone.
- Perform with superior wear resistance to reduce wear debris and avoid excessive metal ion release.
- Achieve quick and strong osseointegration or chondrointegration for long-term anchorage; prevent excessive fibrous tissue growth and inflammatory response.

In the following sections, the biomechanical and biological properties of titanium and cobalt–chromium alloys will first be summarized. Their advantages and disadvantages as hip and knee implants will be discussed. Additionally, some emerging novel methods to help current metallic hip and knee implants meet the above criteria will be reviewed.

2.3 Material fundamentals of titanium and cobalt–chromium alloys used in hip and knee replacement

2.3.1 Titanium and titanium alloys used in hip and knee replacements

Titanium has two allotropes: alpha and beta. Alpha phase titanium has a hexagonal closed-packed (hcp) crystal structure and exists at room temperature. Beta phase titanium is a body-centered cubic (bcc) structure and appears when titanium solidifies to equilibrium from liquid or titanium is heated over 883 ºC. For titanium alloys, alpha-stabilizing elements include aluminum, tin, and oxygen and beta-stabilizing elements include niobium, molybdenum, chromium, iron, and vanadium, which can achieve stable crystal structures at room temperature.

Mechanical properties

Today, the most widely used titanium alloy in hip replacements is titanium alloyed with aluminum and vanadium. This is because typically alpha–beta alloys can achieve optimum properties necessary for demanding loading-bearing applications (i.e., hip replacement) by balancing the amounts of alpha and beta stabilizers. Some of the mechanical properties of two alpha–beta alloys (Ti-6Al-4V and Ti-6Al-7Nb) are shown in Table 2.3.

Mechanical and thermal treatment

The mechanical properties of titanium alloys are principally determined by their microstructure assuming the same composition, which in turn can be defined by manufacturing processes (e.g., casting, forging, powder metallurgy) and subsequent thermal treatment (e.g., solution heat treatment, hot isostatic pressing (HIP), sintering). Mechanical processes can result in elongated grains in the working direction while the final heat treatment can recrystallize the elongated structure into an equiaxed structure. The as-worked elongated structures exhibit higher anisotropic tensile strength and lower ductility while the recrystallized equiaxed structures exhibit lower non-directional strength but have higher ductility. For example, the ultimate tensile strength of commercially pure titanium (grade 1) increased from 410 to 560 MPa after 40% cold deformation while at the same time its elongation at fracture decreased from 30% to 16% (Black and Hastings, 1998).

Generally, cast materials may have microscopic voids that can lead to reduced mechanical properties. In comparison, forging can achieve the best mechanical properties for metallic prostheses. Specifically, both Ti-6Al-4V and

Table 2.3 Mechanical properties of selected titanium, titanium alloys and bone (Niinomi, 1998)

Material and designation (or condition)	Young's modulus (GPa)	Tensile strength (MPa)	Yield strength (MPa)
Ti ASTM Grade 1 (alpha)	102.7	240	170
Ti ASTM Grade 2 (alpha)	102.7	345	275
Ti ASTM Grade 3 (alpha)	103.4	450	380
Ti ASTM Grade 4 (alpha)	104.1	550	485
Ti-6Al-4V (alpha/beta; annealed)	110–114	895–930	825–869
Ti-6Al-7Nb (alpha/beta)	105–123	900–1050	880–950
Ti-6Al-4V ELI (alpha/beta)	101–110	860–965	795–875
Ti-13Nb-13Zr (beta; aged)	79–84	973–1073	836–908
Ti-12Mo-6Zr-2Fe (beta; annealed)	74–85	1060–1100	1000–1060
Ti-35.3Nb-5.1Ta-7.1Zr	55	597	547
Cortical bone	17–28	130	–

Ti-6Al-7Nb can be forged into hip implant components at temperatures between 900 and 950 ºC (Windler and Klabunde, 2001). This is because hot forging or other thermo-mechanical treatments can inherently close the pre-existing voids and improve mechanical and fatigue properties of the same material.

Strength and elasticity

Titanium alloys usually have higher strength and elasticity than bone. A low Young's modulus enables more physiological transmission of loads to the femur and can avoid proximal stress shielding and bone resorption in the proximal femur. Although titanium alloys already have a relatively low elasticity (110 GPa) compared with CoCr alloys (210 GPa), recent research has focused on developing novel titanium alloys which possess even lower elasticity (Kuroda *et al.*, 1998). This issue will be discussed in detail in later sections.

Fatigue strength

The fatigue properties of titanium alloys used for hip implants are very important because they will be subjected to high dynamic loading of millions of cycles during its lifetime. The fatigue strength of titanium alloys is significantly higher than pure titanium and is affected by its microstructure and surface treatment. For example, forged and polished Ti-6Al-7Nb has a fatigue strength of about 600 MPa which is excellent compared with its static strength (Windler and Klabunde, 2001). However, it is known that titanium alloys are sensitive to fatigue induced by notches. Therefore, an appropriate hip design as well as choice of material is critical here. In other words, the design should minimize excessive stress due to construction notches in order to avoid hip fracture.

Wear resistance

Untreated titanium alloys usually do not have high enough wear resistance for use in articulating situations which appear in both hip and knee replacements. Therefore, research has improved the tribological properties of titanium alloys through various surface treatments. For example, a layer of hard coatings of TiN (Coll and Jacquot, 1988; Liu *et al.*, 2003) and diamond-like carbon (McNamarta *et al.*, 2001; Platon *et al.*, 2001) up to several microns can be deposited onto titanium alloy surfaces by chemical or physical deposition. However, the main challenge for hard coating methods lies in the insufficient adhesive strength of the coatings and the potential presence of wear particles. Hence, so far, such coatings are not a practical choice for femoral heads of hip implants and articulating parts of knee implants. Some other techniques to enhance titanium and cobalt–chromium alloy wear resistance will be discussed in later sections.

Biocompatibility

It has been found that elements such as vanadium (often alloyed with titanium) have corrosion and cytotoxicity risks (Wapner, 1991). As a result, toxic-free titanium alloys such as Ti-13Nb-13Zr and Ti-15Mo have been developed to achieve higher biocompatibility properties since the 1980s (Okazaki *et al.*, 1996). Beside the composition of titanium alloys, the outermost oxide layer of titanium-based orthopedic implants is a main factor influencing biocompatibility properties. Titanium dioxide is the most stable titanium oxide and is resistant to most chemical events. The excellent corrosion resistance of titanium and its alloys is to a large extent due to this oxide layer (containing titanium dioxide and other oxides like Al_2O_3, Nb_2O_5, etc.). For this reason, titanium is usually considered biocompatible when used as an orthopedic implant (Textor *et al.*, 2001). Numerous *in vitro* and *in vivo* studies have confirmed the biocompatibility properties of titanium and titanium alloys (Bordji *et al.*, 1996; Larsson *et al.*, 1996; Long and Rack, 1998; Sittig *et al.*, 1999; Shin *et al.*, 2005). In addition, numerous clinical studies on different cementless titanium hip prostheses with various surface treatments confirmed a high survival rate. For example, Zenz *et al.* (1995) observed a 97.9% success rate after 10 years of implantation for rough grit-blasted Ti-6Al-4V and Ti-6Al-7Nb stems. McLaughlin and Lee (1997) found a 96% survival rate after 10 years for titanium plasma-sprayed Ti-6Al-4V stem implants.

Though titanium and titanium alloys generally perform well as hip implant materials (in the scale of 5 to 10 years), it is still a challenge to obtain an effective longevity over 20 years. One of the problems with current titanium alloy implants (regardless of chemistry and crystallinity) is that their surfaces lack enough bioactivity to promote and sustain bone cell functions necessary for quick and strong osseointegration, i.e., there is a lack of direct structural and functional connections between living bone and the surface of load-bearing titanium-based implants. As a result, numerous researchers have focused on improving titanium implant surface properties to prevent interposition of non-bone (fibrous) tissue and to support better new bone growth.

2.3.2 Cobalt–chromium alloys used in hip and knee replacements

Mechanical and tribological properties

There are four cobalt–chromium alloys commonly used for hip and knee replacements today (Table 2.4). Among them, F75 has been widely used in the fabrication of femoral stems because of its corrosion resistance in chloride environments due to the oxidized surface. As mentioned before, large grain sizes develop during the casting process, which results in decreased yield strength. In addition, casting defects may cause fatigue fracture of a femoral stem. To

Table 2.4 Typical mechanical properties of CoCr alloys (Brunski, 2004)

ASTM designation	Condition	Young's modulus (GPA)	Yield strength (MPa)	Tensile strength (MPa)	Fatigue endurance limit (at 107 cycle, $R = -1$) (MPa)
F75	As-cast/annealed	210	448–517	655–889	207–310
	Powder metallurgy product, hot-isostatically pressed	253	841	1277	725–950
F799	Hot forged	210	896–1200	1399–1586	600–896
F90	Annealed	210	448–648	951–1220	Not available
	44% Cold worked	210	1606	1896	586
F562	Hot forged	232	965–1000	1206	500
	Cold worked, aged	232	1500	1795	689–793 (axial tension $R = 0.05$, 30 Hz)

$R = \alpha_{max}$

remove these problems, powder metallurgical methods are usually used for decreasing grain sizes as well as formulating finer distributions of carbides, which leads to better fatigue properties and higher yield strength. F799 has a similar chemical composition to F75 but has been treated by hot forging after casting. As a result, its mechanical properties (such as yield, fatigue, and ultimate tensile strength) increase by 100% compared with as-cast F75. The mechanical properties of F90 are also twice as high as those for F75, due to the addition of Ni and processed by cold work. F562, which is processed by cold working and aging, is one of the strongest materials for implant applications.

Cobalt–chromium alloys are mostly used for bearing components due to its excellent wear resistance. Table 2.5 lists clinical wear behavior for cobalt–chromium alloys used in total hip replacements. Compared with currently used metal-on-cross-linked UHMWPE bearings, second generation (reintroduced into the field in the late 1980s) metal-on-metal bearings exhibit much better wear properties. They can even compete with ceramic-on-ceramic bearings while they are much stronger than ceramics for loading-bearing situations.

Biocompatibility

Although cobalt–chromium alloys are generally considered biocompatible, they are not considered as optimal as titanium alloys in term of new bone tissue

Table 2.5 Wear behavior of CoCr alloys used in total hip replacement (Dumbleton and Manley, 2005; Windler and Klabunde, 2001)

Femoral head	Cup	Linear wear (μm/y)	Debris size (μm)
CoCr	UHMWPE	100–300	0.5
Ceramic	UHMWPE	50–150	0.2
CoCr	CoCr	2–5	0.05
Ceramic	Ceramic	2–5	0.2

integration. This is because elements such as cobalt, chromium, and nickel included in cobalt–chromium alloys have controversial effects on immune responses and cytotoxicity (Spriano *et al.*, 2005).

The cobalt–chromium alloys used in the second generation of total hip replacements proved to be successful after short- to medium-term follow-up clinical studies. For example, Doerig *et al.* (1999) observed a 96% survival rate out from a total of 218 hip stems after 2–6 years. Korovessis *et al.* (2002) found a 96.8% survival rate for such stem after 4.3 years and 99.4% for cups after 7.6 years. However, large patient numbers and long-term clinical follow-up will be needed to further confirm the efficacy of cobalt–chromium alloys.

Biological issues related to cobalt–chromium alloys used in load-bearing applications continue to be a concern today. Specifically, metal ions released may have carcinogenic effects and wear debris from cobalt–chromium alloys may be toxic to cells (Spriano *et al.*, 2005). Thus, a harder and more protective cobalt–chromium surface is desirable to address these problems.

2.4 Advances in titanium and cobalt–chromium alloys used for joint implant

So far the advantages and disadvantages of titanium and cobalt–chromium alloys used as in joint replacements have been reviewed. As stated earlier, continued innovations have been made in these fields and some of them are discussed here.

2.4.1 Selection of new composition alloys

As mentioned above, Ti-6Al-4V ELI is the most widely used titanium alloy in hip prostheses (stems and cups). Other first generation titanium alloys include Ti-6Al-7Nb (Semlitsch *et al.*, 1992) and Ti-5Al-2.5Fe (Borowy and Kramer, 1995). Nb and Fe are used to substitute V in response to concerns about potential cytotoxicity of V and adverse tissue reactions.

To enhance biocompatibility and lower the modulus of hip prostheses, second generation titanium alloys have been recently developed. Some earlier examples

include beta titanium alloys based on the Ti-Mo system (Ti-12Mo-6Zr-2Fe, Ti-15Mo-5Zr-3Al, and Ti-15Mo-3Nb-3O) (Steingemann *et al.*, 1993; Wang *et al.*, 1993a,b). These alloys have a Young's modulus around 80 GPa (compared with 110 GPa for Ti-6Al-4V). Since Mo is still considered potentially detrimental, Mo-free titanium alloys such as Ti-15Zr-4Nb-2Ta-0.2Pd and Ti-15Sn-4Nb-2Ta-0.2Pd have been developed (Okazaki *et al.*, 1993). However, elements such as Sn and Pd may still lack biocompatibility. Finally, titanium alloys using only biocompatible elements such as Nb, Ta, and Zr have been developed. One example is Ti-13Nb-13Zr which is considered to be completely biocompatible and possess a Young's modulus of 79 GPa (Kovacs and Davidson, 1993; Mishra *et al.*, 1993). Another example is Ti-35Nb-5Ta-7Zr, which has a Young's modulus as low as 55 GPa (Ahmed *et al.*, 1995). The improved biocompatibility of these Ti-Nb-Zr alloys is closely associated with their corrosion resistance. Electrochemical measurements of Ti-13Nb-13Zr revealed that Nb and Zr helped to form and tended to be incorporated into a highly protective passive layer on the alloy surface. As a result, this alloy has a much lower potential electrochemical interaction than Ti-6Al-4V and has no adverse effect resulting from dissolved metal ions as Al and V do.

2.4.2 Porous metal prostheses

Compared with solid metal implants, porous metal prostheses, either only surface or total bulk porosity, may have advantages in the following fields: first, a tailored modulus that can match the modulus of bone and avoid stress shielding; second, improved fixation by allowing bone ingrowth, i.e., osseointegration. In this light, a variety of fabrication techniques have been developed over the years and the interaction between porous metals and tissues have been investigated (Hirschhorn *et al.*, 1971; Bobyn *et al.*, 1990, 1992; Ryan *et al.*, 2006).

Obviously, porous metals may have a few challenges when serving as hip implants. First of all, a porous metal matrix might have reduced fatigue strength. For instance, researchers found that the high cyclic fatigue strength of porous coated Ti-6Al-4V is about one-third of the solid alloy (Wolfarth and Ducheyne, 1994). Therefore, a partly or fully porous coated solid metal substrate instead of a fully porous metal is more appropriate for hip applications to provide sufficient mechanical strength; porous coated metals are usually avoided at highly stressed surface areas. Furthermore, to address this concern, optimization of the porosity, pore size and shape, pore distribution, and interconnectivity can be critical. Wolfarth and Ducheyne (1994) predicted a doubling of fatigue strength when optimizing these porous geometries using finite element analysis. Heat treatment is another method to increase the fatigue properties of porous metals. Cook *et al.* (1988) showed a 15% improvement in fatigue strength of porous Ti-6Al-4V via post-sintering heat treatments that produced microstructures more resistant to

crack formation. Second, a highly porous metal matrix with increased surface area may exhibit higher corrosion rates than its solid counterpart (Reclaru *et al.*, 2005). To address this concern, surface treatment of porous metals is necessary prior to implantation.

Although porous metals are promising for titanium and cobalt–chromium alloy hip implants, it is only now that researchers are starting to understand the multifactorial design criteria that include mechanical properties under loading conditions, corrosion resistance, bone attachment and ingrowth, and, finally, parameters such as pore size, shape, and distribution that will optimize mechanical/corrosion properties and bone ingrowth.

2.4.3 Bioactive coatings

Hydroxyapatite (HA) has been used as a surface coating on metallic hip implants (mostly on femoral stems and limited use on acetabular components) since the mid-1980s (Geesink, 1989; Furlong and Osborn, 1991). HA is the inorganic mineral component of bone and it exhibits excellent biocompatibility and bioactivity, such as quick bone bonding capability and osteoconductivity (Stephenson *et al.*, 1991; Cook *et al.*, 1992). Clinical practice with HA-coated hip prostheses indicates that HA coatings generally achieved earlier fixation and stability with more bone in- and on-growth (Capello *et al.*, 1997; Donnelly *et al.*, 1997; Nelissen *et al.*, 1998; Roynesdal *et al.*, 1998). However, the long-term performance of such HA-coated prostheses depends on the quality of the HA coating, that is, the purity, crystallinity, Ca/P ratio, microstructure, porosity, thickness, and implant surface properties.

Specifically, two major concerns exist in achieving continued bone fixation via HA coatings. First, degradation or resorption of HA coatings may result in the loss of interfacial bonding strength. Second, delamination or disintegration of the HA coating with the formation of granular debris may increase wear, thus leading to osteolysis and finally implant loosening. These should be addressed by improving the HA coating quality via optimizing the deposition techniques and implant surface properties.

HA coatings are usually applied to both titanium and cobalt–chromium alloys using a plasma spray method. This process involves high velocity spraying of HA powders and high temperatures (up to 30 000 K) so conventional plasma-sprayed HA coatings are composed of micron-size HA particles. Before plasma spraying, the surface of metallic implants can be grit blasted to create microroughness, macrostructured to form patterns, or made porous (as discussed in the previous section) to enhance coating adhesion strength and implant fixation. Studies have shown that compared with CoCr alloys, titanium alloys had a 33% increase in bonding strength to the HA coatings *in vitro*, which might be a result of chemical bond between Ti and HA. Moreover, titanium showed a closer coefficient of thermal expansion ($9–10 \times 10^{-6}/^{o}C$) to HA ($12 \times 10^{-6}/^{o}C$)

as opposed to CoCr alloys (16×10^{-6}/ºC) (Sun *et al.*, 2001). As a result, titanium alloys are more suitable for the HA coating method.

Nano-HA coatings have received a lot of attention recently due to its biomimicking nano-size and enhancement in long-term bone growth compared with conventional micron-size HA coatings by plasma spraying. This has been achieved by room-temperature deposition techniques such as electrophoretic deposition (Cornia *et al.*, 2008). It has been claimed that such nano-HA coatings have higher bond strength (60 MPa compared with 30 MPa of plasma sprayed HA coating), higher density and crystallinity (100% crystallinity, thus less degradation and fewer wear problems) to significantly improve the lifetime of HA-coated metal hip prostheses (Zhang *et al.*, 2007).

2.4.4 Novel hip implant surface modification techniques

The aforementioned porous metals and bioactive coatings are two major research directions to improve current titanium and cobalt–chromium alloy hip prostheses. Besides, novel surface modification techniques such as anodization provide a great opportunity to take advantages of nanostructured metal surfaces in order to promote new bone growth (Yao and Webster, 2006).

Anodization to promote tissue integration

Anodization or anodic oxidation is a well-established surface modification technique for valve metals that produce protective layers. During anodization, a constant voltage or current is applied between the anode and cathode, electrode reactions (oxidation and reduction) in combination with field-driven ion diffusion lead to the formation of an oxide layer on the anode surface.

The anodization technique was discovered in the early 1930s and was widely studied in the 1960s to enhance titanium implant osseointegration. These processes usually adopted high voltage anodization (called ASD) of titanium in electrolyte solutions whose ions would be embedded into the oxide coating, resulting in a microporous structure. For electrolytes containing Ca and P, such as calcium glycerophosphate (Ca-GP) and calcium acetate (CA), both Ca and P were contained in the oxide layer with a Ca/P ratio closer to HA (1.67). After an additional hydrothermal treatment (e.g., high pressure steaming), HA crystals were randomly precipitated on the anodic oxide film. This could be an alternative way to create HA coatings on titanium implants as opposed to plasma spraying.

Recently, research efforts have focused on creating biologically inspired nanometer surface structures on titanium implants using specific anodization parameters. Studies have shown that nanoporous structures can be created by anodizing titanium in chromic acid at 10–40 V (Baun, 1980). Another unique surface morphology obtained through titanium anodization is self-ordered nanotubular structures (Fig. 2.2a). For these studies, fluorine electrolyte solutions are

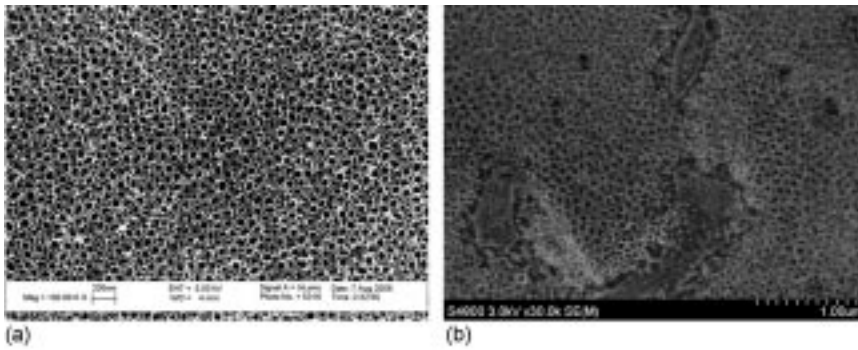

2.2 Scanning electron microscopy (SEM) images of (a) anodized pure titanium, and (b) anodized Ti-6Al-4V in a dilute fluorine-containing electrolyte.

used and the applied voltage must be much lower than the dielectric breakdown. For such titanium nanotubular surfaces, apatite layers can be easily formed by simply soaking anodized crystalline titania in simulated body fluid (SBF) because anodized titanium with anatase and rutile titania surfaces were shown to induce apatite formation *in vitro* (Yang *et al.*, 2004; Oh *et al.*, 2005). This technique could be useful as well as adherent bioactive nano-HA layers on titanium-based implants are created which simulate the size and shape of natural HA in bone.

A preliminary study showed that anodized Ti-6Al-4V in fluorine-containing electrolyte solutions displayed nanotubular structures similar to the anodized titanium all over the surface except where the β phase was present (Fig. 2.2b). Both bone and cartilage cells exhibited increased activity on anodized Ti surfaces compared with untreated Ti (Fig. 2.3). Numerous studies confirmed that such anodized titanium alloys can promote osseointegration compared with untreated surfaces (Yao *et al.*, 2008; Das *et al.*, 2009; Lee *et al.*, 2009).

CoCr alloys can also be anodized to possess nanoscale features. A Co-33.4Cr-3.3Mo alloy was successfully anodized in both fluorine-containing and fluorine-free acidic electrolytes. The resulting surface possessed numerous micron features as well as nanoporous structures all over the surface (Fig. 2.4). The size of such heterogeneous porous structures was about 20 to 30 nm under 10 V. Under lower voltages (2 V), the resulting topography was less rough in the micron-scale while nano rough features looked similar to the surfaces created under 10 V (Fig. 2.4). Anodized CoCrMo had an oxide layer composed of CoO, Co_3O_4, and Cr_2O_3 (Gallant *et al.*, 2006; Survilienė *et al.*, 2008). The network of –Cr–O–Cr– bridges in the oxide of CoCr alloys are considered to be the main reason for their passivity (McCafferty, 2002). In addition, due to the formation of this oxide layer, the water contact angle of anodized CoCrMo was nearly 30º lower than the unanodized CoCrMo, and, thus, indicated better wettability of the CoCr surfaces for protein adsorption and subsequent cell attachment. This is promising in terms of improving the biocompatibility of CoCr alloys. Pre-

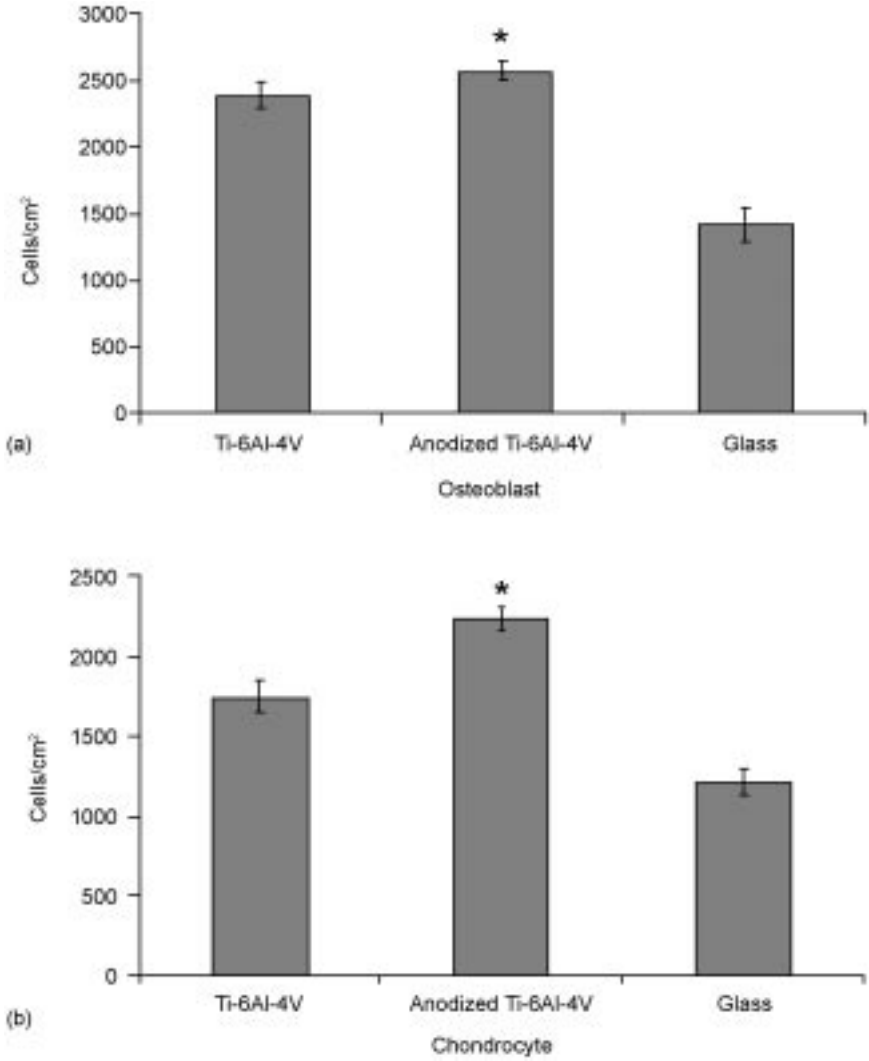

2.3 (a) Osteoblast and (b) chondrocyte adhesion on unanodized Ti-6Al-4V and anodized Ti-6Al-4V after 4 hours. Values are mean ± SEM; $n = 3$; $^{*}p < 0.05$ compared with unanodized Ti-6Al-4V.

liminary results also confirmed that anodized CoCrMo surfaces promote both osteoblast and chondrocyte adhesion (Fig. 2.5).

Surface treatments to increase wear resistance and biocompatibility

The aforementioned hard coating method (diamond-like carbon) on metals is limited by its weak interface strength and, thus, has not been used. In comparison,

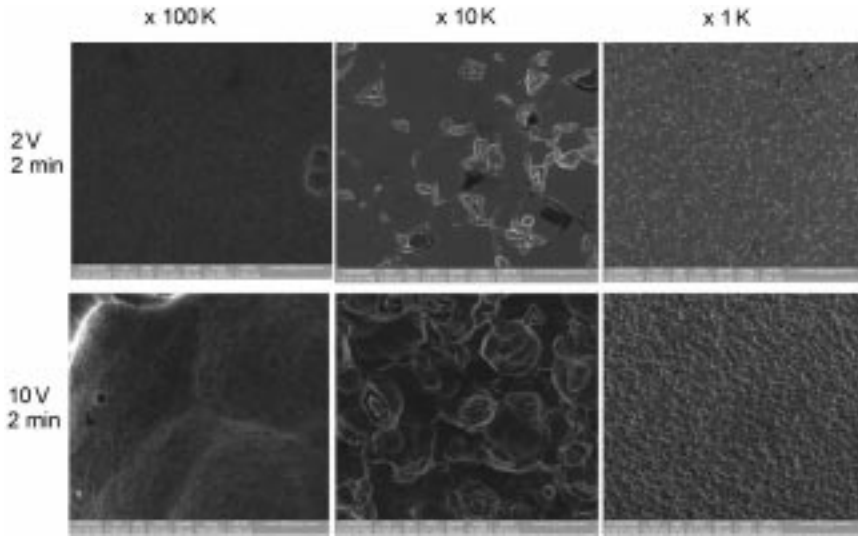

2.4 SEM images of anodized CoCr alloy under 10 and 2 V.

some other methods (such as ion implantation) present no concern for the loss of adhesion and delamination. Basically, the titanium or cobalt–chrome alloy surfaces are bombarded with high-energy ions which penetrate into the metal substrate and change the composition and properties of the surface. Nitrogen, oxygen, and other elements are usually used to increase the hardness of the surface regions and such ion-implanted surfaces have been advocated for articulating joint surfaces especially with UHMWPE (Windler and Klabunde, 2001).

Introduction of biocompatible and corrosion-resistant modifier elements into metal surfaces is another way to improve titanium and cobalt–chromium alloy surface properties. An example is enrichment of tantalum on cobalt–chromium alloy surfaces by heat treatments (Spriano *et al.,* 2005). Tantalum has been used as trabecular constructs to allow bone ingrowth (Findlay *et al.*, 2004). In the study by Spriano *et al.*, a cobalt alloy was thermally treated in molten salts including 47 wt% NaCl, 52 wt% K_2TaF_7, and 1 wt% Ta at 1000 ºC for 60 min (Spriano *et al.*, 2005). Chemical analysis confirmed enrichment of Ta. The water contact angle on treated CoCr alloy was 46º which was 24º lower than the untreated alloy. Scratch tests revealed high scratch resistance of the modified layer. The friction coefficient and abrasive wear rate of Ta-enriched surface were significantly lower than those of the untreated surface. Moreover, metal ion release during wear tests on treated alloys was one magnitude lower than on untreated alloys.

There are many other mechanical, thermal-mechanical, chemical, and electrochemical methods to mediate titanium and cobalt–chromium alloy surface properties. The choice of method should be a comprehensive consideration of the material, the biocompatibility, and wear resistance.

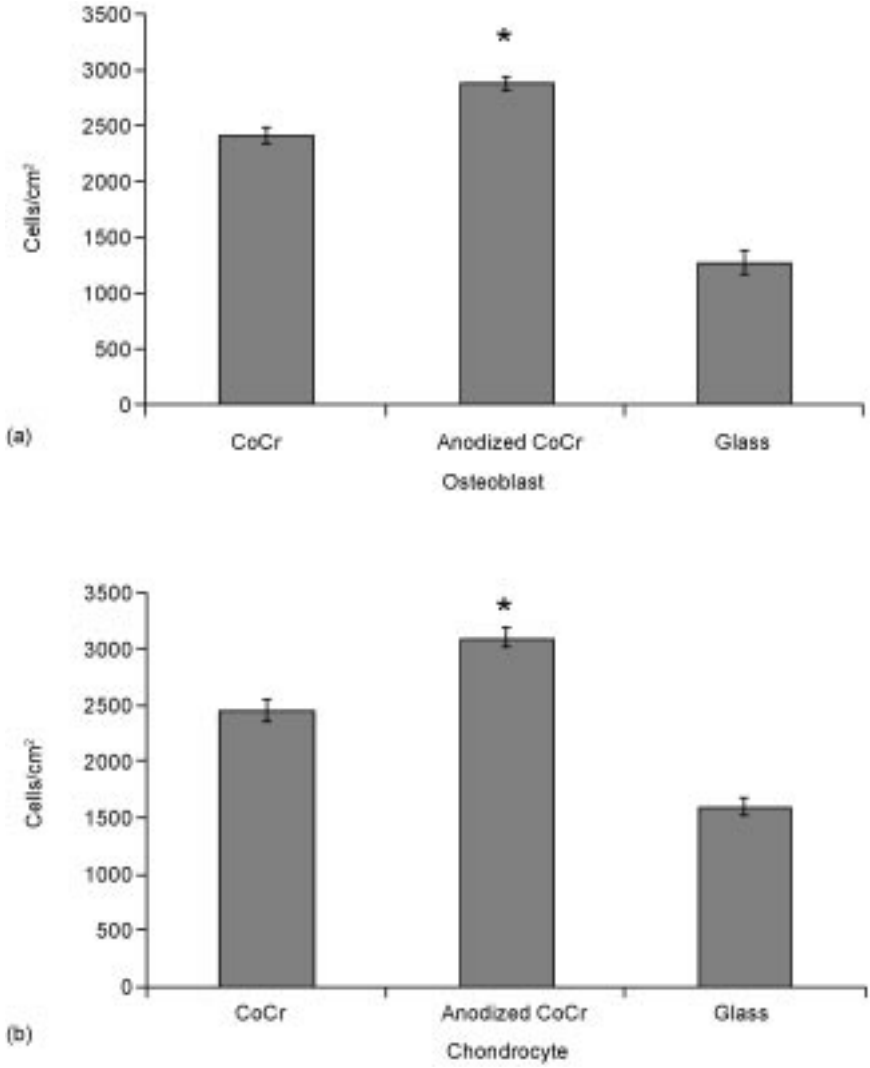

2.5 (a) Osteoblast and (b) chondrocyte densities on unanodized CoCrMo and anodized CoCrMo after 4 hours of culture. Values are mean ± SEM; $n = 3$; $^{*}p < 0.05$ compared with unanodized CoCrMo.

2.5 Conclusions and future trends

The goal of developing novel total hip and knee prostheses with a lifetime over 30 years for younger and more active patients has put high demands on titanium and cobalt–chromium alloys since they are used for most components of these joints.

Wear debris and consequent osteolysis and aseptic loosening are major causes of implant revisions. This is partly a result of using UHMWPE for the articulating bearing components. Some of the clinical studies have already shown promising results of using second generation metal-on-metal bearing systems rather than conventional metal-on-polymer systems. However, the design of novel pure metal joint systems raises questions on their wear resistance and metal ion release. A more detailed understanding of effects of metal particles and ions on the human body is needed in the future. Meanwhile, some methods, such as ion implantation and tantalum-enrichment, have demonstrated promising results in improving titanium and cobalt–chromium alloy tribological properties.

For titanium and cobalt–chromium alloys that are mainly used for stems and metal backs that require tissue integration, quick and strong osseo- or chondrointegration is a major goal. To meet this challenge, either bioactive coatings, porous surface structures, or various surface modification methods (such as anodization) have been employed and have demonstrated some success *in vitro* and *in vivo*. Further investigations to optimize the modification parameters and resulting surfaces are important to achieve more bioactive metal implants.

Last, but not least, a metal hip implant with closer elasticity to bone will add strength and a prolonged implant lifetime. This is partially achieved by selection of metal alloys with new compositions. Some beta titanium alloys are of great interest today due to their superior biocompatibility and low Young's modulus compared with the current widely used Ti-6Al-4V.

In summary, titanium and cobalt–chromium alloys play an important role in today's hip and knee replacements. The development of new metal prostheses designs, new alloy compositions, new processing and heat treatments, new implant surface coatings, and modifications will all contribute to improve the efficacy of current metal joint prostheses and prolong their effective lifetimes. However, in a field that requires maybe decades for a new standard to be accepted, more laboratory work and clinical studies are needed for industrial acceptance.

2.6 References

AAOS (American Association of Orthopedic Surgeons) (2007a), Hip implants. Available from: http://orthoinfo.aaos.org/topic.cfm?topic=A00355 (accessed 5 February 2010).

AAOS (American Association of Orthopedic Surgeons) (2007b), Knee implants. Available from: http://orthoinfo.aaos.org/topic.cfm?topic=A00221 (accessed 5 February 2010).

Ahmed T, Long M, Silvestri J, Ruiz C and Rack HJ (1995), 'A new low modulus, biocompatible titanium alloy', presented at the 8th World Titanium Conference. Birmingham, UK.

Baun WL (1980), 'Chromic acid anodization of Ti6Al4V', *Surf Technol*, **11**, 421–426.
Black J and Hastings G (1998), 'Titanium and titanium alloys', in *Handbook of Biomaterial Properties*, Chapman & Hall, 120–200.
Bobyn JD, Glassman AH, Goto H, Krygier JJ, Miller JE and Brooks CE (1990), 'The effect of stem stiffness on femoral bone resorption after canine porous-coated total hip arthroplasty', *Clin Orthop Relat Res*, 196–213
Bobyn JD, Mortimer ES, Glassman AH, Engh CA, Miller JE and Brooks CE (1992), 'Producing and avoiding stress shielding. Laboratory and clinical observations of noncemented total hip arthroplasty', *Clin Orthop*, 79–96.
Bordji K, Jouzeau JY, Mainard D, Payan E, Netter P, Rie KT, Stucky T and Hage-Ali M (1996), 'Cytocompatibility of Ti-6Al-4V and Ti-5Al-2.5Fe alloys according to three surface treatments, using human fibroblasts and osteoblasts', *Biomaterials*, **17**, 929–940.
Borowy KH and Kramer KH (1995), 'The properties of a new titanium alloy (TiAl5Fe2.5) as implant material', in *Titanium'84 Science and Technology*, vol. 2, Munich, Deutsche Gesellschaft Metallkunde EV, 1381–1386.
Brunski J (2004), 'Classes of material used in medicine: metals', in Ratner BD, Hoffman AS, Schoen FJ and Lemons JE, *Biomaterials Science: An Introduction to Materials in Medicine*, 2nd edn, Elsevier, 137–152.
Capello WD, D'Antonio JA, Feinberg JR and Manley MT (1997), 'Hydroxyapatite-coated total hip femoral components in patients less than fifty years old. Clinical and radiographic results after five to eight years of follow-up', *J Bone Joint Surg*, **79**, 1023–1029.
Capello WN, D'Antonio JA, Feinberg JR and Manley MT (2003), 'Ten-year results with hydroxyapatite-coated total hip femoral components in patients less than fifty years old: a concise follow-up of a previous report', *J Bone Joint Surg Am*, **85A**, 885–889.
Charnley J (1961), 'Arthroplasty of the hip: a new operation', *Lancet*, **1**, 1129–1132.
Coll BF and Jacquot P (1988), 'Surface modification of medical implants and surgical devices using TiN layers', *Surf Coat Technol*, **36**, 867–878.
Cook SD, Thongpreda N, Anderson RC and Haddad RJ (1988), 'The effect of post-sintering heat treatments on the fatigue properties of porous coated Ti-6Al-4V alloy', *J Biomed Mater Res*, **22**, 287–302.
Cook SD, Thomas KA, Dalton JF, Volkman TK, Whitecloud TS III and Kay JF (1992), 'Hydroxyapatite coating of porous implants improves bone ingrowth and interface face attachment strength', *J Biomed Mater Res*, **26**, 989–1001.
Cornia I, Ryana MP and Boccaccini AR (2008), 'Electrophoretic deposition: From traditional ceramics to nanotechnology', *J Europ Ceramic Soc*, **28**, 1353–1367.
Das K, Bose S and Bandyopadhyay A (2009), 'TiO_2 nanotubes on Ti: influence of nanoscale morphology on bone cell-materials interaction', *J Biomed Mater Res A*, **90**, 225–237.
Doerig MF, Odstrcilik E and Jovanovic M (1999), 'Uncemented alloclassic-metasul total hip arthroplasty: early results after 2–6 years', in Rieker C, Wyndler M and Wyss U, *Metasul: A Metal-on-Metal Bearing*, Bern (Swizerland), Hans Huber, 157.
Donnelly WJ, Kobayashi A, Chin TW, Freeman MAR, Yeo H, West M and Scott G (1997), 'Radiological and survival comparison of four fixation of a proximal femoral stem', *J Bone Joint Surg*, **79B**, 351–360.
Dumbleton JH and Manley MT (2005), 'Metal-on-metal total hip replacement: what does the literature say?', *J Arthroplasty*, **20**, 174–188.
Findlay DM, Welldon K, Atkins GJ, Howie DW, Zannettino ACW and Bobyn D (2004), 'The proliferation and phenotypic expression of human osteoblasts on tantalum

metal', *Biomaterials*, **25**, 2215.
Furlong RJ and Osborn JF (1991), 'Fixation of hip prostheses by hydroxyapatite ceramic coatings', *J Bone Joint Surg*, **73B**, 741–745.
Gallant D, Pezolet M and Simard S (2006), 'Optical and physical properties of cobalt oxide films electrogenerated in bicarbonate aqueous media', *J Phys Chem B*, **110**, 6871–6880.
Geesink RGT (1989), 'Experimental and clinical experience with hydroxyapatite-coated hip implants', *Orthopedics*, **12**, 1239–1242.
Hirschhorn J, McBeath A and Dustoor M (1971), 'Porous titanium surgical implant materials', *J Biomed Mater Res Symp*, **2**, 49–67.
Kearns SR, Jamal B, Rorabeck CH and Bourne RB (2006), 'Factors affecting survival of uncemented total hip arthroplasty in patients 50 years or younger', *Clin Orthop Relat Res,* **453**, 103–109.
Korovessis P, Petsinis G and Repanti M (2002), 'Short-term results with the Zweymueller-SL metal-on-metal and other cementless total hip arthroplasty', *Arch Orthop Trauma Surg*, **122**, 283.
Kovacs P and Davidson JA (1993), 'The electrochemical behavior of a new titanium alloy with superior biocompatibility', in *Titanium'92 Science and Technology*, The Minerals, Metals & Materials Society, 2705–2712.
Kuroda D, Niinomi M, Morinaga M, Kato Y and Yashiro T (1998), 'Design and mechanical properties of new β type titanium alloys for implant materials', *Mater Sci Eng A*, **243**, 244–249.
Kurtz SM and Devine JN (2007), 'PEEK biomaterials in trauma, orthopedic, and spinal implants', *Biomaterials*, **28**, 4845–4869.
Larsson C, Thomsen P, Aronsson BO, Rodahl M, Lausmaa J, Kasemo B and Ericson LE (1996), 'Bone response to surface-modified titanium implants: studies on the early tissue response to machined and electropolished implants with different oxide thicknesses', *Biomaterials*, **17**, 605–616.
Lee JE, Heo SJ, Koak JY, Kim SK, Han CH and Lee SJ (2009), 'Healing response of cortical and cancellous bone around titanium implants', *Int J Oral Maxillofac Implants*, **24**, 655–662.
Liu C, Bi Q and Matthews A (2003), 'Tribological and electrochemical performance of PVD TiN coatings the femoral head of Ti-6Al-4V artificial joints', *Surf Coat Technol*, **163–164**, 597–604.
Long M and Rack HJ (1998), 'Titanium alloys in total joint replacement – a materials science perspective', *Biomaterials*, **19**, 1621–1639.
McCafferty E (2002), 'Oxide networks, graph theory, and the passivity of binary alloys', *Corrosion Sci*, **44**, 1393–1409.
McLaughlin JR and Lee KR (1997), 'Total hip arthroplasty with an uncemented femoral component. Excellent results at ten-year follow-up', *J Bone Joint Surg Br*, **79**, 900–907.
McNamarta BP, Murphy H and Morshed MM (2001), 'Adhesion properties of diamond-like coated orthopaedic biomaterials', *Diamond Rel Mater*, **10**, 1098–1102.
Mishra AK, Davidson JA, Kovacs P and Poggie RA (1993), 'Ti-13Nb-13Zr: a new low modulus, high strength, corrosion resistant near-beta alloy for orthopaedic implants', in *Beta Titanium in the 1990's*, The Minerals, Metals & Materials Society, 61–72.
Nelissen RGHH, Valstar ER and Rozing PM (1998), 'The effect of hydroxyapatite on the micromotion of total knee prostheses. A prospective, randomized, double-blind study', *J Bone Joint Surg*, **80A**, 1665–1672.

Niinomi M (1998), 'Mechanical properties of biomedical titanium alloys', *Mater Sci Eng A*, **243**, 231–236.

Oh SH, Finõnes RR, Daraio C, Chen LH and Jin S (2005), 'Growth of nano-scale hydroxyapatite using chemically treated titanium oxide nanotubes', *Biomaterials*, **26**, 4938–4943.

Okazaki Y, Ito Y, Ito A and Tateishi T (1993), 'Effect of alloying elements on mechanical properties of titanium alloys for medical implants', *Mater Trans JIM*, **34**, 1217–1222.

Okazaki Y, Ito Y, Kyo K and Tateishi T (1996), 'Corrosion resistance and corrosion fatigue strength of new titanium alloys for medical implants without V and Al', *Mater Sci Eng A*, **213**, 138–147.

Platon F, Fournier P and Rouxel S (2001), 'Tribological behaviour of DLC coatings compared to different materials used in hip joint prostheses', *Wear*, **250**, 227–236.

Reclaru L, Eschler PY, Lerf R and Blatter A (2005), 'Electrochemical corrosion and metal ion release from Co-Cr-Mo prosthesis with titanium plasma spray coating', *Biomaterials*, **26**, 747–756.

Roynesdal AK, Ambjornsen E, Stovne S and Haanas HR (1998), 'A comparative clinical study of three different endosseous implants in edentulous mandibles', *Int J Oral Maxillofac Implants*, **13**, 500–505.

Ryan G, Pandit A and Apatsidis DP (2006), 'Fabrication methods of porous materials for use in orthopaedic applications', *Biomaterials*, **27**, 2651–2670.

Semlitsch MF, Weber H, Streicher RM and Schon R (1992), 'Joint replacement components made of hot-forged and surface-treated Ti-6Al-7Nb alloy', *Biomaterials*, **13**, 781–788.

Shin D, Arps JH, Sylvia VL and Dean DD (2005), 'Osteoblast response to changes in titanium oxide nanostructure and morphology', *J Dent Res*, **84(A)**, 3–9.

Sittig C, Textor M, Spencer ND, Wieland M and Vallotton PH (1999), 'Characterization of implant materials c.p. Ti, Ti-6Al-7Nb and Ti-6Al-4V with different pretreatments', *J Mater Sci: Mater Med*, **10**, 35–46.

Spriano S, Vernè E, Faga MG, Bugliosi S and Maina G (2005), 'Surface treatment on an implant cobalt alloy for high biocompatibility and wear resistance', *Wear*, **259**, 919–925.

Steingemann SG, Mausli PA, Szmukler-Moncler S, Semlitsch M, Pohler O, Hintermann HE and Perren SM (1993), 'Beta-titanium alloy for surgical implants', in *Titanium'92 Science and Technology*, The Minerals, Metals & Materials Society, 2689–2696.

Stephenson PK, Freeman MA, Revell PA, Germain J, Tuke M and Pirie CJ (1991), 'The effect of hydroxyapatite coating on ingrowth of bone into cavities in an implant', *J Arthroplasty*, **6**, 51–58.

Sun L, Berndt CC, Gross KA, Kucuk A (2001), 'Material fundamentals and clinical performance of plasma-sprayed hydroxyapatite coatings: a review', *J Appl Biomater*, **58**, 570–592.

Survilienė S, Jasulaitienė V, Češūnienė A and Lisowska-Oleksiak A (2008), 'The use of XPS for study of the surface layers of Cr–Co alloy electrodeposited from Cr(III) formate–urea baths', *Solid State Ionics*, **179**, 222–227.

Textor M, Sittig C, Frauchiger V and Tosatti S (2001), 'Properties and biological significance of natural oxide films on titanium and its alloys', in Brunette DM, Tengvall P, Textor M and Thomsen P, *Titanium in Medicine, Material Science, Surface Science, Engineering, Biological Responses and Medical Applications*, Springer, 171–230.

Wang K, Gustavson L and Dumbleton J (1993a), 'The characterization of Ti12Mo6Zr2Fe. A new biocompatible titanium alloy developed for surgical implants', in *Beta Titanium in the 1990's*, The Minerals, Metals & Materials Society, 49–60.

Wang K, Gustavson L and Dumbleton J (1993b), 'Low modulus, high strength, biocompatible titanium alloy for medical implants', in *Titanium'92 Science and Technology*, The Minerals, Metals & Materials Society, 2697–2704.

Wapner KL (1991), 'Implication of metallic corrosion in total knee arthoroplasty', *Clin Orthop*, **271**, 12–20.

Windler M and Klabunde R (2001), 'Titanium for hip and knee protheses', in Brunette DM, Tengvall P, Textor M and Thomsen P, *Titanium in Medicine, Material Science, Surface Science, Engineering, Biological Responses and Medical Applications*, Springer, 703–746.

Wolfarth D and Ducheyne P (1994), 'Effect of a change in interfacial geometry on the fatigue strength of porous-coated Ti-6A1-4V', *J Biomed Mater Res*, **28**, 417–425.

Yang B, Uchida M, Kim HM, Zhang X and Kokubo T (2004), 'Preparation of bioactive titanium metal via anodic oxidation treatment', *Biomaterials*, **25**, 1003–1010.

Yao C and Webster TJ (2006), 'Anodization: a promising nano-modification technique of titanium implants for orthopedic applications', *J Nanosci Nanotechnol*, **6**, 2682–2692.

Yao C, Slamovich EB and Webster TJ (2008), 'Enhanced osteoblast functions on anodized titanium with nanotube-like structures', *J Biomed Mater Res A*, **85**, 157–166.

Zenz P, Pospisil C, Fertschak W and Schwägerl W (1995), '10 years of cementless implantation of total hip endoprosthesis using Zweymüller's stem', *Z Orthop Ihre Grenzgeb*, **133**, 558–561.

Zhang H, Krajewski J, Zhang Z, Masopust M and Xiao DT (2007), 'Nano-hydroxyapatite coated femoral stem implant by electrophoretic deposition', *MRS Symposium Proc*, **975**, 58–63.

3

Polymeric joint bearing surfaces for total joint replacements

E. ORAL, Massachusetts General Hospital/Harvard Medical School, USA

Abstract: Ultrahigh molecular weight polyethylene (UHMWPE) is the polymeric component of hard-on-soft joint replacement implants. This chapter includes an overview of the rationale behind its development, *in vitro* and *in vivo* characterization methods and reasons for failure.

Key words: artificial joints, metal-on-polyethylene, wear, fatigue resistance, vitamin E.

3.1 Introduction

Ultrahigh molecular weight polyethylene (UHMWPE) has been the material of choice for total joint replacements as a part of a 'hard-on-soft' articulation couple since its introduction by Sir John Charnley in the 1960s (Charnley, 1961). Total joint replacement is the most common treatment for end-stage arthritis, which leads to the degradation of bone and cartilage of the joints and results in severe pain and the loss of function of the joints. In the US alone, 46 million people suffer from arthritis (Helmick *et al.*, 2008), about 80% of which is osteoarthritis. Techniques to treat cartilage damage in its early stages are being developed vigorously, including microfracture, osteochondral autograft transplantation (OATS), autologous cartilage implantation (ACI) and mosaicplasty (Hunziker, 2002). The goal of these treatments is to minimize pain, maximize function for the patients and protect undamaged cartilage to delay the need for more invasive surgery such as total joint replacement.

Nevertheless, the total joint replacement operation is considered one of the most successful of our time with Kaplan–Meier implant survival rates of over 80% at 10 years (Murray *et al.*, 1993). It is projected that 1.5 million people in the US alone will undergo hip and knee joint replacement in 2015 (Kurtz *et al.*, 2007). However, after the first decade of service, the survival rates decline, and many patients are required to undergo a revision surgery where part or all of the implant is replaced with a new one. Revision surgery is costly (~50% more than primary surgery) (Bozic *et al.*, 2009) and often very complicated. There is a continual need to reduce the number of revision surgeries to improve the

patients' quality of life as well as the economic burden placed by these operations on the healthcare system.

What are the factors that make implants vulnerable to failure? How can revision rates be decreased? Clinical outcomes of joint arthroplasty operations are dependent on many different factors including the total volume of operations performed by the surgeon, patient variables such as age, weight, bone quality, gender and activity, design parameters of the implant and the material properties. The lack of a widespread registry in the US has precluded the elucidation of the relative importance of some of these factors. Nevertheless, from the available data, it is clear that joint dislocation, implant loosening, peri-prosthetic osteolysis and fractures are some major occurrences requiring the revision of joint implants (Bozic *et al.*, 2009). In the recent years, there have been a surge of technologies involving material development because wear particles associated with articulating surfaces are one problem clearly associated with bone resorption and implant loosening and minimizing wear has been a clear solution. This chapter will focus on UHMWPE and its development as a joint replacement material from this perspective but it is important to keep in mind that clinical outcomes are dependent on a complicated set of factors only one of which is the material.

3.2 Early development of joint bearing couples

There were attempts at repairing damaged joint surfaces by placing materials such as wood in between the joint surfaces in the 1800s, but the first real joint replacement is credited to Smith-Petersen and his mold arthroplasty in 1923, which involved covering the debrided joint surfaces with molds to allow for natural repair of the joint (Smith-Petersen, 1948). He used glass, reinforced glass and other materials such as Formica as interpositional devices. In 1939, a cobalt–chromium alloy called Vitallium was introduced for mold arthroplasty (Venable *et al.*, 1937). An alternative design was the short-stem prosthesis, where the femoral head replacement material was augmented by a short stem fixed into the femur for added stability. Such prostheses were made of polymethylmethacrylate (PMMA) (Judet and Judet, 1950), which was later replaced by cobalt–chromium alloys (Thomson, 1952). Short-stem prostheses were followed by long-stem prostheses, where the length of the intermedullary stem was increased for added stability under weight-bearing conditions (Moore and Bohlman, 1943). The first *total* joint arthroplasty is credited to Wiles in 1938 (Wiles, 1957), where he used a stainless steel ball articulating against a stainless steel acetabular cup. A similar design made of cobalt–chromium designed by McKee and Farrar was the next generation of arthroplasty device overcoming the *in vivo* corrosion observed with stainless steel and decreasing the impingement of the femoral neck on the acetabular rim (McKee and Watson-Farrar, 1966).

The use of acrylic dental bone cement to fix implants to bone reduced loosening of implants and the introduction of a plastic acetabular component to reduce frictional forces in the joint by Charnley revolutionized total joint arthroplasty (Charnley, 1961). Charnley first started using polytetrafluoroethylene (PTFE) but replaced it with UHMWPE due to high wear and catastrophic failures (Charnley, 1963). He called the material he used high density polyethylene (HDPE) at the time because UHMWPE was classified among the HDPEs at the time (Kurtz, 2009c), but it was nevertheless an ultrahigh molecular weight polymer and was more wear resistant (Charnley and Cupic, 1973). Thus, the use of UHMWPE as a joint bearing surface material was initiated.

3.3 Ultrahigh molecular weight polyethylene (UHMWPE)

3.3.1 Structure and properties

UHMWPE is a linear polyolefin with a simple structure ($-[CH_2]_n-$) of a saturated carbon backbone. While polyethylenes can come in a variety of forms based mostly on their molecular weight and branch structure (very low density, linear low density, low density, high density and ultrahigh molecular weight), the molecular weight and linearity of UHMWPE render its morphology and its mechanical/tribological properties interesting. They also present some challenges in its processing and life as a long-term implantable medical device.

UHMWPE is a semicrystalline matrix embedded in an amorphous matrix (Fig. 3.1) with 70–80% crystallinity in resin powder form and 50–60% crystallinity in consolidated form (Table 3.1). When crystallized from the melt at ambient pressures, it has an orthorhombic folded chain crystal structure (crystal unit parameters $a = 7.4$ Å, $b = 4.93$ Å, $c = 2.534$ Å; Bunn, 1939) and crystalline lamellae thickness is approximately 10–50 nm. At room temperature, UHMWPE is well above its glass transition temperature, where the mobility of its chains is enhanced. The mobility of the chains in the crystalline phase can be further enhanced by crystallization at high temperature and pressure (>160 ºC, >300 MPa), where it can grow chain-extended crystals in the hexagonal phase ($a = 8.46$ Å, $b = 4.88$ Å; Bassett and Turner, 1972; Bassett *et al.*, 1974; Wunderlich and Arakawa, 1964). In this phase, the lamellae can grow as thick as several microns (Geil *et al.*, 1964).

The mechanical properties of UHMWPE are strongly dependent on its crystallinity and semicrystalline morphology. The tie-chains between crystalline lamellae (Fig. 3.1) can span a very large distance and multiple lamellae, thus making it a very strongly entangled network. Increasing crystallinity results in increased yield strength and ultimate tensile strength (Brooks *et al.*, 1999; Turell and Bellare, 2004; Simis *et al.*, 2006). High yield strength is combined with a

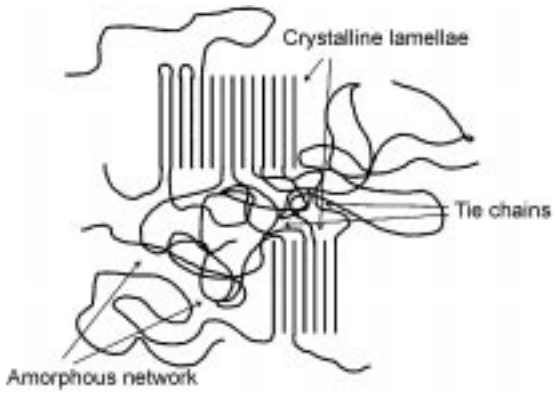

3.1 Semicrystalline morphology of UHMWPE.

high elongation-at-break, which results in increased resistance against fatigue, a clinically relevant deformation mode (Bartel *et al.*, 1986). While the ability of UHMWPE to deform plastically to a large extent leads to high impact and fatigue resistance, it causes wear under multidirectional shear, another clinically relevant loading mode. The orientation of the material in the principal direction of motion weakens the material in the transverse direction (Zhang *et al.*, 2004; Kurtz *et al.*, 2006) and particle breakup is thought to occur when the material is loaded in directions other than the principal orientation direction (Jasty *et al.*, 1997; Fig. 3.2).

Ticona is currently the only producer of medical grade UHMWPE resins (GUR1020 and GUR1050) used by the orthopedic industry to manufacture implants. The history of this resin can be traced in the same company back to the original commercialization of the polymerization of UHMWPE in the 1950s. The consolidation of the resin is performed at either converter companies or at the orthopedic manufacturer.

Table 3.1 Physical and chemical properties of consolidated medical grade UHMWPE

Molecular weight (g/mol)	2–6 million
Density (g/cm^3)	0.92–0.95
Crystallinity (%)	50–60
Glass transition temperature (°C)	~ -160
Melting temperature range (°C)	100–150
Peak melting temperature (°C)	133–137
Elastic modulus (GPa)	1–2
Yield strength (MPa)	$\sim$20
Ultimate tensile strength (MPa)	$\sim$60
Elongation at break (%)	350–500

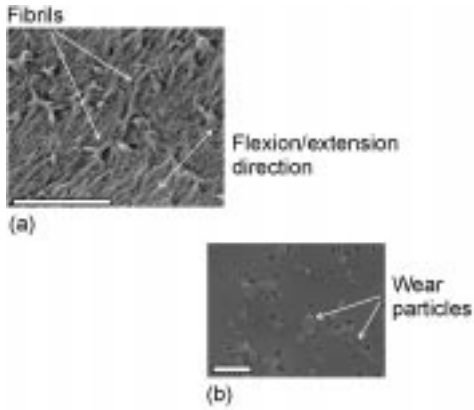

3.2 Orientation on the articular surface of a UHMWPE acetabular liner after retrieval from the patient (scale bar represents 10 μm) (a) and UHMWPE wear particles after being isolated from bovine serum used in hip simulator wear testing of gamma sterilized UHMWPE (scale bar represents 1 μm) (b).

3.3.2 Processing

When temperature is increased above the melting temperature, UHMWPE simply turns from opaque to translucent, but its melt flow rate (MFR) is extremely low, which means that for all practical purposes it behaves as a solid in the melt state. For this reason, traditional polymer processing techniques such as injection molding or screw extrusion are not feasible for processing UHMWPE resin into consolidated form for implant manufacturing. Most commonly, UHMWPE is processed through slab compression molding of powder or using extrusion by impaction with a ram (Kurtz, 2009a). In both cases, high temperatures and high pressures are used to enhance the diffusion of the long polymer chains and the effective fusion of the resin powder. The processing time as well as the cooling (recrystallization) rate can make significant differences to the resultant properties of the material. There are specifications for the properties of consolidated UHMWPE for use in surgical implants (ASTM, 2009).

Implants can be manufactured by machining from UHMWPE stock material consolidated by compression molding or ram extrusion or they can be direct compression molded to the desired implant shape. While the latter offers a single-step process, the effects of any additional processing such as sterilization or crosslinking on the manufacturing tolerances may be significant.

A recent development in the manufacture of polyethylene implant components is the use of antioxidants. Despite the pervasive use of antioxidants in other applications using polyethylene such as food packaging, this was carefully avoided in medical-grade polyethylene mainly due to the fusion defects and sporadic oxidation attributed to the presence of calcium stearate in the past

(Blunn *et al.*, 1997). However, the benefits of using vitamin E, the natural antioxidant in preventing oxidation in polyethylene were demonstrated *in vitro* (see Section 3.4.2) and a vitamin E-containing highly crosslinked UHMWPE was introduced clinically in 2007 (E-Poly^{TM} (now E1), Biomet, Inc.). Therefore, there is a current trend towards using alternative antioxidants and processing conditions in medical-grade UHMWPE; in fact, Ticona has announced a vitamin E-containing GUR UHMWPE resin for use in the medical industry (http://www.ticona.com/home/products/uhmw-pe/gur_uhmw-pe_premium.htm).

3.3.3 *In vitro* characterization methods

Physical characterization

The crystallinity of the polymer is determined by differential scanning calorimetry (DSC). The sample is subjected through a heating cycle, usually at 10 ºC/min. The limits of the run are 0 to 200 ºC and the integration limits are 50–160 ºC (ASTM, 2007). The crystallinity is determined by normalizing the enthalpy of fusion calculated in this manner to that of 100% crystalline UHMWPE. If the limits of integration are extended to 20 ºC, then the crystallinity can increase by approximately 3–5% and care should be taken when comparing results from different sources. As mentioned before, crystallinity can be increased by high pressure crystallizing UHMWPE, which can change its mechanical properties. On the other hand, crystallinity can also increase due to oxidative chain scission and local recrystallization of degraded chains. This crystallinity increase does not result in an increase in mechanical properties because the molecular weight of the polymer is decreased and its network structure is degraded. The DSC thermogram can give important information on crystal populations and crystalline lamellae size as well.

Since the introduction of highly crosslinked UHMWPE (see Section 3.4), methods have been devised to measure the extent of crosslinking in UHMWPE (Muratoglu *et al.*, 1999; ASTM, 2006a, 2008c). These methods are based on the inability of crosslinked UHMWPEs to dissolve in a good solvent such as xylene; gel content of crosslinked UHMWPEs is often above 90%. Instead, they swell until equilibrium is reached and this equilibrium swell ratio can be defined in terms of a crosslink density, the Flory interaction parameter between the polymer and the solvent, and the specific volume of the solvent (Flory, 1953). The measurement is done either by measuring *in situ* linear expansion by contacting a probe with the sample or gravimetrically. A typical crosslink density for highly crosslinked UHMWPE is around 0.170–0.300 mol/dm^3.

Wear

The abundance of UHMWPE wear particles has been linked to peri-prosthetic osteolysis, the resorption of bone around implants (Dumbleton *et al.*, 2002).

Thus, one of the most important *in vitro* validation techniques for UHMWPE materials is wear testing. Pin-on-disk (POD) wear testing is a common comparative method to quantify the wear rate of UHMWPE load-bearing materials (Wang *et al.*, 1998b; Muratoglu *et al.*, 1999; Saikko *et al.*, 2001; ASTM, 2006b). Cylindrical pins machined of UHMWPE are articulated against a smooth counterface disc made out of implant-finish metal, commonly cobalt–chromium alloy (CoCr, Ra ~ 0.05 μm) in a bidirectional path (Bragdon *et al.*, 2001). This motion is especially designed after the hip joint, where the principal arc of motion in the flexion-extension direction is accompanied by transverse motions in the abduction/adduction and internal/external rotation axes at the articulating surface (Ramamurti *et al.*, 1998). Wear is determined gravimetrically as UHMWPE does not absorb significant amounts of testing medium during the 1–2 million cycles over which POD tests are typically performed. The wear rate is calculated as the linear regression of wear against the number of cycles disregarding the first 200 000–500 000 cycles where creep deformation of the pin occurs and surface asperities are eliminated.

To obtain more clinically relevant results, simulators have been designed for wear testing (Scales *et al.*, 1969; Dumbleton *et al.*, 1972; Shaw and Murray, 1973; Walker *et al.*, 1997). Simulators have been designed to match the *in vivo* wear rate, wear debris size and shape of UHMWPE as well as the surface morphology observed in explanted components by replicating *in vivo* attributes such as component positioning, temperature, loading and kinematics of normal gait (Paul, 1966; Johnston and Schmidt, 1969; Bergmann *et al.*, 1993; Ramamurti *et al.*, 1996, 1998), all of which are known to affect the wear rate of UHMWPE. The simulator tests are typically carried out at 1–2 Hz, at 37–40 ºC bovine serum to simulate joint temperature. Wear is assessed gravimetrically and can be measured also by a volumetric method using a coordinate measuring machine, which can measure the three-dimensional shape of the articular surface. When measuring wear volumetrically, creep deformation of UHMWPE has to be separated from wear; this can be done by melting the component after testing is completed as UHMWPE has excellent shape memory and creep deformation can be eliminated by re-melting the component (Muratoglu *et al.*, 2005b). Limitations of simulators are the choice of kinematics, which is usually limited to normal gait kinematics in contrast to a complex variety of activities of daily living. Another factor affecting wear in the simulator is the testing environment. While bovine serum is the accepted analogue for synovial fluid, dilution of bovine serum with water to obtain protein concentrations relevant to *in vivo* conditions is commonly used. However, wear of conventional (gamma sterilized) UHMWPE has been shown to increase with bovine serum dilution (Wang *et al.*, 1998a). At high water concentration, non-physiological wear mechanisms can dominate the wear process (Liao *et al.*, 1999). Other factors that may affect the outcome are surface finish of the metallic counterface, stress levels and loading mode (dynamic vs. constant) (Haider, 2009).

Mechanical properties

In addition to tensile mechanical testing, there are a few mechanical testing methods that are commonly used in assessing the properties of UHMWPEs designed for joint implants. One of these is the so-called small punch test (Kurtz, 1999; ASTM, 2008b) using deformation of small discs of UHMWPE resulting in a load–displacement curve, an ultimate load at failure and a work-to-failure which is calculated as the area under this curve. These can be used to compare materials with different processing history and it has the advantage of using small enough samples to allow mechanical analysis of explanted components (Kurtz *et al.*, 2005), which is not possible by other characterization methods.

There are compressive and shear forces on UHMWPE during articulation, and there may be residual tensile stresses that arise from accumulated stress during repeated load cycles (Sathasivam and Walker, 1998). The reversal of stress direction causes fatigue cracks to initiate causing delamination, especially in total knee implants (Bartel *et al.*, 1986, 1995). Fatigue crack initiation and propagation resistance of UHMWPE is a crucial property for predicting long-term performance of joint implants especially under adverse loading conditions. Fatigue testing is performed in cyclic tension on a compact tension specimen (ASTM, 2008a), which is designed to concentrate applied stress at a notch tip with an existing crack. A stress factor at crack inception (ΔK_i) is calculated as a measure of fatigue crack propagation resistance. This is the stress factor range (dependent on the load ratio, sample geometry and crack length), at which the crack growth rate exceeds 10^{-6} mm/cycle. The ΔK_i of unirradiated UHMWPE is reported as 1.6–2.0 MPa $m^{1/2}$ (Baker *et al.*, 2000; Oral *et al.*, 2009). The temperature at which the testing is performed (25 vs. 40 ºC), the frequency used in the test, testing environment (air vs. water) and the crack initiation method are some factors that account for the variation in the results obtained from different laboratories.

Impact testing is performed by fracturing a double notched Izod impact specimen by contacting with a swinging pendulum and calculating the work-to-fracture (ASTM, 2009).

Oxidative properties

Oxidation in UHMWPE takes place through a cascade of reactions (Fig. 3.3). The macroalkyl/macroallyl radicals in UHMWPE react with oxygen to form peroxy free radicals, which then attack unreacted polymer chains to form hydroperoxides, generating new free radicals which can fuel the oxidative reactions. The thermal decomposition of the hydroperoxides into carbonyl-containing species is accompanied by chain scission and molecular degradation. What is termed ‘oxidation’ in UHMWPE is the amount of detectable carbonyl containing species by vibrational spectroscopy, commonly Fourier transform infrared spectroscopy (FTIR) (ASTM, 2006c). It has been shown that there can be absorbed lipid species in UHMWPE *in vivo* (Costa *et al.*, 2001), some of

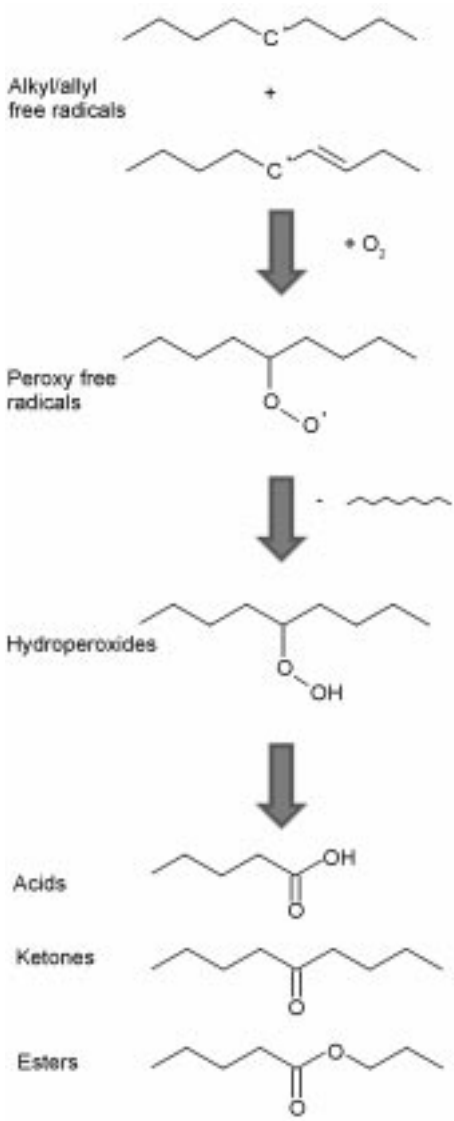

3.3 Oxidation cascade in UHMWPE.

which are esters of cholesterol. These compounds can show up as oxidation in the FTIR analysis of components (James *et al.*, 1993), therefore, oxidation is measured after extraction of extractable species from UHMWPE without changing the morphology of the polymer by a suitable organic solvent with a low boiling point, commonly hexane or heptane.

Although the intermediate hydroperoxides are not detectable by FTIR, they can be stained by nitric oxide gas to give primary nitrates, which can then be

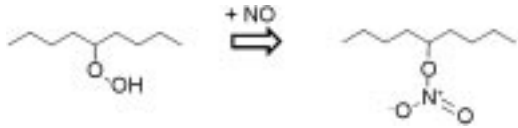

3.4 The staining of hydroperoxides by nitric oxide gas.

detected (Fig. 3.4; Carlsson *et al.*, 1990; Costa *et al.*, 1998). This hydroperoxide index can be interpreted as an oxidation potential since the decomposition of these hydroperoxides will eventually lead to oxidation products.

As mentioned before, free radicals initiate oxidation in UHMWPE. While most free radical species are very mobile and can react or recombine readily, the free radicals induced in the crystalline domains of UHMWPE commonly by radiation (for sterilization or crosslinking) have very low mobility due to the rigidity and spacing between crystalline chains and can persist in UHMWPE for years (Jahan *et al.*, 2001). These free radicals are measured using electron spin resonance (ESR), which can provide insight into the type of free radicals as well as the amount (Jahan, 2009). However, there exists a stable 'oxygen-induced radical' (OIR) in UHMWPE, the structure of which is yet to be determined (Fig. 3.5).

Aging methods

Since most problems associated with UHMWPE have occurred in the second decade of service, the development of methods that can simulate the oxidative

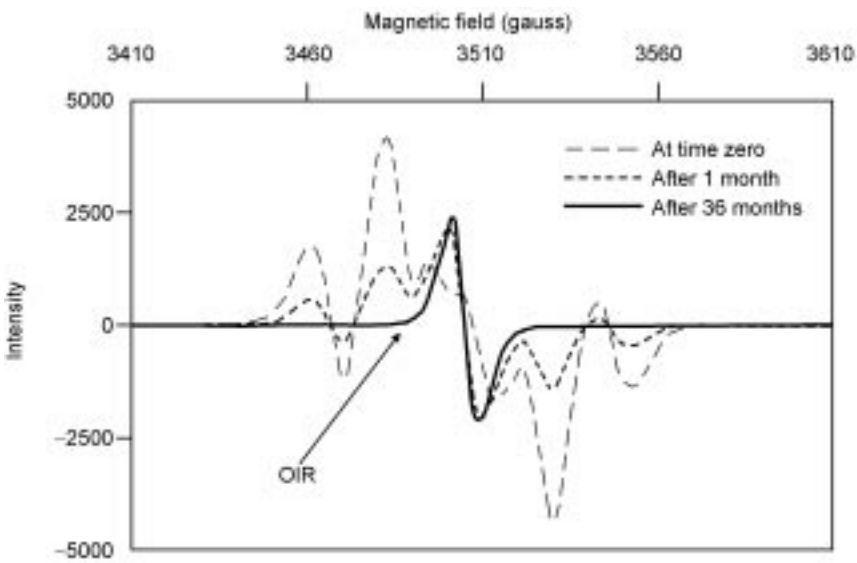

3.5 The free radical signature of 100 kGy irradiated UHMWPE as a function of aging time in water at 40 °C.

changes in UHMWPE materials *in vivo* are crucial to predict the stability of joint implants in the long term. Commonly used accelerated aging techniques involve high temperature and/or high oxygen concentration; for example, 80 ºC in air for 5 weeks or 70 ºC in 5 atm. of oxygen for 2 weeks (Kurtz *et al.*, 1999). Although neither method accurately simulates the subsurface oxidation peaks that are commonly observed in explanted oxidized UHMWPEs, they have nevertheless provided methods to compare the relative oxidative stability of UHMWPEs in development to conventional UHMWPE. However, it appears that the use of antioxidants will necessitate the revision of these aging methods into more aggressive ones as it is very difficult to differentiate between these relatively highly oxidation-resistant UHMWPEs (Rowell *et al.*, 2008).

3.3.4 *In vivo* assessment tools

There are very few methods to measure the performance of total joint implants *in vivo*. *In vivo* penetration (creep and wear) is determined by using two-dimensional or three-dimensional radiographic methods (Dumbleton *et al.*, 2002). The most commonly used radiographic method is the Martell technique (Martell and Berdia, 1997), which uses computer-assisted definition of boundaries and has been adapted to allow 3-D assessment (Hui *et al.*, 2003). A more accurate technique is radiostereometric analysis (RSA), which measures the distance between tantalum beads placed in the implant and in the pelvic bone at implantation to triangulate the exact position of the components *in vivo*. Both of these methods appear to differentiate between the femoral head penetration rates of gamma sterilized conventional UHMWPE liners into the acetabulum from those of highly crosslinked UHMWPE liners (Manning *et al.*, 2005; Digas *et al.*, 2007), which have shown 70–90% reduced in wear in hip simulator studies (McKellop *et al.*, 1999; Muratoglu *et al.*, 2004). It is not clear if these methods will be able to differentiate the *in vivo* performance of different highly crosslinked UHMWPEs with very low wear rates.

3.3.5 Sterilization methods and 'conventional' polyethylene

Gamma irradiation is the preferred method of sterilizing UHMWPE medical implants. Unlike the alternative techniques of gas plasma or ethylene oxide gas sterilization, radiation penetration through components of various thicknesses is not limiting. Typically, a radiation dose of 25–40 kGy is used for sterilization. Historically, gamma sterilization in air was used to sterilize total joint implants until the mid-1990s, when it was widely acknowledged that radiation caused oxidative embrittlement of implants in the long term.

Ionizing radiation induces free radicals by radiolytic cleavage of C–C and C–H bonds on the polymer backbone. Owing to the relative immobility of chains of this high molecular weight polymer, C–C bonds are mostly recombined and

chain scission is not a prevalent phenomenon in UHMWPE. On the other hand, hydrogens have higher mobility than the macroalkyl radicals of the polymer and C–H bonds are not readily recombined. In the amorphous phase, crosslinks between polymer chains are formed by the combination of two free radicals on different chains (H crosslinks) or by the reaction of a macroalkyl radical with a terminal vinyl group (Y crosslinks). On the other hand, the free radicals in the crystalline phase do not undergo recombination but are trapped until they can migrate to the crystalline/amorphous interface. This migration takes a very long time, which is proportional to the thickness of the crystalline lamellae. When the free radicals have escaped the crystalline phase, they can react with diffused oxygen and start a cascade of reactions (Fig. 3.3), which result in the formation of oxidation products and chain scission. Molecular weight degradation due to chain scission and recrystallization of degraded chains results in the deterioration of mechanical properties of the material.

Gamma sterilized UHMWPE is slightly more wear resistant than UHMWPE sterilized without radiation sterilization because even the low dose of irradiation causes some crosslinking in the material, reducing its plasticity (Affatato *et al.*, 2002). However, wear of UHMWPE coupled with the detrimental mechanical degradation resulting from oxidation caused was linked to severe osteolysis and implant loosening (Wroblewski, 1988; Amstutz *et al.*, 1992; Jasty and Smith, 1992; Buechel *et al.*, 1994). Therefore, in the next decade, the focus was on finding methods to minimize wear and oxidation. One method to combat oxidation was gamma sterilization in inert atmosphere. While this eliminates most oxidation on the shelf, the implants oxidized *in vivo*. Also, radiation crosslinking was introduced to decrease wear.

3.4 The introduction of high dose crosslinking

The first highly crosslinked UHMWPEs were used in the 1970s and 1980s in small cohorts of patients (DuPlessis *et al.*, 1977; Oonishi *et al.*, 1992; Wroblewski *et al.*, 1996). The industry-wide acceptance of highly crosslinked UHMWPE came in the late 1990s, when large orthopedic manufacturers started producing highly crosslinked UHMWPEs (Table 3.2).

3.4.1 First generation highly crosslinked UHMWPEs

Radiation crosslinking of UHMWPE was introduced to decrease the wear rate observed with gamma sterilized conventional UHMWPE (Muratoglu *et al.*, 1999), which was associated with the occurrence of osteolysis and implant loosening. Radiation doses ranging from 50 to 100 kGy were used (Table 3.2). Since radiation-induced free radicals were determined to be the cause of oxidation, post-irradiation thermal treatments were used in first generation highly crosslinked UHMWPEs to reduce or eliminate the presence of free radicals. One

Table 3.2 First generation highly crosslinked UHMWPEs

Tradename	Manufacturer	Radiation dose (kGy)	Post-irradiation thermal treatment	Sterilization method
Marathon™	Depuy	50	Melting	Gas plasma
Longevity™	Zimmer	100	Melting	Gas plasma
Crossfire™	Stryker	75	Annealing	Gamma irradiation
Prolong™	Zimmer	65	Melting	Ethylene oxide
Durasul™	Zimmer	95	Melting	Ethylene oxide
XLPE™	Smith & Nephew	100	Melting	Ethylene oxide
ALTRX™	DePuy	75	Melting	Gas plasma

method is melting the crystals to allow the recombination of the trapped free radicals in the crystals. This method eliminates all detectable free radicals (Muratoglu *et al.*, 2001a), but it is detrimental to the mechanical properties and fatigue resistance of UHMWPE (Baker *et al.*, 2003). Radiation crosslinking reduces mechanical properties with increasing radiation dose due to decreased plasticity, and post-irradiation melting decreases these properties further due to the loss of crystallinity during melting (Oral *et al.*, 2006b). This UHMWPE has been in clinical use for over 10 years and has shown good wear resistance *in vivo* up to 5 years (Digas *et al.*, 2007). However, the reduction in fatigue strength of crosslinked UHMWPEs is a concern for increased risk of fracture, especially under adverse loading conditions (Halley *et al.*, 2004; Tower *et al.*, 2007).

In contrast, the mechanical properties of crosslinked UHMWPE are maintained when post-irradiation thermal annealing is used below the melting point. However, annealing below the melting point reduced but did not eliminate the residual free radicals, a problem exacerbated by the terminal gamma sterilization of this first generation highly crosslinked material, which introduced new free radicals. Thus, this material was not resistant to oxidation (Wannomae *et al.*, 2006; Currier *et al.*, 2007).

3.4.2 Second generation highly crosslinked UHMWPEs

Second generation highly crosslinked UHMWPEs (Table 3.3) were developed to overcome the shortcomings of the first generation highly crosslinked UHMWPEs; namely, the low mechanical properties for irradiated and melted UHMWPEs and low oxidation resistance for irradiated and annealed UHMWPE.

The fatigue strength loss due to post-irradiation melting of crosslinked UHMWPE could be eliminated by the introduction of the antioxidant vitamin E into crosslinked UHMWPE (Oral *et al.*, 2004). Vitamin E can be incorporated into UHMWPE by two methods (Fig. 3.6): one is blending of the antioxidant into UHMWPE resin powder followed by consolidation and radiation

Table 3.3 Second generation highly crosslinked UHMWPEs

Tradename	Manufacturer	Radiation dose (kGy)	Post-irradiation treatment	Sterilization method
E-Poly (E1)™	Biomet	100	Vitamin E diffusion	Gamma irradiation
X3™	Stryker	90 (3×30)	Sequential annealing	Gas plasma
ArComXL™	Biomet	50	Mechanical deformation	Gas plasma

crosslinking, the other is the diffusion of the antioxidant into radiation crosslinked UHMWPE. In addition to protecting UHMWPE against oxidation initiated by radiation-induced free radicals (Oral *et al.*, 2004, 2006c), vitamin E reacts with primary free radicals induced on the polymer chains during radiation and prevents crosslinking with increasing concentration (Parth *et al.*, 2002; Oral *et al.*, 2005). In fact, crosslink density reaches a saturation level and at a vitamin E concentration of 0.3 wt% (3000 ppm) or above, it is not possible to crosslink UHMWPE to a level equivalent to that of 100 kGy irradiated virgin UHMWPE (Oral *et al.*, 2008). Therefore, if blending followed by radiation crosslinking is to be used, the antioxidant concentration and the radiation dose have to be carefully optimized to obtain good wear resistance and enough vitamin E to protect the UHMWPE against oxidation in the long term. The vitamin E-containing UHMWPE currently in clinical use (introduced in hips in 2007 and in knees in 2008) is prepared by post-irradiation diffusion of vitamin E using a two-step doping and homogenization process to ensure the penetration of vitamin E throughout the entire thickness of components (Oral *et al.*, 2007). This material has a uniform vitamin E concentration profile.

Vitamin E-stabilized, highly crosslinked UHMWPE has about 35% more fatigue resistance than irradiated and melted UHMWPE due to the elimination

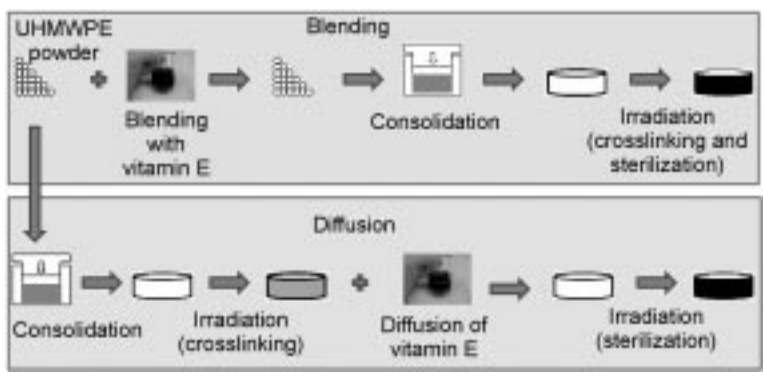

3.6 Vitamin E incorporation methods in highly crosslinked UHMWPE.

of the crystallinity loss during post-irradiation melting (Oral *et al.*, 2006a). Its crosslink density is comparable to that of 100 kGy irradiated and melted UHMWPE; thus wear resistance is comparable as well (Oral *et al.*, 2006a).

Another second generation method introduced in crosslinked UHMWPE was sequential irradiation and annealing. This material is irradiated at 30 kGy and subsequently annealed below the melting point and this process is repeated three consecutive times. The rationale for using this approach was to enhance chain mobility during thermal annealing by using lower doses of irradiation at a time and eliminate free radicals more efficiently. The terminal gamma sterilization was replaced by gas plasma sterilization so as not to induce new free radicals. While *in vitro* wear resistance is high, the free radical concentration of X3™ is low but still detectable at a level comparable to that of conventional, gamma sterilized UHMWPE (Wang *et al.*, 2006). It is too early to determine what the effect of these free radicals will be on the long-term performance of this material as a joint bearing surface.

Another second generation UHMWPE was ArComXL™, which was prepared by solid-state deformation following radiation crosslinking. The manufacturer states that the tensile mechanical properties of the material are 30% improved in a directional manner. This material also had 90% less free radicals than control UHMWPE (Kurtz *et al.*, 2006) as mechanical deformation is known to also induce mobility in the crystalline lamellae and enhance free radical recombination (Muratoglu *et al.*, 2005a). It showed high oxidation resistance after accelerated aging for 4 weeks, while conventional UHMWPE oxidized heavily.

The clinical introduction of these second generation crosslinked UHMWPEs is based on the promise that they can improve the longevity of joint implants by obtaining wear, oxidation and fatigue resistance simultaneously. There is a continued effort in the community to improve the material properties to make it more forgiving under more demanding conditions. This is especially important as more young and active patients (age < 60) are undergoing total joint replacement with the expectation of full functionality and long implant life.

As much as we, orthopedic researchers, would like to believe new materials will solve more problems associated with the outcomes of total joint replacement, some material modifications in UHMWPE have led to clinical failures. I briefly discuss these in the next section.

3.5 Failures in material development

3.5.1 PTFE

Dr Charnley's rationale for using PTFE as part of the joint bearing couple was to minimize friction between the articular surfaces. However, surprisingly, PTFE showed tremendously high wear rate with most implants having to be revised within a couple of years (Charnley, 1963). Similarly, modifications of PTFE

such as glass-filled PTFE resulted in similar wear rates (Kurtz, 2009b). To date, there have been attempts at decreasing the wear of joint implants by decreasing friction, but the relationship is yet to be established.

3.5.2 Carbon fiber-reinforced UHMWPE (Poly II™)

PolyII™ was a carbon fiber-reinforced UHMWPE composite, whose development was based on improved wear properties of the composite. However, the material was a clinical failure (Wright *et al.*, 1988) due presumably to the lack of integrity of the carbon fiber–polymer matrix interface under load among other factors (Connelly *et al.*, 1984).

3.5.3 Highly crystalline UHMWPE (Hylamer™)

Hylamer™ was a highly crystalline UHMWPE with extended chain morphology and increased yield and ultimate tensile strength as well as a higher elastic modulus. Although *in vitro* wear tests initially showed wear behavior similar to conventional gamma sterilized UHMWPE (McKellop *et al.*, 2000), clinical revision rates due to excessive wear were very high (Chmell *et al.*, 1996; Livingston *et al.*, 1997). One reason could have been oxidation caused by gamma irradiation and the possibly more severe effects of oxidation on this highly crystalline material compared to conventional UHMWPE (Collier *et al.*, 1998). Hylamer was gamma sterilized in air for a period of time, after which it was gamma sterilized in nitrogen and after 1995, it was sterilized using gas plasma. Although the reasons remain unclear, it appeared that the clinical performance of Hylamer™ was not an improvement over that of conventional UHMWPE and the use of it was discontinued in 1997.

3.6 Joint-specific challenges and alternatives

3.6.1 Hip

A prevalent reason for revision surgery is dislocation of the implant in total hip implants (22.5%; Bozic *et al.*, 2009). Typically, larger femoral head sizes are used to improve the stability of the joint and reduce dislocation rates. While this is one of the main advantages of using metal-on-metal or ceramic-on-ceramic implants, this presented a problem with conventional UHMWPE because the wear rate was significantly increased with increasing head size (Livermore *et al.*, 1990). However, highly crosslinked UHMWPE wear appears to be largely independent of femoral head size, possibly allowing the use of thinner UHMWPE liners (Muratoglu *et al.*, 2001b). This presents a new challenge, as the use of thin liners increases the risk of fracture in these liners and improving the fatigue and mechanical properties become essential.

As younger patients require joint replacements, hip resurfacing is becoming more popular (Daniel *et al.*, 2004) due to the conservation of bone stock and the potential reduction rate in dislocation. The improvement of the mechanical properties of highly crosslinked UHMWPEs may present a feasible UHMWPE to be used in this more demanding application.

3.6.2 Knee

Fatigue-induced delamination wear is a major concern in total knees. The lower fatigue resistance of highly crosslinked UHMWPEs compared with unoxidized conventional UHMWPE is more of a concern due to increased contact stresses in the knee. This can be especially important for adverse cases such as cam impingement of the post, which is a geometrical design feature in some total knee implants to provide stability to the joint in the absence of a posterior cruciate ligament. Highly crosslinked UHMWPEs have been used in the knee for close to a decade and there is growing interest in them (Durasul™, Zimmer since 2001, Prolong™, Zimmer since 2002, X3™, Stryker since 2005, XLK™, DePuy since 2005, XLPE™, Smith and Nephew since 2008 and E-Poly™, Biomet since 2008), but there are currently no clinical studies reporting on their performance.

3.6.3 Spine

I have discussed the development of UHMWPE mainly in total hip and knee replacements because these large volume operations and the patient outcomes associated with them have been the driving force behind these developments. At the same time, the same articular pair, cobalt–chromium against UHMWPE, is used in the replacement of other joints. Most notably, two aritifical discs (CHARITÉ and ProDisc), which are used in total (intervertebral) disc replacement (CHARITÉ was discontinued as of March 2010 and will be replaced by In Motion, DePuy Spine) have been approved for single level replacement in the US in 2004 and there are several others in development (Kurtz, 2006). The driving force behind this development was the belief that 'dynamic stabilization' of the vertebrae following the degeneration of the supporting disc would perform better functionally than the fusion of the adjacent segments, the most common alternative.

The total disc replacement operation is relatively new and the interpretation of its outcomes is complex as the problems surrounding the spine are less well established especially in the presence of a synthetic device. The expected benefit of these devices is the reduction in the operation rate at the adjacent levels, which is known to be a progression associated with fusion (Lee, 1988).

One concern in spine implants is the use of conventional, gamma sterilized UHMWPE based on the long history of the occurrence of wear and oxidation of

this in materials in total hip and knee implants. A recent study analyzing total disc implants with up to 16 years' *in vivo* service has found significantly increased penetration rates with increasing implantation time (Kurtz *et al.*, 2008).

3.7 Future trends

Despite some problems, total joint arthoplasty is one of the most successful medical operations with low mortality and high functional outcomes. It is also the only feasible option for patients with end-stage arthritis. Today, joint replacement operations are increasing at a fast pace and the average of the patients is decreasing (Kurtz *et al.*, 2007). There is more demand than ever on the performance of the materials.

It appears that crosslinked UHMWPEs are gaining more acceptance clinically as they finish their first decade of service because of the clearly superior wear resistance provided by crosslinking. If the additional concerns involving the mechanical properties and oxidation resistance of these materials are addressed satisfactorily, then UHMWPE offers benefits over alternative hard-on-hard bearing couples, which suffer from their own associated problems such as metal hypersensitivity (Willert *et al.*, 2005; Daniel *et al.*, 2006; Jacobs and Hallab, 2006), aseptic lymphocyte-dominated vasculitis-associated lesion (ALVAL) (Counsell *et al.*, 2008), pseudotumors (Pandit *et al.*, 2008) for metal-on-metal implants and squeaking (Jarrett *et al.*, 2009) and fracture (Park *et al.*, 2006; Rahaman *et al.*, 2007) for ceramic-on-ceramic implants.

Aside from the surgeons', researchers' and manufacturers' views of successful materials for total joint replacement, economics also plays an important role, especially when complicated payment plans are involved as in the US. Implant 'average selling price' has increased 135% from 1996 to 2007 (*Orthopaedic Network News*, 2009). In 2009, total hip implants pairing uncoated femurs with polyethylene liners were listed at $9989, coated femurs and polyethylene liners were listed at $12 433 compared with $13 843 for metal-on-metal implants and $13 112 for ceramic-on-ceramic implants. Implant list prices have increased substantially, which may be partly due to increased costs of implant manufacture, but the cost of making UHMWPE implants remains less than the alternative hard-on-hard bearings.

3.8 References

Affatato, S., Bersaglia, G., Foltran, I., Taddei, P., Fini, G. & Toni, A. (2002) The performance of gamma- and EtO-sterilised UHWMPE acetabular cups tested under severe simulator conditions. Part 1: role of the third-body wear process. *Biomaterials*, **23**, 4839–4846.

Amstutz, H., Campbell, P., Kossovsky, N. & Clarke, I. (1992) Mechanism and clinical significance of wear debris-induced osteolysis. *Clin Orthop*, **276**, 7–18.

ASTM (2006a) D2765-01 Standard test method for determination of gel content and swell ratio of crosslinked ethylene plastics. West Conshohocken, PA, ASTM International.

ASTM (2006b) F732-00 Standard test method for wear testing of polymeric materials used in total joint prostheses. West Conshohocken, PA, ASTM International.

ASTM (2006c) F2102 – 06e1 Standard guide for evaluating the extent of oxidation in ultra-high-molecular-weight polyethylene fabricated forms intended for surgical implants, West Conshohocken, PA, ASTM International.

ASTM (2007) F2625-07 Standard test method for measurement of enthalpy of fusion, percent crystallinity, and melting point of UHMWPE by means of differential scanning calorimetry. West Conshohocken, PA, ASTM International.

ASTM (2008a) E647-08 Standard test method for measurement of fatigue crack growth rates. West Conshohocken, PA, ASTM International.

ASTM (2008b) F2183-02 Standard test method for small punch testing of UHMWPE used in surgical implants. West Conshohoken, PA, ASTM International.

ASTM (2008c) F2214-02 Standard test method for in situ determination of network parameters of crosslinked UHMWPE. West Conshohocken, PA, ASTM International.

ASTM (2009) F648-07 Standard specification for UHMWPE powder and fabricated form for surgical implants. West Conshohocken, PA, ASTM International.

Baker, D. A., Hastings, R. S. & Pruitt, L. (2000) Compression and tension fatigue resistance of medical grade ultra high molecular weight polyethylene: the effect of morphology, sterilization, aging and temperature. *Polymer*, **41**, 795–808.

Baker, D. A., Bellare, A. & Pruitt, L. (2003) The effect of degree of crosslinking on the fatigue crack initiation and propagation resistance of orthopedic-grade polyethylene. *J Biomed Mater Res*, **66A**, 146–154.

Bartel, D. L., Bicknell, V. L. & Wright, T. M. (1986) The effect of conformity, thickness, and material on stresses in ultra-high molecular weight components for total joint replacement. *J Bone Joint Surg (Am)*, **68**, 1041–51.

Bartel, D. L., Rawlinson, J. J., Burstein, A. H., Ranawat, C. S. & Flynn, W. F. (1995) Stresses in polyethylene components of contemporary total knee replacements. *Clin Orthop Rel Res*, **317**, 76–82.

Bassett, D. & Turner, B. (1972) New high-pressure phase in chain-extended crystallization of polyethylene. *Nature Phys Sci*, **240**, 146–148.

Bassett, D. C., Block, S. & Piermarini, G. (1974) A high-pressure phase of polyethylene and chain-extended growth. *J Appl Phys*, **45**, 4145.

Bergmann, G., Graichen, F. & Rohlmann, A. (1993) Hip joint loading during walking and running, measured in two patients. *J Biomechanics*, **26**, 969–990.

Blunn, G. W., Joshi, A. B., Minns, R. J., Lidgren, L., Lilley, L., Ryd, L., Engelbrecht, E. & Walker, P. S. (1997) Wear in retrieved condylar knee arthroplasties: a comparison of wear in different designs of 280 retrieved condylar knee prostheses. *J Arthroplasty*, **12**, 281–290.

Bozic, K., Kurtz, S., Lau, E., Ong, K., Vail, T. & Berry, D. (2009) The epidemiology of revision total hip arthroplasty in the United States. *J Bone Joint Surg*, **91**, 128–133.

Bragdon, C. R., O'Connor, D. O., Lowenstein, J. D., Jasty, M., Biggs, S. A. & Harris, W. H. (2001) A new pin-on-disk wear testing method for simulating wear of polyethylene on cobalt–chrome alloy in total hip arthroplasty. *J Arthroplasty*, **16**, 658–665.

Brooks, N., Duckett, R. & Ward, I. (1999) Effects of crystallinity and stress state on the yield strain of polyethylene. *Polymer*, **40**, 7367–7372.

Buechel, F. F., Drucker, D., Jasty, M., Jiranek, W. & Harris, W. H. (1994) Osteolysis around uncemented acetabular components of cobalt-chrome surface replacement hip arthroplasty. *Clin Orthopaed Rel Res*, 202–211.

Bunn, C. (1939) The crystal structure of long-chain normal paraffin hydrocarbons. The 'shape' of the CH_2 group. *Trans Faraday Soc*, **35**(1), 482–491.

Carlsson, D., Chmela, S. & Lacoste, J. (1990) On the structures and yields of the first peroxyl radicals in γ-irradiated polyolefins. *Macromolecules*, **23**, 4934–4938.

Charnley, J. (1961) Arthroplasty of the hip: a new operation. *Lancet*, **1**, 1129–1132.

Charnley, J. (1963) Tissue reactions to polytetrafluorethylene [letter]. *Lancet*, **2**, 1379.

Charnley, J. & Cupic, Z. (1973) The nine and ten year results of the low-friction arthroplasty of the hip. *Clin Orthop*, **95**, 9–25.

Chmell, M. J., Poss, R., Thomas, W. H. & Sledge, C. (1996) Early failure of Hylamer acetabular inserts due to eccentric failure. *J Arthroplasty*, **11**, 351–353.

Collier, J., Bargmann, L., Currier, B., Mayor, M., Currier, J. & Bargmann, B. (1998) An analysis of Hylamer and polyethylene bearings from retrieved acetabular components. *Orthopaedics*, **21**, 865–871.

Connelly, G., Rimnac, C., Wright, T., Hertzberg, R. & Manson, J. (1984) Fatigue crack propagation behavior of UHMWPE. *J Orthopaed Res*, **2**, 119–125.

Costa, L., Luda, M. P., Trossarelli, L., Brach del Prever, E. M., Crova, M. & Gallinaro, P. (1998) Oxidation in orthopaedic UHMWPE sterilized by gamma radiation and ethylene oxide. *Biomaterials*, **19**, 659–668.

Costa, L., Bracco, P., del Prever, E. B., Luda, M. P. & Trossarelli, L. (2001) Analysis of products diffused into UHMWPE prosthetic components *in vivo*. *Biomaterials*, **22**, 307–315.

Counsell, A., Heasley, R., Arumulli, B. & Paul, A. (2008) A groin mass caused by metal particle debris after hip resurfacing. *Acta Orthopaedica Belgica*, **74**, 870–874.

Currier, B. H., Currier, J. H., Mayor, M. B., Lyford, K., Collier, J. P. & van Citters, D. W. (2007) Evaluation of oxidation and fatigue damage of retrieved Crossfire polyethylene acetabular cups. *J Bone Joint Surg*, **89**, 2023–2029.

Daniel, J., Pynsent, P. & McMinn, D. (2004) Metal-on-metal resurfacing of the hip in patients under the age of 55 years with osteoarthritis. *J Bone Joint Surg*, **86B**, 177–184.

Daniel, J., Ziaee, H., Salama, A., Pradhan, C. & McMinn, D. (2006) The effect of the diameter of metal-on-metal bearings on systemic exposure to cobalt and chromium. *J Bone Joint Surg*, **88B**, 443–448.

Digas, G., Karrholm, J., Thanner, J. & Herberts, P. (2007) 5-year experience of highly crosslinked polyethylene in cemented and uncemented sockets – two randomized studies using radiostereometric analysis. *Acta Orthopaedica*, **78**, 746–754.

Dumbleton, J., Miller, D. & Miller, E. (1972) A simulator for load bearing joints. *Wear*, **20**, 165–174.

Dumbleton, J., Manley, M. & Edidin, A. (2002) A literature review of the association between wear and osteolysis in total hip arthroplasty. *J Arthroplasty*, **17**, 649–661.

DuPlessis, T., Grobbelaar, C. & Marais, F. (1977) The improvement of polyethylene prostheses through radiation crosslinking. *Radiat Phys Chem*, **9**, 647–652.

Flory, P. (1953) *Principles of Polymer Chemistry*. Ithaca, Cornell University Press.

Geil, P., Anderson, F., Wunderlich, B. & Arakawa, T. (1964) Morphology of polyethylene crystallized from the melt under pressure. *J Polym Sci: Part A: Polym Chem*, **2**, 3707–3720.

Haider, H. (2009) Tribological assessment of UHMWPE in the knee. In Kurtz, S. (Ed.) *UHMWPE Biomaterials Handbook*, 2nd edn. New York, Elsevier.

Halley, D., Glassman, A. & Crowninshield, R. (2004) Recurrent dislocation after revision total hip replacement with a large prosthetic femoral head. *J Bone Joint Surg*, **86A**, 827–830.

Helmick, C., Felson, D., Lawrence, R. & Gabriel, S. (2008) Estimates of the prevalence of arthritis and other rheumatic conditions in the United States. *Arthritis Rheumatism*, **58**, 15–25.

Hui, A., McCalden, R. W., Martell, J. M., MacDonald, S. J., Bourne, R. B. & Rorabeck, C. (2003) Validation of two and three-dimensional radiographic techniques for measuring polyethylene wear after total hip arthroplasty. *J Bone Joint Surg*, **85A**, 505–511.

Hunziker, E. (2002) Articular cartilage repair: basic science and clinical progress. *Osteoarthritis Cartilage*, **10**, 432–463.

Jacobs, J. & Hallab, N. (2006) Loosening and osteolysis associated with metal-on-metal bearings – a local effect of metal hypersensitivity. *J Bone Joint Surg*, **88**, 1171–1172.

Jahan, M. (2009) ESR insights into macroradicals in UHMWPE. In Kurtz, S. (Ed.) *UHMWPE Biomaterials Handbook*, 2nd edn. New York, Elsevier.

Jahan, M. S., King, M. C., Haggard, W. O., Sevo, K. L. & Parr, J. E. (2001) A study of long-lived free radicals in gamma-irradiated medical grade polyethlene. *Radiat Phys Chem*, **62**, 141–144.

James, S. P., Blazka, S., Merrill, E. W., Jasty, M., Lee, K. R., Bragdon, C. R. & Harris, W. H. (1993) Challenge to the concept that UHMWPE acetabular components oxidize *in vivo*. *Biomaterials*, **14**, 643–647.

Jarrett, C., Ranawat, A., Bruzzone, M., Blum, Y., Rodriguez, J. & Ranawat, C. (2009) The squeaking hip – a phenomenon of ceramic-on-ceramic total hip arthroplasty. *J Bone Joint Surg*, **91A**, 1344–1349.

Jasty, M. & Smith, E. (1992) Wear particles of total joint replacements and their role in periprosthetic osteolysis. *Curr Opin Rheumatol*, **4**, 204–209.

Jasty, M. J., Goetz, D. D., Lee, K. R., Hanson, A. E., Elder, J. R. & Harris, W. H. (1997) Wear of polyethylene acetabular components in total hip arthroplasty. An analysis of 128 components retrieved at autopsy or revision operation. *J Bone Joint Surg*, **79A**, 349–358.

Johnston, R. C. & Schmidt, G. L. (1969) Measurement of hip-joint motion during walking. *J Bone Joint Surg (Am)*, **51A**, 1083.

Judet, J. & Judet, R. (1950) The use of an artificial femoral head for arthroplasty of the hip joint. *J Bone Joint Surg (Br)*, **32B**, 166–173.

Kurtz, S. M. (1999) A miniature specimen mechanical testing technique scaled to articulating surface of polyethylene components for total joint arthroplasty. *J Biomed Mater Res*, **48**, 75–81.

Kurtz, S. M. (2006) Total disc arthroplasty. In Kurtz, S. M. & Edidin, A. (Eds) *Spine Technology Handbook.* New York, Elsevier.

Kurtz, S. M. (2009a) From ethylene gas to UHMWPE component: the process of producing orthopaedic implants. In Kurtz, S. M. (Ed.) *UHMWPE Biomaterials Handbook*, 2nd edn. New York, Elsevier.

Kurtz, S. M. (2009b) The origins of UHMWPE in total hip arthroplasty. In Kurtz, S. M. (Ed.) *UHMWPE Biomaterials Handbook*, 2nd edn. New York, Elsevier.

Kurtz, S. M. (2009c) A primer on UHMWPE. In Kurtz, S. M. (Ed.) *UHMWPE Biomaterials Handbook*, 2nd edn. New York, Elsevier.

Kurtz, S. M., Muratoglu, O. K., Evans, M. & Edidin, A. A. (1999) Advances in the processing, sterilization, and crosslinking of ultra-high molecular weight

polyethylene for total joint arthroplasty. *Biomaterials*, **20**, 1659–1688.
Kurtz, S. M., Hozack, W., Turner, J., Purtill, J., MacDonald, D., Sharkey, P., Parvizi, J., Manley, M. & Rothman, R. (2005) Mechanical properties of retrieved highly cross-linked crossfire liners after short-term implantation. *J Arthroplasty*, **20**, 840–849.
Kurtz, S. M., Mazzucco, D., Rimnac, C. M. & Schroeder, D. (2006) Anisotropy and oxidative resistance of highly crosslinked UHMWPE after deformation processing by solid-state ram extrusion. *Biomaterials*, **27**, 24–34.
Kurtz, S. M., Ong, K., Lau, E., Mowat, F. & Halpern, M. (2007) Projections of primary and revision hip and knee arthroplasty in the United States from 2005 to 2030. *J Bone Joint Surg (Br)*, **89**, 780–785.
Kurtz, S. M., Patwardhan, A., MacDonald, D., Ciccarelli, L., van Ooij, A., Lorenz, M., Zindrick, M., O'Leary, P., Isaza, J. & Ross, R. (2008) What is the correlation of *in vivo* wear and damage patterns with *in vitro* TDR motion response? *Spine*, **33**, 481–489.
Lee, C. (1988) Accelerated degeneration of the segment adjacent to a lumbar fusion. *Spine*, **13**, 375–377.
Liao, Y.-S., Benya, P. & McKellop, H. (1999) Effect of protein lubrication on the wear properties of materials for prosthetic joints. *J Biomed Mater Res*, **48**, 465–473.
Livermore, J., Ilstrup, D. & Morrey, B. (1990) Effect of femoral head size on wear of the polyethylene acetabular component. *J Bone Joint Surg*, **72A**, 518–528.
Livingston, B. J., Chmell, M. J., Spector, M. & Poss, R. (1997) Complications of total hip arthroplasty associated with the use of an acetabular component with a hylamer liner. *J Bone Joint Surg*, **79A**, 1529–1538.
Manning, D. W., Chiang, P. P., Martell, J. M., Galante, J. O. & Harris, W. H. (2005) *In vivo* comparative wear study of traditional and highly cross-linked polyethylene in total hip arthroplasty. *J Arthroplasty*, **20**, 880–886.
Martell, J. M. & Berdia, S. (1997) Determination of polyethylene wear in total hip replacements with use of digital radiographs. *J Bone Joint Surg (Am)*, **79**, 1635–1641.
McKee, G. & Watson-Farrar, J. (1966) Replacement of arthritic hips by the McKee-Farrar prosthesis. *J Bone Joint Surg*, **48B**, 245–259.
McKellop, H., Shen, F.-W., Lu, B., Campbell, P. & Salovey, R. (1999) Development of an extremely wear resistant ultra-high molecular weight polyethylene for total hip replacements. *J Orthop Res*, **17**, 157–167.
McKellop, H., Shen, F.-W., Lu, B., Campbell, P. & Salovey, R. (2000) Effect of sterilization method and other modifications on the wear resistance of acetabular cups made of ultra-high molecular weight polyethylene – a hip-simulator study. *J Bone Joint Surg*, **82A**, 1708–1725.
Moore, A. & Bohlman, H. (1943) Metal hip joint: a case report. *J Bone Joint Surg*, **25**, 688–692.
Muratoglu, O. K., Bragdon, C. R., O'Connor, D. O., Jasty, M., Harris, W. H., Gul, R. & McGarry, F. (1999) Unified wear model for highly crosslinked ultra-high molecular weight polyethylenes (UHMWPE). *Biomaterials*, **20**, 1463–1470.
Muratoglu, O. K., Bragdon, C. R., O'Connor, D. O., Jasty, M. & Harris, W. H. (2001a) 1999 HAP Paul Award. A novel method of crosslinking UHMWPE to improve wear, reduce oxidation and retain mechanical properties. *J Arthroplasty*, **16**, 149–160.
Muratoglu, O. K., Bragdon, C. R., O'Connor, D. O., Perinchief, R. S., Estok, D. M., Jasty, M. & Harris, W. H. (2001b) Larger diameter femoral heads used in conjunction with a highly cross-linked ultra-high molecular weight polyethylene: a new concept. *J Arthroplasty*, **16**, 24–30.

Muratoglu, O. K., Bragdon, C. R., Jasty, M., O'Connor, D. O., von Knoch, R. & Harris, W. H. (2004) Knee simulator testing of conventional and crosslinked polyethylene tibial inserts. *J Arthroplasty*, **19**, 887–897.

Muratoglu, O. K., Oral, E., Burroughs, B., Christensen, S., Malhi, A., Spiegelberg, S., Wannomae, K. & Harris, W. (2005a) Two second generation crosslinked UHMWPEs show improved mechanical properties and fatigue strength. *Transactions*, *51st Annual Meeting of the Orthopaedic Research Society.* Washington, DC.

Muratoglu, O. K., Wannomae, K., Christensen, S., Rubash, H. E. & Harris, W. H. (2005b) *Ex vivo* wear of conventional and cross-linked polyethylene acetabular liners. *Clin Orthop Relat Res*, **438**, 158–64.

Murray, D., Carr, A. & Bulstrode, C. (1993) Survival analysis of joint replacements. *J Bone Joint Surg*, **75B**, 697–704.

Oonishi, H., Takayama, Y. & Tsuji, E. (1992) Improvement of polyethylene by irradiation in artificial joints. *Radiation Phys Chem*, **39**, 495–504.

Oral, E., Wannomae, K. K., Hawkins, N. E., Harris, W. H. & Muratoglu, O. K. (2004) α-Tocopherol doped irradiated UHMWPE for high fatigue resistance and low wear. *Biomaterials*, **25**, 5515–5522.

Oral, E., Greenbaum, E. S., Malhi, A. S., Harris, W. H. & Muratoglu, O. K. (2005) Characterization of irradiated blends of alpha-tocopherol and UHMWPE. *Biomaterials*, **26**, 6657–6663.

Oral, E., Christensen, S., Malhi, A., Wannomae, K. & Muratoglu, O. (2006a) Wear resistance and mechanical properties of highly crosslinked UHMWPE doped with vitamin E. *J Arthroplasty*, **21**, 580–591.

Oral, E., Malhi, A. & Muratoglu, O. (2006b) Mechanisms of decrease in fatigue crack propagation resistance in irradiated and melted UHMWPE. *Biomaterials*, **27**, 917–925.

Oral, E., Rowell, S. & Muratoglu, O. (2006c) The effect of alpha-tocopherol on the oxidation and free radical decay in irradiated UHMWPE. *Biomaterials*, **27**, 5580–5587.

Oral, E., Wannomae, K. K., Rowell, S. L. & Muratoglu, O. K. (2007) Diffusion of vitamin E in ultra-high molecular weight polyethylene. *Biomaterials*, **28**, 5225–5237.

Oral, E., Godleski Beckos, C., Malhi, A. & Muratoglu, O. (2008) The effects of high dose irradiation on the cross-linking of vitamin E-blended UHMWPE. *Biomaterials*, **29**, 3557–3560.

Oral, E., Godleski Beckos, C., Lozynsky, A., Malhi, A. & Muratoglu, O. (2009) Improved resistance to wear and fatigue fracture in high pressure crystallized vitamin E-containing ultrahigh molecular weight polyethylene. *Biomaterials*, **30**, 1870–1880.

Orthopaedic Network News (2009) Hip and knee implant list prices: 2008–2009. *Orthopaedic Network News*, **20**, 1–14.

Pandit, H., Glyn-Jones, S., McLardy-Smith, P., Gundle, R., Whitwell, D., Gibbons, C., Ostlere, S., Athanasou, N., Gill, H. & Murray, D. (2008) Pseudotumors associated with metal-on-metal hip resurfacings. *J Bone Joint Surg*, **90B**, 847–851.

Park, Y., Hwang, S., Choy, W., Kim, Y., Moon, Y. & Lim, S. (2006) Ceramic failure after total hip arthroplasty with an alumina-on-alumina bearing. *J Bone Joint Surg*, **88A**, 780–787.

Parth, M., Aust, N. & Lederer, K. (2002) Studies on the effect of electron beam radiation on the molecular structure of ultra-high molecular weight polyethylene under the influence of alpha-tocopherol with respect to its application in medical implants. *J Mater Sci Mater Med*, **13**, 917–921.

Paul, J. P. (1966) Forces transmitted by joints in the human body. *Proc Instn Mech Engrs*, Pt 3F, **8**, 181.

Rahaman, M., Yao, A., Bal, B., Garino, J. & Ries, M. (2007) Ceramic for prosthetic hip and knee replacement. *J Am Ceramic Soc*, **90**, 1965–1988.

Ramamurti, B., Bragdon, C., O'Connor, D., Lowenstein, J., Jasty, M., Estok, D. & Harris, W. (1996) Loci of movement of selected points on the femoral head during normal gait. Three-dimensional computer simulation. *J Arthroplasty*, **11**, 845–852.

Ramamurti, B. S., Estok, D. M., Jasty, M. & Harris, W. H. (1998) Analysis of the kinematics of different hip simulators used to study wear of candidate materials for the articulation of total hip arthroplasties. *J Orthop Res*, **16**, 365–369.

Rowell, S., Oral, E. & Muratoglu, O. (2008) Oxidation and oxidation potential of radiation crosslinked vitamin E/UHMWPE blends. *Transactions of the 54th Annual Meeting of the Orthopaedic Research Society.* San Francisco, CA.

Saikko, V., Calonius, O. & Keranen, J. (2001) Effect of counterface roughness on the wear of conventional and crosslinked ultrahigh molecular weight polyethlene studied with a multi-directional motion pin-on-pin device. *J Biomed Mater Res*, **57**, 504–512.

Sathasivam, S. & Walker, P. (1998) Computer model to predict subsurface damage in tibial inserts of total knees. *J Orthopaed Res*, **16**, 564–571.

Scales, J., Kelly, P. & Goddard, D. (1969) Friction torque studies of total joint replacements. The use of a simulator. *Ann Rheum Dis*, **28**, Suppl, 30–35.

Shaw, J. A. & Murray, D. G. (1973) Knee joint simulator. *Clin Orthop*, **94**, 15–23.

Simis, K. S., Bistolfi, A., Bellare, A. & Pruitt, L. A. (2006) The combined effects of crosslinking and high crystallinity on the microstructural and mechanical properties of ultra high molecular weight polyethylene. *Biomaterials*, **27**, 1688–1694.

Smith-Petersen, M. (1948) Evolution of mold arthroplasty of the hip joint. *J Bone Joint Surg (Br)*, **30B**, 59–75.

Thomson, J. (1952) A prosthesis for the femoral head: a preliminary report. *J Bone Joint Surg*, **34A**, 175–182.

Tower, S. S., Currier, J. H., Currier, B. H., Lyford, K. A., van Citters, D. W. & Mayor, M. B. (2007) Rim cracking of the cross-linked longevity polyethylene acetabular liner after total hip arthroplasty. *J Bone Joint Surg (Am)*, **89**, 2212–2217.

Turell, M. & Bellare, A. (2004) A study of the nanostructure and tensile properties of ultra-high molecular weight polyethylene. *Biomaterials*, **25**, 3389–3398.

Venable, C., Stuck, W. & Beach, A. (1937) The effects on bone of the presence of metals, based upon electrolysis – an experimental study. *Annals Surg*, **105**, 917–938.

Walker, P., Blunn, G., Broome, D., Perry, J., Watkins, A., Sathasivam, S., Dewar, M. & Paul, J. (1997) A knee simulating machine for performance evaluation of total knee replacements. *J Biomechanics*, **30**, 83–89.

Wang, A., Essner, A., Polineni, V., Stark, C. & Dumbleton, J. H. (1998a) Lubrication and wear of UHMWPE in total joint replacements. *Tribol Int*, **31**, 17–33.

Wang, A., Polineni, V., Stark, C. & Dumbleton, J. (1998b) Effect of femoral head surface roughness on the wear of UHMWPE acetabular cups. *J Arthroplasty*, **13**, 615–620.

Wang, A., Zeng, H., Yau, S.-S., Essner, A., Manely, M. & Dumbleton, J. (2006) Wear, oxidation and mechanical properties of a sequentially irradiated and annealed UHMWPE in total joint replacement. *J Phys D: Appl Phys*, **39**, 3213–3219.

Wannomae, K., Bhattacharyya, S., Freiberg, A., Estok, D., Harris, W. & Muratoglu, O. (2006) *In vivo* oxidation of retrieved crosslinked UHMWPE acetabular components with residual free fadicals. *J Arthroplasty*, **21**, 1005–1011.

Wiles, P. (1957) The surgery of the osteoartritic hip. *Br J Surg*, **45**, 488–497.

Willert, H., Buchhorn, G., Fayyazi, A., Flury, R., Windler, M., Koster, G. & Lohmann, C. (2005) Metal-on-metal bearings and hypersensitivity in patients with artificial hip joints. *J Bone Joint Surg*, **87A**, 28–36.

Wright, T. M., Astion, D. J., Bansal, M., Rimnac, C. M., Insall, J. N. & Robinson, R. P. (1988) Failure of carbon fiber-reinforced polyethylene total knee-replacement components. *J Bone Joint Surg*, **70A**, 926–932.

Wroblewski, B. M. (1988) Wear and loosening of the socket in the Charnley low-friction arthroplasty. *Orthop Clin North Am*, **19**, 627–630.

Wroblewski, B. M., Siney, P. D., Dowson, D. & Collins, S. N. (1996) Prospective clinical and joint simulator studies of a new total hip arthroplasty using alumina ceramic heads and cross-linked polyethylene cups. *J Bone Joint Surg*, **78B**, 280–285.

Wunderlich, B. & Arakawa, T. (1964) Polyethylene crystallized from the melt under elevated pressure. *J Polym Sci: Part A*, **2**, 3697–3706.

Zhang, X., Elkoun, S., Ajji, A. & Huneault, M. (2004) Oriented structure and anisotropy properties of polymer blown films: HDPE, LLDPE and LDPE. *Polymer*, **45**, 217–229.

4

Biomaterials for pacemakers, defibrillators and neurostimulators

M. J. EBERT, Medtronic Cardiac Rhythm Disease Management, USA, S-P. LYU, Medtronic Strategy and Scientific Operations, USA, M. T. RISE, Medtronic Neuromodulation, USA and M. F. WOLF, Medtronic Strategy and Scientific Operations, USA

Abstract: This chapter discusses the materials used to make functional electrical stimulation devices, including implantable pacemakers, defibrillators, and neurostimulators. It focuses on the use of the materials in terms of structures, functions, and biological responses of these devices, and engineering principles to solve problems related to material biocompatibility, biostability, and unmet needs.

Key words: functional electrical stimulation, implantable electrical stimulation devices, pulse generator, leads, cardiac stimulation, neuromodulation, implantable biomaterials.

4.1 Introduction

4.1.1 Overview of electrical stimulation devices

Artificial cardiac pacing is a therapy to restore the rhythm functions of a diseased heart through electrical stimulation. This therapy is generated and delivered to the heart by a cardiac pacemaker. A pacemaker has two components: a pulse generator, or 'can', that produces electric pulses (therapy) after analyzing the signals that it senses from the diseased heart; and one or more leads that deliver the therapy. In their initial clinical applications, pacing therapies focused on the treatment of slow heart rate problems (bradycardia). Gradually, pacemakers evolved to treat fast rate problems (tachycardia), irregular beating problems (arrhythmia/fibrillation), and neurological disorders. Today, electrical stimulation is established as a unique, safe, and effective therapy and is becoming a competitive alternative to pharmaceutical therapies for many chronic diseases. The therapies are different for different diseases, but the stimulation devices are similar; they have similar structures, functions, and biological requirements. The materials used to make these devices are similar as well. This chapter focuses on the materials for cardiac pacemakers, defibrillators, and neural stimulators.

The first artificial pacemakers were external devices commonly attributed to Hyman (1930, 1935) and Lidwell (1929), (Mond *et al.*, 1982). Hyman used a hand-cranked pulse generator and needle electrodes inserted in the myocardium transthoracically. Lidwell's device used a myocardial needle as one electrode and a saline-soaked plate as another electrode placed on the skin. The early pacemakers used AC electricity from wall outlets and, as a result, limited patient mobility to the length of power cords, making uninterrupted power supply critical. The first fully portable, battery-powered, and transistorized external pulse generator was developed by Bakken and applied clinically by Lillehei in 1957 (Lillehei *et al.*, 1960). This simple, yet foundational, invention solved the pacemaker power supply problem. Most importantly, this work greatly promoted clinical use, research and development, and public acceptance of electrical stimulation devices; it opened a new industry.

In the following years, a few breakthroughs substantially advanced pacemaker technology. One was the introduction of the totally implantable pacemaker by Senning and Elmqvist in 1958 (Elmqvist and Senning, 1960). Their first device worked for only a short time, but brought the concept of an implantable device to the forefront. In 1960, Chardack, Gage, and Greatbatch implanted another self-contained battery-powered device. This device was combined with the electrodes developed by Hunter and Roth (i.e., Hunter–Roth electrodes) that could be sutured to the patient's heart and more effectively concentrate the pacemaker's current where it was needed (Chardack *et al.*, 1960). The system required about 70% less current than existing electrode technology of that time; the devices worked for 18 months. Another breakthrough was the development of a transvenous lead insertion technique by Furman in 1958 (Furman and Robinson, 1958). Furman added a wire to the lumen of a Cournand catheter and passed it into the right ventricle of the patient's heart through a vein. The use of this insertion technique and an endocardial electrode eliminated the need to cut the chest open. By combining an endocardial lead and an implantable pulse generator, Lagergren achieved a totally implantable transvenous system on 5 June 1962. Parsonnet accomplished a full transvenous implantation a few months later. In 1965, Medtronic commercially introduced a wholly implantable transvenous system (Furman, 2000). These achievements established the fundamental form of today's pacemakers.

As transvenous leads evolved, it became obvious that they were easier, safer, and less traumatic to implant than those requiring transthoracic approaches; however, the results of this method of implantation were not as reliable. Complications such as dislodgment, myocardial perforation, conductor fracture, exit block, and failure to sense required corrective reoperation in a significant percentage of implants. Thus, during the 1970s, a plethora of transvenous lead designs were developed with mechanisms intended to reduce the acute reoperation rate.

In 1968, Mirowski began developing the implantable cardioverter defibrillator (ICD) to stop heart fibrillation (irregular beating) by delivering a high voltage and high energy shock (Efimov *et al.*, 2008). It took several years to develop the circuitry, battery, and capacitor suitable for an implantable device. The first device was implanted in 1980. The transvenous defibrillation lead system was approved in the 1990s, allowing patients to avoid the more invasive thoracotomy procedure. Later, tiered therapy was added to the ICD so the device could provide various therapies at an escalating energy scale for defibrillation.

While the use of electrical stimulation of excitable tissue for therapeutic purposes began with the heart, expansion of this technology to new therapy modalities involving other specialized tissues such as the brain and nervous tissues was forthcoming. Many different therapeutic applications have been explored with this technology throughout the years. While it is impractical to review all of them here, a few therapies that have gained relatively widespread commercial use are representative of the broader field of these applications and are relevant for review in this chapter.

One such therapeutic application, neurostimulation (as it has broadly become known), involves technology that spun off from pacing technology. This therapy has been developed from an understanding of the nervous system 'wiring diagram' for a particular body function. The advent of Melzack and Wall's *Gate Control Theory of Pain* in the latter half of the 1960s, proposing endogenous neural circuits capable of inhibiting pain perception, led to several approaches to stimulate these neurological circuits (Melzack and Wall, 1965). Norm Shealy, working with Mortimer, developed a neurostimulator designed to stimulate the dorsal columns of the spinal cord (Shealy *et al.*, 1967). The dorsal columns function to convey somatosensory information from the periphery and are part of the pain inhibition circuitry. Initially, they performed a laminectomy and opened the dura to place a flat electrode with its stimulating surface directly against the spinal cord.

As with pacemakers, these techniques have evolved. Modern techniques employ a Tuohy needle to insert a cylindrical lead into the epidural space between the dura and dorsal aspect of the spinal column. Alternatively, a paddle-shaped lead is inserted through a laminotomy to lie over the dorsal columns. These various techniques, specifically referred to as spinal cord stimulation (SCS), are in widespread commercial use as a pain treatment modality used primarily for neurogenic pain, or pain caused by damage to the nervous system itself.

Further understanding of endogenous pain suppression circuitry within the brain led to techniques to activate opioid responsive nerve cells deep inside the brain. Hosobuchi and Adams implanted electrical stimulation leads into the periventricular gray to treat pain. The cylindrical leads were inserted through a small burr hole in the skull using stereotaxic surgery (Hosobuchi *et al.*, 1977). While this particular therapy is employed infrequently today, the technology of

deep brain stimulation (DBS) has since been further developed and used for several commercially approved therapies treating motor symptoms of Parkinson's disease, essential tremor, and dystonia, and the psychiatric condition of obsessive compulsive disorder (OCD). DBS is also under investigation for treatment of epilepsy and depression.

Arguably, the easiest way to apply stimulation to the nervous system is through a peripheral nerve. Neurostimulators designed to stimulate sacral nerves are used commercially to treat urinary incontinence (Jonas *et al.*, 2001) and chronic pain. Researchers have been pursuing therapeutic applications, referred to as functional electrical stimulation (FES), wherein motor nerves or the muscles themselves are stimulated to return motor control to persons with spinal cord injury or stroke survivors (de Kroon *et al.*, 2005). The cochlear nerve has been successfully stimulated to return some auditory function to persons with hearing loss. Therapeutic applications of neurostimulation have recently undergone a nomenclature shift and are now referred to as neuromodulation. Currently, a wide array of applications are in commercial use, with many more being developed or in a research phase. The materials and components used for these device designs share many common properties and have borrowed heavily from technology developed to advance cardiac pacing.

4.1.2 Biocompatibility and biostability

Any object placed inside the body for medical purposes must meet strict controls and undergo rigorous testing to ensure that the material and the device itself are biocompatible and biostable. A well-accepted definition of biocompatibility was stated by David Williams in 1987: 'biocompatibility is the ability of a material to perform with an appropriate host response in a specific application' (Williams, 1987). This definition is based on the performance of the device. It does not rule out the existence of certain host responses; rather, it proposes accepting them as natural and tolerable (and inevitable) reactions as long as device performance together with patient safety and quality of life are maintained.

From an evaluation standpoint, biocompatibility testing attempts to establish and rate, within a risk management process, the potential of undesirable responses of the host to the implant. Biocompatibility assessments tend to focus on areas of cytotoxicity (toxic to cells), sensitization (allergic response), pyrogenicity (fever producing), hemolysis (red blood cell damage), thrombogenicity (causing thrombus formation), inflammation, and mutagenicity and/or chromosomal aberrations (damage to DNA). Biostability, on the other hand, refers to the ability of a device to resist undesirable effects by normal host biological defence mechanisms. These mechanisms can manifest their actions as fracture of components, corrosion of metallic and ceramic parts, degradation of polymeric materials, or failure at the component interfaces due to reactive chemicals,

cellular elements, or their combined presence. Factors that may affect the biocompatibility and biostability of devices primarily include material properties, device designs, contacting tissues, and implantation techniques.

At the chemical and cellular level, biocompatibility and biostability of a device or material depend on the type of chemicals and cellular responses that occur at the host–device interfaces. Implanted devices must withstand the humoral (bulk) environment within the body that consists of water, electrolytes, proteins, fatty acids, glucose, urea, lactic acid, creatinine and more. The inflammation or 'foreign body response' of the host to the device is a term that describes cellular reactions to the implant. Once implanted, a cascade of reactions starts and results in the device being covered with a layer of foreign body giant cells and/or macrophages, and a fibrotic capsule composed primarily of collagen. The cellular components of the foreign body reaction can have significant effects on the biostability of the materials in the device. These cells can release a number of enzymes and oxidants to destroy the foreign body (device and materials). The compounds in tissues that seem to have the greatest effect on polymer biostability are water, oxidants and free radicals, and hydrolytic enzymes. Along with the chemical and cellular environment around the implant, the body also exerts mechanical loads (forces) upon the device by interactions or juxtaposition with bones, muscles, and organs. A patient's own physical activity and occasional inadvertent actions can also affect the device. Therefore, an implanted device must withstand routine physical activity as well as the mechanical environment within the body.

A great deal of research has been done to understand the biological reactions to materials including protein adsorption, blood coagulation and thrombosis, inflammation, cellular reactions, and tissue remodeling. Yet, no material has been discovered and recognized to have a zero or null inflammatory reaction. On this point researchers have learned a number of important lessons: first, a certain level of biological reactions, such as an inflammatory response or thrombotic reaction, may not be adverse. Biological reactions at certain levels are acceptable although the levels depend on specific tissues and applications; second, combining drugs with the devices can be an effective means to control biological reactions compared with inventing new materials or new surface treatment methods. Steroid releasing leads are an excellent example of using a drug to minimize the inflammation reaction to the pacing electrodes. Such drugs incorporated in the tips of lead electrode effectively reduce the inflammatory response that gives rise to high pacing thresholds; third, although biocompatibility is always considered with high priority, in reality the majority of device failures are due to poor biostability of materials, especially when unexpected interactions among different materials and biological factors are present in the biological environment.

Most materials pass biocompatibility testing as long as they do not release toxic levels of additives, monomers, contaminants, degradable products,

corrosion products, or particulates. Whether such materials can perform satisfactorily in devices depends on their ability to maintain the chemical and mechanical stabilities necessary for the designed functions under the intended clinical conditions and anticipated implant durations. Therefore, practical biocompatibility combines acute and chronic biological reactions, biostability, and physical and biological functions of the whole device.

Establishing biocompatibility and biostability of implant devices and materials is a highly regulated and evolving field. In addition, given the globalization of development and use of modern medical technology, international standards have arisen for carrying out such safety testing prior to use in humans. As such, the testing strategy for much of the needs described in this chapter can be found in the horizontal standard referred to as ISO (International Standards Organization) 10993: Biological Evaluation of Medical Devices (Table 4.1). In this standard, devices and materials are first evaluated on the basis of constituent materials and their chemical characterizations with a risk management and toxicological perspective, e.g., identifying what materials are present and at what risk level. Then, depending on this information and known and unknown risks in each application, a series of *in vitro* and *in vivo* tests are prescribed that may be required by regulatory bodies worldwide to establish safety prior to clinical investigations and commercialization. This horizontal standard is supplemented by several specific vertical standards (e.g., ISO 14708-2 and ISO 5841-3) for the fields of cardiac pacing (Tables 4.1 and 4.2).

Fortunately, in spite of many potentially adverse biological responses to implants (and vice versa), a number of materials have been tested and used extensively throughout the device industry for implantable medical devices. Most implantable pulse generators (IPGs), e.g., pacemakers, neurostimulators, implantable cardioverter defibrillators, are constructed with relatively common materials such as titanium metal for the pulse generators (cans) and polyurethane or silicone rubber for the leads and the connectors between the can and leads. These materials have been the primary components of the implantable devices for decades and are backed by literally billions of patient hours in the field with a high degree of reliability and demonstrated biocompatibility. However, the safe use history of these materials and the high cost of developing new materials have led to the rather short list of materials employed in such devices today.

4.2 Pacemakers

4.2.1 Pacemaker overview

The heart has it own natural pacemaker, the sinoatrial (SA) node, which acts as the primary pacemaker of the heart to regulate the rate at which it beats. The SA node is located within the wall of the right atrium and it is this specialized group of cells that generates the primary pulses that stimulate atria contraction. These

Table 4.1 International Organization for Standardization ISO 10993: Biological Evaluation of Medical Devices Standard, by Parts

Part	Title (publication year: status)	Focus
1	Evaluation and testing within a risk management process (2009)	General instruction on how to use the standard
2	Animal welfare requirements (2006)	General instruction on proper and ethical use of animals in testing
3	Tests for genotoxicity (G), carcinogenicity (C), and reproductive toxicity (RT) (2003: CD)	*In vitro* and *in vivo* tests to assess the materials capacity to cause G, C, and RT
4	Selection of tests for interactions with blood (2006: to be revised)	*In vitro* and *in vivo* tests to assess the material/device interactions with blood
5	Tests for *in vitro* cytotoxicity (1999: under revision)	*In vitro* tests to assess the potential for the material to cause a cytotoxic response
6	Tests for local effects after implantation (2007)	*In vivo* tests for general implantation response
7	Ethylene oxide (ETO) sterilization residuals (1995: under revision)	General instruction on safe ETO sterilization practice
8	Withdrawn standard	NA
9	Framework for identification and quantification of potential degradation products (1999: under revision)	General instruction on chemical characterization for material degradation products
10	Tests for irritation and delayed-type hypersensitivity (DTH) (2006: to be revised)	*In vivo* tests for material-related irritation and DTH
11	Tests for systemic toxicity (2006)	*In vivo* tests for material tissue toxicity
12	Sample preparation and reference materials (2002: under revision)	General instruction on proper controls and preparation of material samples
13	Identification and quantification of degradation products from polymeric medical devices (1998: under revision)	*In vitro* analytical tests for chemical characterization of polymeric materials
14	Identification and quantification of degradation products from ceramics (2001)	*In vitro* analytical tests for chemical characterization of ceramic materials
15	Identification and quantification of degradation products from metals and alloys (2000)	*In vitro* analytical tests for chemical characterization of metallic materials
16	Toxicokinetic study design for degradation products and leachables (1997: to be revised)	*In vivo* tests for toxicokenetic assessment of material degradation products and leachables
17	Establishment of allowable limits for leachable substances (2002)	Instruction on allowable limits of leachable materials
18	Chemical characterization of materials (2005)	*In vitro* analytical tests for chemical characterization of materials
19	Physicochemical, morphological, and topographical characterization of materials (2006)	*In vitro* analytical tests for surface analysis of materials
20	Principles and methods for immunotoxicology testing of medical devices (2006)	*In vivo* tests to assess material/device immunotoxicity

Table 4.2 Pacing, ICD, and neuromodulation system components arranged by most common material, tissue interface, and relevant standard(s). (Note: Lead conductor materials (e.g., MP35N) and internal can components generally do not contact tissue and are not listed)

Components	Selected materials	Primary tissue contacts	Applicable standards
Pacemaker pulse generator	Titanium	Subcutaneous and muscle	ISO 10993 ISO 14708-1 (CEN EN 45502-1) ISO 14708-2 ISO 14708-3 CENELEC EN 45502-2-1 ISO 14708-6 (CENELEC EN 45502-2-2) Guidance for Industry (12)
Connector module of pulse generator	Polyether polyurethane (rigid, e.g., 75D)	Subcutaneous and muscle	ISO 5841-3 (IS-1) ISO 11318 (DF1) ISO 27186 (IS4) ISO 10993
Adhesives	Silicone or polyurethane	Subcutaneous and muscle	ISO 10993 ISO 14708-1 (CEN EN 45502-1) ISO 14708-2 ISO 14708-3 CENELEC EN 45502-2-1 ISO 14708-6 (CENELEC EN 45502-2-2) Guidance for Industry (12)
Lead connector	Polyether polyurethane	Subcutaneous and muscle	ISO 10993 ISO 14708-1 (CEN EN 45502-1) ISO 14708-2 ISO 14708-3 CENELEC EN 45502-2-1 ISO 14708-6 (CENELEC EN 45502-2-2) Guidance for Industry (12)
Lead insulation	Silicone or polyether polyurethane	Subcutaneous and muscle, venous tissue, blood, cardiac tissues	ISO 10993 ISO 14708-1 (CEN EN 45502-1) ISO 14708-2 ISO 14708-3 CENELEC EN 45502-2-1 ISO 14708-6 (CENELEC EN 45502-2-2) Guidance for Industry (12)
Lead electrode	Titanium nitride, platinum, platinum–iridium alloys, or activated carbon	Blood, cardiac tissues	ISO 10993 ISO 14708-1 (CEN EN 45502-1) ISO 14708-2 ISO 14708-3 CENELEC EN 45502-2-1 ISO 14708-6 (CENELEC EN 45502-2-2) Guidance for Industry (12)

Table 4.2 Continued

Components	Selected materials	Primary tissue contacts	Applicable standards
Fixation	Silicone, polyether polyurethane, or lead electrode metals	Blood, cardiac tissues	ISO 10993 ISO 14708-1 (CEN EN 45502-1) ISO 14708-2 ISO 14708-3 CENELEC EN 45502-2-1 ISO 14708-6 (CENELEC EN 45502-2-2) Guidance for Industry (12)
Drug release components	Silicone or polyether polyurethane	Blood, cardiac tissues	ISO 10993 ISO 14708-1 (CEN EN 45502-1) ISO 14708-2 ISO 14708-3 CENELEC EN 45502-2-1 ISO 14708-6 (CENELEC EN 45502-2-2) Guidance for Industry (12)

pulses also travel through special conduction pathways to a second specialized group of cells localized between the atria and ventricles. These cells are referred to as the atrioventricular (AV) node. The time delays in the signal conducting from the SA node and the AV node synchronize the beating rhythms of the atria and ventricles for optimum blood outputs. Pacemakers are used if a heart beats too slowly (bradycardia) because of diseases in the heart's own pacemaker or electrical conduction system (such as the AV node or HIS–Purkinje system abnormalities).

A pacemaker is implanted just under the skin either over or under the pectoral muscle. The pacemaker is connected to the heart via a lead (or leads) that is inserted through a vein and positioned in the heart muscle. Leads may be inserted in the muscle of the right atrium, right ventricle, or indirectly to regions of the left ventricle via cardiac veins accessible from the right side of the heart, i.e., the coronary sinus. A schematic of an implantable pacemaker and leads is shown in Fig. 4.1. The lead carries both the electrical impulse generated by the pacemaker to the heart and the heart's electrical signals back to the pacemaker for analysis. The pacemaker contains a battery and a tiny computer that interprets the heart's signals and formulates pulses to stimulate the heart to contract.

A pacemaker may have one, two, or three leads, depending on the type of heart problem diagnosed. A single chamber pacemaker uses one lead, either in the right atrium or right ventricle, to increase the heart rate. A dual chamber pacemaker paces both the right atrium and right ventricle. A biventricular

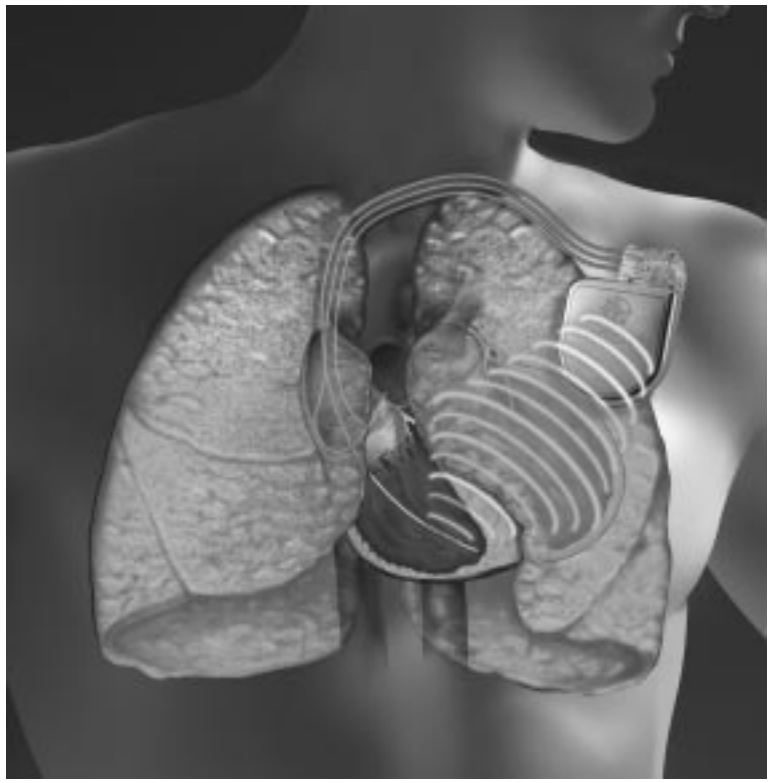

4.1 Schematic of an ICD system showing two pacing leads, the pulse generator, and positioning within the thoracic region (courtesy of Medtronic, Inc.).

pacemaker uses three leads: one placed in the right atrium, one placed in the right ventricle, and one placed in the left ventricle indirectly. The biventricular device imparts what is commonly referred to as cardiac resynchronization therapy (CRT).

4.2.2 Pacemaker pulse generators

Pacemakers are also called pulse generators or pacemaker cans. While a pulse generator and leads work together, the generator is implanted separately from the leads. It has its own implant site and can be removed or replaced with different units. The earliest pacemakers were simple in their designs, requiring only a power source and a few transistors to provide a stable series of electrical output pulses to stimulate the cardiac tissue.

Modern pacemakers provide a wide array of functions including on-board microprocessors for signal processing and therapy optimization, wireless telemetry for communication to the outside world, and diagnostic data storage.

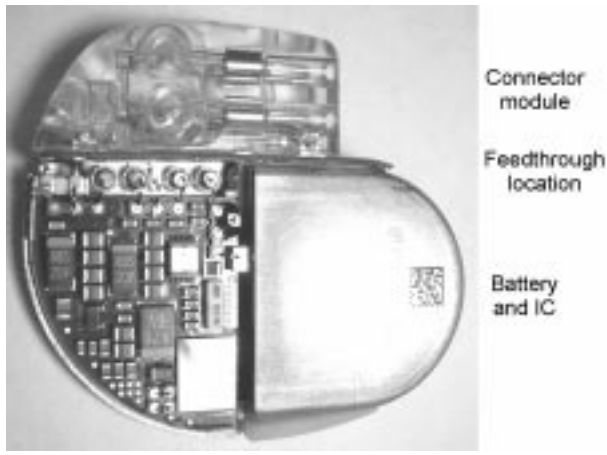

4.2 Internal view of a pacemaker. The component at the top is referred to as the connector module (courtesy of Medtronic, Inc.).

These features provide the crucial sensing and pacing functions and opportunity for remote monitoring and reprogramming by physicians.

Figure 4.2 shows an implantable pacemaker with one half of the shield removed to show internal components, including integrated circuits (ICs), discrete components, electrical feedthroughs, and the battery. These components are housed inside titanium shields which are welded shut to prevent moisture ingress into the electronics. The transference of signals between the inside and the outside of the cans is completed by the wires leading out of the cans through special components called feedthroughs. These feedthroughs are highly insulated, sealed against moisture permeation, and mechanically fixed to the cans.

Epoxy resin and stainless steel were used in some of the earlier pulse generators. Today, titanium is the most commonly used material. Titanium has been proven to be well accepted upon implantation in the human body (biocompatible) and quite stable against corrosion under biological environments (biostable). It is lighter than stainless steel, yet rigid and strong enough to protect the electric components inside the cans from mechanical damage. Its good electric conductivity allows it to function, when needed, as an additional electrode, e.g., in unipolar systems. In certain cases, a Parylene coating (polyparaxylylene) is partially applied to the surface of cans to further improve its biocompatibility and biostability.

One complication with pacemaker pulse generators is bacterial infection. The rate of infection has been low (1–7%) (Darouiche, 2001). However, if infection happens, the device is often replaced even though its function is intact. This is because the bacteria aggregate and form a biofilm on the surface or corners of the implant, making treatment with antibiotics often poor or ineffective.

4.2.3 Pacemaker connector modules

A connector module is the component that physically and electrically connects the pulse generators with leads (Fig. 4.2). It has a metal scaffold, typically made of stainless steel, embedded into a molded polymeric block, usually made of rigid polyether polyurethane or epoxy. The connector module is bonded to the can directly on top of the feedthroughs. The metal scaffold connects the wires from the feedthroughs to the electrodes of the leads inserted into the module. The connector module contacts host tissue with its polyether polyurethane surface. A critical feature for the connector to properly function is its bonding with the pulse generator. Surface cleaning and treatment to promote adhesion are necessary steps in manufacturing. Electric insulation between the multiple electrodes and conducting wires is also critical for the device function and reliability. The stability of conductor modules, especially chronic stability associated with chemical degradation and mechanical creep, must be carefully considered.

4.2.4 Pacemaker leads

Pacing leads are 'wires' that carry the electricity from the pacemaker to the heart. Pacemaker leads are implanted through a vein in the chest and fixed to the inside of the heart chamber. The functions of leads are simple, but they have a number of components to ensure proper performance. Maintaining proper functionality of leads relates in part to a constant relative movement between the heart and lead(s) as the heart beats. A heart beats approximately 32 million times a year (at 60 beats/minute). Along with being biocompatible and biostable, the various components of the lead must withstand these cyclical mechanical interactions. At the heart itself, lead fixation to the endocardial surface of the heart is critical, and is made possible with a tip fixation component. At the opposite end is the critical connector that allows the lead to be fastened to the connector module of the pacemaker. The other crucial lead components are: an electrical conductor that carries electric signals between the can and the pacing site; insulation material that isolates the conductors; and the important electrode tip that senses and delivers the electrical therapy. A picture of a whole lead is shown in Fig. 4.3.

Lead fixation

Once inside the heart, a pacing lead must be affixed to the heart muscle to provide proper electrical pacing pulse. Fixation is either active (traumatic fixation), achieved from an extendible/retractable screw-in electrode, or passive (atraumatic), accomplished by using tines that can be trapped in the trabeculae of the heart (Fig. 4.4). Tines are made of flexible polymers such as polyether polyurethane. Proper fixation is critical to prevent dislodging of electrodes

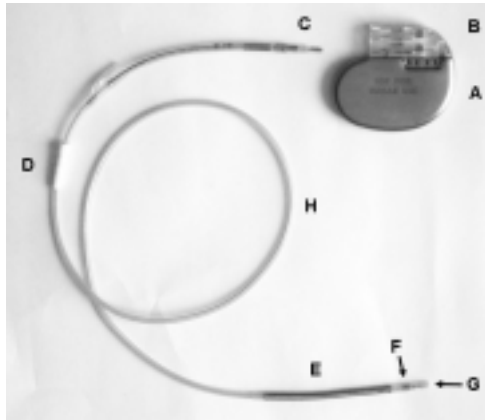

4.3 Picture of an entire lead with functional segments. A, pulse generator; B, connector module; C, lead connector. C is inserted into B by the surgeon in the operation room. D, suture ring; E, defibrillation coil; F, ring anode (for pacing); G, tip cathode (for pacing); H, lead body (courtesy of Medtronic, Inc.).

within the first few days to weeks after implantation. Over time, the implanted leads are integrated into the heart muscle.

Lead connector

Pacing leads are manufactured and packaged separately from pulse generators. After preparing the pectoral pocket and positioning the leads in the patient, the surgeon connects the leads and pulse generator by inserting the connector ends of the leads into the cavities on the connector module of the pulse generator. The function of the lead connector is to secure the mechanical and electrical connection between the generator and leads so that the electrical therapy generated in the can is uninterrupted and properly delivered to the heart. The lead connector is made of strong and rigid materials for this purpose. Resistance to corrosion and

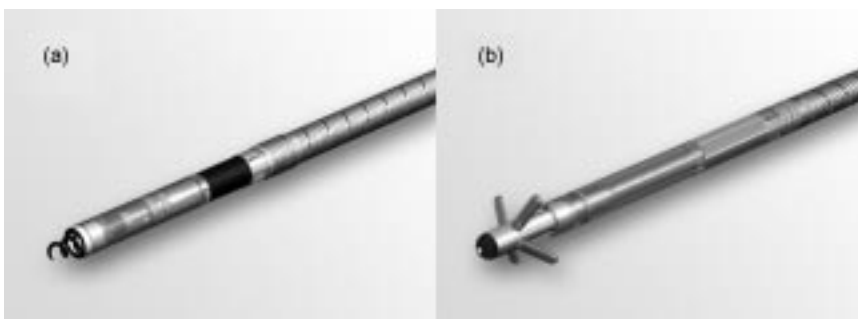

4.4 (a) Active fixation, extendible/retractable helix electrode. (b) Passive fixation, a tined tip electrode (courtesy of Medtronic, Inc.).

creep, and good electrical insulation performance are required for this component of the leads.

Conducting wires

Lead wires do not directly contact tissue, but they do perform the most important function: they carry the electric signals. The two major types of conductor designs in pacing leads are coils and cables (Fig. 4.5).

The coil, first suggested by Chardack, has been greatly attributed to reducing incidents of conductor fracture. Initially, wire used in coils was stainless steel, which occasionally corroded. Platinum and platinum alloys were used to reduce corrosion, but they were very expensive and wire fracture remained an issue. These materials were eventually replaced by the super-alloy MP35N, which has excellent corrosion properties and mechanical properties, making it ideal for use in coils. MP35N coils were improved upon by using multiple smaller diameter wires. Multiple smaller diameter wires allowed the electrical resistance to drop and extended the life of the coil. To further reduce the electrical resistance, a

4.5 Cross-section of a defibrillator lead body showing the small cable conductors and one larger coil conductor. Outside tubing insulates the conductors. The conductors themselves are mounted in a multilumen tubing that separates and further insulates the individual conductors (courtesy of Medtronic, Inc.).

drawn filled tube (DFT) was used. In the DFT wire, the core of the MP35N wire was filled with silver, which dramatically reduced resistance. Corrosion-resistant MP35N on the outside of the wire protected the silver from corroding.

Cables composed of many strands of pure MP35N or silver cored MP35N wires were implemented to further reduce electrical resistance in defibrillator leads. However, both coils and cables are still susceptible to fatigue fracture within the body under certain conditions. Moreover, by-products from MP35N corrosion, such as cobalt ions, have been implicated in the degradation of polyether polyurethanes' insulation materials, as seen in the complex metal ion induced oxidation process discussed below.

Insulation

Teflon® (polytetrafluoroethylene) and polyethylene were used as insulation in early leads. Both materials had a demonstrated history of use in tissue-contacting applications. However, Teflon bonded poorly to other parts of the lead, making production difficult. The use of polyethylene insulation also ended because it made stiff leads which can increase the possibility of perforating the heart. Its biostability has also come into question due to oxidation degradation associated with the inflammatory response. Polyester polyurethanes were tried because of their excellent mechanical properties but were ultimately rejected because they are subject to rapid hydrolytic degradation in water. Silicone rubber became the material of choice for insulation; it was nontoxic, chemically inert and biostable. Because of low tear strength, however, silicone rubber also needs thicker walls to minimize mechanical damage. It also has a high coefficient of friction in blood which made passing two leads in the same vein difficult. As a result, dual chamber pacing did not realize its full potential until after the 1970s.

Use of polyether polyurethane as a lead insulation began when it was found to be an almost ideal material for lead insulation. Polyether polyurethane showed acceptable biocompatibility for the application; it demonstrated hydrolytic stability; it showed high mechanical strength and lubricious properties when wetted with blood; it could be bonded to other materials; and it was much more flexible. The increased mechanical properties allowed the insulation thickness to be downsized. Smaller size, combined with lubricious surface in blood, made placement of two leads in one vein easier, which made dual chamber pacing a practical therapy. This evolution of materials applications demonstrates how a material itself can make complicated therapies possible.

Polyether polyurethanes are copolymers made through condensation reactions among polytetramethyleneoxide (PTMO), methylene diphenyl diisocyanate (MDI), and 1,4-butanediol (BDO) (Fig. 4.6). The percentage of PTMO and its molecular weights determine the mechanical properties of the end product. Polyurethanes with high PTMO contents and/or high PTMO molecular

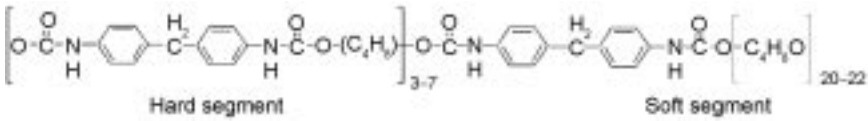

4.6 Chemical structure of an example of polyether polyurethane. The structure consists of distinct repeating hard and soft segments.

weights are soft and flexible, making them superior for lead insulation. Polyurethanes with low PTMO contents, however, are rigid and strong, making them more suitable for use in connector modules or lead connector ends. Commodity polyether polyurethanes are readily available (e.g., Pellethane® from Lubrizol), while medical-grade materials are made by only a few manufacturers. Examples of the latter include the brand names Elasthane® and Tecothane®.

Though polyether polyurethanes seemed to be an excellent insulating material early on, the softer grade polyether polyurethanes were found to be subject to two previously unknown failure mechanisms: metal ion oxidation (MIO) and environmental stress cracking (ESC). MIO was identified after a discovery of brittle cracking in lead insulation made of the soft grade polyether polyurethane. These cracks started from the insulation surface, at the side contacting the conducting metal wires it protected. This cracking developed when polyurethane insulation reacted with the metal ions that resulted from the corrosion reactions of conducting wires. MP35N has a very slow corrosion reaction and is not usually detected for commodity applications. Despite extensive prior preclinical and clinical tests, however, this rare reaction caused significant insulation failure of pacing leads (Fig. 4.7).

Unlike MIO, ESC is a ductile cracking that can appear on the lead external surface i.e., where direct tissue contact occurs and residual stress resides (Fig. 4.8). This failure was found to occur only *in vivo*. The term ESC is the same term as that used for a commonly observed failure mechanism that occurs in amorphous polymers (such as bisphenol A polycarbonate) that contact small molecular weight chemicals and are under mechanical stress (Ward and Hadley, 1993). However, these two mechanisms are fundamentally different. *In vivo* ESC in polyether polyurethane surfaces results from chemical degradation reactions of the polyether segments by the oxidative agents produced by inflammatory cells in the surrounding tissues. When foreign materials are implanted, the body defends itself in a series of biological reactions that attempt to destroy and wall-off the implant. Inflammation reactions are part of the defence action that occurs immediately after implantation. Cells such as neutrophils and monocytes migrate to the implant surfaces and produce oxidative agents in the attempt to degrade the foreign material. If an implant is large and stable, and does not release toxic chemicals and particulates, the inflammation reactions will demonstrate the pathway of a common foreign body response. Fibrous capsules form and separate the implant from the surrounding body

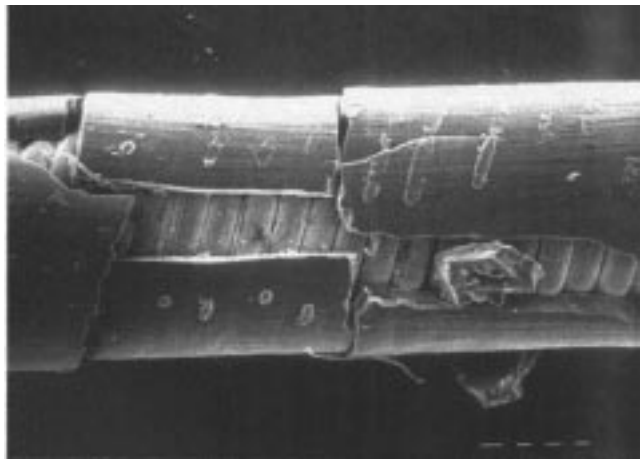

4.7 Metal ion oxidation (MIO) breach in inner insulation of lead made of a polyether polyurethane (courtesy of Medtronic, Inc.).

tissue. Inside the capsule are foreign body giant cells that directly contact the materials and continuously secrete oxidative agents in the attempt to degrade the structures.

After years of investigation, these oxidative agents were found to be responsible for the environmental stress cracking of the lead insulation. Here, specific polyether components on the outside surface of the lead insulation were observed to be oxidized by these agents. This combined chain breakage and residual stress resulted in ductile cracking in the insulation surface (Zhao *et al.*, 1991; Casas *et al.*, 1999; Lyu and Untereker, 2009). This degradation reaction is a unique, biological mechanism that is difficult to predict by simple *in vitro* tests. Nonetheless, some progress has been made in this area and its importance is addressed in ISO 10993, Part 13: Identification and Quantification of Degradation Products from Polymeric Devices (ISO 10993, 1997).

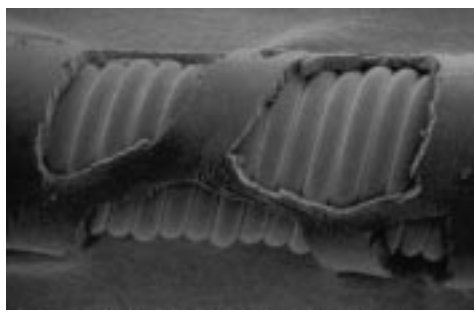

4.8 Biological environmental stress cracking (ESC) breach in outer insulation of lead made of polyether polyurethane (courtesy of Medtronic, Inc.).

Electrodes

Early transvenous leads had a relatively large electrode diameter (e.g., 4 mm). Irnich showed that the theoretical optimum (spherical) electrode radius for stimulation was approximately 0.7–1 mm, corresponding to the thickness of the fibrous capsule layer that frequently forms around it (Irnich, 1973). Under a given voltage, the highest electrical field should be in the tissue surrounding an electrode of optimum size. However, determining the optimum electrode size is a complicated matter. On one hand, a smaller size electrode has higher pacing impedance, resulting in lower current drain and longer pacemaker longevity. On the other hand, a smaller electrode has higher electrode polarization, which affects its cardiac sensing functions and pacing efficiency.

In the late 1970s, small electrodes with porous surface were introduced (Fig. 4.9). These structures produced high pacing impedance because of their small size (radius), but their increased surface area from the porosity resulted in much lower polarization, providing better sensing than polished electrodes. This development solved the problem caused by the two constraints mentioned above. The pores might also facilitate tissue ingrowth, which aided fixation to the cardiac wall tissue. Porous surface coatings used today include platinum black, titanium nitride, iridium oxide and activated carbon.

A problem for early lead electrodes was that the pacing threshold increased over time. A pacing threshold is the minimum voltage electrodes need to apply to tissues for them to respond. An increased threshold can cause failure of pacing and/or increase in energy consumption that reduces the longevity of the device. An increased threshold was found to be associated with inflammatory

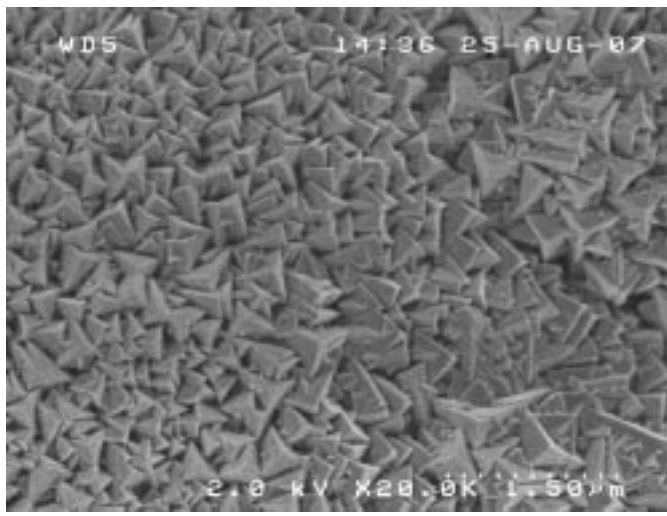

4.9 Scanning electron microscope (20 000×) of a titanium-nitride coated electrode (courtesy of Medtronic, Inc.).

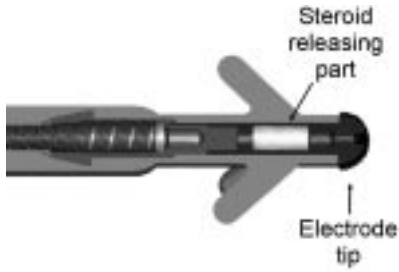

4.10 Cross-section of steroid eluting electrode (courtesy of Medtronic, Inc.).

reaction at the electrode tip insertion site. In particular, formation of the foreign body fibrous capsule surrounding the electrode resulted in an increased impedance of the electrode–tissue interface.

The steroid-eluting electrode, invented by Stokes in early 1980s, was the breakthrough technology that solves this problem. The steroid was combined with silicone to form a plug that was positioned inside the electrode shank behind the porous tip (Fig. 4.10). The steroid elution through the porous material thus mitigated the foreign body response at the electrode tip. This combined electrode technology was seen to result in a minimal-to-no threshold rise as a function of implant time. Like the introduction of thinner biostable polyurethanes, the introduction of the steroid-releasing lead reshaped electrical stimulation device technology, in this case, by allowing more reliable pacing, longer battery life, and more accurate sensing.

Electrode materials used in early transthoracic temporary pacemakers included tantalum, silver plated copper, and stainless steels. Silver-plated copper and stainless steel gave way to more corrosion-resistant materials such as platinum, platinum–iridium alloys, and activated carbon. Titanium has also been used. Under controlled conditions, oxides of varying structures can be grown on titanium electrode surfaces. These oxides are stable in the body, even when charged. Titanium oxide electrodes have been used successfully in Europe for more than 25 years. The negative aspect of titanium is its poor radiopacity, which makes implant placement difficult because of poor tip visibility with X-ray imaging methods.

4.3 Defibrillators

An implantable cardioverter defibrillator (ICD) detects tachycardia and fibrillation, and shocks the heart to restore the normal rhythm. ICDs provide a tiered therapy that escalates in energy to defibrillate the heart. If the device detects a tachyarrhythmia, or fibrillation, it first attempts to pace the heart out of fibrillation (anti-tachycardia pacing). If pacing fails, the ICD escalates to deliver a low energy shock. If the low energy shock fails to stop the tachyarrhythmia,

then high energy shocks (30–35 J) are delivered at about 800 V to stop the tachyarrhythmia. Additionally, ICDs can deliver 'back-up' pacing if bradycardia occurs.

An ICD can be thought of as a derivative of the pacemaker. Both share basic structures, working principles, materials, biocompatibility, and implantation procedures. Like the pacemaker, an implantable defibrillator device includes a pulse generator and leads. The pulse generator is made of titanium, the connector module is made of rigid polyurethane, its lead insulation is made of soft polyurethane or silicone, and its electrodes are made with platinum or platinum-plated metals.

These defibrillators, however, have more functions than pacemakers. They deliver a much higher energy (30–35 J in less than 1 second) at a much higher voltage than pacemakers. No battery in a current implantable device can have a discharge rate high enough for this fast, high energy delivery. Therefore, ICD pulse generators have capacitors to form and store high energy packages for delivery within a short period of time, as needed. The ICD battery and capacitor occupy about half to two-thirds of its volume. The ICD lead has one or two long defibrillation coils to deliver cardioversion (low energy) or defibrillation (high energy) shocks. These coils have large surface areas to increase defibrillation efficacy and, at the same time, reduce failure risk from corrosion. One coil is always in the right ventricle. A second coil is in the superior vena cava.

ICD cans are an integral portion of the circuit, similar to unipolar pacemakers whose titanium cans on the devices that become part of the electrical circuit formed between the device and the human body. The shock electrical field is between the device and the right ventricle coil, when one coil is used. An electric field between the superior vena cava coil and the right ventricle coil is added when a second coil is used. The device is used as one electrode, permitting more efficient delivery of high energy from the ICD to the cardiac muscle. Without the can in the defibrillation circuit, the device would require a great deal more energy and/or different, possibly less comfortable device and lead configurations within the body to supply the high energy shocks across the heart needed to stop a life-threatening arrhythmia.

4.4 Neurostimulators

Researchers and engineers developing neurostimulation devices borrowed extensively from cardiac stimulation technology since many fundamental design requirements of both technologies are similar, and numerous cardiac pacing technologies were already standard-of-care therapies. Neurostimulation applications do, however, include a number of different requirements for the various therapies. The sections that follow describe some well-developed neurostimulation applications that emerged from pacing technologies.

4.4.1 Structures and functions of neurostimulators in comparison with pacemakers

Neurostimulation therapies consist essentially of exposing the electrically excitable tissue of the central or peripheral nervous system to voltage pulses applied to electrodes located in close proximity to the nervous tissue. These voltage pulses cause a depolarization or hyperpolarization of the nerve cells. As in real estate, the effectiveness is extremely dependent on 'location, location, location'. Voltage pulses must be applied to the appropriate spot in the 'wiring diagram' of the nervous system to obtain the desired effect. Like pacing, different lead designs are required for different therapy applications. Moreover, neurostimulation leads present distinctly different designs compared with pacing leads because of the critical nature of the implant site location.

Structurally, neurostimulators are similar to pacemakers and defibrillators. That is, a hermetically sealed electronic package is implanted subcutaneously and connected to lead wires containing electrodes for delivering stimulation to a unique anatomical target required for the specific therapy. In current commercial

4.11 Deep brain stimulation (DBS). Brain leads are implanted using stereotactic procedures and connected to an extension wire tunnelled under the skin along the neck. This latter then connects to the stimulation electronics located in a subcutaneous pocket inferior to the clavicle (courtesy of Medtronic, Inc.).

applications of neurostimulation, the leads may be placed in the brain parenchyma, in the spinal column over the dura mater covering the dorsal aspect of the spinal cord, or in close proximity to a peripheral nerve. The electronics package, or implanted neurostmulator (INS), may be located in a subcutaneous pocket just inferior to the clavicle for deep brain stimulation (DBS) therapy (Fig. 4.11). The INS may be located in a subcutaneous pocket in the abdomen, the flank, or the buttocks for SCS therapy involving the thoracic spine or sacral nerve stimulation (Fig. 4.12).

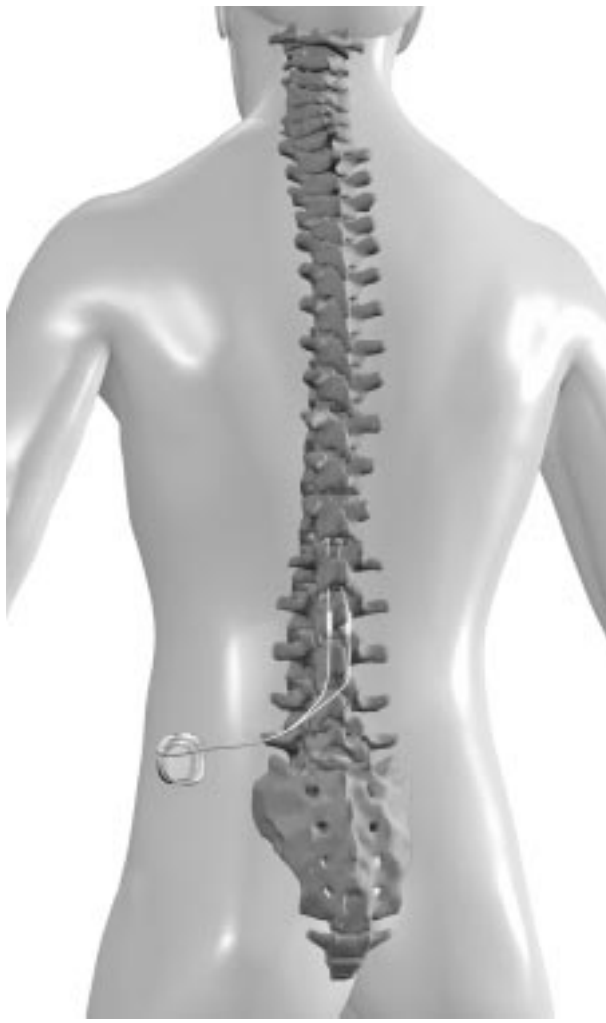

4.12 Spinal cord stimulation (SCS). Leads are inserted into the epidural space at a spinal segment appropriate for the location of the presenting pain (courtesy of Medtronic, Inc.).

When applications require leads to traverse a relatively long distance, an extension lead is inserted in the circuit. This extension may have a more robust design than the lead in order to address the design requirements. For example, DBS applications often make use of an INS implanted in a subcutaneous pocket inferior to the clavicle. Here, an extension lead traverses the neck, making connection to the main lead at a location behind the ear on the skull. This configuration allows the main lead to be designed for implanting in the brain, while the extension lead can be designed for the significant mechanical demands of traversing the neck region.

The leads used in neurostimulation are specifically designed for the particular anatomical target being stimulated. Most important is the configuration of electrodes on the lead. An electrode array design is used to optimize the ability of the clinician to couple the stimulation voltage to the appropriate nervous tissue (Figs 4.13 and 4.14). The wide variety of anatomical locations targeted for neurostimulation can be grouped into two broad categories: those outside the blood–brain barrier (SCS and peripheral nerve stimulation), and those that

4.13 Two versions of electrode spacing in DBS leads. Individual electrodes can be programmed to be positive, negative, or off. The Model 3389 lead, on the right, has electrodes more closely spaced together. This feature allows more alternatives for stimulation within a smaller space, compared with the Model 3387 lead seen on the left (courtesy of Medtronic, Inc.).

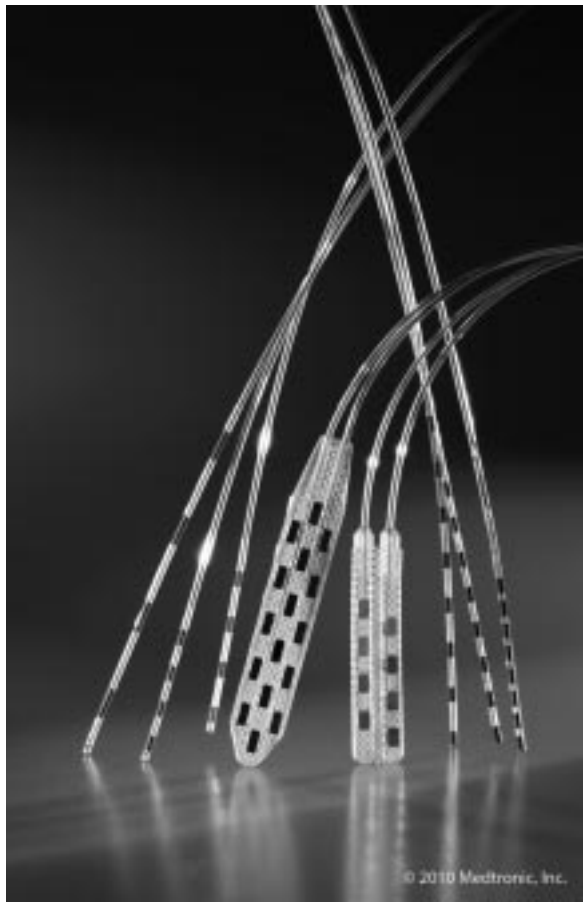

4.14 Variety of leads available for SCS. The cylindrical leads may be passed through a needle into the epidural space. The flat paddle leads require a laminotomy procedure to remove the bone for insertion. The individual electrodes may be programmed to be positive, negative, or off. Electrode choices facilitate stimulation of the appropriate nerve fibers matching the distribution of pain (courtesy of Medtronic, Inc.).

traverse the dura and have a portion of the lead within the cerebral spinal fluid compartment, such as DBS therapies.

4.4.2 Materials for neurostimulators

Materials used for components of neurostimulators are similar to those in cardiac pacing and defibrillation technologies. The INS electronics, like pacemakers, are packaged in a titanium case. Some neurostimulation applications require considerably more energy than cardiac pacing therapies because of

unique and much higher stimulation rates required to achieve a therapeutic effect in neurostimulation. As a result, some INS models use rechargeable battery technology to extend the life of the device.

Neurostimulation leads consist of multiple conductors, each electrically insulated using high performance materials such as fluoropolymers. Individual conductors can be made of MP35N or Pt-Ir alloys, and formed into helical coils or a braided wire. These conductors are further insulated within an insulating polymer jacket that may be made from a silicon polymer or a polyether polyurethane polymer.

4.5 Engineering approaches to solve material problems

Material scientists and engineers often try to develop new materials or modify existing materials to meet design requirements for new product development concepts. In the medical device industry, given the expense associated with the development, testing, and qualification of new materials for medical applications, the most common approach is to design new technologies using materials with a demonstrated history of safe use in particular applications. For medical devices, especially implantable devices, patient safety and risk mitigation must always be given the highest priority. However, unexpected problems are always possible given the demand for increasingly complex medical devices to work in the complicated milieu of the biological environment, and the fact that *in vitro* tests and animal models often used in development are not perfectly predictive. Importantly, many unmet material needs can be solved by applying fundamental engineering principles. The success of this approach requires careful attention to specific device design, functions, manufacturing, and testing efforts.

One example of applying fundamental engineering principles, mentioned previously, addressed the problem of pacing threshold increases in response to inflammatory reaction occurring at an electrode–cardiac tissue interface. A natural response may have been to seek out a new electrode material or surface treatment that did not trigger an inflammation reaction. After decades of research, however, a material has yet to be found that does not cause an inflammatory reaction. A few materials have demonstrated minimal or no inflammation reactions in certain research laboratories, but there is no record indicating similar results in a chronic implantation. The use of a simple existing technology – a monolithic controlled-release of anti-inflammatory steroid at the electrode tip – successfully reduced inflammatory reaction to a level that did not cause significant increases in pacing thresholds. This approach not only provided a very effective way to solve the threshold increase problem for pacing leads, but also suggested a principle to solve problems related to material–biological interactions by combining devices with biologically active agents. Today's drug eluting stents, antimicrobial coatings, and rhBMP2-charged,

lumbar-tapered fusion devices are examples of this direction. This combination product approach is expected to continue producing more examples of synergistic devices and biological engineering products.

Similar combination ideas have been used at all levels of device design. MIO is another example mentioned previously. MIO resulted when metal ions from conducting wire corrosion reacted with the lead insulation polymer. MIO was successfully minimized by applying a barrier layer to the wire, which effectively prevented metal corrosion and release of ions into the polymer insulation.

In a final example, recall the lead design used in DBS therapy. This particular design offered a very simple approach to the design of a neurostimulation device that meets the needs of the two mechanically different implant environments. Here, the solution was not a single complex lead that met the two requirements, but rather a two-lead solution: a fine lead for positioning in the brain, and a more robust lead to handle the mechanically dynamic neck region.

4.6 Reliability and testing

Though materials and engineering principles used for implantable medical devices are essentially the same as those for other products, strict requirements exist for patient safety, demonstrated effectiveness and reliability. The scrutiny required to meet these requirements is intense, and as expected this adds a very heavy burden and risk to device manufacturers.

Even with the best of intentions, things can go awry. For example, prior to Food and Drug Administration (FDA) regulations enacted in 1976, a pacemaker called Xytron was introduced. To ensure the device reliability, extra engineering measures were used. The device circuitry was first encased in an epoxy pocket, then sealed in a metal case. Later, it was discovered that the seal of the soldered case could fail, allowing moisture to enter the case, permeate the epoxy pocket, and reach the circuitry imbedded inside. The moisture combined with the ionic residual of the solder aid made a conductive path in the pocket. The leaking current gradually caused the growth of dendrites (metal crystals) which shorted out the circuitry. Clearly, systems that ensure product reliability and test methods that capture failure modes are critical to prevent device complications and failures.

Downsizing, adding more functions, and increasing longevity have been constant driving forces in the device industry. These development goals must be combined with the universal goal of improving device reliability. There may be a conflict with this direction down the road.

Figure 4.15 shows the downsizing trends of some leads developed from 1980 to 2000. As mentioned, the defibrillation voltage is about 800 V. A typical polymer insulation material has an electrical strength of 20 V/μm. This high voltage would require the insulation layer to be at least 40–50 μm thick. With the effort of lead downsizing, we may soon approach this limit.

4.15 Various Medtronic lead designs from 1980 to 2000. Over time, technology and market forces have lead to the development of smaller diameter leads (courtesy of Medtronic, Inc.).

Many device failure examples indicate that device problems are often caused by unexpected failure mechanisms. Testing is one of the most critical steps to ensure reliability in product development. Prior to testing, a failure mode and effects analysis is conducted for an intended application. Cross-interactions among the components of the same devices are considered. A full or partial biocompatibility assessment in accordance with ISO 10993 and relevant *in vitro* and *in vivo* chemical and mechanical stability tests are performed.

Commonly used factors for chemical stability tests include pH, lipid, metal ions (relevant to metals in the same devices), enzymes, per-oxidative agents (for inflammation), biological agents (combination products), and corrosion products (for metals). Mechanical tests include material property assessments (e.g., tensile, fracture, and bending) and long-term stability assessments (e.g., creep and stress relaxation, environmental cracking, and wearing). These screening tests provide valuable information to grade the acceptability of a material for its intended application.

If the materials pass the test criteria, they are made into the intended parts and assembled with other parts into individual modules or a whole device, and tested *in vitro* following the application requirements. If passed, the whole devices are tested *in vivo* for safety and efficacy. Upon passing these tests in this sequence, the development work moves on to clinical trials. This is the general process for introducing completely new materials or devices, and is required by regulatory bodies worldwide before a device may be released into the market. But, research does not stop here. Manufacturers continue to conduct post-market surveillance on products implanted in the patients for a number of years to monitor product safety. This leads to a deeper and broader understanding of the device performance and provides feedback for the device manufacturers to continuously improve their devices.

Except for ISO 10993 and a few other vertical device guidance documents, there are few other standard procedures (Tables 4.1 and 4.2). Testing protocols and *in vivo* models are designed according to specific device applications, though none has been found to be entirely predictive of human applications. Applying sound rationales and having experience can be invaluable when interpreting some of these standards. In many cases, test work can be easier if the development work is to replace an existing material or component with an

equivalent one, particularly if the new material has a demonstrated history of safe use in a similar application. In these cases, the tests are simply designed to prove the replacement is truly equivalent to the old one.

4.7 Future electrical stimulation devices

Electrical stimulation devices have evolved from pacemakers into defibrillators and neural stimulators, and will continue to move in new directions to bring forth numerous new therapeutic treatments. Recently, there has been a rise in the research of neural interfacing, neural prostheses, and neural signal processing and imaging, as well as an expansion of neurostimulation (He, 2005). These research activities are expected to open new areas of electrical stimulation and sensing technologies to augment physical abilities of healthy individuals and help neurologically impaired people.

Another exciting development is the application of electrical stimulation to the gastrointestinal (GI) tract. The first such application for the treatment of post-operative ileus was reported as early as 1963 (Bilgutay *et al.*, 1963). Research on gastroparesis, a debilitating gastric motor disorder, led to the development of Enterra therapy that has been demonstrated to be effective in suppressing certain symptoms (Abell *et al.*, 2002, 2003).

In the past decade, there has been growing interest in electrical stimulation of the GI tract as a potential therapy for obesity. Much of the recent work has focused on the ability of gastric stimulation to modulate activity along the brain–gut axis in a manner consistent with the down-regulation of feeding. For example, gastric electrical stimulation (GES) has been shown to modulate gastrointestinal motility (Sarnelli *et al.*, 2003; Ouyang and Chen, 2007; Song *et al.*, 2007, 2009; Zhang *et al.*, 2009a), the central nervous system (Qin *et al.*, 2005, 2007; Sun *et al.*, 2006; Zhang *et al.*, 2009b), and the level of peptides known to be involved in the regulation of feeding (Tang *et al.*, 2006; Zhang and Chen, 2006; Xu *et al.*, 2007; Liu *et al.*, 2008). Similar to neurostimulation, the magnitude of all of these effects depends upon the stimulation targets and parameters. However, the parameters that appear to be most effective in this area are outside the range of most implantable neurostimulation devices. Therefore, a new generation of engineering designs and biomaterials for 'gut stimulation' devices may be required.

It is fair to say that medical device trends are strongly affected by other technologies. Many research activities of electric stimulation can be attributed to the successes in other areas. Rapid progress in imaging and navigation technologies made neurostimulator implantation possible. The wide uses of magnetic resonance imaging (MRI) techniques created a need for MRI-compatible devices. Rapid advances in drug delivery technology helped drive the development of drug–device combination products. Sensing, wireless, and IT technologies combined to provide opportunities to merge biological sensing,

monitoring, and remote access functions with the existing devices. Electrical stimulation has been an exciting arena of research and development for six decades, and will continue to be a field rich in new technology and therapy development opportunities for years to come.

4.8 Acknowledgements

The authors thank Dr Warren Starkebaum for the contribution of writing the review of gastric electrical stimulation. The authors also thank Medtronic Inc., for support in preparing this chapter.

4.9 Sources of further information and advice

ISO 10993:1997 Biological evaluation of medical devices Parts 1–20. 1997

ISO 11318:2002 Cardiac defibrillators – connector assembly DF-1 for implantable defibrillators – dimensional and test requirements, Second Edition, 1 August 2002.

ISO 5841-3:2000 Implants for surgery – cardiac pacemakers – Part 3: Low-profile connectors (IS-1) for implantable pacemakers, 15 October 2000.

ISO 27186:2010 (FDIS), Active implantable medical devices – Four-pole connector system for implantable cardiac rhythm management devices – Dimensional and test requirements, November 2009. (Note: This document is being circulated as a Final Draft International Standard.)

CEN EN 45502-1, Active implantable medical devices – Part 1: General requirements for safety, marking and information to be provided by the manufacturer, 1 August 1997.

CENELEC EN 45502-2-1, Active implantable medical devices – Part 2-1: Particular requirements for active implantable medical devices intended to treat bradyarrhythmia (cardiac pacemakers), 1 December 2003.

CENELEC EN 45502-2-2, Active implantable medical devices – Part 2-2: Particular requirements for active implantable medical devices intended to treat tachyarrhythmia (includes implantable defibrillators), 1 March 2008.

ISO 14708-1:2000, Implants for surgery – Active implantable medical devices – Part 1: General requirements for safety, marking and for information to be provided by the manufacturer, 15 November 2008.

ISO 14708-2:2005, Implants for surgery – Active implantable medical devices – Part 2: Cardiac pacemakers, 2nd Edition, January 2008.

ISO 14708-3:2008, Implants for surgery – Active implantable medical devices – Part 3: Implantable neurostimulators, 15 November 2008.

ISO 14708-6:2010 (FDIS), Implants for surgery – Active implantable medical devices – Part 6: Particular requirements for active implantable medical devices intended to treat tachyarrhythmia (including implantable defibrillators), December 2009. (Note: This document is being circulated as a Final Draft International Standard.)

CDRH Guidance for Industry: Guidance for the Submission of Research and Marketing Applications for Permanent Pacemaker Leads and for Pacemaker Lead Adaptor 510(k) Submissions, US Department of Health and Human Services, Food and Drug Administration, Center for Devices and Radiological Health, Interventional Cardiology Devices Branch, Division of Cardiovascular and Respiratory Devices,

Office of Device Evaluation: 1 November 2000, http://www.fda.gov/downloads/MedicalDevices/
DeviceRegulationandGuidance/GuidanceDocuments/UCM073684.pdf, accessed 9 February 2010.

4.10 References

Abell T L, Van Cutsem E, Abrahamsson H, Huizinga J D, Konturek J W, Galmiche J P, VoelIer G, Filez L, Everts B, Waterfall W E, Domschke W, des Varannes S B, Familoni B O, Bourgeois I, Janssens J and Tougas G (2002), 'Gastric electrical stimulation in intractable symptomatic gastroparesis', *Digestion*, **66**, 204–212.

Abell T L, McCallum R, Hocking M, Koch K, Abrahamsson H, LeBlanc I, Lindberg G, Konturek J, Nowak T, Quigley E M M, Tougas G and Starkebaum W (2003), 'Gastric electrical stimulation for medically refractory gastroparesis', *Gastroenterology*, **125**, 421–428.

Bilgutay A M, Lillehei C W, Wingrove R, Griffen W O and Bonnabeau R C (1963), 'Gastrointestinal pacing: a new concept in the treatment of ileus', *Biomed Sci Instrum*, **1**, 377–383.

Casas J, Zhao Q, Donovan M, Schroeder P, Stokes K and Untereker D (1999), '*In vitro* modulation of macrophage phenotype and inhibition of polymer degradation by dexamethasone in a human macrophage/Fe/stress system', *J. Biomed Mater Res*, **46**, 475–484.

Chardack W M, Gage A A and Greatbatch W (1960), 'A transistorized, self-contained implantable pacemaker for the long-term correction of complete heart block', *Surgery*, **48**, 643–654.

Darouiche R O (2001), 'Device-associated infections: a macroproblem that starts with microadherence', *Clinical Infectious Diseases*, **33**, 1567–1572.

De Kroon J R, Ijzerman M J, Chae J, Lankhorst G L and Zilvold G (2005), 'Relation between stimulation characteristics and clinical outcome in studies using electrical stimulation to improve motor control of the upper extremity in stroke', *J Rehabil Med*, **37**, 65–74.

Efimov I R, Kroll M W and Tchou P J (2008), *Cardiac Bioelectric Therapy: Mechanisms and Practical Implications*, New York, Springer-Verlag.

Elmqvist R and Senning A M (1960), 'An implantable pacemaker for the heart', in Smyth CN, *Proceeding of the Second International Conference of Medical Electronic*, Paris, June 24–27, 1959, London, Iliffe, 253–254.

Furman S (2000), 'Introduction: history of cardiac pacing', in Ellenbogen K, Kay G N and Wilkoff B L, *Clinical Cardiac Pacing and Defibrillation*, London, W. B. Saunders Company, 1–13.

Furman S and Robinson G (1958), 'The use of an intracardiac pacemaker in the correction of total heart block', *Surg Forum*, **8**, 245–248.

He B (2005), *Neural Engineering*, New York, Kluwer Academic/Plenum Publishers.

Hosobuchi Y, Adams J E and Linchitz R (1977), 'Pain relief by electrical stimulation of the central gray matter in humans and its reversal by naloxone', *Science*, **197**, 183–186.

Hyman A S (1930), 'Resuscitation of the stopped heart by intracardiac therapy', *Arch Intern Med*, **46**, 553–568.

Hyman A S (1935), 'Resuscitation of the stopped heart by intracardiac therapy IV. Further use of the artificial pacemaker', *US Navy Med Bull*, **33**, 205–214.

Irnich W (1973), 'Considerations in electrode design for permanent pacing' in Thalen H J, *Cardiac Pacing*: *Proceedings of the Fourth International Symposium of Cardiac Pacing*, 268–274.

Jonas U, Fowler C J, Chancellor M B, Elhilali M M, Fall M, Gajewski J B, Grünewald V, Hassouna M M, Hombergh U, Janknegt R, van Kerrebroeck P E, Lylcklama a Nijeholt A A, Siegel S W and Schmidt R A (2001), 'Efficacy of sacral nerve stimulation for urinary retention: results 10 months after implantation', *J Urology*, **165**, 15–19.

Lidwell M C (1929), 'Cardiac disease in relation to anaesthesia', in *Transactions of the Third Session*, Australia Medical Congress, Sydney, Australia, 2–7 September 1929, 160.

Lillehei C W, Gott V L, Hodges P C, Long D M and Bakken E E (1960), 'Transistor pacemaker for treatment of complete atrioventricular dissociation', *JAMA*, **172**, 2006–2010.

Liu S, Tang M, Tao S and Chen J D (2008), 'Central expressions of ghrelin and cholecystokinin in rats with gastric electrical stimulation', *Obes Surg*, **18**, 109–114.

Lyu S P and Untereker D (2009), 'Degradability of polymers for implantable biomedical devices', *Int J Mol Sci*, **10**, 4033–4065.

Melzack R and Wall P D (1965), 'Pain mechanisms: a new theory', *Science*, **150**, 971–979.

Mond H G, Sloman J G and Edwards R H (1982), 'The first pacemaker', *PACE*, **5**, 278–282.

Ouyang H and Chen J D (2007), 'Long-pulse gastric electrical stimulation at tachygastrial frequency reduces food intake by inhibiting proximal gastric tone', *Scand J Gastroenterol*, **42**, 702–707.

Qin C, Sun Y, Chen J D and Foreman R D (2005), 'Gastric electrical stimulation modulates neuronal activity in nucleus tractus solitarii in rats', *Auton Neuro Sci*, **119**, 1–8.

Qin C, Chen J D, Zhang J and Foreman R D (2007), 'Modulatory effects and afferent pathways of gastric electrical stimulation on rat thoracic spinal neurons receiving input from the stomach', *Neurosci Res*, **57**, 29–39.

Sarnelli G, Caenepeel P, Geypens B, Janssens J and Tack J (2003), 'Symptoms associated with impaired gastric emptying of solids and liquids in functional dyspepsia', *Am J Gastroenterology*, **98**, 784–788.

Shealy C N, Mortimer J T and Reswick J B (1967), 'Electrical inhibition of pain by simulation of the dorsal columns: preliminary clinical report', *Anesth Analg*, **46**, 489–491.

Song G Q, Hou X, Sun Y, Yang B, Qian W and Chen J D (2007), 'Effects of retrograde gastric electrical stimulation with pulse trains on gastric emptying of solids and plasma hormones in dogs', *Am J Surg*, **194**, 122–127.

Song G Q, Zhu H B, Lei Y, Yuan C, Starkebaum W and Chen J D Z (2009), 'Gastric electrical stimulation with wider pulses inhibits food intake and gastric motility in dogs', *Gastroenterology*, **136**, A-134.

Sun X, Tang M, Zhang J and Chen J D (2006), 'Excitatory effects of gastric electrical stimulation on gastric distension responsive neurons in ventromedial hypothalamus (VMH) in rats', *Neurosci Res*, **55**, 451–457.

Tang M, Zhang J, Xu L and Chen J D (2006), 'Implantable gastric stimulation alters expression of oxytocin- and orexin-containing neurons in the hypothalamus of rats', *Obes Surg*, **16**, 762–769.

Ward I M and Hadley D W (1993), *An Introduction of Mechanical Properties of Solid Polymers*, New York, John Wiley & Sons.

Williams D F (1987), *Definitions in Biomaterials, Progress in Biomedical Engineering*, Vol. 4, New York, Elsevier.

Xu J, McNearney T A and Chen J D (2007), 'Gastric/intestinal electrical stimulation modulates appetite regulatory peptide hormones in the stomach and duodenum in rats', *Obes Surg*, **17**, 406–413.

Zhang J and Chen J D (2006), 'Systematic review: applications and future of gastric electrical stimulation', *Alimentary Pharmacol Therapeut*, **24**, 991–1002.

Zhang J, Tang M and Chen J D (2009a), 'Gastric electrical stimulation for obesity: the need for a new device using wider pulses', *Obesity*, **17**, 474–480.

Zhang J, Maude-Griffin R, Zhu H, Sun Y, Starkebaum W, Firestone E and Chen J D Z (2009b), 'Gastric electrical stimulation alters ventral medial hypothalamic activity and food intake parameter-dependently in obese rats', *The 27th Annual Obesity Society Meeting*, Washington DC, October.

Zhao Q, Tonpham N, Anderson J M, Hiltner A, Lodoen G and Payet D R (1991), 'Foreign-body giant cells and polyurethane biostability: *in vivo* correlation of cell adhesion and surface cracking', *J Biomed Mater Res*, **25**, 177.

5

Mechanical and bioprosthetic heart valves

M. N. HELMUS, Biomedical Consultant, USA and
C. M. CUNANAN, Cunanan Consulting, USA

Abstract: Replacement heart valves routinely save thousands of lives each year, to replace damaged or diseased native valves and restore sufficient cardiac function for the patient. The clinician has a number of factors to consider when choosing an appropriate prosthetic valve for a patient, including their age and life expectancy, lifestyle and quality of life, and other comorbidities. The two main types of tissue heart valves include a valve fabricated from a native porcine aortic valve, or one fabricated with leaflets made from bovine pericardium. Clinical experience demonstrates that pericardial valves have a longer duration than porcine valves. There have been significant developments in both types of valves over the years, including improvements on valve design, materials, treatments, and fabrication methods. Future advances in heart valves include mechanical valves with improved hemodynamics and reduced damage to blood elements, percutaneous heart valves which can be implanted minimally invasively, and tissue engineered heart valves which have the ability to repair and grow.

Key words: heart valve, mechanical, tissue, bioprosthesis, prosthesis, replacement, pyrolytic carbon, porcine, bovine pericardium, xenograft, suture ring, biomaterials, biocompatibility.

5.1 Introduction

There are four valves in the heart which help direct the one-way flow of blood through the body. Figure 5.1 shows these four valves, and replacement valves have been made for each of them. Which valve(s) need replacement is a function of the patient's disease and history. Historically, the most common disease to affect the heart valves is rheumatic fever, which primarily attacks the mitral valve. Congenital defects can also require valve replacement for correction, and depending upon the severity of the defect, it may not become symptomatic until the patient is in their 40s. Aortic stenosis is the most common valve disease in developed countries, where calcification of the native valve results in a stiffening of the leaflets and overall degeneration of function. Stenosis of the aortic valve is a progressive condition with many similarities to coronary artery disease and patients typically become symptomatic in their fifth or sixth decade of life.

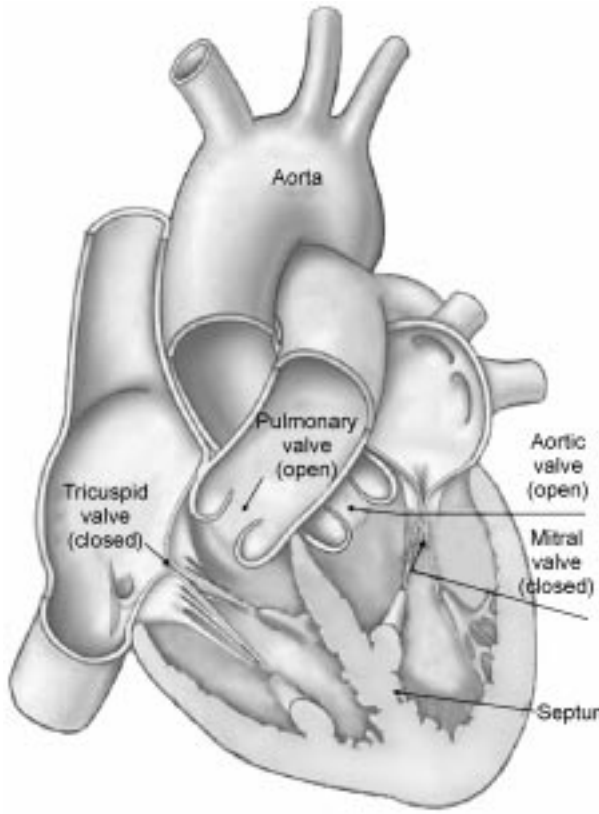

5.1 Cross-section of the heart, showing the location of the four valves of the heart. (Image adapted from Cleveland Clinic Foundation patient education website, www.ccf.org, 'your heart and blood vessels'.)

Patients with coronary artery and valve disease have a decreased life expectancy compared with healthy patients of the same age, and these patients may survive only 10–12 years after valve replacement surgery (Jones *et al.*, 1994; Puvimanasinghe *et al.*, 2003).

Valve replacement surgery became possible with the development of cardiopulmonary bypass, a technique which uses an external machine to oxygenate and pump the blood, allowing the heart to be stopped so it can be repaired. In the 1960s, human donor allografts were being used for heart valve replacement procedures, although it was not until the Starr–Edwards™ mechanical valve was commercially available a few years later that heart valve replacement became a viable option for most patients (Matthews, 1998). Because of the need for anticoagulants to control the thrombosis which would otherwise cause a mechanical valve to fail (Wittkowsky *et al.*, 2004), and because allograft valves were only available from cadavers, research continued into other sources of

biological valves which did not require anticoagulants or human donors. Porcine aortic valve isolations were successfully used in humans once a means of sterilizing the tissue was found. Buffered formaldehyde was used initially with short-term success, but these valves ultimately failed. It was not until Alain Carpentier introduced the use of dilute solutions of glutaraldehyde in 1968 to sterilize the tissue that long-term implants fabricated from animal-derived tissues became possible.

Today, the clinician has a variety of options to consider when a patient needs a valve replaced. Table 5.1 contains an overview of the different classes of replacement valves, an example of the most popular valve in that category, as well as a list of the advantages and disadvantages of each class. Through the diligent efforts of engineers and scientists working closely with surgeons, heart valve replacement surgery has saved millions of lives worldwide. Given the marked improvement in quality of life and longevity, despite the limitations of today's current valves, it is a certainty that advances in heart valve technology will continue.

5.2 Mechanical valves

A mechanical heart valve is a good illustration of the problems of multivariate design issues in heart valves. Mechanical heart valves typically consist of a circular support attached to a fabric sewing cuff or ring, supporting either a single or bileaflet valve. The mechanical requirements of the bileaflet valve (Fig. 5.2) have to do mainly with wear and fatigue resistance. The leaflets are in nearly constant motion and contact the support at the pivot and closure points, and they are stressed at a relatively high frequency. They may also be a nidus for thrombosis and subsequent septic colonization. The high shear in the pivots causes localized damage to blood elements leading to a high propensity for

5.2 Classical mechanical valves. Left, the Regent™ mechanical heart valve, a modern bileaflet pyrolytic carbon valve from St. Jude Medical. Right, the Starr-Edwards™ ball-and-cage valve, the first commercial heart valve. (Regent™ is a trademark of St. Jude Medical, Inc. Reprinted with permission of St. Jude Medical™, © 2010 All Rights Reserved. Starr-Edwards™ is a trademark of Edwards Lifesciences Corporation. Reprinted with permission of Edwards Lifesciences LLC, All Rights Reserved.)

Table 5.1 Representative examples of the different types of valves currently available

Valve type	Representative example	Advantages	Disadvantages
Mechanical bileaflet pyrolytic carbon		Lifetime durability	Quality of life restrictions due to Coumadin Potential for thromboembolic event
Tissue, porcine, stentless		Good hemodynamics and biocompatibility No need for Coumadin	Difficult surgical procedure Limited durability due to structural deterioration, calcification
Tissue, porcine, stented		Fair hemodynamics Good biocompatibility No need for Coumadin Long clinical history	Standard surgical method Limited durability due to structural deterioration, calcification
Tissue, equine pericardial, stentless		Good hemodynamics Good biocompatibility No need for Coumadin	More difficult surgical method Short clinical experience
Tissue, bovine pericardial, stented		Good hemodynamics Good biocompatibility No need for Coumadin Long history of clinical success	Standard surgical method Durability limited to calcification

thrombosis. This requires permanent anticoagulation, typically with warfarin (Coumadin) for the rest of the patient's life. Tissue integration is required at the sewing cuff and fabrics of polyethylene terephthalate (PET) or polytetrafluoroethylene (PTFE) are commonly employed. The sewing cuff may be a site for thrombosis and bacterial attachment and growth, so it must promote rapid tissue integration and endothelial cell coverage without extensive thrombus and platelet attachment.

5.2.1 Design considerations

A detailed list of heart valve design criteria is contained in Table 5.2. The hemodynamics of the mechanical heart valve is extraordinarily critical. If regions of low flow exist around some areas of the valve, thrombotic complications are likely. The pivot point (the region where the leaflet's pivot protrusion rests within the ring support's pivot cavity) may be such a region of low flow, which is poorly washed by the incoming blood. Thrombosis may result and this region may become a nidus for calcification, which may restrict the leaflet's movement. Areas of turbulent flow, as well as the cavitation that results when the valve opens and closes, can cause platelet and cellular destruction, with potential thrombosis and embolization. Thus, the materials requirements and the design of the device are intimately connected.

5.2.2 Mechanical heart valve materials

Pyrolytic carbon is a glassy carbon, deposited at high temperatures by pyrolysis of a carbon gas such as acetylene, used as heart valve components, particularly as pyrolytic carbon in the leaflets and housings of mechanical valves. These materials demonstrate good biocompatibility and thromboresistance, as well as high lubricity and resistance to wear, in this application. Graphite is used as the substrate for many of the pyrolytic carbon coatings. Typically the pyrolytic carbon is deposited on the graphite substrate and then machined and polished to the final shape. Conversely, the orifice can be deposited on a graphite core that is machined out, so that the orifice has no graphite substrate. Strength and durability are imparted by the pyrolytic coatings. The use of a graphite substrate can reduce residual stresses that become significant in thick pyrolytic coatings. The substrate has the potential to act as a barrier to crack propagation within the pyrolytic coating. Low-temperature isotropic coatings (LTI) can be used to coat more heat-sensitive polymeric substrates such as the heart valve sewing cuff.

Silicone is a rubber-like polymer. It is normally crosslinked in a mold or during extrusion. The most common silicone used is room temperature vulcanizing (or RTV) silicone. The first commercially-viable heart valve, the Starr–Edwards valve, used a peroxide heat-cured silicone ball in a cage. However, when first used, these silicone balls absorbed lipids and swelled, causing

Table 5.2 Parameters for heart valves

Surgical and patient parameters		Parameters relating to device function		Factors relating to device design	
Treatment and surgical parameters	Patient health and medication	Design parameters	Failure modes	Device configuration	Material properties
Approach to heart • Surgical • Minimally invasive • Catheter delivery by cut-down or percutaneous	Medication pre-op, peri-op, and post-op	Surgical vs percutaneous delivery	Thrombus/emboli	Catheter design for percutaneous valve	Strength
Valve size and difficulty in placement	Anticoagulant/anti-platelet/ thrombolytic regimen	Method of attachement to heart	Tissue overgrowth from sewing ring or pannus, hyperplasia at stent/ valve interface	Ability to mount for percutaneous delivery	Compliance
Placement and suturing techniques or percutaneous stent placement	Prophylactic antibiotics	60 to 160 beats/ min	Infection	Ball in cage	Creep resistance
Preservation of chordae tendons and papillary muscle	Adverse coagulation states, e.g., hyperco-agulable	$>$ 20 year lifetime	Hemolysis	Disk in cage	Fatigue resistance
	Diabetes: inhibition of fibrosis/healing of grafts	Large effective orifice area	Destruction of blood elements	Tilting disk	Fracture toughness
	Diseases, e.g. congestive heart failure	Minimum regurgitation	Degradation/ calcification of bioprosthetic tissue valves	Bileaflets	Lubricity
	Previous valve or annuloplasty ring	Fluid flow modeling: Hemodynamics of valve to approximate natural valve	Fatigue of valve components	Flexible polymer leaflet	Porosity (tissue ingrowth into cuff)
			Fracture	Porcine heart valve	Lack of chronic inflammatory response in chronic applications
			Stress corrosion	Bovine pericardial valve	Lack of thrombus and emboli
				Homograft valve	Biostability
					Sterilizability

Length of procedure		Eliminate high shears Eliminate cavitation erosion Eliminate areas of stasis and vortex formation Effective washing of all blood contacting areas of valve, including pivots Stress modeling: limit sites of excessive stress	Cavitation erosion in mechanical valves Paravalvular leak Dehiscence Movement of valve, particularly percutaneously placed valve	Tissue engineered valve • Scaffolds of biostable, tissue or bioresorbable materials • Bioreactor tissue neogenesis • *In situ* tissue neogenesis

premature failure of the valves due to processing issues. These problems were corrected and a small number of these valves are still implanted today. It is not uncommon that explants are recovered 30 to 40 years after implantation showing no degradation, minor wear, and only discoloration of the silicone ball. Many of the silicones currently used are platinum-cured systems.

Metallic alloys commonly used in mechanical heart valves include austenitic stainless steels, cobalt–chrome–molybdenum (Co-Cr-Mo), tantalum, and titanium. Stainless steels are not as widely used for permanent implants because their passive layer is not as durable as the other implant metals and alloys. Furthermore, the release of nickel ions can result in nickel hypersensitivity (Gibbons, 1980). However, 316 LVM (low carbon vacuum melt) is currently used for endovascular stents and the stented portion of percutaneous valves. This material provides the needed mechanical and biocompatibility requirements for these applications.

Titanium alloys are used for heart valves and artificial heart structural components because of their low density, high strength, low corrosion rate, and biocompatibility. The Sorin heart valve uses a Ti-6V-4Cr alloy coated with a low temperature isotropic carbon for the orifice. Percutaneous heart valves also use a nickel–titanium alloy referred to as Nitinol, which allows self-expansion of a stent as it remembers its original shape. Finishing techniques for Nitinol are very important in imparting corrosion resistance and biocompatibility to the material. Co-Cr alloys have also been used as cast or machined orifices for heart valves.

5.2.3 Advances in mechanical heart valves

The focus is on two approaches:

- Reduction of the mechanical damage to blood elements in the pivot points of the valve, by reduction of cavitation effects and closing of the valve leafets. This approach relies heavily on computational fluid dynamics and designs that demonstrate improved hemodynamics.
- New designs based on polymeric leaflets of biostable polymers of polyurethane or new generation materials such as styrene–isobutylene–styrene (SIBS) block copolymers (Duraiswamy *et al.*, 2009). The key to making this approach successful is the lack of thrombus and emboli, prevention of leaflet tearing and prevention of material calcification. These valves would then have the theoretical advantage of a bioprosthetic valve without the failure modes of bioprostheses.

5.3 Tissue valves

There are several primary components to consider in the success of tissue valves, including the tissue, the stent, and how the tissue is processed. Each of

these components will be discussed in the context of the various elements of the valve, including its design, the materials, and the processing. Ultimately, the success of the valve is due to the combined successful interaction of all of these components, and various valves have failed from the ultimate failure of only one component.

5.4 Design considerations

5.4.1 Orifice area

There are a number of design considerations that must be taken into account with a bioprosthetic heart valve as outlined in Table 5.2. Of paramount importance is the orifice area of the valve, particularly in elderly women and people with a small aortic root. A bioprosthetic valve does not have the same orifice area as the native valve, as it requires additional support elements, such as the stent or aortic wall tissue. Since the replacement valve is intended to improve blood flow to the patient, every element which reduces the orifice area can be considered to reduce the theoretical maximum benefit that a patient would receive from the implant. The valve size should match the patient's heart annulus size as closely as possible, to avoid prosthesis–patient mismatch. Mismatch in the valve size implanted in the patient's annulus leads to early structural valve degeneration (SVD) in the bioprosthesis (Flameng *et al.*, 2010).

5.4.2 Valve design type

The tissue component is, necessarily, an essential part of a bioprosthetic valve. In valves utilizing a synthetic material as a frame (also called the stent), the tissue component is reserved to the leaflets, and all commercially successful valves utilize three leaflets in their designs. Historical publications include reports on unileaflet (Soots *et al.*, 1986) and bileaflet (Black *et al.*, 1986) tissue valve designs, although durability testing showed these designs to be inferior to trileaflet designs in long-term durability. Other types of valves utilize tissue for the leaflet material and for the supporting structure of the leaflets, with minimal synthetic material used at all. These valves are called stentless valves. A new type of valve design beginning to enter the marketplace is the minimally invasive percutaneous valve. Figure 5.3 contains photos of percutaneous valves from Medtronic and Edwards Lifesciences that are approved for sale in Europe.

Figure 5.4 contains representative examples of tissue valves where the tissue is supported on a synthetic frame (stented valves) or the entire porcine aortic valve isolation is processed intact to form a stentless valve. Stented valves have a reduced orifice area compared with stentless valves, although the surgical implantation of a stentless valve is much more difficult than that of a stented valve, so most surgeons will use a stented valve for its ease of use and

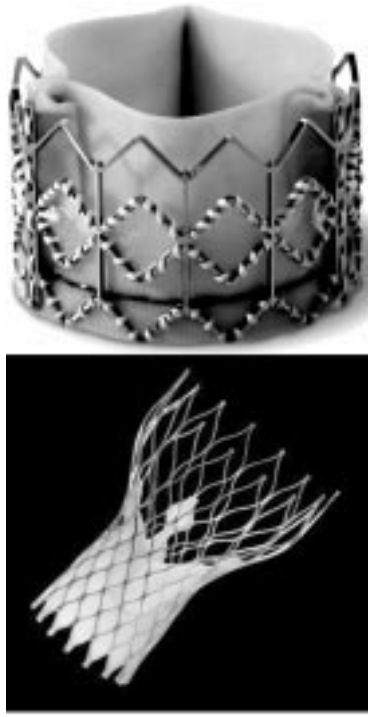

5.3 Photos of two percutaneous valves commercially available in Europe. Top, the Edwards Lifesciences SAPIEN™ Transcatheter Aortic Heart Valve. Bottom, the Medtronic CoreValve® Transcatheter Aortic Valve. (SAPIEN™ is a trademark of Edwards Lifesciences Corporation. Reprinted with permission of Edwards Lifesciences LLC, All Rights Reserved. CoreValve® is a registered trademark of Medtronic CV Luxembourgh S.a.r.l. Reprinted with permission of Medtronic, Inc. All Rights Reserved.)

consistency of results postoperatively. Nonetheless, the use of a stentless valve seems to minimize prosthesis–patient mismatch, which may ultimately lead to longer durability for the patient (Flameng *et al.*, 2010).

Some stented valve designs endeavor to improve the effective orifice area of the valve by placing the valve above the aortic annulus, rather than directly in the annulus. This supra-annular position requires a different shape to the stent of the valve, as shown in Fig. 5.5 (Carpentier and Lane, 1984). At the extreme, Lane has designed a valve which fits entirely in the sinuses of valsalva, resulting in a trilobal shape, rather than a circular design (Lane, 2002). Such a design offers a theoretical improvement in orifice area of 17% over a similarly sized circular valve. Preclinical testing of this valve demonstrated improved hemodynamics over the PERIMOUNT® valve design, when tested in the adolescent sheep model (Flameng *et al.*, 2008). Figure 5.6 shows a valve fabricated with a trilobal shape.

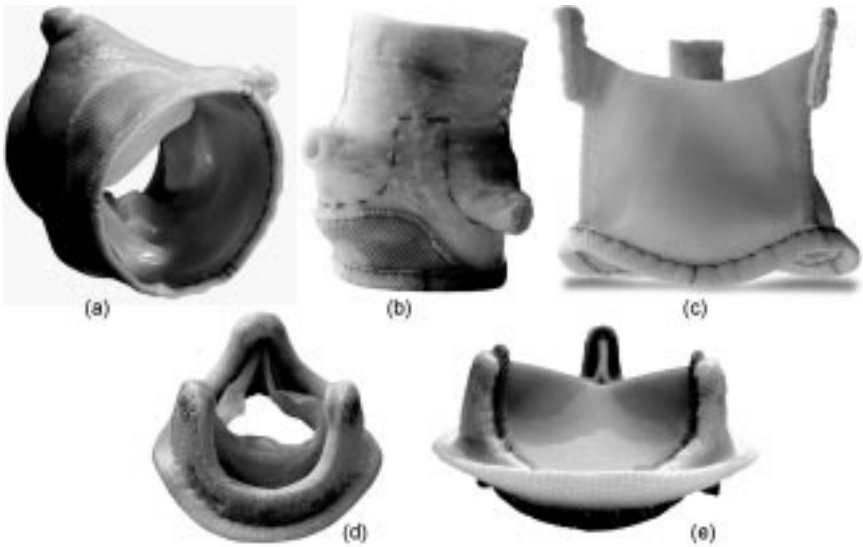

5.4 Product photos of stentless and stented valves: (a) Medtronic Freestyle® Stentless porcine aortic valve; (b) Edwards Lifesciences Prima Plus® Stentless porcine aortic valve; (c) ATS 3f® Aortic Bioprosthesis, a stentless bovine pericardial valve; (d) Medtronic Mosaic® stented porcine valve; (e) Edwards Lifesciences PERIMOUNT® bovine pericardial stented valve. (Freestyle® and Mosaic® are registered trademarks of Medtronic, Inc. Reprinted with permission of Medtronic, Inc. All Rights Reserved. Prima Plus® and PERIMOUNT® are registered trademarks of Edwards Lifesciences Corporation. Reprinted with permission of Edwards Lifesciences LLC, All Rights Reserved. ATS 3f® is a registered trademark of ATS Medical. Reprinted with the permission of ATS Medical, Inc. (now owned by Medtronic). All Rights Reserved.)

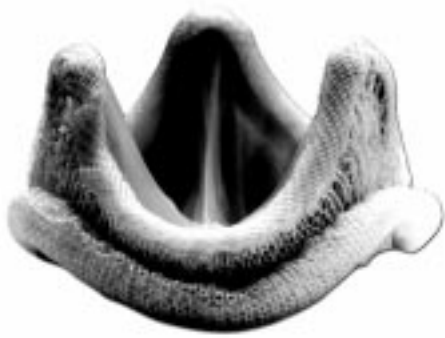

5.5 The scalloped shape of the Edwards Lifesciences S.A.V.™ porcine bioprosthesis is designed to fit above the aortic valve annulus. Such a supra-annular placement should enable a valve with a larger effective orifice area to be used. (Edwards Lifesciences S.A.V.™ is a trademark of Edwards Lifesciences Corporation. Reprinted with permission of Edwards Lifesciences LLC, All Rights Reserved.)

5.6 Prototypes of a new valve designed to fit within the aortic sinuses. Since the sinuses are not circular, the valve is not circular. The trilobal design is particularly evident from the inflow side of the valve. The advantages of such a valve design are increased orifice area and improved hemodynamics. (Photos reprinted with permission from Arbor Surgical Technologies, Inc. (now owned by Medtronic).)

Stentless valves fabricated from isolated porcine aortic valves were the first examples of commercial bioprostheses made from xenogeneic tissues. In some aspects, porcine stentless valves are easier to fabricate because the manufacturing process does not alter the leaflet size, shape or alignment, as these issues were determined by the pig itself. Stentless valves can also be fabricated entirely from bovine pericardium. Porcine aortic valve isolations can be trimmed down and fitted to a frame to create a porcine stented valve, although care must be taken during the trimming process to avoid trimming too far and thus weakening the attachment of the aortic leaflets to the wall tissue. In the case of a stented porcine valve, the stent is there more for the surgical implantation, rather than the leaflet support, as the leaflets are still attached to the native aortic wall. Figure 5.7 shows a photo of a trimmed porcine aortic valve isolation placed inside a metallic wire stent where the aortic wall was trimmed too thin to permit long-term leaflet attachment during use. The high pressure environment in the bloodstream placed a tremendous amount of force on the leaflet at the tip of the commissure, and the trimmed aortic wall was unable to provide sufficient attachment support to the leaflet under these conditions. The solution to this problem is to avoid trimming the aortic wall so thin during construction.

The most frequently implanted valve in use today is the Carpentier–Edwards PERIMOUNT® valve line (Lane, 1985). This valve design succeeded in part by learning from others' failures, in particular, the failure of the Ionescu–Shiley pericardial valve. Comparing these two valves highlights other important design features, including the following:

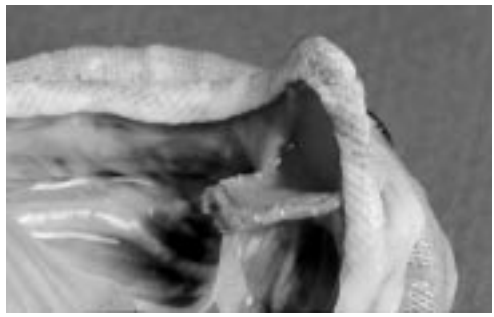

5.7 Photo of an explanted Edwards Lifesciences S.A.V.® valve, showing the problems of excessive trimming of the aortic wall during production. The too-thin wall tissue was unable to support the leaflets during use and they pulled out from the surrounding stent. The solution to this problem was to provide adequate wall tissue to provide the necessary support for the leaflets. (Photo taken from Jamieson WRE, *et al.* (1999), 'Carpentier-Edwards standard and supra-annular porcine bioprostheses: comparison of technology,' *Ann Thorac Surg*, 67, 10. Reprinted with permission from The Society of Thoracic Surgeons. All Rights Reserved.)

- Are the leaflets inside or outside the stent? The Ionescu–Shiley valve wrapped the tissue around the outside of the stent, giving the valve maximum orifice area, while the PERIMOUNT® valve wrapped the tissue around the inside of the stent. Ultimately, the Ionescu–Shiley valve failed due to poor long-term durability. This is because the leaflets were being rubbed against the cloth-covered stent during valve closure, which is a period of maximum pressure. The PERIMOUNT® design resulted in leaflets occasionally contacting the stent during valve opening, which is relatively low pressure. Tissue contact to the stent during valve closure resulted in maximum abrasion and, thus, significantly shorter durability for the Ionescu–Shiley valve. Figure 5.8 depicts the differences between these two valves and shows a close-up photograph of a leaflet in close proximity of a cloth-covered stent. Recently, St. Jude Medical has commercialized the Trifecta™ valve, where the leaflets are wrapped outside of the stent, but the stent is covered with thin pericardium, to try to minimize tissue abrasion. Long-term results will be required to determine if this approach will be successful in preventing tissue abrasion.
- How are the leaflets attached to the stent, particularly at the commissure tips? A critical design flaw of the Ionescu–Shiley valve was the use of an aligning suture over the top of the leaflets over the stent. As shown in Fig. 5.9, this alignment suture became the site of early failure, due to stress concentration around the suture, causing the tissue to yield and ultimately tear. Later design iterations removed this alignment suture and lowered the profile of the valve, but the valve still failed clinically due to stent abrasion. In accelerated wear testing this abrasion resulted in perforation of the leaflet all along the attachment line to the stent, beginning at the top of the commissure, the site of maximum stress.

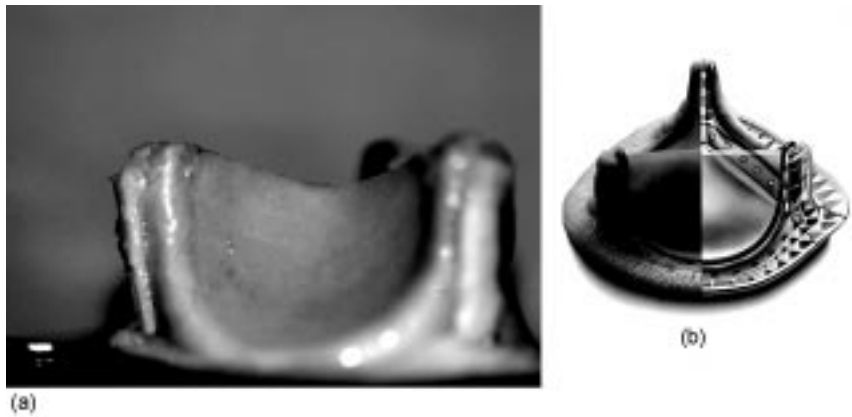

5.8 Photos of two valves with different tissue mounting techniques. In (a), the Ionescu–Shiley pericardial valve wraps the tissue on the outside of the stent; in (b) the Edwards PERIMOUNT® valve wraps the tissue on the inside of the stent. During valve closure, the tissue will rub against the stent when the tissue is wrapped on the outside of the stent; when the tissue is wrapped inside the stent, the tissue rubs against tissue during valve closure. Tissue abrasion against a cloth-covered stent was the primary mechanism of failure for the Ionescu–Shiley valve. (Photos reprinted with permission from Edwards Lifesciences LLC. PERIMOUNT® is a registered trademark of Edwards Lifesciences Corporation. All Rights Reserved.)

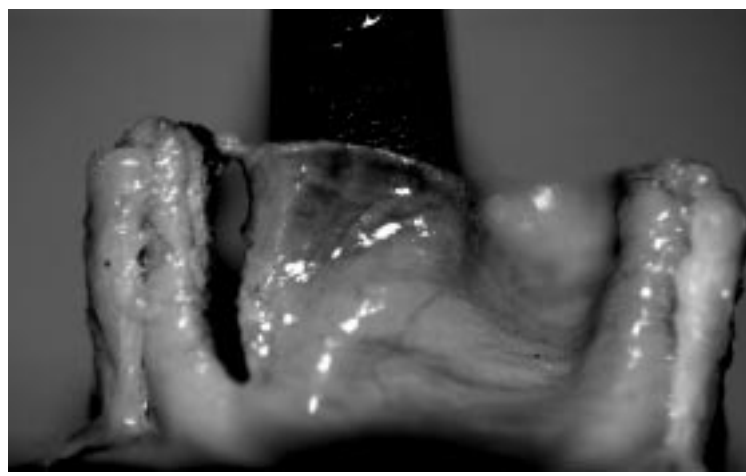

5.9 Photo of an Ionescu–Shiley valve which had undergone typical accelerated aging testing in a standard durability tester. Note how the leaflet tissue tore all along the area next to the cloth. (Photo reprinted with permission from Edwards Lifesciences LLC.)

5.4.3 Design stress analysis

Other key design considerations include the stresses that the design places on the tissue. Minimizing stress is an important design objective that will improve durability and long-term use. This consideration is so important, in fact, that it is a required analysis of a new heart valve design to conduct a finite element analysis (FEA) of the design (Sacks *et al.*, 2006; Sacks and Yoganathan, 2007). The PERIMOUNT® valve has a central opening at rest, and this is because the leaflet design has been developed to take into account the 5º angulation of the stent posts and the flexible nature of the stent material, which provides some flexure during peak stresses, such as valve closure. Because the commissures deflect inward under peak stresses (Drury *et al.*, 1986), the leaflets move forward, closing the central opening to create a competent valve during closure. If the leaflets were designed to be fully closed at rest (zero pressure condition), then once the valve was pressurized, the leaflets would be too large and thus would necessarily rub against each other excessively, particularly in the center (Fisher and Wheatley, 1987). This situation does not hold true for many percutaneous valves, however, where now the stent is held rigidly to the aortic wall and there are no commissures to flex under the load. In this case, the leaflets have to be designed to be closed at rest or the valve would be incompetent under pressurization (Webb *et al.*, 2009).

5.4.4 Hemodynamics

Hemodynamics is another key attribute to a successful design, and the hemodynamics of a valve can be evaluated both *in vitro* and *in vivo*. When tested outside the bloodstream, this is called hydrodynamic testing, and it is commonplace for every valve to be optimized utilizing a pulsatile flow loop which exposes the valve to normal pressurization cycles and measures a variety of valve parameters, including the resistance to valve opening, the amount of fluid leaking through the valve before valve closure, and the pressure differential across the valve (Walker *et al.*, 1986; Yoganathan and Woo, 1986). These parameters are shown diagrammatically in Fig. 5.10. Viewing the valve under normal cycling conditions also enables the designer to observe the leaflet motion, or kinematics, to ensure proper valve opening and closing behavior. As discussed in the area of leaflet design and stent movement, it is important to observe the valve design and ensure that the individual leaflets actually touch each other during closure. The area where the leaflets touch is called the coaptation area. If the leaflets do not coapt completely, the valve will leak even when it is closed. Excessive coaptation area can result in leaflet 'fluttering' where the ends of the leaflet flutter in the flow, like a flag flutters in the wind. Fluttering is very damaging to tissue and can result in a tattered and torn edge. Figure 5.11 contains a series of photos of both a standard PERIMOUNT® valve

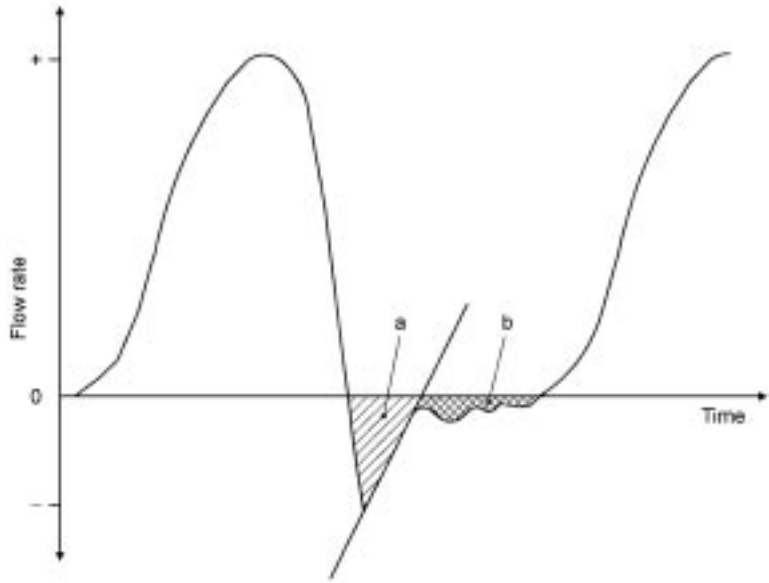

5.10 Example of a single waveform taken from a pulse duplicator apparatus, required for valve development, as described in ISO 5840:2005 guidelines. The pulse duplicator records the flow of liquid through the valve during a simulated heart beat. The hatched area 'a' represents the closing volume, or the volume of fluid required to close the valve. The cross-hatched area in area 'b' represents leakage volume, or the volume of fluid which leaks through the valve, even after it is closed. Different valve designs will require different amounts of fluid to close the leaflets, and some designs may experience residual leakage, depending upon valve design, leaflet design, and overall construction techniques. (Figure adapted from ISO 5840:2005 guidelines, 'Cardiovascular implants – cardiac valve prostheses', available at www.ISO.org.)

and a percutaneous valve prototype during the entire cycle. Note that, despite the differences in the valve designs and placement techniques, both valves still need to operate similarly.

5.4.5 Implantation method/ease of use

Implant method and ease of use are additional design considerations which are very important to the overall success of a procedure. While frequently glossed over at an engineering level, these considerations are quite important to the success of the valve, and thus are covered extensively in regulatory testing and submissions. This would include the use of ancillary devices, such as sizers, which are used to verify the correct annulus size before the valve is implanted, as well as valve fixtures and holders, such as used in packaging. In the mitral position, because the struts of the valve are pointed downward, into the ventricle, it is not possible for the surgeon to directly visualize the struts prior to

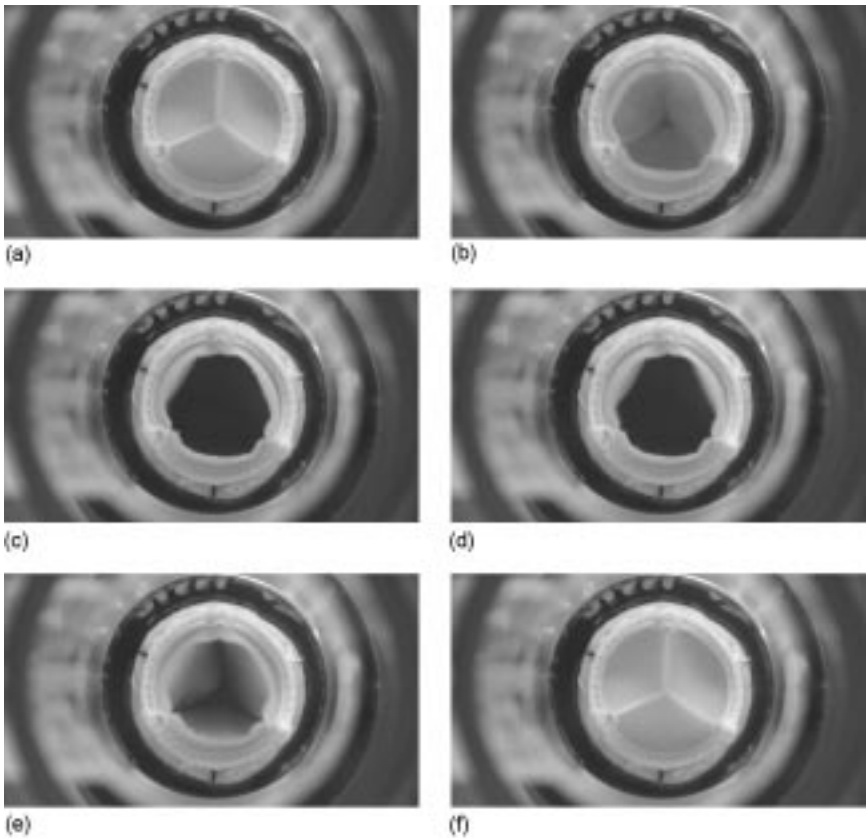

5.11 Series of still photographs of two different types of valves in an accelerated wear tester, showing the behavior of the leaflets during opening and closing. Series (a) through (f) demonstrate the leaflet behavior of a surgical valve, the Edwards PERIMOUNT® pericardial valve. Series (g) through (l) demonstrate the leaflet behavior of a prototype percutaneous valve, the Sadra Lotus™ valve. Note that the delivery method of the valve is irrelevant when evaluating the valve and both surgical and minimally-invasive valves are expected to perform adequately once implanted. (Photos a–f reprinted with permission from Edwards Lifesciences. PERIMOUNT® is a registered trademark of Edwards Lifesciences Corporation. All rights reserved. Photos g–l reprinted with permission from Sadra Medical. Lotus™ is a trademark of Sadra Medical. All rights reserved.)

closure. Because surgeons were finding a tendency for their sutures to get wrapped around the struts during implantation (a condition called suture looping), some companies developed proprietary 'caps' to their mitral valve holders which would prevent the sutures from being able to wrap around the struts during implantation. Figure 5.12 shows two examples of such a solution to the problem.

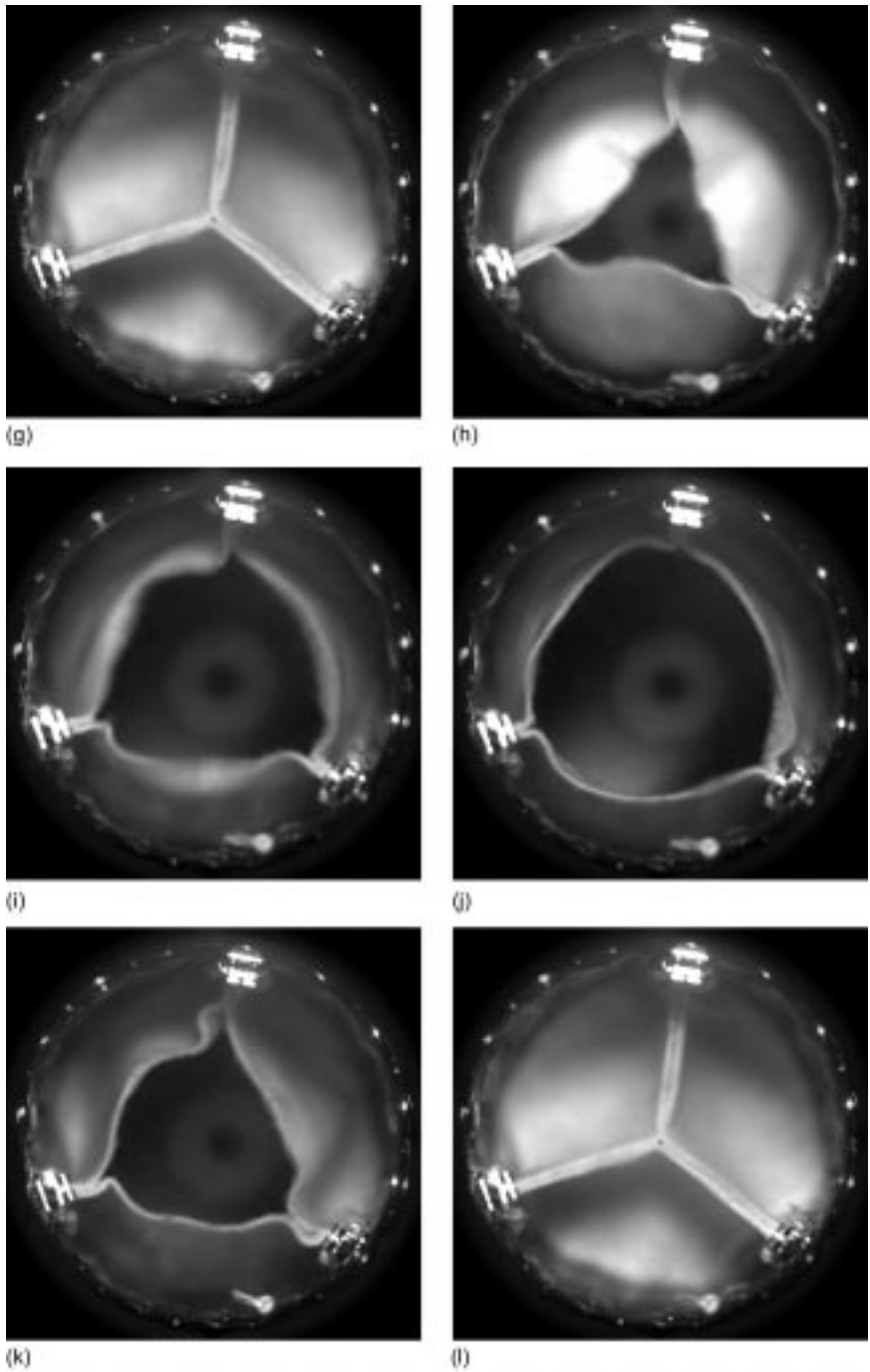

5.11 Continued

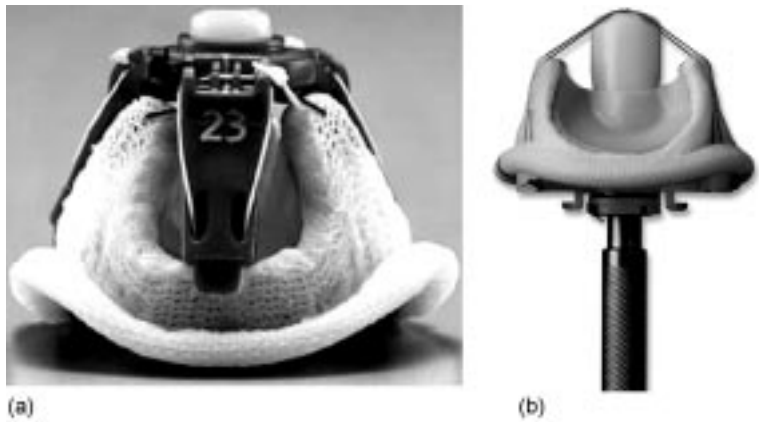

5.12 Two examples of specialized holders for mitral valves which minimize suture looping during implantation. (a) the Cinch® Implant System, from Medtronic, Inc.; (b) the Tricentrix™ Holder System, from Edwards Lifesciences. (Cinch® is a registered trademark of Medtronic, Inc. Reprinted with permission from Medtronic, Inc. All Rights Reserved. Tricentrix™ is a trademark of Edwards Lifesciences Corporation. Reprinted with permission from Edwards Lifesciences LLC. All Rights Reserved.)

5.4.6 Service environment of the valve

Finally, it is essential to consider the service environment of the valve and all the ancillary devices. While many of the standardized tests include test conditions which attempt to simulate various ranges of the service environment (e.g., low flow conditions, high pressure conditions), sometimes the specifics of the service environment are not known or not well defined. Such would be the case when trying to understand how a new surface chemistry would react once implanted. There have been several cases where currently available animal implant models failed to replicate problems experienced in elderly patients. For example, in elderly sick patients, the cloth on a valve sewing ring fails to heal quickly. When a radically new fixation method was introduced that did not employ glutaraldehyde (tradenamed PhotoFix), the increased elongation of the tissue prepared with this new fixation method resulted in excessive tissue abrasion and leaflet perforation within 2 years in patients, despite the fact that no abrasion was seen during the chronic animal studies (Schoen, 1998). In another instance of delayed cloth healing, patients implanted with Silzone-coated sewing rings experienced higher rates of thromboembolism, infection and perivalvular leaks than patients implanted with untreated sewing rings (Schaff *et al.*, 2002). In a third example, the CoreValve® percutaneous valve used in Europe has been associated with a high incidence of heart rhythm disruption (left-bundle branch block, LBBB). Apparently the long stent design exerts forces on critical areas in the heart associated with normal electrical conduction, and patients fitted with

this valve may require a permanent pacemaker in order to maintain normal sinus rhythm postoperatively (Baan *et al.*, 2010).

In each of these cases, the unique characteristics of the elderly sick patient were not duplicated in young healthy animals during the preclinical studies, and thus these problems could not be detected until clinical use. Another aspect of the service environment that has to be considered is the hospital or surgical environment. How are the sizers going to be resterilized between cases? What particular challenges does your new product pose to the institution? Will you require refrigeration of the product or the use of new equipment during rinsing or implantation? Changes like these can lead to unforeseen problems which can be disastrous and result in early clinical failures. Because of the importance of the service environment, sponsoring companies are required to conduct extensive risk analysis and risk management processes as a part of the product development process.

5.5 Material considerations

5.5.1 Leaflet material

The choice of leaflet material is one that has been hotly debated throughout the history of bioprosthetic valves. In the early period of valve development, valves were fabricated from various autologous tissues including the diaphragm, veins, and aortic wall. Pericardium was most often utilized because of its availability and its properties of pliability, resistance, and thinness, which was very similar to the aortic valve tissue (Duran, 1986). Despite the lack of immunogenicity issues with an autologous tissue, and the apparent suitability of autologous pericardium, these tissues ultimately failed as valves, as they were rapidly absorbed by the body. Thus, chemical stabilization of the tissue is an essential component to its use as a valve, regardless of the source. Because of the impracticality of using glutaraldehyde in the operating room (the need for freshly made dilute solutions, the time required for crosslinking, and the chemical residuals in the tissue), homologous tissues were quickly abandoned in favor of xenogeneic tissues, which could be prepared by commercial laboratories under standardized conditions. Allograft valves and valved conduits are still in use today, however due to the limited supply of cadaver tissue these do not represent a practical option for most patients requiring treatment.

5.5.2 Tissue type

Since 1976, with the commercialization of the Ionescu–Shiley bovine pericardial valve, there has been a proliferation of tissue valves of various designs made with a variety of animal tissues. Practical considerations such as supply, size, and other factors generally limited the choices to porcine aortic valve

5.13 Contegra® Conduit is a pulmonary valved conduit, available under a Humanitarian Device Exemption from Medtronic, Inc. The conduit is fabricated from an isolated bovine jugular vein and preserved in glutaraldehyde. The conduit is used in certain pediatric applications. (Contegra® is a registered trademark of Medtronic, Inc. Reprinted with permission from Medtronic, Inc. All Rights Reserved.)

isolations, because they are of similar size to the human aortic valve, and bovine pericardium, because it has tissue properties similar to the aortic valve tissue. Nonetheless, consideration of other materials and other animal sources has periodically surfaced. Isolated valves from the bovine jugular vein are used to treat pediatric congenital defects and are available as a humanitarian-use device from Medtronic. These devices are used to reconstruct the right ventricular outflow tract (see Fig. 5.13).

Other tissue sources that have been proposed for use in bioprostheses include pericardium from cows (Lee *et al.*, 1989a), calves (Gibbons, 2009), horses (Eckstein *et al.*, 2004), pigs (Naimark *et al.*, 1992), sheep (Naimark *et al.*, 1992), dogs (Lee and Boughner, 1981), kangaroos (Neethling *et al.*, 2002), and ostriches (Maestro *et al.*, 2006). Comparative studies documenting the different properties of these tissues are available. Figure 5.14 shows the comparative data on tissue thickness, often a design specification for valve designs. Tissue thickness is a key design parameter for percutaneous valves, as tissue thickness is essential in determining the smallest packing volume of the valve (see Fig. 5.15). Except for percutaneous valves, the importance of tissue thickness is unclear, and in the authors' opinion, narrow thickness specifications, in the absence of discrete design requirements, are inappropriate and a burden to manufacturing. Published studies demonstrate that the mechanical properties of tissues cannot be predicted by tissue thickness, and that uniform tissue thickness does not ensure uniform mechanical properties (Mikus *et al.*, 1986).

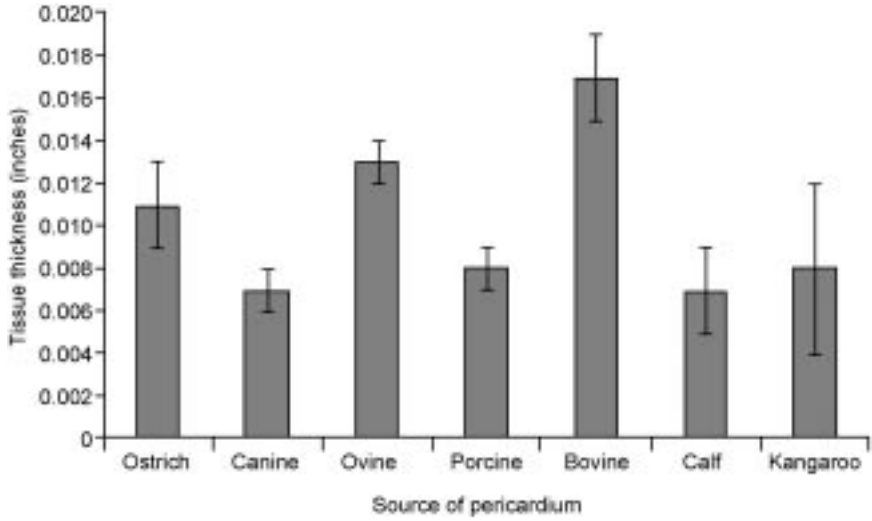

5.14 Thickness comparison between different sources of pericardial tissue (1 inch = 25.4 mm). While thickness does not equate to strength per se, it is often specified as a design criteria. In the case of a percutaneous valve, however, thickness is indeed a critical design specification, as it determines the minimum packing volume for the valve.

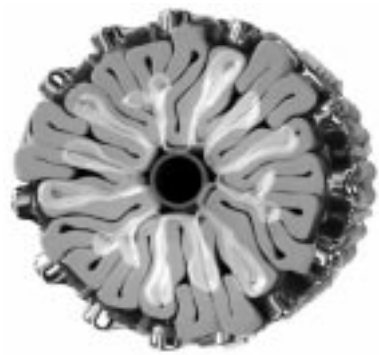

5.15 Schematic diagram of the Edwards Lifesciences RetroFlex 3® Transfemoral Delivery System, showing the percutaneous heart valve in its retracted, or packed, state. Note the tight packing of the tissue leaflets within the frame, with a central opening for the guidewire to direct insertion. Clearly, thicker tissue would require a greater packing volume compared to thinner tissue. As such, tissue thickness is an important design constraint for percutaneous valve designs. (Image reprinted with permission from Edwards Lifesciences LLC. RetroFlex 3® is a registered trademark of Edwards Lifesciences Corporation. All Rights Reserved.)

5.5.3 Mechanical properties

Mechanical properties are important for several reasons: first, the tissue must be strong enough to withstand the forces exerted on the valve during use. As the peak loads on the tissue are estimated at 1 MPa at the commissures, the ultimate tensile strength (UTS) of the tissue must exceed 1 MPa (Zioupos *et al.*, 1994). Further, continuous use can cause the tissue to break down with time, leading to lower mechanical parameters (Sacks, 2001; Sun *et al.*, 2004). Since no one knows how continuous wear correlates with changes in mechanical strength *in vivo*, it is not possible to define precisely what the UTS of a material should be at the point of manufacture in order to provide a specified number of years of durability. Suffice to say, however, that a healthy 'safety factor' is appropriate, and choosing materials with UTS values close to 1 MPa could be a durability concern. This is where porcine aortic valves fall short, their UTS values range from 0.6 to 1.2 MPa in the circumferential direction (along the axis of the major collagen bundles), whereas bovine pericardial tissue has UTS values ranging from 5 to 26 MPa or more (Sacks *et al.*, 2006). The increased strength of pericardial tissue is due to the increased amount of collagen in the tissue, as well as its lower water content. A porcine leaflet contains 94% moisture, leaving only 6% of the mass of the tissue composed of structural proteins and other components. Bovine pericardium, however, contains only 78% moisture and contains twice as much collagen as a porcine leaflet (Cunanan *et al.*, 2001).

Second, natural pericardium has a wide range of intrinsic mechanical properties, and if thickness does not correlate with mechanical properties, how does one ensure proper valve behavior? Figure 5.16 contains elongation data for nine different pieces of bovine pericardium, each considered suitable for valve

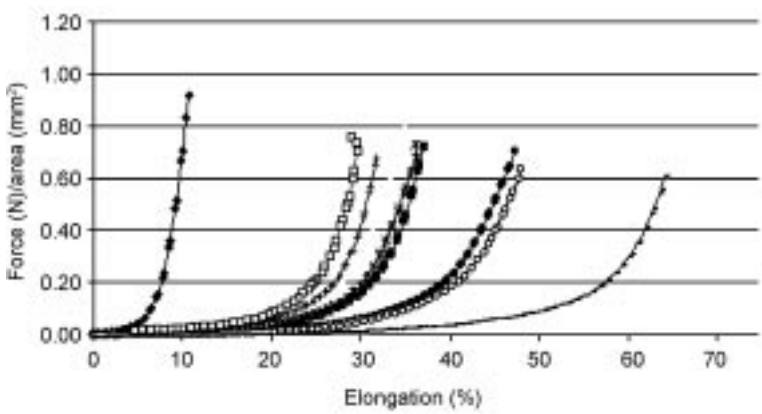

5.16 Stress–strain curves for nine random samples of bovine pericardial tissue. All tissues were considered suitable for use in valve production and were of similar thickness. Note significant differences in elasticity between tissues. (Figure reprinted with permission from Arbor Surgical Technologies, Inc. (now owned by Medtronic.)

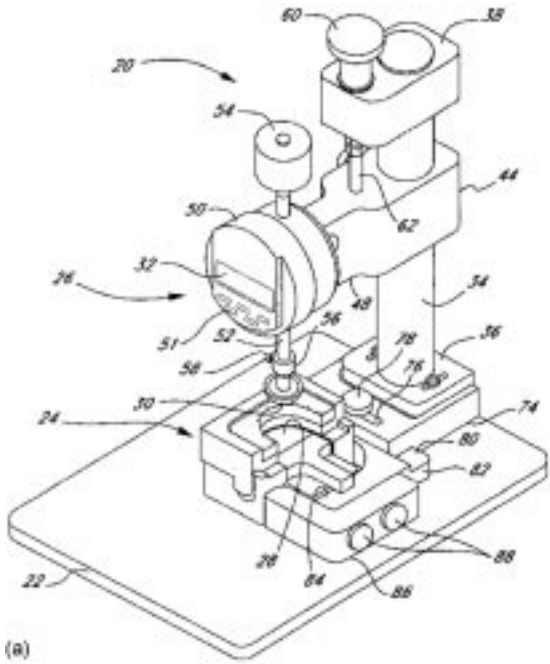

(a)

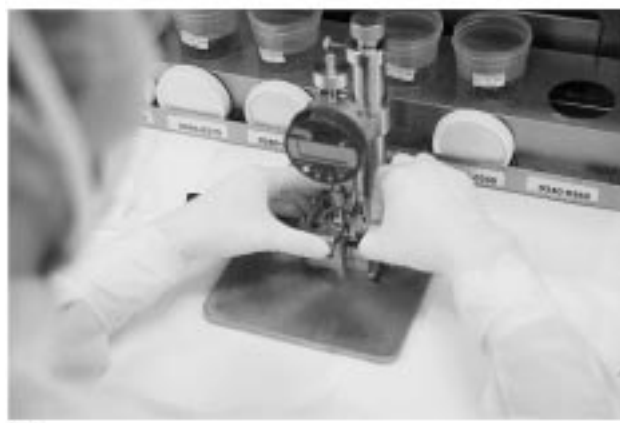

(b)

5.17 (a) Leaflet deflection tester described in US Patent 6,413,275. The tester measures the displacement of tissues under a dynamic load, thereby simulating the forces experienced by the tissues during valve closure. Use of such a device enables tissues to be matched with specific biomechanical characteristics, which are important for proper valve functioning. (Reprinted with permission from Edwards Lifesciences Corporation. All Rights Reserved.) (b) Photo of a dynamic leaflet deflection tester used in the Edwards Lifesciences pericardial valves. Each leaflet is tested for elasticity under a load and then sorted by elasticity, in order to construct valves with leaflets of similar mechanical properties.

fabrication. The tissues were also matched for thickness, as one would do in manufacturing. As is immediately evident from the data, not all tissues with uniform thickness and acceptable cosmetics behave similarly. The consequences of this have been long appreciated since pericardial valves were first used clinically; that is, that this mismatch in mechanical properties between leaflets can cause asynchronous closing of the leaflets and result in poor valve functioning. As early as 1986, manufacturers implemented selection criteria 'according to standardized techniques and exacting methods for tissue selection and correct matching of leaflets for uniformity of function' (Ionescu *et al.*, 1986).

Every manufacturer which produces a pericardial valve must address the issue of mechanical property mismatch between leaflets and each have developed different approaches to this problem. One particularly effective method that has been implemented by Edwards Lifesciences involves measuring the displacement of an isolated leaflet when subjected to a standardized dynamic load (Nguyen *et al.*, 2002). An example of a leaflet displacement tester is shown in Fig. 5.17. Use of such a system enables close matching of leaflet mechanical properties and can be utilized to match tissue properties across the range of *in vivo* forces to which the valve is exposed.

Another approach to the problem of mechanical mismatch is to subject the tissue to an applied force during fixation, thereby removing some of the intrinsic variability in elongation of the tissue prior to valve fabrication. Numerous studies have been published which document the effects of the exposure of applied forces to pericardial tissue, in either one or two directions, and compared with untethered values (Lee *et al.*, 1989a,b). Figure 5.18 demonstrates the effects of a load when applied in one direction; the extensibility of the tissue along the axis of the applied load is reduced compared with untethered tissues.

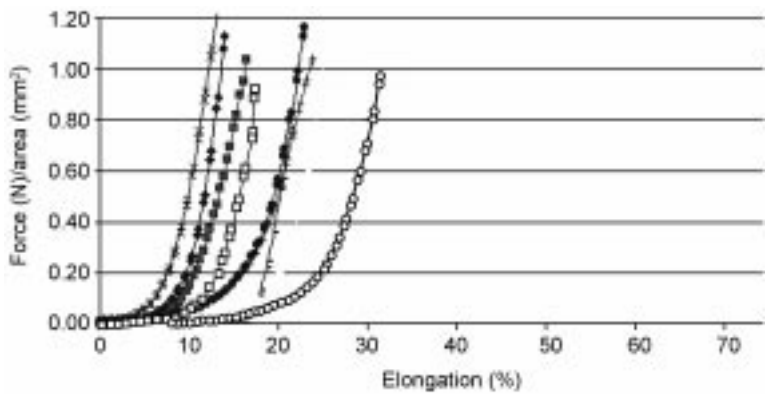

5.18 Stress–strain curves for nine random samples of bovine pericardial tissue crosslinked in glutaraldehyde with an applied load for 30 minutes. Note the significant reduction in variability in elasticity between tissues, compared with Fig. 5.16. (Figure reprinted with permission from Arbor Surgical Technologies, Inc. (now owned by Medtronic.)

Perhaps most significantly, the elongation of different pieces of tissue are more similar compared with untethered tissues. In this way, the application of a uniaxial load during fixation can generate tissues with more consistent mechanical properties, thereby addressing the problem of mechanical mismatch. Further, the application of a uniaxial load during fixation generates anisotropy in the pericardial tissue which mimics the native valve leaflet (Sacks *et al.*, 2009a) and porcine aortic valve leaflet (Sacks *et al.*, 2006) tissues.

5.5.4 Non-tissue materials

The support and finishing elements of a bioprosthetic heart valve are made from materials similar to those used in mechanical valves. All valves contain some cloth to assist in fixation of the tissue to the stent or to the heart tissue of the patient. The cloth is typically made of PET or PTFE and permits ingrowth of cells into the cloth which helps hold the valve in place.

Stented heart valves can use a variety of materials for the support structure. The Edwards PERIMOUNT® valve has a stent formed from Elgiloy™ wire, while the Medtronic Hancock® valve has a stent made from Delrin® (homo-acetal). In either case, the choice of the material must be justified and tested to show that it has sufficient durability for the demanding job of a heart valve stent. Early clinical explants with the Hancock® standard orifice porcine aortic valves showed that these polymeric stents had a tendency to creep with time, ultimately bowing down into the central orifice and reducing the area for blood flow (Schoen and Cohn, 1986). Today, stent creep testing is a standard component of the test regimen required of any new heart valve design.

Valves with a sewing ring may contain additional support elements to provide annular rigidity and integrity to support the many sutures that are used to fixate the valve in the patient's heart. The Edwards PERIMOUNT® valve contains a silicone waffle-like ring which helps the surgeon fixate the sutures in the sewing ring. The Medtronic Mosaic® valve contains radio-opaque markers at the stent tips which help visualize the valve stent during imaging procedures.

All valves are held together with sutures, and the construction of a heart valve is complex and very labor-intensive. There are so many fine stitches used to construct the valve that the assembly workers build the valves under magnification, and it may take a day or two for a worker to finish just one valve. The choice of suture material(s) is an important consideration, and it may be appropriate to choose different types of suture materials for different applications. For example, it may be desirable to use a stretchy suture with some compliance when suturing the tissue to the frame. This may help prevent the type of tearing seen with the Ionescu–Shiley valve, where the sutures tore through the tissue, resulting in early failure. When attaching non-tissue elements together, it may be desirable to use high tensile strength suture materials which are very non-compliant, to ensure a solid construction. Different types of sutures have

different effects on the tissue (Paez *et al.*, 2001), and even the use of different sizes of needles can influence the mechanical properties of sewn tissue (Lim and Cheong, 1994). While it may seem like a small detail, the choice of suture material and needle used in construction can have an important effect on the overall durability of the finished device.

5.6 Process considerations

There are a number of ways for valves to fail, and most testing plans are designed to test a new valve design for all known failure modes. Early failure modes include mechanical failure due to leaflet mismatch or construction issues where tissues tear or abrade. If a valve does not fail due to early failure modes, it can fail later due to durability issues. Late failure modes include mechanical degradation of the tissue, with resulting tearing, which is most common for porcine aortic valve designs (Ishihara *et al.*, 1981; Sacks and Schoen, 2002). Calcification is another late failure mode which is only partly due to design, and all valves are required to be tested for calcification potential during the development process.

5.6.1 Calcification models

Much work has been done in the early days of heart valve development on developing various models to test for calcification. While some proposed the use of *in vitro* calcification test models, these methods proved to be difficult to execute and required constant maintenance, particularly for the super-saturated solutions that were specified. Animal implant models proved to be more reliable, and have been rapidly adopted for testing purposes.

Large animal models were developed first, led primarily by the pioneering work by Drs Jones and Ferrans at the National Heart, Lung and Blood Institute and Dr Hilbert at the Center for Devices and Radiological Health (CDRH) of the Food and Drug Administration (FDA) (Jones *et al.*, 1986, 1989). They utilized juvenile sheep 4–8 months old and implanted the prostheses in the mitral position. During the in-life portion of the study, the valves were studied for their hemodynamic performance. After a period of 150 days, the animals were sacrificed and the explanted valves were examined and analyzed for calcification. Calcification was evaluated in a number of ways, including macroscopically, microscopically via histopathology, and analytically using chemical methods such as atomic absorption spectroscopy.

Since then, the model has been applied to every known valve in use today. In particular, Professor Flameng's group in Leuven, Belgium has tested and published results on hundreds of valve implants, looking at the effects of valve type (stented vs. stentless), leaflet material (porcine vs. pericardial), treatment type (anticalcification treatment vs. none), implant duration, implant location,

and animal age (Flameng *et al.*, 2006). While juvenile sheep have an aggressive calcification response, their rapid growth during the 150 day study results in hemodynamic complications due to valve–annulus mismatch. Flameng correlated results in juvenile sheep to results in adolescent sheep, where sheep are 8–11 months old. At this age, the growth rate of the animal has slowed, so it will not outgrow the valve during the study duration, greatly reducing the complications associated with valve–annulus mismatch. The calcification response of the adolescent animal is reduced compared with a juvenile animal, but it will still calcify, and the relative level of calcification between common valves is still evident. This also provides a more representative assessment of the hemodynamic performance of the valve (Flameng *et al.*, 2006).

While large animal models enable evaluation of the finished valve in the orthotopic position, it is expensive and not amenable for research purposes. Towards that end, Drs Schoen and Levy have popularized the application of the rat subcutaneous implant model, which has become the most commonly used small animal model (Levy *et al.*, 1983). Briefly, young rats are used, 21–28 days old, and strips or coupons of processed tissue are implanted subcutaneously in the abdomen or across the back, with multiple samples implanted in each animal. This enables a direct comparison of test and control materials in the same animal, an important feature, as there can be significant between-animal variability in calcification levels.

5.6.2 Baseline calcification levels

Baseline levels of calcification were determined from clinical explants, which were analyzed in much the same way as the animal study explants. Evaluating valves which were explanted due to dystrophic calcification, Schoen *et al.* (1987) report that as little as 67 and 34 μg calcium/mg dry tissue weight were sufficient to result in clinical failure in the aortic and mitral positions, respectively.

To date, evaluation of materials and processes in various models have revealed that the initiating sites of calcification are associated with cell membranes, which come from endogenous degenerated cells and infiltrating cells once implanted in the host (Harasaki *et al.*, 1986). Additional sites of calcification include insudated proteins (sometimes called the sponge phenomenon), collagen and elastic fibers (Schoen and Levy, 1986), and bacterial remnants (Levy *et al.*, 1977; Rumisek *et al.*, 1985). Calcification begins very quickly upon implantation, within 48 hours (Schoen *et al.*, 1986). These deposits are visible only ultra-microscopically at first, but the calcium deposits grow in size and number with time (Schoen *et al.*, 1994). Porcine aortic leaflets and bovine pericardial tissues calcify similarly. An in-depth protocol for explants analysis has been published (Schoen, 1995).

5.6.3 Tissue treatments

Once calcification was realized as a primary limitation to long-term valve durability, the field has focused on various treatments to reduce calcification. Since those initial studies conducted in the early 1980s, several technologies have been commercialized, focused on removing phospholipids (Nashef and Ahmed, 1989; Lentz and Pollock, 1982). These technologies remove the binding sites for the calcium, and the correlation between quantitative phospholipid levels and calcification levels has been reported (Cunanan *et al.*, 2001). While the use of an anionic surfactant has been associated with increased incidence of thromboembolism clinically, the use of a non-ionic surfactant has been widely used with the Edwards Lifesciences brand of porcine and pericardial valves (Hartz *et al.*, 1986). Alcohol also reportedly reduces phospholipid levels in tissues (Levy and Hirsch, 1998) and has been incorporated in the St. Jude Medical treatment called Linx™ (Connolly *et al.*, 2004).

Other theories have been proposed to explain the pathophysiology of calcification, as summarized by Schoen and Levy (1999). One such theory that has reached commercialization is to block residual aldehyde groups using 2-aminooleic acid (AOA®) (Girardot, 1990). This technology has been applied to the Medtronic Mosaic® and Freestyle® porcine valves (Gott *et al.*, 1992). Figure 5.19 shows the comparative performance of these commercial processes in the rat subcutaneous model.

Surprisingly, while all treatments were developed with the intent of reducing calcification, none of the treatments commercialized has been optimized to

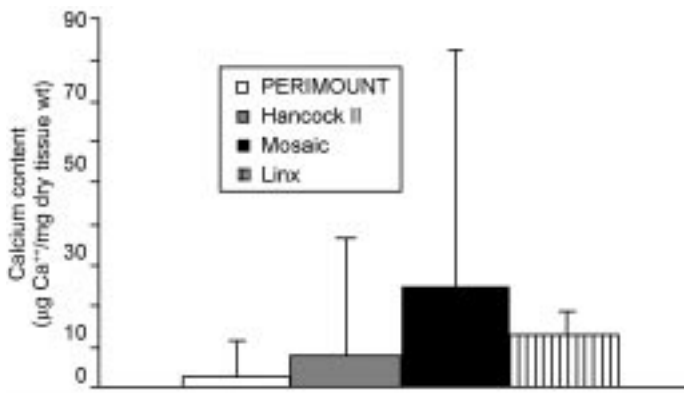

5.19 Comparative analysis of calcium content (mg Ca^{++}/mg dry tissue weight) for various commercial tissue processes, as evaluated in the rat subcutaneous implant model. Data for PERIMOUNT®, Hancock II®, and Mosaic® taken from Cunanan *et al.* (2001) after 90 days implantation. Data for Linx™ taken from Connolly *et al.* (2004) after 21 days implantation. (PERIMOUNT® is a registered trademark of Edwards Lifesciences Corporation. Hancock II® and Mosaic® are registered trademarks of Medtronic, Inc. Linx™ is a trademark of St. Jude Medical, Inc.)

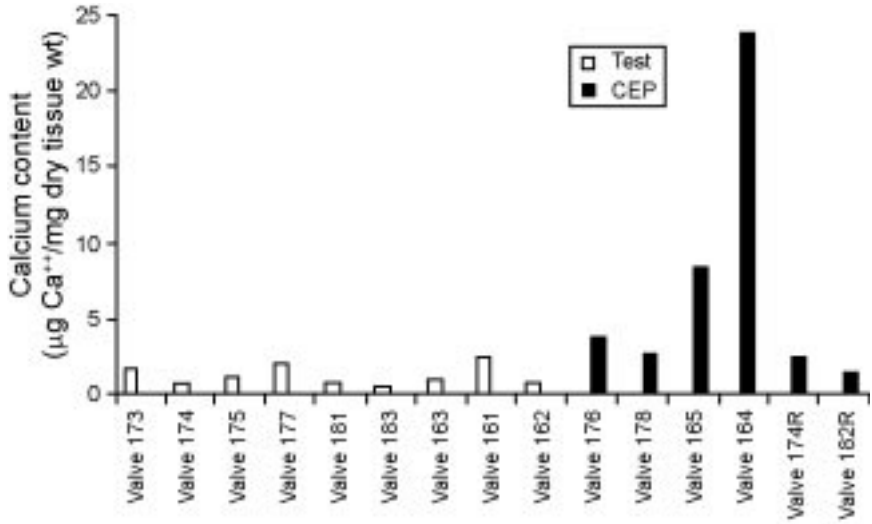

5.20 Calcification comparison between a prototype valve produced with an optimized process and the Edwards PERIMOUNT® (CEP) valve. The calcium content for each valve is reported (mg Ca^{++}/mg dry tissue weight). Both valve types use Tween-80™ as a calcification mitigation treatment; however, the prototype process has been optimized to ensure effective treatment of every tissue. By contrast, an individual PERIMOUNT® valve can occassionally demonstrate moderate to significant calcification levels. (Figure reprinted with permission from Arbor Surgical Technologies, Inc. (now owned by Medtronic). PERIMOUNT is a registered trademark of Edwards Lifesciences, Inc.)

reduce calcification in all samples, and all processes demonstrate a significant standard deviation in mean calcium content within a group. This is evident in the early studies reported by Jones *et al.* (1986), as well as more recent studies reported by Flameng *et al.* (2006). Several recent processes have been described which have been optimized to reduce calcification in all specimens, as determined by the rat subcutaneous implant model at 90 days (Cunanan *et al.*, 2004, 2009). This was accomplished by approaching the problem using a chemical engineering approach, which considers variability in the process. By the application of variability-reducing methods such as design of experiments (DOE), the critical inputs were identified and optimized for the desired output – consistently low calcium content after implantation. Demonstration of the success of this approach has been reported in sheep (Flameng *et al.*, 2008). As shown in Fig. 5.20, every valve implanted with the optimized process demonstrated very low calcification levels, all below 3 μg calcium/mg dry tissue weight. In contrast, the PERIMOUNT® valves tested in this study had calcium levels as high as 23.8 μg calcium/mg dry tissue weight. As a patient may only receive one replacement heart valve, it is an important concept to ensure that every heart valve has a similarly low propensity to calcify.

5.7 Additional considerations

5.7.1 Overall process design

In the initial processes which were employed, many companies took a minimalist view towards glutaraldehyde, believing it to be the source of irritation and toxicity, and resulting in calcification. With that view, they strove to reduce glutaraldehyde concentrations as low as possible and to eliminate glutaraldehyde wherever possible. In at least one case, the use of very low levels of glutaraldehyde was associated with the persistence of viable *Mycobacterium chelonei* in commercial product (Levy *et al.*, 1977; Rumisek *et al.*, 1985).

As a result of this experience, every commercial producer has implemented a bioburden-reducing process into their valve manufacturing protocol. The key process steps to a commercial process are thus: receipt of tissue from abattoir/supplier; isolating desirable tissue and crosslinking it; exposing the tissue to a bioburden-reducing treatment; implementing an optional calcification mitigation treatment; cutting out the leaflets and fabricating the valve; and finally, sterilizing the finished product. While it is beyond the scope of this chapter to discuss each of these steps in detail, there are several items worth noting.

5.7.2 Tissue sourcing

An important consideration is the source of the tissue, not just the animal species, but also the location and practices of the supplier of the tissues. In most cases, this is the abattoir or a tissue broker. As was demonstrated in the 1980s, it is possible for humans to develop disease by eating beef from cattle infected with bovine spongiform encephalopathy (BSE) (Erdtmann and Sivitz, 2004). Given the seriousness of the resulting disease, new variant Creutzfeld–Jacob disease (nvCJD), and the inability of most known bioburden-reducing practices to inactivate the organism responsible for disease transmission, the World Health Organization (WHO) has worked with regulatory agencies worldwide to adopt a policy of safe sourcing (EMEA, 2004).

Safe sourcing is a series of best-practices designed to safeguard the public by minimizing the risk of transmitting BSE to humans through medicinal products and devices. It includes demonstration of source controls to ensure that feed does not contain proteins from ruminant sources. It continues with a demonstration of good veterinary practices, both at the farm and at the abattoir. Abattoirs are required to employ trained veterinarians to inspect animals prior to slaughter, as well as inspect the carcass during the slaughter process, in order to evaluate the lymph nodes and other tissues which might signal a latent or undetected disease in the animal. Abattoirs must have a means to isolate questionable carcasses until further evaluation can be performed, and in general to keep the tissues most likely to transmit BSE (specified risk materials, SRMs) away from other tissues and organs that will be used in food, medicines, and

medical devices. The details of the guidance can be found published in the *Official Journal of the European Union* (EMEA, 2004), as well as identified in a series of International Standards Organization (ISO) guidance documents, ISO 22442-1, -2, and -3 (2007).

Compliance with safe sourcing practices has become a requirement for companies wishing to commercialize their products. In the US, this is regulated by a joint review of the product application by the US Department of Agriculture (USDA) and Food and Drug Administration (FDA). In Europe, notified bodies prefer that sponsors obtain European Directorate for Quality in Medicines and Healthcare (EDQM) approval prior to submission of their product dossiers for CE mark approval. The EDQM is an organization which harmonizes and coordinates the guidelines on ensuring a safe supply of medicines, blood products, and cell- and animal tissue-derived products. They review a sponsor's submission packet to ensure adherence to the safe sourcing practices, and will issue a Certificate of Suitability if the submission is approved. The Certificate is very specific for sponsors using specified suppliers and documented practices. If a tissue supplier is changed, the Certificate is no longer valid, and the sponsor must reapply for a new EDQM approval.

While the argument still persists that the absence of detectable disease does not prove absence of disease, there are several helpful safeguards which every manufacturer can implement. First, scientific studies done in the United Kingdom by Gerald Wells and colleagues have shown that BSE takes some time to develop, even if animals are intentionally inoculated with the infectious agent. This time is about 32 months, so limiting tissue procurement to animals younger than 30 months of age is typically done for the heart valve industry. Second, Mr Wells has studied the pericardium and heart valves (including the aortic and mitral heart valves) from animals with clinical disease, and he was unable to demonstrate transmission of infectivity from these tissues (EMEA, 2004). The lack of infectivity of these tissues, even when taken from animals with known disease, is another safeguard in mitigating the risk of BSE transmission through a bioprosthetic heart valve. Owing to the proteinaceous nature of the BSE infectious agent, it cannot be isolated or destroyed in the tissue without destroying the tissue itself. Until genetically engineered tissues can be manufactured with sufficient properties and in adequate supply, safe sourcing is an important component of an overall risk management strategy to ensure the continued development and commercialization of products that are safe for human use.

5.7.3 Tissue preservation

It is important to preserve the tissue architecture prior to fixation. If the tissue is swollen or damaged prior to fixation, fixation can only 'lock in' that state, it cannot reverse any damage that has already been done. While it is traditional to ship isolated tissues in isotonic saline, this may not be sufficient to prevent tissue

swelling, and new processes have been described which attempt to better preserve the tissue architecture prior to fixation (Cunanan *et al.*, 2009).

5.7.4 Crosslinking

Crosslinking of the tissue can be done either with or without an applied force, as discussed previously (Lee *et al.*, 1989a,b). Determining the completion of crosslinking is an important parameter in controlling the process. While many believe shrinkage temperature to be a measure of crosslinking, it is not in a pure sense of the term (Lee *et al.*, 1995). Shrinkage temperature is defined as the temperature at which the tissue shrinks by 1%. While it is true that the shrinkage temperature of crosslinked tissue is greater than the shrinkage temperature of fresh tissue (Cunanan *et al.*, 2001), this merely demonstrates that the tissue has a greater resistance to thermal denaturation after crosslinking. A better measure of the degree of crosslinking would be to measure the consumption of the reactants involved in the crosslinking reaction. Since it is difficult to accurately measure minute changes in glutaraldehyde during the reaction (because it is present in great excess), it is easier to measure the component to which the glutaraldehyde reacts, that is, the amino acid lysine.

Lysine can be easily measured using amino acid analysis, of which many commercial systems are available. Because of sampling difficulties, it is best to normalize the amount of lysine to another amino acid present in collagen which is not consumed in the crosslinking reaction. Glycine is a particularly abundant amino acid in collagen which cannot participate in the cross-linking reaction, due to its non-reactive side chain. This then leads to the development of a Lys/Gly ratio (L/GR) and a percentage crosslinked, as defined below:

$$\text{Lys/Gly ratio} = \frac{\text{residues of lysine in the sample (per 1000 amino acids)}}{\text{residues of glycine in the sample (per 1000 amino acids)}} \quad 5.1$$

$$\%\ \text{crosslinked} = \frac{\text{L/GR}_{\text{initial}} - \text{L/GR}_{\text{final}}}{\text{L/GR}_{\text{initial}}} \quad 5.2$$

As lysine is consumed in the crosslinking reaction, amino acid analysis will reveal a decline in the lysine content with time. At the point where the reaction has reached a steady state, the percentage crosslinking will remain unchanged with further reaction time. This is the point of complete fixation.

An important point worth mentioning is that the lysine content will never be zero in an intact crosslinked tissue. This is because some of the lysine side chains will be protected by other molecules in the tissue and thus are sterically hindered from reacting with the glutaraldehyde. Table 5.3 contains some amino acid data published by Schoen *et al.* (1986). In this study he characterizes the kinetics of glutaraldehyde incorporation into the tissue using tritium-labeled glutaraldehyde. This is an elegant way to measure crosslinking; however, if

Table 5.3 Amino acid analysis of bovine pericardial tissues

Amino acid	Fresh tissue	Glut-fixed tissue	Explanted tissue
Glycine	257	334	295
Lysine	31	8	15
Lys/Gly ratio	0.121	0.024	0.051
% Crosslinked	0%	83%	58%

Data from: Schoen *et al.* (1986).

radioactive compounds are unavailable or cost-prohibitive, amino acid analysis is an alternative approach. As shown in Table 5.3, fresh tissue has Lys/Gly ratio of about 0.12, or 31 lysine residues/257 glycine residues. After glutaraldehyde crosslinking, this value drops to about 0.02, or 8 lysine residues/334 glycine residues. Thus at completion of the reaction, 83% of the lysines in the tissue have reacted with glutaraldehyde adducts.

Interestingly, he also evaluated explanted tissues, which demonstrate a Lys/Gly ratio of 0.05. Assuming the tissue was made from the same initial lot, this leads to the conclusion that only 58% of the lysines in the implanted tissue are still reacted with glutaraldehyde adducts. This implies that, after implantation in the body, some glutaraldehyde reactions with tissue are not permanent, and thus can reverse their reaction with lysine. In order to prevent glutaraldehyde reversibility, the double bond formed in the reaction must be reduced to a stable, single, carbon–carbon bond with sodium borohydride (Connolly *et al.*, 2004). Typically this is not done in commercial processes, so there is the potential for some glutaraldehyde reversibility. If the data are typical, we can assume that it is a relatively small amount of glutaraldehyde overall, although it represents a high percentage of the crosslinks initially formed. That is, while the Lys/Gly ratio increases by 0.03 after implantation, this represents about 30% of the crosslinks initially formed. In a similar manner, amino acid analysis can be used as a measure of tissue stability during the shelf-life of the product.

5.7.5 Bioburden

For products manufactured from animal tissues which have been sourced from an abattoir, the tissues are not sterile. The amount of viable microorganisms on the tissue is called bioburden. Many things influence bioburden, including cleanliness, chemicals, staff, and environmental conditions. As a tissue valve manufacturer, it is your goal to process non-sterile starting materials in such a way as to produce sterile, functional heart valves without damaging the delicate tissue structure or components.

It is an important mindset to always consider the bioburden and how it affects your processes, and how your processes affect the bioburden. For example, it is a

requirement of the heart valve regulations to demonstrate a sterility assurance level (SAL) of 10^{-6} (ISO 5840, 2005). This can also be stated as the need to develop a process which can demonstrate a 6-log reduction in bioburden. If your incoming tissue is highly contaminated, however, it can have a bioburden of more than 10^6 viable microorganisms per tissue. If that is the case, a process that provides a SAL of 10^{-6} will not provide a sterile product. That is, the incoming tissue was so contaminated that its bioburden level overwhelmed the process's ability to kill microorganisms, and thus some extraordinary actions must then be taken. Because of the risk of a non-sterile product, the usual action that is taken in such a case is to discard the tissue. As this has an associated cost in terms of monetary loss, as well as loss in starting materials, this cannot be a regular occurrence. If it is, then something about the process must be changed to prevent this from occurring regularly. In a manufacturing environment with a well-established quality system, there should be alert levels and action levels established on bioburden, in order to ensure that the incoming bioburden never exceeds the SAL of the process.

Ideally, you would never receive tissue with more than a million viable microorganisms, but this can easily occur, especially when working with abattoirs that are not sensitive to the high cleanliness standards of the medical/pharmaceutical industry. Other factors can also contribute to higher incoming bioburden, such as extended shipping times, or delays in receiving fresh tissues. This is particularly a problem for US-based companies wishing to comply with worldwide regulations on minimizing the risk of BSE. One universally accepted way of meeting those regulations is to source tissues from a country with a minimal risk of BSE, such as Australia or New Zealand. While it is possible to express-freight a chilled cooler of tissue to the US in 24 hours, it can be difficult to ensure the shipment will be released through US Customs, FDA, and USDA, all in the same day that it was received. It is likely that a delay of at least 24–48 hours will occur during this release process, before the tissue can be shipped to your facility. If it is a Friday by then, will you process the tissue immediately, or place it in the refrigerator for the weekend? Delays in processing will also increase the bioburden of the tissue.

From the moment the tissue is received, it should be your goal to try to reduce bioburden. This can be accomplished via a number of different mechanisms. First, prompt processing of the tissue once it is received. Second, vigorous rinsing of tissue is useful in mechanically removing microorganisms from the tissue. A typical rinsing regimen will involve a series of rinses, usually three consecutive rinses, prior to selecting tissue for fixation. Fixation with glutaraldehyde will reduce the bioburden significantly, and thus was its original intent when Professor Carpentier fashioned the first glutaraldehyde-treated porcine aortic valves. But how much does your fixation process reduce bioburden, and does it affect all the possible microorganisms that might be contained on your tissue? As we have seen from previous examples, if you use a

0.2% solution of glutaraldehyde, you will not have a process that is entirely effective in killing viable *Mycobacterium cholonei*. Therefore it is essential in any good manufacturing process to measure your incoming bioburden, understand how changes in vendors and shipping and other parameters can affect it, and to also characterize the main species within your bioburden. Do you have aerobic bacteria? Anaerobic bacteria? Molds and fungi? While this chapter is not intended to provide an extensive training on microbiology, it should educate you on the important issues that you will face in a heart valve development project. In the case of microbiology, make sure you work with someone who is well trained and has experience in heart valve manufacturing and quality assurance.

After the tissue has been crosslinked, the initial bioburden will be reduced, but it will not necessarily be completely eliminated. Therefore it is necessary to introduce a bioburden reducing step, which is usually composed of a more aggressive chemical cocktail, such as a mixture of formaldehyde–ethanol–Tween (Nashef and Ahmed, 1989) or a high concentration of glutaraldehyde with alcohol (Lentz and Pollock, 1982). The exact composition and exposure conditions would depend upon your residual incoming bioburden after fixation, but they could include prolonged exposure times, elevated temperatures, or both, if necessary. A process of systematic determination of bioburden reduction rates as a function of solution composition and concentration, as well as optimization of process time and temperature, combined with the knowledge of your residual bioburden after fixation, will help you determine the precise processing conditions required. The goal at this point should be complete elimination of the incoming bioburden without placing unnecessary restrictions on the manufacturing department.

Once you have sterilized the tissue from its incoming bioburden, you must continue to monitor bioburden, as the process of manufacturing a valve will also contribute bioburden to the tissue. The amount of bioburden added by the process during valve fabrication is very much a matter of the cleanliness of your facility, the operating environment and its control, the number of personnel in the room and their work practices, and the cleanliness of everything going in to the process/product/environment. All these factors must be considered and controlled to minimize the contamination of the valve by the process. After the valve is fabricated and tested, it is typical to subject the valve once again to a bioburden reduction step, to protect the valve from the bioburden generated by the process. Ensuring the bioburden reducing step is effective will be done by measuring, on a regular basis, the bioburden of the product as it is built, and characterizing its species. Because this bioburden was caused by the manufacturing process, it is likely to be different from the incoming bioburden from the abattoir. It is possible that the two bioburden reducing steps will require two different chemical solutions, or at least different conditions of time and/or temperature. Again, these parameters will have to be developed specifically for

the given operating environment. Proving that the conditions chosen will effectively mitigate bioburden is part of the validation process.

As you can now appreciate, bioburden measurement and determination are essential aspects of any facility manufacturing a tissue-based product (ISO 11737-1, 2006). Not only is it important to do this during the initial development and validation of the process, but it is also important to do this routinely, to make sure the bioburden has not changed significantly, either in amount (in which case, the SAL of 10^{-6} may not be sufficient) or in the type of micro-organism. Every manufacturing change that is considered must also be evaluated from the perspective of its effect on the bioburden, whether it is a change in supplier, cleaning procedures, or expanding production capacity by adding another work shift. These and other changes have the potential to greatly increase bioburden, and if you are not measuring it, you will not know it – that is, until the Center for Disease Control and the FDA appear at your door, and by then it will be too late! It is best to keep your destiny in your control, and regularly measure the parameters that have the most risk for creating a harmful product. Bioburden is one of those critical parameters.

5.7.6 Sterilization

Sterilization of a bioprosthetic valve is complicated and unlike most other devices. Because of the mixture of different synthetic and biologic materials used, the traditional methods of sterilization including autoclaving, gamma irradiation, e-beam treatment, ethylene oxide exposure, or peroxide plasma sterilization typically are not used. Because of the increasingly widespread use of bioprostheses and other tissue-based products, guidelines have been published on the use of liquid chemical sterilants to ensure terminal sterilization of the device (ISO 14160, 1998). These guidelines include a discussion of the quality system requirements for the manufacturer, a description of process development and product compatibility with the proposed terminal liquid sterilization (TLS) method, and a detailed discussion of the validation of the method.

There are a number of considerations that go into designing a suitable TLS method. First, the sponsor must know the bioburden (amount and type) of the product prior to application of the TLS method. Second, they must know that the product can still perform adequately after the sterilization process, and typically this is tested after worst-case conditions, such as excessively long exposure times which may simulate an equipment failure, or the need to repeat a sterilization cycle. The test methods themselves must be validated prior to use in the sterilization validation, to ensure that the methods do not generate erroneous results. For example, residual liquid chemical sterilant must be neutralized prior to culturing for surviving microorganisms.

The choice of microorganisms used in the performance qualification of the device is essential. It is important to test both representative microorganisms that

have been isolated from the product, but also to choose highly resistant organisms that could someday be encountered in the bioburden. The inactivation kinetics of each of these microorganisms to the proposed process is determined, and at least five time-points must be included, with at least a demonstration of 10^3 kill rate of the process for each organism. The inactivation curves are used to establish the sterilization times, where the time is based on the most resistant organism tested. Such a method ensures at least a 10^{-6} SAL of the process. ISO 14160 (1998) contains informative guidance in the annexes of the document to assist in understanding what must be done, but it is highly recommended that an experienced microbiologist be hired or used as a consultant during the development and validation of the sterilization process.

While liquid chemical sterilization is the method of sterilization used today for bioprosthetic heart valves, it has its disadvantages, particularly for the user of the device. Residual chemical sterilant must be repeatedly rinsed from the device before implantation, and this can lead to delays during the surgical procedure. The remaining liquid sterilant in the container must be disposed of by the hospital staff, and typically this must be collected and discarded as chemical waste. Because of these inconveniences, which also represent safety hazards at some basic level, there is continued interest in challenging the previous thought that some of the more routine sterilization methods could not be used for bioprosthetic valves.

Duran *et al.* (2001) have developed a means of treating tissues with a water-soluble polar solvent to replace the water in the tissue with a mixture of low and high molecular weight ethylene glycols. Thereafter, the tissue can be freeze-dried for storage, while retaining its flexibility. Donnelly *et al.* (1973) reported that freeze-drying produces large vacuoles in the porcine aortic valve tissue, and questioned its utility in valve sterilization. Chen and Wika (2003) developed a means of drying tissues with glycerol, which stabilizes the tissue dimensionally such that the process can be applied to finished heart valves. The dried tissue can then be sterilized using ethylene oxide or ionizing radiation. When the valve is ready to be used, it can be implanted dry or rehydrated before use, and the tissue will return to its original physical dimensions and mechanical properties. Shamis and coworkers (2009) have evaluated the use of microwave radiation as a new sterilization technique for bovine pericardial tissues. Their studies demonstrated that the use of nonthermal microwave radiation did not alter the mechanical properties of the pericardium, although they did not achieve complete sterilization in their study.

Modern e-beam facilities enable biological materials to be irradiated frozen or refrigerated, thereby reducing the damage that e-beam-generated free radicals can cause to the biological material without interfering with its ability to kill the microorganisms (Calhoun *et al.*, 2008). The e-beam dose can be delivered in two separate treatments, with a cooling period between the two treatments, to further minimize damage to sensitive biological materials. Sometimes the delivery rate

of the treatment can be increased to deliver a sterilizing dose of electrons without permitting the degradation that could occur using a standard sterilization cycle. Today, an electron beam is being used to sterilize combination products, including drugs, biologics, and nanoparticles. Wright Medical utilizes e-beam to sterilize demineralized bone (DMB) products for orthopedic applications. E-beam minimizes damage to osteo-inductive protein, which is a key component of DMB. They found that ethylene oxide was inappropriate for their product composition and that gamma irradiation was more destructive to the osteo-inductive protein activity. Synovis Surgical, which manufactures bovine pericardial patches for orthopedic reconstruction, uses an electron beam to terminally sterilize their product (Calhoun *et al.*, 2008).

Given the advances in our understanding of sterilization technologies, it may be possible in the future to employ techniques such as e-beam or microwave to sterilize bioprosthetic heart valves. For now, however, tissue valves are sterilized using liquid chemical sterilization, using ingredients and process conditions which are determined empirically during process development. Regular measurement of the bioburden is essential in guiding those efforts, as well as ensuring that the process is under control.

5.8 Emerging technology

5.8.1 Percutaneous and minimally invasive valves

As mentioned several times in the previous sections, percutaneous valves are one of the biggest developments in heart valves since the use of glutaraldehyde to preserve and sterilize animal tissues. There are two leading valve companies with percutaneous valves approved for sale outside the US, Edwards Lifesciences and Medtronic. Both companies expect that commercialization of these valves in the US will be much slower than in Europe, in part because the guidelines do not distinguish between the requirements for a percutaneous valve and those for a traditional, or surgical, valve.

Because the delivery of a percutaneous valve is done in a beating heart through an artery or the apex of the heart, the surgeon cannot prepare the implant location for the valve, as is typically done for a surgical valve. For example, in a surgical valve, the old calcified leaflets are usually excised from the annulus, and the surgeon debrides as much embedded calcium from the annulus as possible before sewing in the valve. For a percutaneous valve, however, he cannot do these things, and must simply identify the best location possible and deploy the valve. His ability to image the location is limited to the view through angiography, rather than direct imaging of the implant site, as is done with a surgical valve. The result is that there is a significant incidence of leakage around the stent of a percutaneous valve, as well as the potential for embolism and thromboembolism.

Since the percutaneous valve is not sutured in place, it can migrate with time. Also the need to collapse the entire valve structure, both the stent and the tissue, into a very small cross-sectional area may damage the tissue, resulting in reduced durability.

As discussed previously on valve design, many percutaneous valves are fixed rigidly to the aortic wall, unlike a surgical valve where the stent is suspended somewhat in the central orifice. While the stent on a surgical valve can flex and provide some compliance to the tissue when it is under heavy loads, a percutaneous valve cannot. Therefore, the commissures of the leaflets on a percutaneous valve remain in a fixed position during periods of heavy loads, which greatly increases the forces on the tissue. If the forces exceed the mechanical properties of the tissue, the leaflet can tear prematurely, resulting in reduced durability.

The limitations of current percutaneous valve technology stand in stark contrast to the relative success of traditional surgical valves, but proponents argue that it is a risk–benefit discussion (Chiam and Ruiz, 2008). Percutaneous valves are intended for use in high risk patients who are too sick to survive open heart surgery (Webb *et al.*, 2009). As such, these patients have a greatly reduced life expectancy compared with the traditional surgical patient, and any theoretical reduction in long-term durability is sufficiently balanced by the immediate benefits to the patient of improved cardiac output and extension of life. There also remains the interesting possibility that these terminally ill patients may recover additional cardiac function once the defective valve is replaced. Such recovery is seen in terminal patients awaiting a heart transplant who have been implanted with a ventricular assist device (Klotz *et al.*, 2008).

An additional difficulty in the development of percutaneous valves is that it greatly disrupts the current practice of medicine, where the cardiovascular surgeon is no longer the implanting clinician. Because percutaneous valves are usually implanted through the femoral artery, the skills of interventional cardiologists and radiologists are more appropriate. This has added a considerable amount of debate to the issue, although the groups seem to be realizing and appreciating the skills of the other, and in Europe, a team-based approach is emerging, which will undoubtedly provide the best level of care for the patient.

A final dynamic that is certainly important to investors and others who look at the financial aspects of new technology development is that the manufacturer can obtain much higher payments for a percutaneous valve than for a traditional surgical valve. True, a percutaneous valve requires the development of an entire system of products, not just the valve, but also the catheter, the specialized stent, and development of the implantation procedure. Still, those features were also required when surgical valves were originally developed, although today's surgical valves benefit from the investments in the tools and techniques made years ago. The upside is substantial, and while Edwards Lifesciences reports average selling prices of $4500–5000 for a traditional surgical valve, with

upcharges of 10–20% for new technological features, such as the Magna™ design or the Thermafix™ process (Mussallem, 2006), these prices fall far short of the US$30 000 they are projecting for the sale of a percutaneous valve system (Wood, 2009). It is no wonder that the development of the Edwards' percutaneous valve system has generated tremendous interest among investors and no fewer than a dozen start-up companies have begun to develop their own versions of percutaneous valve technology. When Medtronic announced the purchase of start-up valve company CoreValve in February 2009 for $700 million (Beach, 2009), it was clear that investors want percutaneous valve technology to reach commercialization and that they are willing to take the risks and make the investments required to do so. Figure 5.21 illustrates two of the leading second-generation percutaneous valves that have begun clinical investigation. Both valves enable the physician to reposition the valve prior to final deployment, thereby ensuring an optimal placement of the valve in the aortic position.

5.8.2 Tissue engineered valves

While tissue engineering is being covered in Chapter 10, a few words are warranted here, in light of the discussion on percutaneous valve technologies.

A reality of new technology development is that there has to be some financial reward for the investors who bravely invest the time and money in a new concept and support the company as it works through the hurdles and setbacks intrinsic in new technology development (Cardis *et al.*, 2001). Most of the investment dollars for new technology comes from venture capital firms, which are, in turn, paid to invest others' money and generate an extraordinary rate of return that would not be achievable in more conventional investment methods. As such, venture capitalists must show their partners a return on their investment within some reasonable period of time, say 5 to 10 years. This makes it difficult for traditional money sources to support the development of paradigm-shifting new technologies like tissue engineering, where commercialization is still decades away, particularly for a tissue engineered heart valve.

So it is unlikely that you will see the excitement and fervor around tissue engineered heart valves as you see around percutaneous valves, at least for some period of time. This is despite the fact that a tissue engineered heart valve will likely contribute more significantly to the treatment of valve disease than any other technology, and it has the ability to provide a real cure to the problem, particularly in children. Currently children with congenital or acquired valve disease are subjected to suboptimal treatments with valves developed for adults. As they grow, they must endure repeated open heart surgeries to replace the implanted valves with larger valves. Also, because children are rapidly growing, including their bones, they rapidly calcify traditional bioprosthetic valves.

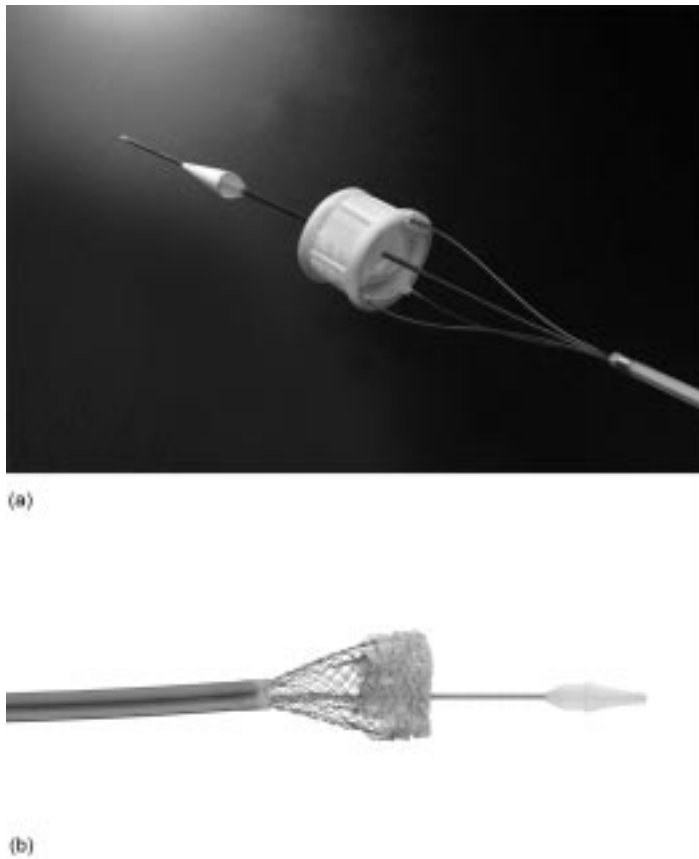

5.21 Two second-generation percutaneous valves in clinical development. (a) The Direct Flow Medical percutaneous valve, which utilizes an inflatable polymeric stent and bovine pericardial leaflets. (b) The Sadra Lotus™ Valve System, with a repositionable nitinol stent and bovine pericardial tissue leaflets. Both valves were designed to enable clinicians to examine initial valve placement, particularly in relation to the coronary arteries, and reposition, if necessary, prior to permanent implantation. (Reprinted with permission from Direct Flow Medical, Inc. All Rights Reserved. Lotus™ is a trademark of Sadra Medical. Reprinted with permission from Sadra Medical. All Rights Reserved.)

Therefore children cannot benefit from traditional bioprosthetic valves and must use mechanical valves and be subjected to Coumadin therapy, with all the limitations on their quality of life that the blood thinner imposes.

A key hurdle in advancing tissue engineered heart valves to commercial reality will be to reduce the technical risks on such a project. An excellent overview of the challenges for heart valve tissue engineering was recently published (Sacks *et al.*, 2009b). This review envisions an implantable synthetic device containing living cells and a supporting biomatrix. Another interesting

approach to creating a living valve is to implant a valve matrix which attracts the right cells from the body and induces them to remodel the matrix and create a living tissue (De Visscher *et al.*, 2007). Preliminary research indicates that the body does contain the right kinds of cells required for such a task (De Visscher *et al.*, 2008), and early research is underway to attract those cells to the valve matrix using the appropriate homing factors (De Visscher *et al.*, 2010). Undoubtedly, the concepts and technologies being developed for a tissue engineered heart valve will continue to evolve as we understand how to address the many challenges posed by such a device. Only time will tell when a tissue engineered heart valve will become a commercial reality.

5.9 Applicable standards

There are numerous ISO guidelines regulating the design, development and testing of heart valves, both mechanical and biologic. ISO 5840 describes the specific test methods that need to be performed to demonstrate the safety of the valve. Informative Annex K in ISO 5840 describes a number of relevant standards applicable to testing the materials and components of heart valve substitutes. While these are too numerous to list here, the Annex includes specifications for metals, tensile testing of metals, durability crack initiation and endurance limit testing of metals, fatigue crack growth rate testing, hardness, microstructure determination, thermal expansion testing, fracture toughness, and fatigue life. Testing which may be required for polymers include viscosimetry, melt flow index, determination of breaking strength under a static load, tensile testing to failure, tensile properties determination, determination of dynamic mechanical properties, resistance to surface wear, resistance to scratching, flexural properties and the determination of breaking strength under dynamic bending load, fatigue crack initiation determination and measurement of fatigue crack growth rate, determination of compressive properties, material specifications for various common medical polymers, density, liquid diffusivity, hardness, wear resistance, creep, fracture toughness, and hydraulic expansion.

The Annex also identifies relevant standards for ceramics and carbons, including characterization of physical and chemical properties, measurement of fatigue crack growth rates, hardness, thermal expansion and fracture toughness. While there are no specific standards or guidance documents describing the mechanical testing of biological materials, the Annex identifies some potentially relevant test methods which might be adapted to the determination of the tensile properties of biological materials. The Annex also identifies testing to be completed on the cloth used in the valve. The ISO 10993 series is applicable to the biocompatibility testing of the device, which is detailed more fully in Part 1. The FDA has recently distributed its draft guidance on heart valves (Vaughn, 2010).

There are also numerous ISO guidelines relating to the overall systems at the sponsoring company, including ISO 13485, which describes the quality systems requirements, and ISO 14971, which describes the application of risk management to medical devices. ISO 14937 covers general requirements for sterilization of a device and ISO 14630 describes general requirements of a non-active surgical implant. ISO 11134 covers moist heat sterilization (needed to cover sterilization of containers, tools, and equipment used in manufacturing), ISO 14160 covers terminal liquid sterilization, and ISO 22442-1/-2/-3 cover animal sourcing practices. ISO 11607 discusses packaging for terminally sterilized devices; ISO 14155 covers the clinical investigation of the device.

5.10 Conclusions and future trends

The challenges required to develop a new heart valve are considerable, and the list does not get any shorter as new designs and applications are developed. Pushing the envelope and developing new technologies will benefit existing patients with improved therapies and reduced complications and benefit new patients not currently serviced by existing valve technologies. The trend is towards reduced use of mechanical valves, because of the significant compromises to the patients' quality of life. The development of a mechanical valve which does not require Coumadin and is more hemocompatible would be a tremendous advancement which would enable a new mechanical valve to displace bioprosthetic valves. Until that material advancement occurs, bioprosthetic valves are destined to continue to dominate the market and grow as the technologies improve, primarily to address the current limitations and shortcomings of bioprostheses. The successful development of a tissue engineered heart valve would ensure complete market conversion to bioprosthetic valves, and offer the greatest therapeutic option for patients.

5.11 Sources of further information and advice

- ASM International. www.asminternational.org. Extensive materials database available as well as workshops and other resources. Database can be accessed at http://products.asminternational.org/meddev/index.aspx
- Company websites: Edwards Lifesciences, www.edwards.com. Medtronic, Inc., www.medtronic.com. St. Jude Medical, www.sjm.com. Direct Flow Medical, www.directflowmedical.com. Sadra Medical, www.Sadramedical.com.
- Websites from leading heart valve research institutions and organizations: American Heart Association: www.americanheart.org; Cleveland Clinic: www.clevelandclinic.org; Texas Heart Institute: www.texasheartinstitute.org. Society for Heart Valve Disease: www.shvd.org.

5.12 Dedication

Ralph Kafesjian (1934–2008)

This chapter is dedicated to Ralph Kafesjian, who worked tirelessly during his 31 year career at Edwards Lifesciences to develop and improve many life-saving technologies, particularly heart valves. His contributions focused on using science and engineering to provide practical solutions to problems in the real world environment of manufacturing and device development, and his expertise in metallurgy, biomaterials, ceramics, material fatigue/failure analysis, and materials processing directly benefited the patients who received those life-saving devices, many of which became market-leading technologies.

Ralph leaves behind his wife June, his children, and many colleagues who have been fortunate enough to work with him and call him a friend. Ralph, you are missed, but we thank you for always being willing to teach us and working tirelessly to improve the performance of medical implants. We know the millions of patients whose lives you've touched also thank you.

5.13 References

Baan J Jr, Yong ZY, Koch KT, *et al.* (2010), 'Factors associated with cardiac conduction disorders and permanent pacemaker implantation after percutaneous aortic valve implantation with the CoreValve prosthesis', *Am Heart J*, **159**, 497–503.

Beach D (2009), 'Medtronic to acquire CoreValve Inc.', available at: http://wwwp.medtronic.com/Newsroom/NewsReleaseDetails.do?itemId=1235395903862&format=print&lang=en_US [accessed 7 April 2010].

Black M M *et al.* (1986), 'The Sheffield bicuspid valve: concept, design and *in vitro* and *in vivo* assessment', In Yacoub M and Bodnar E, *Biologic & Bioprosthetic Valves*, New York, Yorke Medical Books, 709–17.

Calhoun R, Stephan T, Periman S (2008), 'Electron-beam sterilization more versatile than you think', *Medical Design*, December, 50–3.

Cardis J, Kirschner S, Richelson S, *et al.* (2001), *Venture Capital: The Definitive Guide for Entrepreneurs, Investors, and Practitioners*, New York, John Wiley & Sons, Inc.

Carpentier A and Lane E (1984), 'Supra-annular aortic valve', US Patent 4,451,936, issued June 5, 1984.

Chen J F and Wika K (2003), 'Processing of implantable animal tissues for dry storage', US Patent 6,534,004, issued March 18, 2003.

Chiam P T L and Ruiz C E (2008), 'Percutaneous transcatheter aortic valve implantation: assessing results, judging outcomes, and planning trials', *J Am Coll Cardiol Intv*, **1**, 341–50.

Connolly J M, Alferiev I, Kronsteiner A, *et al.* (2004), 'Ethanol inhibition of porcine bioprosthetic heart valve cusp calcification is enhanced by reduction with sodium borohydride', *J Heart Valve Dis*, **13**, 487–93.

Cunanan C M, Cabiling C M, Dinh T T, *et al.* (2001), 'Tissue characterization and calcification potential of commercial bioprosthetic heart valves', *Ann Thorac Surg*, **71**, S417–21.

Cunanan C M, Dinh T T, Rubalcaba R (2004), 'Enhanced phospholipid reduction and calcification mitigation of biological materials', US Patent Application 20040093674, published May 20, 2004.

Cunanan C M, Ochoa A, Cambron R E (2009), 'Methods for processing biological tissue', US Patent 7,622,276, issued November 24, 2009.

De Visscher G, Vranken I, Lebacq A, *et al.* (2007), '*In vivo* cellularization of a cross-linked matrix by intraperitoneal implantation: a new tool in heart valve tissue engineering', *Eur Heart J*, **28**, 1389–96.

De Visscher G, Blockx H, Meuris B, *et al.* (2008), 'Functional and biomechanical evaluation of a completely recellularized stentless pulmonary bioprosthesis in sheep', *J Thorac Cardiovasc Surg*, **135**, 395–404.

De Visscher G, Lebacq A, Mesure L, *et al.* (2010), 'The remodeling of cardiovascular bioprostheses under the influence of stem cell homing signal pathways', *Biomaterials*, **31**, 20–8.

Donnelly R J, Aparicio S R, Dexter F, *et al.* (1973), 'Gamma-radiation of heart valves at 4 ºC; a comparative study using techniques of histochemistry and electron and light microscopy', *Thorax*, **28**, 95–101.

Drury P J, Dobrin J, Bodnar E, Black M M (1986), 'Distribution of flexibility in the porcine aortic root and in cardiac support frames', in Yacoub M and Bodnar E, *Biologic & Bioprosthetic Valves*, New York, Yorke Medical Books, 580–7.

Duraiswamy N, Choksi T D, Pinchuk, L *et al.* (2009), 'A phospholipid-modified polystyrene–polyisobutylene–polystyrene (SIBS) triblock polymer for enhanced hemocompatibility and potential use in artificial heart valves', *J Biomater Appl*, **23**, 367–79.

Duran C G (1986), 'Tissue valves: A perspective from a vintage point of view', in Yacoub M and Bodnar E, *Biologic & Bioprosthetic Valves*, New York, Yorke Medical Books, 487–94.

Duran C M G, Cheung D T, Pang D C (2001), 'Compliant dehydrated tissue for implantation and method for making same', US Patent 6,277,555, issued August 21, 2001.

Eckstein F S, Twvaearai H, Keller D, *et al.* (2004), 'Early clinical experience with a new tubular equine pericardial stentless aortic valve', *Heart Surg Forum*, **7**, E498–502.
EMEA (2004), 'Note for guidance on minimising the risk of transmitting animal spongiform encephalopathy agents via human and veterinary medicinal products', EMEA/410/01 Rev 2, adopted by the Committee for Proprietary Medicinal Products (CPMP) and by the Committee for Veterinary Medicinal Products (CVMP), 2004/C 24/03.
Erdtmann R and Sivitz L B (2004), 'Advancing prion science: guidance for the national prion research program', Washington DC, The National Academies Press.
Fisher J and Wheatley D J (1987), 'An improved pericardial bioprosthetic heart valve. Design and laboratory evaluation', *Eur J Cardiothorac Surg*, **1**, 71–9.
Flameng W, Meuris B, Yperman J, *et al.* (2006), 'Factors influencing calcification of cardiac bioprostheses in adolescent sheep', *J Thorac Cardiovasc Surg*, **132**, 89–98.
Flameng W, Meuris B, DeVisscher G, *et al.* (2008), 'Trilogy pericardial valve: hemodynamic performance and calcification in adolescent sheep', *Annals Thorac Surg*, **85**, 587–92.
Flameng W, Herregods MC, Vercalsteren M, *et al.* (2010), 'Prosthesis-patient mismatch predicts structural valve degeneration in bioprosthetic heart valves', *Circulation*, **121**, 2123–9.
Gibbons D (1980), 'Final Report: Effect of surface texture by ion beam sputtering on implant biocompatibility and soft tissue attachment', NASA-CR-1; 76517.
Gibbons J (2009), Internal data on file, *Southern Lights Biomaterials*, www.slv.co.nz.
Girardot J M (1990), 'Prevention of prosthesis calcification', US Patent 4,976,733, issued December 11, 1990.
Gott J P, Chih P, Dorsey L M A, *et al.* (1992), 'Calcification of porcine valves: a successful new method of antimineralization', *Ann Thorac Surg*, **53**, 207–16.
Harasaki H, Kiraly R, Nose Y (1986), 'Three mechanisms of calcification in tissue valves', in Yacoub M and Bodnar E, *Biologic & Bioprosthetic Valves*, New York, Yorke Medical Books, 433–41.
Hartz R S, Fisher E B, Finkelmeier B, *et al.* (1986), 'An eight-year experience with porcine bioprosthetic cardiac valves', *J Thoracic Cardiovasc Surg*, **91**, 910–17.
Ionescu M I, Tandon A P, Silverton N P, *et al.* (1986), 'Long-term durability of the pericardial valve', in Yacoub M and Bodnar E, *Biologic & Bioprosthetic Valves*, New York, Yorke Medical Books, 165–76.
Ishihara T, Ferrans V J, Boyce S W, *et al.* (1981), 'Structure and classification of cuspal tears and perforations in porcine bioprosthetic cardiac valves implanted in patients', *Am J Cardiology*, **48**, 665–78.
ISO 5840 (2005), 'Cardiovascular implants – cardiac valve prostheses,' available at www.iso.org.
ISO 10993-1 (1997), 'Biological evaluation of medical devices – evaluation and testing,' available at www.iso.org.
ISO 11134 (1994), 'Sterilization of healthcare products – requirements for validation and routine control – industrial moist heat sterilization,' available at www.iso.org.
ISO 11607 (2003), 'Packaging for terminally sterilized medical devices,' available at www.iso.org.
ISO 13485, 'Medical devices – quality management systems – requirements for regulatory purposes,' available at www.iso.org.
ISO 14155-1 (2003), 'Clinical investigation of medical devices for human subjects – Part 1: general requirements,' available at www.iso.org.
ISO 14630, 'Non-active surgical implants – general requirements,' available at www.iso.org.

ISO 14937, 'Sterilization of healthcare products – general requirements for characterization of a sterilizing agent and the development, validation and routine control of a sterilization process for medical devices,' available at www.iso.org.
ISO 14971 (2000), 'Medical devices – application of risk management to medical devices,' available at www.iso.org.
ISO 11737-1 (2006), 'Sterilization of medical devices – microbiological methods – Part 1: Determination of a population of microorganisms on products', available at www.iso.org.
ISO 14160 (1998), 'Sterilization of single-use medical devices incorporating materials of animal origin – Validation and routine control of sterilization by liquid sterilants', available at www.iso.org.
ISO 22442-1 (2007), 'Medical devices utilizing animal tissues and their derivatives – Part 1: Application of risk management', available at www.iso.org.
ISO 22442-2 (2007), 'Medical devices utilizing animal tissues and their derivatives – Part 2: Controls on sourcing, collection and handling', available at www.iso.org.
ISO 22442-3 (2007), 'Medical devices utilizing animal tissues and their derivatives – Part 3: Validation of the elimination and/or inactivation of viruses and transmissible spongiform encephalopathy (TSE) agents', available at www.iso.org.
Jones E L, Weintraub W S, Craver J M, Guyton R A, Shen Y (1994), 'Interaction of age and coronary disease after valve replacement: implications for valve selection' *Annals Thoracic Surg*, **58**, 378–85.
Jones M, Eidbo E E, Walters S M, *et al.* (1986), 'Effects of two types of preimplantation processes on calcification of bioprosthetic valves', in Yacoub M and Bodnar E, *Biologic & Bioprosthetic Valves*, New York, Yorke Medical Books, 451–61.
Jones M, Eidbo E E, Hilbert S L, *et al.* (1989), 'Anticalcification treatments of bioprosthetic heart valves: In vivo studies in sheep', *Journal of Cardiac Surgery*, **4**, 69–73.
Klotz S, Jan Danser AH, Burkhoff D (2008), 'Impact of left ventricular assist device (LVAD) support on the cardiac reverse remodeling process', *Prog Biophys Mol Biol*, **97**, 479–96.
Lane E (1985), 'Method of leaflet attachment for prosthetic heart valves', US Patent 4,501,030, issued February 26, 1985.
Lane E (2002), 'Bioprosthetic heart valve', US Patent 6,371,983, issued April 16, 2002.
Lee J M and Boughner D R (1981), 'Tissue mechanics of canine pericardium in different test environments. Evidence for time-dependent accommodation, absence of plasticity, and new roles for collagen and elastin', *Circ Res*, **49**, 533–44.
Lee J M, Haberer S A, Boughner D R (1989a), 'The bovine pericardial xenograft: I. Effect of fixation in aldehydes without constraint on the tensile viscoelastic properties of bovine pericardium', *J Biomed Mater Res*, **23**, 457–75.
Lee J M, Corrente R, Haberer S A (1989b), 'The bovine pericardial xenograft: II. Effect of tethering or pressurization during fixation on the tensile viscoelastic properties of bovine pericardium', *J Biomed Mater Res*, **23**, 477–89.
Lee J M, Pereira C A, Abdulla D, *et al.* (1995), 'A multi-sample denaturation temperature tester for collagenous biomaterials', *Med Eng Phys*, **17**, 115–21.
Lentz D J and Pollock E M (1982), 'Method for inhibiting mineralization of natural tissue during implantation', US Patent 4,323,358, issued April 6, 1982.
Levy C, Curtin J A, Watkins A, *et al.* (1977), '*Mycobacterium chelonei* infection of porcine heart valves', *NEJM*, **297**, 667–8.
Levy R J and Hirsch D (1998), 'Method of making calcification-resistant bioprosthetic tissue', US Patent 5,746,775, issued May 5, 1998.

Levy R J, Schoen F J, Levy J T, *et al.* (1983), 'Biologic determinants of dystrophic calcification and osteocalcin deposition in glutaraldehyde-preserved porcine aortic valve leaflets implanted subcutaneously in rats', *Am J Pathol*, **113**, 143–55.

Lim K O and Cheong K C (1994), 'Effect of suturing on the mechanical properties of bovine pericardium – implications for cardiac valve bioprosthesis', *Med Eng Phys*, **16**, 526–30.

Maestro M M, Turray J, Olmo N, *et al.* (2006), 'Biochemical and mechanical behavior of ostrich pericardium as a new biomaterial', *Acta Biomaterialia*, **2**, 213–19.

Matthews A M (1998), 'The development of the Starr–Edwards heart valve', *Tex Heart Inst J*, **25**, 282–93.

Mikus P M, Arpesella G, Gargiulo G, *et al.* (1986), 'Does pericardial thickness guarantee an homogenous bioprosthetic product?', in Yacoub M and Bodnar E, *Biologic & Bioprosthetic Valves*, New York, Yorke Medical Books, 605–9.

Mussallem M (2006), Transcript from 3Q2006 investor conference call, available from: http://ht.edwards.com/resourcegallery/investorrelations/ew-transcript-2006-final.pdf [Accessed 7 April 2010].

Naimark W A, Lee J M, Limeback H, Cheung D T (1992), 'Correlation of structure and viscoelastic properties in the pericardia of four mammalian species', *Am J Physiol*, **263**, H1095–H1106.

Nashef A W and Ahmed A I (1989), 'Surfactant treatment of implantable biological tissue to inhibit calcification', US Patent 4, 885, 005, issued December 5, 1989.

Neethling W M, Cooper S, Van Den Heever J J, *et al.* (2002), 'Evaluation of kangaroo pericardium as an alternative substitute for reconstructive cardiac surgery', *J Cardiovasc Surg (Torino)*, **43**, 301–6.

Nguyen T, Lam H L, Zhou J, *et al.* (2002), 'Apparatus for testing bioprosthetic heart valve leaflets', US Patent 6,413,275, issued July 2, 2002.

Paez J M G, Carrera A, Herrero E J, *et al.* (2001), 'Influence of the selection of the suture material on the mechanical behavior of a biomaterial to be employed in the construction of implants. Part 1: Calf pericardium', *J Biomater App*, **16**, 47–67.

Puvimanasinghe J P, *et al.* (2003), 'Choice of a mechanical valve or a bioprosthesis for AVR: does CABG matter?', *Eur J Cardiothorac Surg*, **23**, 688–95; discussion 695.

Rumisek J D, Albus R A, Clarke J S (1985), 'Late *Mycobacterium chelonei* bioprosthetic valve endocarditis: activation of implanted contaminant?', *Annals Thorac Surg*, **39**, 277–9.

Sacks M S (2001), 'The biomechanical effects of fatigue on the porcine bioprosthetic heart valve', *J Long-Term Effects Med Implants*, **11**, 231–47.

Sacks M S and Schoen F J (2002), 'Collagen fiber disruption occurs independent of calcification in clinically explanted bioprosthetic heart valves', *J Biomed Mater Res*, **62**, 359–71.

Sacks M S and Yoganathan A P (2007), 'Heart valve function: a biomechanical perspective', *Phil Trans R Soc B*, **362**, 1369–91.

Sacks M S, Mirnajafi A, Sun W, Schmidt P (2006), 'Bioprosthetic heart valve heterograft biomaterials: structure, mechanical behavior and computational simulation', *Expert Rev Med Devices*, **3**, 817–34.

Sacks M S, Merryman W D, Schmidt D E (2009a), 'On the biomechanics of heart valve function', *Journal of Biomechanics*, **42**, 1804–24.

Sacks M S, Schoen F J, Mayer J E (2009b), 'Bioengineering challenges for heart valve tissue engineering', *Annu Rev Biomed Eng*, **11**, 289–313.

Schaff H V, Carrel T P, Jamieson W R, *et al.* (2002), 'Paravalvular leak and other events

in Silzone-coated mechanical heart valves: a report from AVERT', *Ann Thorac Surg*, **73**, 785–92.

Schoen F J (1995), 'Approach to the analysis of cardiac valve prostheses as surgical pathology or autopsy specimens', *Cardiovascular Pathology*, **4**, 241–55.

Schoen F J (1998), 'Pathological findings in experimental clinical bioprosthetic valves fabricated from photooxidized bovine pericardium', *J Heart Valve Dis*, **7**, 174–9.

Schoen F J and Cohn L H (1986), 'Explant analysis of porcine bioprosthetic heart valves: modes of failure and stent creep', in Yacoub M and Bodnar E, *Biologic & Bioprosthetic Valves*, New York, Yorke Medical Books, 356–65.

Schoen F J and Levy R J (1986), 'Pathophysiology of bioprosthetic heart valve calcification', in Yacoub M and Bodnar E, *Biologic & Bioprosthetic Valves*, New York, Yorke Medical Books, 418–29.

Schoen F J and Levy R J (1999), 'Tissue heart valves: current challenges and future research perspectives', *J Biomed Mater Res*, **47**, 439–65.

Schoen F J, Tsao J W, Levy R J (1986), 'Calcification of bovine pericardium used in cardiac valve bioprostheses', *Am J Pathol*, **123**, 134–45.

Schoen F J, Kujovich J L, Webb C L, Levy R J (1987), 'Chemically determined mineral content of explanted porcine aortic valve bioprostheses: correlation with radiographic assessment of calcification and clinical data', *Circulation*, 1061–6.

Schoen F J, Hirsch D, Bianco R W, Levy R J (1994), 'Onset and progression of calcification in porcine aortic bioprosthetic valves implanted as orthotopic mitral valve replacements in juvenile sheep', *J Thorac Cardiovasc Surg*, **108**, 880–7.

Shamis Y, Patel S, Taube A, *et al.* (2009), 'A new sterilization technique of bovine pericardial biomaterial using microwave radiation', *Tissue Engineering: Part C*, **15**, 1–10.

Soots G, *et al.* (1986), 'Preliminary clinical results with Meadox-Gabbay unicusp pericardial heart valve bioprosthesis', in Yacoub M and Bodnar E, *Biological & Bioprosthetic Valves*, New York, Yorke Medical Books, 699–708.

Sun W, Sacks M, Fulchiero G, *et al.* (2004), 'Response of heterograft heart valve biomaterials to moderate cyclic loading', *J Biomed Mater Res*, **69A**, 658–69.

Vaughn C (2010), 'Heart Valves – Investigational Device Exemption (IDE) and Premarket Approval (PMA) Applications', Available from: http://www.fda.gov/Medical Devices/Device RegulationandGuidance/GuidanceDocuments/ucm193096.htm [accessed 7 April 2010].

Walker D K, Scotten L N, Nugent A H, Brownlee R T (1986), '*In vitro* assessment of the Ionescu-Shiley III, Mitral Medical, and Edwards pericardial valves', in Yacoub M and Bodnar E, *Biologic & Bioprosthetic Valves*, New York, Yorke Medical Books, 588–95.

Webb J G, Altwegg L, Masson J B, *et al.* (2009), 'A new transcatheter aortic valve and percutaneous valve delivery system', *J Am Coll Cardiol*, **53**, 1855–8.

Wittkowsky A K *et al.* (2004), 'Effect of age on international normalized ratio at the time of major bleeding in patients treated with warfarin', *Pharmacotherapy*, **24**, 600–5.

Wood L (2009), 'Edwards Lifesciences Investor Conference, Day 2: THV – Wood & Webb', available at: http://phx.corporate-ir.net/External.File?item=UGFyZW50SUQ9MjM1NzN8Q2hpbGRJRD0tMXxUeXBlPTM=&t=1 [accessed 7 April 2010].

Yoganathan A P and Woo Y-R (1986), '*In vitro* fluid dynamics of tissue valves: old versus new designs', in Yacoub M and Bodnar E, *Biologic & Bioprosthetic Valves*, New York, Yorke Medical Books, 596–604.

Zioupos P, Barbenel J C and Fisher J (1994), 'Anisotropic elasticity and strength of glutaraldehyde fixed bovine pericardium for use in pericardial bioprosthetic valves', *J Biomed Mater Res*, **28**, 49–57.

6

Small intestinal submucosa and other decellularized matrix biomaterials for tissue repair

M. HILES and J. HODDE, Cook Biotech Incorporated, USA

Abstract: Extracellular matrix (ECM) is an essential component of every tissue in our bodies, but it has been relatively misunderstood for decades. More recently, knowledge regarding the role of the ECM in biology and in medicine has been significantly expanded, and its study has greatly added to the world of regenerative medicine in a real and practical sense. This chapter seeks to address the concepts of *in situ* tissue engineering through the provision of an ECM as a scaffold for regrowth of functional tissue. Whether harvesting and decellularizing an ECM from a tissue source or building it *de novo*, the many variables encountered in tissue processing affect the physicochemical aspects of the ECM material, the results achieved after *in vivo* implantation, and the resulting clinical utility of the implants made from such materials. Furthermore, even the most robust ECM materials are affected by procedural and patient-related variables that together affect clinical outcomes for tissue reconstructions with ECM. Advanced biomaterials that consist, either wholly or partially, of ECMs can form the basis for many therapeutic modalities, but clinical medicine must play a role in defining the procedures and the patients that will best benefit from these materials in the future.

Key words: decellularized materials, extracellular matrix, crosslinking, biologic grafts, matrix signals, clinical lessons.

6.1 Introduction

In the whole hierarchy of cells, tissues, organs, systems, and organisms, the roles of the scaffolds and signals of the traditional tissue engineering triad (Fig. 6.1) are lost, or at least obscured. Cells are 'nesters', meaning that they tailor their environment to suit their needs and often the needs of other cells around them or that are likely coming to visit (more on this later). The cells plus this 'nest' become the true basis for tissues, and conversely, harvesting tissues and removing the cells become the basis for the extracellular matrix-based materials that are the focus of this chapter. Herein, we will take a more in-depth look at the extracellular matrix (ECM), but not so much from the point of view of the molecular biologist. We will instead look at the ECM from the point of view of a biomedical or tissue engineer seeking to use it as a building block for medically useful constructs.

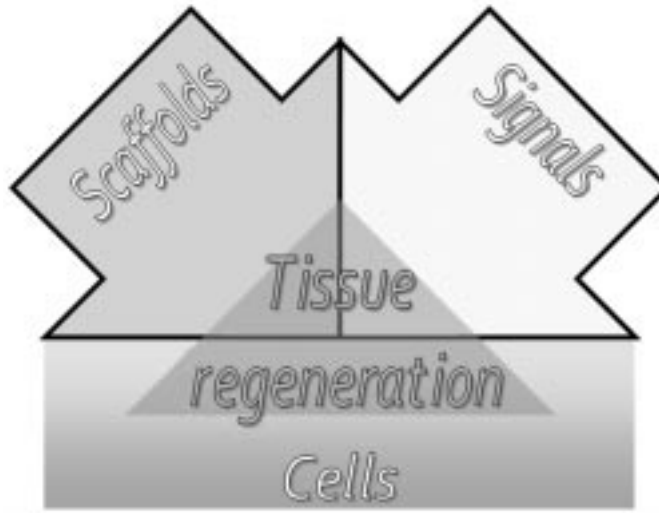

6.1 The triad of cells, scaffolds and signals come together in *in situ* tissue engineering to result in tissue regeneration. In this paradigm, the cells necessary are provided by the recipient in response to exogenous scaffolds and signals.

6.2 *In situ* tissue engineering

The notion-turned-reality of tissue engineering has more traditionally followed the thought process of providing cells, scaffolds, and signals in an already determined, often three-dimensional construct ready for implantation in, or application on, the patient. The goal is to provide the 'right' construct with the cells still alive and able to properly interface with the host's (patient's) cells and systems.

In situ tissue engineering is differently described as the idea that some parts of the tissue engineering triad required for tissue regeneration can somehow be coaxed out of the recipient's physiology to affect and complete the reparative processes. Thus, the elegant example of salamander whole limb regeneration after amputation is perhaps also the ultimate example of *in situ* tissue engineering because none of the three components of the triad must be exogenously applied for total tissue regeneration to occur. In the absence of this ability, a great deal of time and effort, research and development is spent trying to determine how the non-cellular components of scaffolds and signals can be harnessed for healing. Some fundamental questions for *in situ* tissue engineering are as follows:

- What is the minimum exogenous stimulus necessary to get the healing process rolling if stalled or alter the healing process if somehow deemed aberrant or undesirable?

- Is that which is minimally necessary to drive the healing process also sufficient for functional tissue regeneration or is more than the minimum often needed?
- Are the necessary and sufficient provisions different for each tissue, disease, and species treated and approach used to treat?

Remarkably, in many cases of soft and hard tissue repair, surprisingly little exogenous stimulus is required for quite exceptional repairs. Demineralized bone powder has had a long track record for repairing osseous defects (Glowacki *et al.*, 1981), yet in the grand scheme of tissue engineering, it is a relatively simple and effective solution. Similarly, wound dressings for chronic skin wounds made simply of purified, type I collagen and a cellulosic material have shown clear benefit in getting some of these recalcitrant wounds to close (Ghatnekar *et al.*, 2002).

Further, we find that the amount of exogenous stimulus required is not only a function of the disease processes present, but also a strong function of the application procedures and the suitability for healing inherent in the recipient. For example, proper tissue attachment with closely spaced sutures facilitates tissue ingrowth from adjacent, viable tissue into an ECM scaffold, and less attachment can result in graft failure, premature graft degradation, or other failure modes. Also, it is well known that the diabetic state has a dramatically negative effect on wound healing. Thus, it is no surprise that diabetic recipients require a greater stimulus, such as a bioactive matrix, to get their wounds to heal (Niezgoda *et al.*, 2005).

6.2.1 ECM and all its constituents as signals

The ECM is complex in both structure and composition. Both structure and composition appear to be tissue-specific, meaning that, for example, the ECM of the dermis and the ECM of the intestinal submucosa are both collagen-rich but very different in thickness, structural fiber orientation, and biochemical composition (Orberg *et al.*, 1983; Hodde, 2002; Yasui *et al.*, 2004; Derwin *et al.*, 2006; Hodde *et al.*, 2007; Gilbert *et al.*, 2008). It is quite reasonable to consider both the molecules themselves as well as their structural arrangement within the ECM as signals to incident or invading cells.

We learn in basic biochemistry that the non-lipid[1] part of molecular biology is constituted by a spectrum of molecules ranging from pure proteins to pure carbohydrates, with names like proteoglycans, glycoproteins, and glycosaminoglycans. These molecules come together in a complex and well-orchestrated structure known as the ECM. Much like each instrument in the orchestra has a

1. Interestingly, the lipid-containing molecules of the ECM remain largely unstudied, at least in terms of their roles for cell-signaling and matrix interactions. Of course, there are some exceptions, but like outer space this realm remains fertile for new exploration.

part to play, so too does each molecule of the ECM have a part to play in the symphony of wound healing. Each part that is played can be characterized, in a biological sense, as signaling.

The structure itself can help or hinder cellular penetration and other cellular activities. Although significant self-assembly of macromolecules takes place in the ECM (Rabinovitch and Anderson, 1976; Chung *et al.*, 2008), the ECM is clearly the result of cell-based synthetic and excretory pathways. The presence of hydration states, vascular and lymphatic channels, and the cells themselves necessitates that the ECM be porous in its origins, and much evidence of cellular invasion patterns in decellularized matrices shows that porosity is an important property for cellular repopulation (Wei *et al.*, 2005; Yeong *et al.*, 2007; Liu *et al.*, 2009). Density, pore size and frequency, hydrophilicity, and fibrous structural integrity all play a role in cell interaction, invasion, and matrix degradation.

The overall structure of the ECM can affect long-term results and end-stage tissue composition. For example, dermis is known to contain a fair amount of elastin, and Harper showed that an acellular human dermis graft used in breast fascia showed significant amounts of persistent elastin in a biopsy taken more than 2 years after grafting (Harper, 2005). Elastin is a structural protein found in some, but not all, ECMs from various tissues, not typically found in significant quantities in fascia, and extremely slow to turn-over (more on this below). These facts may contribute to late-term changes and failures that take place in hernia repairs made with elastin-rich materials such as human or animal dermis (Hiles *et al.*, 2009).

There is much evidence in the published literature that the individual components of the ECM have effects on cellular function. More than 30 years ago Postlethwaite *et al.* (1978) showed that various collagen types and their fragments were chemoattractants for cells. Hyaluronic acid is known to bind growth factors, maintain moisture, and decrease inflammation (Belford *et al.*, 1993; Polubinska *et al.*, 2000; Vazquez *et al.*, 2003). Heparan sulfate proteoglycan is known to stimulate angiogenesis (Klagsbrun, 1992). Fibronectin is known to facilitate cell attachment and stimulate cell migration (Carter *et al.*, 1981; Baron-van Evercooren *et al.*, 1982). Growth factors such as TGF-β, CTGF, and FGF-2 are commonly found in the ECM and known to stimulate cell proliferation, differentiation, and excretion of other factors and ECM proteins (McDevitt *et al.*, 2003; Hodde *et al.*, 2005; Yamanaka *et al.*, 2008). Davis *et al.* (1987) showed *in vitro* that hepatic cells synthesize varying amounts of differing collagen types in response to changes in their ECM substrate.

Conversely, there is a growing body of evidence that the cells that create the ECM tailor it to their specific needs. This can happen as part of the normal course of development of tissues, or cells taking part in various disease states can also dramatically affect the ECM composition. For example, dermis and fascia are known to have different compositions, and even various layers of the dermis have strikingly different mechanical properties, as shown by Ventre *et al.*

(2009). Of particular note, Belluci *et al.* (2007) showed that the diseased state associated with familial Alzheimer's significantly affect collagen, glycosaminoglycan, and growth factor production of ECM in skin fibroblasts.

What was not well known until recently is how to retain many of these signals in the ECM while still making it safe for use in the medical arena. There is a long history of harvested tissues, such as porcine heart valves, for use in humans, but classical processing methods include harsh chemical treatments such as stripping and crosslinking to render tissues more mechanically stable, biologically predictable and sterile. Such processes sacrifice biological activity (bioactivity) and complete remodeling in favor of short-term handling characteristics.

6.2.2 Harnessing healing and measurable bioactivity

Healing can be defined as the process of bringing a diseased or wounded tissue back into synchronization with the adjacent, viable tissues. In other words, lost or necrotic tissue needs to be brought back up in metabolic state to heal, and a hypertrophic tissue may need to be brought down in metabolic state to properly heal.

Not surprising, ECM plays a big role in all stages of the healing process. One of the very first processes in healing, the creation of the provisional matrix of the fibrin clot, is an example of the formation of an ECM very suitable for cellular invasion, repopulation, and breakdown for tissue replacement. Applying a 'more complete' ECM, or at least a different ECM, can dramatically affect the host response on the cellular level in the healing environment.

A variety of cellular functions including attachment, migration, proliferation, secretion, differentiation, and probably even apoptosis are necessary parts of the healing process. Signals, in their broadest sense, that more actively than passively stimulate cells to perform one of these functions are said to be 'bioactive.' Thus, an ECM can be quite bioactive, and assays can and have been developed to measure bioactivity – even the bioactivity that may be present in a fresh, frozen, or processed ECM.

These bioactivity assays can be *in vitro* or *in vivo* and can test by direct contact or sample extracts. One of the most straightforward of these assays is a cell proliferation measurement often tested with various material extracts. Purified growth factors and naive media are often used as controls. A modified version of this test can be conducted by growing the cells of interest directly on the materials of the test. Cell proliferation can be measured in a variety of ways from DNA synthesis measures to metabolism of target substrates.

Another bioactivity assay can measure the ability of various materials or extracts to affect cellular differentiation (Sano *et al.*, 1988). Of course, the ability for any material or extract to cause cellular differentiation may be as much a function of the cell type and culture conditions as it is a measure of the

bioactivity of the test articles, so careful selection of controls, blocking agents, and test conditions are often necessary.

An ECM harvested from the submucosa of the small intestine (SIS) has been shown to have significant, measurable bioactivity (Nihsen *et al.*, 2008). *In vitro* assays of cell proliferation, stimulation of cell differentiation, and promotion of cell signaling to cause excretion of another growth factor have all been observed with SIS. Still further, an *in vivo* bioactivity measure of cellular migration and angiogenesis has been developed using a mouse subcutaneous implant model (Sung *et al.*, 2005). These assays can be used to test a variety of implant materials and shows that SIS stimulates a robust angiogenic response but chemical stripping of SIS with acids, bases and salts nearly obliterates this response (Hodde *et al.*, 2007; Nihsen *et al.*, 2008).

6.2.3 Turn-over versus a long-term foreign body

All tissues of the body turn over – some imperceptibly slow, such as bone – and some very rapidly, such as the cornea. A properly healed wound is no exception, and restoring this turn-over is an overarching goal of tissue regeneration therapies. In contrast, the very idea of placing a permanent mesh or metallic implant is, by definition, not in keeping with this philosophy of harnessing healing. That is not to say that these therapies are not effective, because they often are. They are simply not tissue regeneration therapies; they are tissue replacement therapies.

Tissue replacement implants are recognized as a foreign body and attacked by innate immunity. If it cannot be broken down and removed from the site, the body will mount a chronic inflammatory response around the implant. This response may simply serve to encapsulate and wall-off the implant from other tissues, or it may serve to dramatically drive an adaptive and progressively stronger inflammatory response that can result in sterile abscesses, seromas or rejection-like phenomena (Rosch *et al.*, 2003; Tsui *et al.*, 2005).

Tissue regeneration therapies, such as those of bioactive ECMs, are also recognized as a foreign body and attacked by innate immunity, but the sequelae are quite different (Allman *et al.*, 2001). Breakdown by cell-secreted matrix metalloproteinases (MMPs) results from cellular ingrowth and migration and causes the release of breakdown products that are themselves bioactive (Postlethwaite *et al.*, 1978). Further, the breakdown of a matrix under mechanical stress serves to transfer that stress to other areas that may have already be invaded by host cells, and these mechano-stimulated cells respond by laying down new ECM (Badylak *et al.*, 1995, 2001; Silverman *et al.*, 2004). Thus, in turn, the ECM implant is replaced by host ECM, and the cycle of living tissue turnover begins.

Achieving the goal of harnessing tissue turnover means that an implant can become completely 'self' – a living part of the patient. It also means that the

implant will not stay static, but indeed can grow with the patient. This is the case as reported by several investigators using SIS implants in children (Smith and Campbell, 2006; Murphy and Corbally, 2007; Hayn *et al.*, 2009; Karpelowsky *et al.*, 2009). A living graft can also be defended from bacterial invaders and avoid early- and late-term infections often seen in permanent synthetic implants (Badylak *et al.*, 1994; Butler *et al.*, 2005; Shell *et al.*, 2005).

6.3 Harvest from nature or build from scratch

Bringing an ECM biomaterial into widespread clinical use clearly requires a source for sufficient quantities of raw material. ECMs traditionally have been harvested from an animal or human source, but the idea of creating a useful ECM from the 'ground up' is very attractive. If this could be done, then the exact composition, microstructure, macrostructure, and even release kinetics for drugs and the like could be precisely specified.

6.3.1 ECM sources similarities and differences

ECM for clinical use has been harvested from a wide variety of sources. These include dermis, pericardium, fascia lata, dura mater, intestinal submucosa, bone, ligament, heart valve, blood vessel, and many others that have only been tested in preclinical studies. Aside from the tissue location of ECM harvest, such materials can originate from autograft (self), allograft (different individual of the same species), or xenograft (different species) sources – all of which have been used widely in clinical medicine. Xenograft materials that have been used clinically have been harvested from pigs, sheep, cows, and even horses.

ECMs that have proven most successful in clinical medicine have a few important characteristics in common. First, they have a readily available and economically accessible source for tissue acquisition and processing. Also, in the case of soft-tissue repairs, they have relative mechanical strength that allows them to be sutured in place and readily able to resist the stresses encountered in load-bearing sites. In the case of bone, they have the ability to be placed in a bony defect and stimulate a functional repair of osseous tissue. They are all biocompatible, meaning that they will pass a standard battery of biological tests, and can be processed aseptically, terminally sterilized, or both. Finally, successful decellularized ECMs do not stimulate immune rejection, sensitization, or promotion of neoplastic cell growth. In fact, some studies even show that some ECMs can alter neoplastic cell phenotypes and even reduce neoplastic growth *in vivo* (Hurst *et al.*, 2003; Hodde *et al.*, 2004).

Although each combination of tissue and source species can result in a harvestable ECM, they are by no means equivalent in their structure, composition, availability, or utility (Table 6.1). Of course, each harvested ECM inherits many of the characteristics that describe the original tissue. Thus, ECM

Table 6.1 Comparison of harvested ECM biomaterials (commercially available in the US) for important similarities and differences

	Acellular human dermis (AHD)	Acellular porcine dermis (APD)	Crosslinked porcine dermis (CPD)	Fetal bovine dermis (FBD)	Small intestinal submucosa (SIS)
Intact, bioactive ECM with known, measurable bioactivity	No (stripped)	No (stripped)	No (crosslinked)	No (stripped)	Yes
Fully remodeled scaffold (complete turn-over)	No	No	No	No	Yes
Significant elastin content	Yes	Yes	Yes	Yes	No
Published strength over time data (preclinical)	No	Yes	No	No	Yes
Published short-term (<2 yr) data in any human clinical use	Yes	No	Yes	No	Yes
Long-term (>2 yr) multi-application published results in humans	No	No	No	No	Yes
Proven, validated, published anti-viral safety and sterility	No	No	Yes	No	Yes

materials harvested from arteries or dermis are much more elastic and elastin-containing than those harvested from pericardium, fascia lata, or submucosa. Further, growth factors and other biologically potent cell stimulators vary widely from tissue to tissue and alter what is even possible to keep present through the processing steps.

6.3.2 Problems with *de novo* ECM synthesis

Building a complete ECM *de novo* is not a simple task. Solubilizing and reconstituting type I collagen is not all that difficult, but restructuring the collagen to form a porous, recognizable, and structurally strong matrix is quite difficult. Most purified collagen constructs are reformed into dense sheets or films but lack structural integrity and resistance to degradation without strong chemical crosslinking (Weadock *et al.*, 1983; Charulatha and Rajaram, 2003). Further, virtually all natural ECMs have been shown to contain various collagen types other than type I, many forms of glycosaminoglycans, glycoproteins,

growth factors, and other structural or signal proteins (Hodde *et al.*, 2007). Recreating these complex structures, especially in a biologically relevant context, has yet to be achieved.

Bowlin and colleagues were successful in creating very porous and fiber-oriented structures from electro-sprayed collagen I and other ECM molecules such as elastin (Matthews *et al.*, 2002; Boland *et al.*, 2004). These structures were implanted in animal models and showed remarkable tissue integration. Their work represents very promising steps toward *de novo* ECM development, but to date their results still suffer from lack of structural integrity for load-bearing applications and biological complexity that are likely necessary for surgical applications and directing cellular fate (Newton *et al.*, 2009).

6.3.3 Safety issues real and perceived

Many myths or half-truths surround the use of ECM in clinical medicine, and yet some safety issues are quite real and must be addressed by the developers. With any medical device improper sterilization can lead to bacterial disease transmission, but no reports exist in the literature describing the transmission of an animal disease to humans from an implantable or topical xenogenic ECM device. This is not the case for human allograft tissues such as tendon, dermis, and bone, which have a finite risk of disease transmission given by the US Centers for Disease Control as approximately four transmissions per million grafts used (CDC, 2005).

When developing an ECM biomaterial from an animal tissue source, many source-related considerations must be addressed. Herd controls for source animals, regular assessment by properly trained veterinary medical personnel, food and drug regimens, and harvest facility exclusivity, handling, and cleanliness procedures must all be addressed to ensure safety and limit cross-contamination potential for the target tissues.

Even when source controls and processing techniques are stable and well designed, all but the most extremely chemically modified ECMs are subject to bacterial and inflammatory degradation, which can present safety issues. For example, premature degradation of a hernia repair device can lead to reherniation, evisceration, bowel strangulation, or even patient death (Helton *et al.*, 2005). It is very important that products designed with an ECM component take into account potential levels and modes of bacterial contamination in their use.

The immunological aspects of an ECM, especially those from animal origin, must be carefully considered and controlled for. Perhaps the single biggest factor in determining immunocompatibility of ECM and host is the processing used to prepare the ECM. The processing aspects will be further addressed in the next section, but it is important to state here that cellular debris, contaminants such as endotoxin, and endogenous factors such as immunoglobulins need to be considered and reduced or eliminated in the overall process. Further, validated

antiviral and terminal sterilization processing steps are necessary to provide safety assurance and, in most cases, to achieve regulatory approvals (Hodde and Hiles, 2002).

6.4 The extreme importance of processing

ECM materials are full of proteins and other biologically important molecules that can be rinsed away, altered, destroyed, or simply rendered mute by the many steps of processing in an attempt to make them safe for human use. Many of these steps can affect the mechanical and physical properties of the resultant grafts, but perhaps more subtle are their effects on the biological properties both for short-term complications and for long-term outcomes in the recipients. These effects can also extend to cell-culture applications where a cell-friendly matrix is of utmost importance for cellular tissue engineering.

6.4.1 Process similarities and differences

Virtually all commercially viable tissue harvesting processes involve one or more steps of mechanical isolation, chemical washes, thorough rinses, dehydration, freezing, and gas or radiation sterilization. Not every graft material includes every step, but all grafts undergo processes that alter them from their original, *in situ* composition and structure. The extent of this alteration is one of the main determinants that affect its fate in the patient.

Mechanical steps involve cutting, delaminating, or grinding the source organ or tissue to form a sheet or powdered material that can be further processed. This is often done at a location away from the manufacturing facility, such as a packing plant or morgue, in order to facilitate transport and allow for quick storage methods to be used.

Chemical steps often used are focused on the goals of decellularization, disinfection, and sometimes crosslinking for mechanical 'stabilization.' Decellularization is an art that ultimately means that no living cells survive the process. Lipid content measurements, histologic methods, or DNA extractions can all be used to help quantify the extent of decellularization, but there is little consensus on exact definitions of what constitutes complete and necessary decellularization. For example, DNA is often left behind in decellularized grafts, but in the absence of strands long enough to code for complete genes or known viruses, little or no harm can be attributed to DNA remnants.

Chemical disinfection is of utmost importance in the processing of tissues to make them safe. Most regulatory bodies reviewing processes for animal tissues require the manufacturers to provide extensive data on the overkill of various resistant viruses that might be found in their source animals. This involves spike and recovery studies with several logs of kill built into the process as a safety factor (Hodde and Hiles, 2002). Achieving this extensive overkill of bacteria and

viruses without destroying many important aspects of the target tissue is a balancing act, for sure, and the subject of numerous patents in this field. One of the oldest and most effective methods for disinfection involves the use of aldehydes such as glutaraldehyde. They are very effective at disinfection and impart a chemical crosslink between the collagen fibers that is directly akin to making leather. These crosslinks render the source tissue much more resistant to degradation by enzymes but also render it inert with respect to host remodeling or at least cell signaling attributes.

Dehydration steps are often part of a tissue process. These can be solvent-based or done with vacuum pumps, and the goal is to provide a more stable material for shelf storage. Much research has gone into the effects of various freezing and freeze-drying techniques on the structure of the resulting matrix, yet some ECM materials appear to be rather robust and affected very little by freeze–thaw cycles. Drying a tissue means that for most applications it must be rehydrated before use, typically in sterile saline in the operating room. Another, less obvious benefit of drying is that a dry product offers many more standard options for sterilization.

Decellularized tissues of animal origin are regulated by the US Food and Drug Administration (FDA) and many other regulatory bodies as medical devices. As such, they must be terminally sterilized to exacting standards with a sterility assurance of 10^{-6} (i.e. less than 1 device in a million can have a single living organism present). Terminal sterilization of collagen-based materials is not simple because many modes adversely affect the materials. For example, intense heat from steam autoclaves causes collagen shrinkage and denaturization.[2] Gamma radiation is an effective sterilization method for many materials but for collagen-based materials it leads to chain scission and decreased tissue strength and increased degradation rates (Seto *et al.*, 2009). This may be desirable for some applications, but not for most of the strength-bearing uses of ECM grafts. Although some biochemical degradation is seen, ethylene oxide sterilization at suitably low temperatures appears to be quite compatible with ECMs, and even some of the newer methods, such as gas plasma sterilization, are showing some promise for sterilization with tissue preservation (Markowicz *et al.*, 2006).

Decellularized tissues from human origin are regulated in the US as banked tissues and not subject to the same sterilization rules. Their processes often involve chemical disinfections and aseptic handling without the use of terminal sterilization. This means that a much more rigorous process for screening donors must be employed to help assure graft safety.

2. Although probably not appropriate for collagen implants, collagen shrinkage from boiling water was the basis for shrunken heads in the jungles of South America. Don't try this at home.

6.4.2 Consequences in cellular and tissue responses

When deciding to undertake a product development program, the tissue engineer should consider the cellular responses to all components involved, including the selection of a matrix scaffold. Differences in processing can dramatically affect the interplay between cells and the ECM, and these differences can be seen both *in vitro* and *in vivo*.

Perhaps the best side-by-side comparison of ECM process effects found in the literature was presented by Cook *et al.* (2008). They found that crosslinking of ECMs significantly reduced the cellular penetration and cell growth rate of several cell types in culture, and these same materials were significantly slower to repopulate with cells in a rat abdominal wall implant model. This finding is consistent with a recent publication by Becker *et al.* (2009) who found in a randomized clinical study that crosslinked collagen membranes are more prone to wound infections than their non-crosslinked counterparts. Cook *et al.* also found that non-crosslinked but chemically stripped materials, such as acellular human dermis, were also not nearly as 'cell friendly' in culture as the less-processed ECMs.

A comparison highlighting the effects of chemical stripping can be found in work done in the author's laboratory and mentioned above. In a mouse subcutaneous implant model of angiogenesis there is a dramatic difference in the extent of vascular penetration and overall cellularity of intact SIS versus chemically stripped SIS (Fig. 6.2). The incident cells find a much more suitable matrix for repopulation in the intact ECM implants.

One benefit clearly conferred by chemical crosslinking is the reduction in degradation rate of the ECM itself (Liang *et al.*, 2004). This may be advantageous in some settings where high stresses are encountered or large tissue defects have to be spanned. Defect spanning can limit the tissue ingrowth opportunities to edge-only effects and significantly alter the healing response by favoring tissue degradation processes. Unfortunately, chemical crosslinking can lead to seriously aberrant tissue responses including graft encapsulation (Trabuco *et al.*, 2007) and heterotopic ossification (Chanda *et al.*, 1997). These responses are related to the fact that crosslinked materials are often recognized as foreign bodies by host cells and stimulate a localized chronic inflammation.

6.5 Clinical lessons learned

Just because an ECM is naturally derived does not mean that it can be used clinically without any complications. In fact, when any graft material – whether biologic or synthetic – is implanted into the body, the risk of complications rises because the graft material is seen as a foreign object that the body wishes to remove. While surgeons are used to dealing with complications associated with

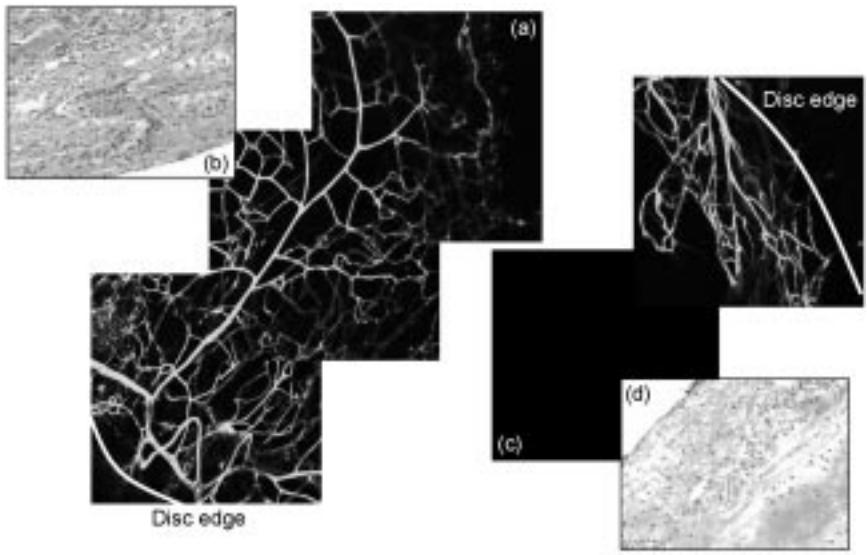

6.2 Fluorescent microangiographs of angiogenesis into 6 mm ECM discs implanted subcutaneously in the mouse and evaluated at 21 days. Intact SIS (a) shows actively growing (leaky) capillaries penetrating to a depth of nearly 3 mm from disc edge, whereas the stripped SIS implants (c) showed much fewer actively-branching capillaries and a penetration depth of less than 1 mm from disc edge. Further, note the difference in cellularity between the implants with the intact SIS (b) showing significantly more cellularity than the stripped SIS (d).

synthetic graft materials, many are not familiar at dealing with complications that can be seen when biologic graft materials are utilized to restore tissue function.

The idea that a biologic implant is simple to implant and use simply because it is naturally derived has been the thought of surgeons in the recent past, but experience in using biologic materials derived from human dermis and porcine intestinal submucosa suggests that the more complex the implant, the more difficult it is to implant without complications. Because biologic graft materials are able to interact with the body, they do not act like inert synthetics. Close and secure tissue approximation with healthy tissue is essential to ensuring that the material is able to interact with the patient's surrounding tissues and become repopulated with fibroblasts. If suture spacing is so great that relative motion can occur between the graft and the patient tissue, the biologic graft will likely be walled off or prematurely degraded and will not incorporate into the surrounding tissues. Likewise, if the patient is in such ill-health or the adjacent tissues are so diseased or necrotic that fibroblasts cannot migrate into the graft, the biomaterial will not become incorporated but instead will act as an inert nidus for seroma formation, wound dehiscence, or infection. Therefore, achieving success when

using ECM-based graft materials for tissue repair depends greatly on not only the implant material, but also on the ability of the patient to accept such a bioactive implant that requires 'self' to be successful and the surgical technique that is used to implant it.

Evidence suggests that healthy people are less likely to have complications when biologic grafts are implanted than are the elderly and frail. Consider, for example, the years of successful outcomes in preclinical animal models where healthy animals were used to test biologic implant grafts, or the high rates of success and minimal complications observed when trained athletes are implanted with biologic mesh to treat 'sports' hernias (Edelman and Selesnick, 2006). Conversely, obese, diabetic patients who also use nicotine on a regular basis are a more challenging lot and are susceptible to poorer outcomes and a higher incidence of complications (Misra *et al.*, 2008). It has been shown, for example, that people who smoke or have diabetes are less likely to achieve successful closure of their anal fistulas following placement of a biologic mesh plug than are their non-smoking or non-diabetic counterparts (Schwandner *et al.*, 2009). Clearly, we have much more to learn about the individual patient characteristics that can affect clinical outcome when biologic implants are used for tissue repair, but it is obvious that since the ECM graft depends on intimate interaction with the patient's tissues to be successful, the health of the graft recipient is a determining factor in the eventual outcome achieved. That is not to say that success cannot be achieved in the face of critically ill patients. Clearly, biologic graft materials have been successful in treating diabetic skin ulcers (Niezgoda *et al.*, 2005) and have their place in treating grossly contaminated wounds (Helton *et al.*, 2005); however, the healthier the patient, the better the likely outcome.

In addition to the nature of the graft and the characteristics of the individual patient recipient playing a role in the outcome of a biologic implant, pristine surgical technique that adheres to historical surgical tenets is critical to achieving a successful outcome absent of complications. For example, Edelman and Selesnick (2006) and Fine (2006) report recurrences that occurred following implant of a biologic graft material to repair direct inguinal hernias and attribute the failures to inadequate size of the graft material used. Additionally, Knoll (2007) has discovered that, much like synthetic materials, biologic graft materials shrink after implant and that this shrinkage needs to be considered during surgical placement. In his report on treating Peyronie's disease, Knoll reports that oversizing the graft by 30% when sewing it in is important in preventing recurvature of the penis. While the shrinkage observed with synthetics is likely to cause pain and discomfort as the material scars into the surrounding tissues, the shrinkage that occurs when decellularized biologic grafts are used is more likely to cause recurrence. Clearly, broad overlap of the biologic graft with the adjacent tissues – as much as 5 cm in all directions for hernia repair – is essential to preventing recurrence (Klinge *et al.*, 2005).

A successful outcome when decellularized biologic grafts are used in tissue repair depends not only on adequate overlap of the mesh and the adjacent tissues. It also depends on close and frequent tissue approximation. Tacks or sutures spaced at as little as 2 mm intervals adequately secure decellularized biologics into place and allow the patient's adjacent cells to invade the graft. If relative motion between the implant and the surrounding tissues is not minimized, the patient's cells will never populate the graft and it will become walled off or dissolved, leaving a nidus or dead space that can serve as a pocket for fluid accumulation or bacterial colonization.

Because decellularized biologics consist of ECM proteins, they are highly susceptible to enzymatic breakdown by the body's own remodeling mechanisms or by bacteria that may be present. Clearly, a risk of using naturally derived, decellularized graft materials is their inherent susceptibility to colonization by bacteria. Collagen is an excellent growth substrate for microorganisms, and so any successful use of a biologic mesh should take into consideration the effect that contamination may have on the implant. For example, Helton *et al.* (2005) report that repair of the ventral abdominal wall with porcine small intestinal submucosa is more successful and less prone to complications in clean cases than in contaminated ones. Likewise, it is likely that many of the early failures observed following placement of a collagen plug in abscessed anal fistulas are due to contamination of the fistula tract with a collagenase-producing, gram-negative bacterium. Preventing breakdown due to colonization by bacteria is critical to the graft's success and can be achieved only if the patient's adjacent cells bring in a new blood supply. Close and tight approximation of the graft with the surrounding tissues ensures that repopulation of the graft will occur and that the risk of premature degradation due to bacterial colonization or liberation of matrix metalloproteases can be minimized.

The most common areas for biologic graft use include ventral hernia repairs in contaminated or potentially contaminated fields where synthetic grafts are often contra-indicated. A recent systematic review of the literature for hernia repair using biologic grafts found, somewhat surprisingly, that the published experience with biologic grafts was much greater for clean cases than for contaminated ones, and it verified that SIS can be used for a long-term repair extending beyond 7 years (Hiles *et al.*, 2009). Widespread use for ECMs also has arisen in the treatment of chronic wounds, chronic fistulas, plastic surgery, and dura mater repair; but everyday inguinal hernias, pelvic organ prolapse repairs, and many other applications have yet to see much ECM use because of concerns over cost and lack clinical evidence. Nonetheless, in many instances where repeat surgeries for recurrent hernia, late infections or erosions from synthetic incompatibilities, or long-term pain from chronic neuritis can be avoided, ECM-based biologic grafts are growing in popularity and proving that in many instances they can save costs in the long term.

Although well over two million patients have been treated worldwide with ECM-based grafts, the widespread clinical use of decellularized biologic grafts is still in its infancy due to their cost, because many surgeons have tried to use them unsuccessfully, or because many surgeons have simply not bought in to the concept of tissue regeneration. As we continue to learn more about how the product, the patient, and the procedure must interact to achieve a successful outcome when these biologic materials are used, it is likely that more surgeons will develop the necessary skills and meticulous surgical techniques required to overcome the inherent challenges that this new field possesses.

6.6 References

Allman, A. J., McPherson, T. B., Badylak, S. F., Merrill, L. C., Kallakury, B., Sheehan, C., Raeder, R. H. & Metzger, D. W. (2001) Xenogeneic extracellular matrix grafts elicit a TH2-restricted immune response. *Transplantation*, **71**, 1631–40.

Badylak, S. F., Coffey, A. C., Lantz, G. C., Tacker, W. A. & Geddes, L. A. (1994) Comparison of the resistance to infection of intestinal submucosa arterial autografts versus polytetrafluoroethylene arterial prostheses in a dog model. *J Vasc Surg*, **19**, 465–72.

Badylak, S. F., Tullius, R., Kokini, K., Shelbourne, K. D., Klootwyk, T., Voytik, S. L., Kraine, M. R. & Simmons, C. (1995) The use of xenogeneic small intestinal submucosa as a biomaterial for Achilles tendon repair in a dog model. *J Biomed Mater Res*, **29**, 977–85.

Badylak, S., Kokini, K., Tullius, B. & Whitson, B. (2001) Strength over time of a resorbable bioscaffold for body wall repair in a dog model. *J Surg Res*, **99**, 282–7.

Baron-van Evercooren, A., Kleinman, H. K., Seppa, H. E., Rentier, B. & Dubois-Dalcq, M. (1982) Fibronectin promotes rat Schwann cell growth and motility. *J Cell Biol*, **93**, 211–16.

Becker, J., Al-Nawas, B., Klein, M. O., Schliephake, H., Terheyden, H. & Schwarz, F. (2009) Use of a new cross-linked collagen membrane for the treatment of dehiscence-type defects at titanium implants: a prospective, randomized-controlled double-blinded clinical multicenter study. *Clin Oral Implants Res*, **20**, 742–9.

Belford, D. A., Hendry, I. A. & Parish, C. R. (1993) Investigation of the ability of several naturally occurring and synthetic polyanions to bind to and potentiate the biological activity of acidic fibroblast growth factor. *J Cell Physiol*, **157**, 184–9.

Bellucci, C., Lilli, C., Baroni, T., Parnetti, L., Sorbi, S., Emiliani, C., Lumare, E., Calabresi, P., Balloni, S. & Bodo, M. (2007) Differences in extracellular matrix production and basic fibroblast growth factor response in skin fibroblasts from sporadic and familial Alzheimer's disease. *Mol Med*, **13**, 542–50.

Boland, E. D., Matthews, J. A., Pawlowski, K. J., Simpson, D. G., Wnek, G. E. & Bowlin, G. L. (2004) Electrospinning collagen and elastin: preliminary vascular tissue engineering. *Front Biosci*, **9**, 1422–32.

Butler, C. E., Langstein, H. N. & Kronowitz, S. J. (2005) Pelvic, abdominal, and chest wall reconstruction with AlloDerm in patients at increased risk for mesh-related complications. *Plast Reconstr Surg*, **116**, 1263–75; discussion 1276–7.

Carter, W. G., Rauvala, H. & Hakomori, S. I. (1981) Studies on cell adhesion and recognition. II. The kinetics of cell adhesion and cell spreading on surfaces coated

with carbohydrate-reactive proteins (glycosidases and lectins) and fibronectin. *J Cell Biol*, **88**, 138–48.

CDC (2005) Centers for Disease Control and Prevention, FDA, and Health Resources and Services Administration, Department of Health and Human Services Workshop on preventing organ and tissue allograft-transmitted infection: priorities for public health intervention, Atlanta, Georgia, June 2–3.

Chanda, J., Kuribayashi, R. & Abe, T. (1997) Heparin in calcification prevention of porcine pericardial bioprostheses. *Biomaterials*, **18**, 1109–13.

Charulatha, V. & Rajaram, A. (2003) Influence of different crosslinking treatments on the physical properties of collagen membranes. *Biomaterials*, **24**, 759–67.

Chung, H. J., Steplewski, A., Chung, K. Y., Uitto, J. & Fertala, A. (2008) Collagen fibril formation. A new target to limit fibrosis. *J Biol Chem*, **283**, 25879–86.

Cook, J. L., Fox, D. B., Kuroki, K., Jayo, M. & de Deyne, P. G. (2008) *In vitro* and *in vivo* comparison of five biomaterials used for orthopedic soft tissue augmentation. *Am J Vet Res*, **69**, 148–56.

Davis, B. H., Pratt, B. M. & Madri, J. A. (1987) Retinol and extracellular collagen matrices modulate hepatic Ito cell collagen phenotype and cellular retinol binding protein levels. *J Biol Chem*, **262**, 10280–6.

Derwin, K. A., Baker, A. R., Spragg, R. K., Leigh, D. R. & Iannotti, J. P. (2006) Commercial extracellular matrix scaffolds for rotator cuff tendon repair. Biomechanical, biochemical, and cellular properties. *J Bone Joint Surg Am*, **88**, 2665–72.

Edelman, D. S. & Selesnick, H. (2006) 'Sports' hernia: treatment with biologic mesh (Surgisis): a preliminary study. *Surg Endosc*, **20**, 971–3.

Fine, A. P. (2006) Laparoscopic repair of inguinal hernia using Surgisis mesh and fibrin sealant. *JSLS*, **10**, 461–5.

Ghatnekar, O., Willis, M. & Persson, U. (2002) Cost-effectiveness of treating deep diabetic foot ulcers with Promogran in four European countries. *J Wound Care*, **11**, 70–4.

Gilbert, T. W., Wognum, S., Joyce, E. M., Freytes, D. O., Sacks, M. S. & Badylak, S. F. (2008) Collagen fiber alignment and biaxial mechanical behavior of porcine urinary bladder derived extracellular matrix. *Biomaterials*, **29**, 4775–82.

Glowacki, J., Altobelli, D. & Mulliken, J. B. (1981) Fate of mineralized and demineralized osseous implants in cranial defects. *Calcif Tissue Int*, **33**, 71–6.

Harper, J. R. (2005) *Tissue Regeneration using a Human Acellular Tissue Matrix: A Histological Perspective*. LifeCell Corporation.

Hayn, M. H., Bellinger, M. F. & Schneck, F. X. (2009) Small intestine submucosa as a corporal body graft in the repair of severe chordee. *Urology*, **73**, 277–9.

Helton, W. S., Fisichella, P. M., Berger, R., Horgan, S., Espat, N. J. & Abcarian, H. (2005) Short-term outcomes with small intestinal submucosa for ventral abdominal hernia. *Arch Surg*, **140**, 549–60; discussion 560–2.

Hiles, M., Record Ritchie, R. D. & ALtizer, A. M. (2009) Are biologic grafts effective for hernia repair? A systematic review of the literature. *Surg Innov*, **16**, 26–37.

Hodde, J. (2002) Naturally occurring scaffolds for soft tissue repair and regeneration. *Tissue Eng*, **8**, 295–308.

Hodde, J. & Hiles, M. (2002) Virus safety of a porcine-derived medical device: evaluation of a viral inactivation method. *Biotechnol Bioeng*, **79**, 211–16.

Hodde, J. P., Suckow, M. A., Wolter, W. R. & Hiles, M. C. (2004) Small intestinal submucosa does not promote PAIII tumor growth in Lobund-Wistar rats. *J Surg Res*, **120**, 189–94.

Hodde, J. P., Ernst, D. M. & Hiles, M. C. (2005) An investigation of the long-term bioactivity of endogenous growth factor in OASIS Wound Matrix. *J Wound Care*, **14**, 23–5.

Hodde, J., Janis, A., Ernst, D., Zopf, D., Sherman, D. & Johnson, C. (2007) Effects of sterilization on an extracellular matrix scaffold: part I. Composition and matrix architecture. *J Mater Sci Mater Med*, **18**, 537–43.

Hurst, R. E., Kyker, K. D., Bonner, R. B., Bowditch, R. D. & Hemstreet, G. P., 3RD (2003) Matrix-dependent plasticity of the malignant phenotype of bladder cancer cells. *Anticancer Res*, **23**, 3119–28.

Karpelowsky, J. S., Thomas, G. & Shun, A. (2009) Definitive abdominal wall closure using a porcine intestinal submucosa biodegradable membrane in pediatric transplantation. *Pediatr Transplant*, **13**, 285–9.

Klagsbrun, M. (1992) Mediators of angiogenesis: the biological significance of basic fibroblast growth factor (bFGF)-heparin and heparan sulfate interactions. *Semin Cancer Biol*, **3**, 81–7.

Klinge, U., Conze, J., Krones, C. J. & Schumpelick, V. (2005) Incisional hernia: open techniques. *World J Surg*, **29**, 1066–72.

Knoll, L. D. (2007) Use of small intestinal submucosa graft for the surgical management of Peyronie's disease. *J Urol*, **178**, 2474–8; discussion 2478.

Liang, H. C., Chang, Y., Hsu, C. K., Lee, M. H. & Sung, H. W. (2004) Effects of crosslinking degree of an acellular biological tissue on its tissue regeneration pattern. *Biomaterials*, **25**, 3541–52.

Liu, Y., Bharadwaj, S., Lee, S. J., Atala, A. & Zhang, Y. (2009) Optimization of a natural collagen scaffold to aid cell-matrix penetration for urologic tissue engineering. *Biomaterials*, **30**, 3865–73.

Markowicz, M., Koellensperger, E., Steffens, G. C., Frentz, M., Schrage, N. & Pallua, N. (2006) The impact of vacuum freeze-drying on collagen sponges after gas plasma sterilization. *J Biomater Sci Polym Ed*, **17**, 61–75.

Matthews, J. A., Wnek, G. E., Simpson, D. G. & Bowlin, G. L. (2002) Electrospinning of collagen nanofibers. *Biomacromolecules*, **3**, 232–8.

McDevitt, C. A., Wildey, G. M. & Cutrone, R. M. (2003) Transforming growth factor-beta1 in a sterilized tissue derived from the pig small intestine submucosa. *J Biomed Mater Res A*, **67**, 637–40.

Misra, S., Raj, P. K., Tarr, S. M. & Treat, R. C. (2008) Results of AlloDerm use in abdominal hernia repair. *Hernia*, **12**, 247–50.

Murphy, F. & Corbally, M. T. (2007) The novel use of small intestinal submucosal matrix for chest wall reconstruction following Ewing's tumour resection. *Pediatr Surg Int*, **23**, 353–6.

Newton, D., Mahajan, R., Ayres, C., Bowman, J. R., Bowlin, G. L. & Simpson, D. G. (2009) Regulation of material properties in electrospun scaffolds: role of cross-linking and fiber tertiary structure. *Acta Biomater*, **5**, 518–29.

Niezgoda, J. A., van Gils, C. C., Frykberg, R. G. & Hodde, J. P. (2005) Randomized clinical trial comparing OASIS Wound Matrix to Regranex Gel for diabetic ulcers. *Adv Skin Wound Care*, **18**, 258–66.

Nihsen, E. S., Johnson, C. E. & Hiles, M. C. (2008) Bioactivity of small intestinal submucosa and oxidized regenerated cellulose/collagen. *Adv Skin Wound Care*, **21**, 479–86.

Orberg, J., Baer, E. & Hiltner, A. (1983) Organization of collagen fibers in the intestine. *Connect Tissue Res*, **11**, 285–97.

Polubinska, A., Pawlaczyk, K., Kuzlan-Pawlaczyk, M., Wieczorowska-Tobis, K., Chen,

C., Moberly, J. B., Martis, L., Breborowicz, A. & Oreopoulos, D. G. (2000) Dialysis solution containing hyaluronan: effect on peritoneal permeability and inflammation in rats. *Kidney Int*, **57**, 1182–9.

Postlethwaite, A. E., Seyer, J. M. & Kang, A. H. (1978) Chemotactic attraction of human fibroblasts to type I, II, and III collagens and collagen-derived peptides. *Proc Natl Acad Sci USA*, **75**, 871–5.

Rabinovitch, A. L. & Anderson, H. C. (1976) Biogenesis of matrix vesicles in cartilage growth plates. *Fed Proc*, **35**, 112–6.

Rosch, R., Junge, K., Schachtrupp, A., Klinge, U., Klosterhalfen, B. & Schumpelick, V. (2003) Mesh implants in hernia repair. Inflammatory cell response in a rat model. *Eur Surg Res*, **35**, 161–6.

Sano, M., Kato, K., Totsuka, T. & Katoh-Semba, R. (1988) A convenient bioassay for NGF using a new subline of PC12 pheochromocytoma cells (PC12D). *Brain Res*, **459**, 404–6.

Schwandner, T., Roblick, M. H., Kierer, W., Brom, A., Padberg, W. & Hirschburger, M. (2009) Surgical treatment of complex anal fistulas with the anal fistula plug: a prospective, multicenter study. *Dis Colon Rectum*, **52**, 1578–83.

Seto, A., Gatt, C. J., Jr. & Dunn, M. G. (2009) Improved tendon radioprotection by combined cross-linking and free radical scavenging. *Clin Orthop Relat Res*, **467**, 2994–3001.

Shell, D. H. T., Croce, M. A., Cagiannos, C., Jernigan, T. W., Edwards, N. & Fabian, T. C. (2005) Comparison of small-intestinal submucosa and expanded polytetrafluoroethylene as a vascular conduit in the presence of gram-positive contamination. *Ann Surg*, **241**, 995–1001; discussion 1001–4.

Silverman, R. P., Li, E. N., Holton, L. H., 3rd, Sawan, K. T. & Goldberg, N. H. (2004) Ventral hernia repair using allogenic acellular dermal matrix in a swine model. *Hernia*, **8**, 336–42.

Smith, M. D. & Campbell, R. M. (2006) Use of a biodegradable patch for reconstruction of large thoracic cage defects in growing children. *J Pediatr Surg*, **41**, 46–9; discussion 46–9.

Sung, H. J., Johnson, C. E., Lessner, S. M., Magid, R., Drury, D. N. & Galis, Z. S. (2005) Matrix metalloproteinase 9 facilitates collagen remodeling and angiogenesis for vascular constructs. *Tissue Eng*, **11**, 267–76.

Trabuco, E. C., Klingele, C. J. & Gebhart, J. B. (2007) Xenograft use in reconstructive pelvic surgery: a review of the literature. *Int Urogynecol J Pelvic Floor Dysfunct*, **18**, 555–63.

Tsui, K. P., Ng, S. C., Tee, Y. T., Yeh, G. P. & Chen, G. D. (2005) Complications of synthetic graft materials used in suburethral sling procedures. *Int Urogynecol J Pelvic Floor Dysfunct*, **16**, 165–7.

Vazquez, J. R., Short, B., Findlow, A. H., Nixon, B. P., Boulton, A. J. & Armstrong, D. G. (2003) Outcomes of hyaluronan therapy in diabetic foot wounds. *Diabetes Res Clin Pract*, **59**, 123–7.

Ventre, M., Mollica, F. & Netti, P. A. (2009) The effect of composition and microstructure on the viscoelastic properties of dermis. *J Biomech*, **42**, 430–5.

Weadock, K., Olson, R. M. & Silver, F. H. (1983) Evaluation of collagen crosslinking techniques. *Biomater Med Devices Artif Organs*, **11**, 293–318.

Wei, H. J., Liang, H. C., Lee, M. H., Huang, Y. C., Chang, Y. & Sung, H. W. (2005) Construction of varying porous structures in acellular bovine pericardia as a tissue-engineering extracellular matrix. *Biomaterials*, **26**, 1905–13.

Yamanaka, O., Saika, S., Ikeda, K., Miyazaki, K., Kitano, A. & Ohnishi, Y. (2008)

Connective tissue growth factor modulates extracellular matrix production in human subconjunctival fibroblasts and their proliferation and migration in vitro. *Jpn J Ophthalmol*, **52**, 8–15.

Yasui, T., Tohno, Y. & Araki, T. (2004) Characterization of collagen orientation in human dermis by two-dimensional second-harmonic-generation polarimetry. *J Biomed Opt*, **9**, 259–64.

Yeong, W. Y., Chua, C. K., Leong, K. F., Chandrasekaran, M. & Lee, M. W. (2007) Comparison of drying methods in the fabrication of collagen scaffold via indirect rapid prototyping. *J Biomed Mater Res B Appl Biomater*, **82**, 260–6.

7

New ceramics and composites for joint replacement surgery

M. N. RAHAMAN, Missouri University of Science and Technology, USA and B. SONNY BAL, University of Missouri–Columbia, USA

Abstract: Ceramics have been used as an alternative to metal-on-polyethylene in joint replacement surgery of arthritic hips and knees since the 1970s. In prosthetic hip and knee bearings, ceramics offer a major benefit of drastically reduced wear rates and excellent long-term biocompatibility, which can increase the longevity of prosthetic hip and knee joints. This benefit is important clinically because hip and knee replacements have become very common surgical procedures, particularly in the United States and Europe, and because these procedures are increasingly performed in younger patients who place greater demands on the prosthetic bearings. Modern ceramic bearings are safe and reliable if used with components of proven design and durability. However, catastrophic bearing failure *in vivo*, while rare, and the risk of 'squeaking' (audible noise) of ceramic bearings, while low, have served to diminish the enthusiasm of many patients and orthopedic surgeons for ceramic bearings in total joint replacement. Future material improvements are actively being investigated to reduce the risk of ceramic bearing failures even further, and to extend the range of ceramic bearing components available for total joint replacement. In this chapter, the properties, applications, and limitations of ceramics that have been used in orthopedic bearings are reviewed, and the new ceramics and composites that will be available for joint replacement surgery in the near future are discussed.

Key words: total joint replacement, orthopedic implants, ceramics, ceramic matrix composites.

7.1 Introduction

Arthroplasty devices for replacing the hip joint have been under development since the early 1900s, but the basic design for modern total hip arthroplasty (THA) devices is credited to Sir John Charnley who, in the early 1960s, introduced a metal femoral head prosthesis articulating in an ultra-high molecular weight polyethylene (UHMWPE) acetabular component (Charnley, 1961). THA and total knee arthroplasty (TKA) are common operations today, particularly in the US and Europe. More than 500 000 total hip and knee joint replacements are

performed annually, and the future incidence is expected to increase as the population ages and maintains its activity and function level (Crowninshield *et al.*, 2006).

The standard bearing coupling in THA and TKA today consists of a cobalt–chromium (CoCr) alloy articulating against UHMWPE (Fig. 7.1). After 10–15 years *in vivo*, UHMWPE wear particles lead to localized inflammation in the hip joint, periprosthetic bone resorption and, ultimately, aseptic loosening of the

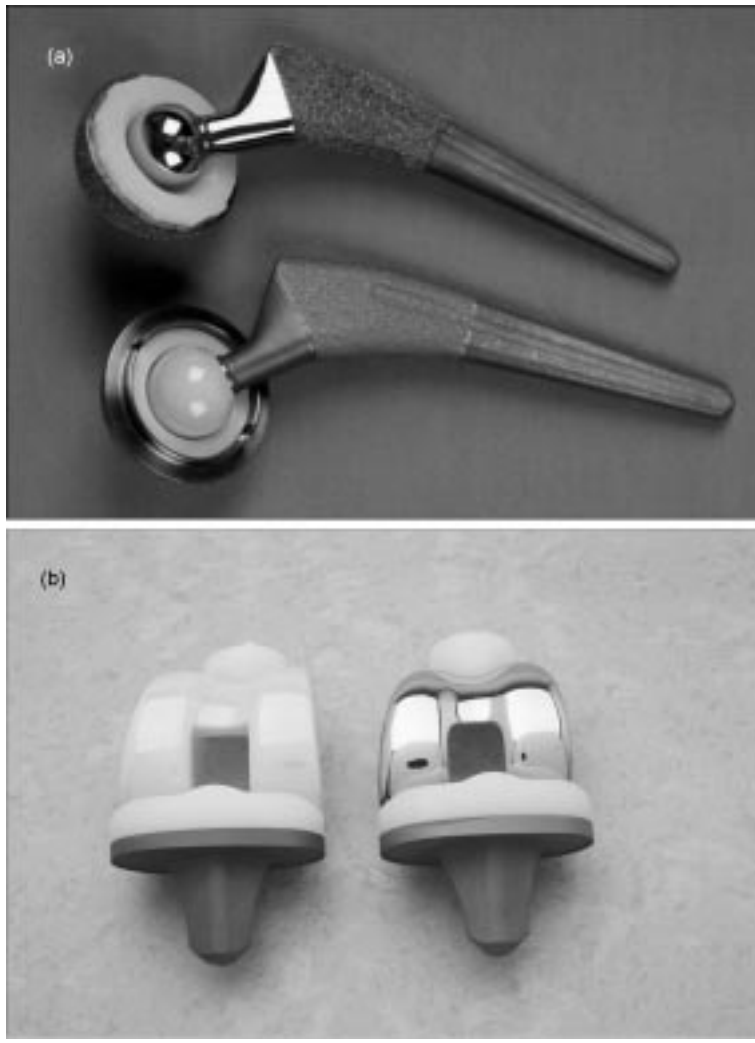

7.1 (a) Prosthetic hip implants with CoCr–UHMWPE bearing couple (top), and Al_2O_3–Al_2O_3 bearing couple (bottom). (b) Prosthetic knee implants with stabilized ZrO_2–UHMWPE bearing couple (left) and CoCr–UHMWPE bearing couple (right).

prosthetic implant. Repeat (revision) joint surgery due to premature failure of the prosthetic joints by aseptic loosening is morbid, risky, and costly. It accounts for approximately 25% of the total hip and knee replacement surgeries performed annually (Crowninshield *et al.*, 2006; Emery *et al.*, 1997).

Ceramics have been used as an alternative to the metal–polyethylene bearing couple in THA and TKA for several decades (Rahaman *et al.*, 2007). Alumina (Al_2O_3), introduced as an orthopedic bearing material in the early 1970s (Boutin, 1971), is by far the most widely used ceramic in THA. The microstructure of the basic Al_2O_3 material has been manipulated in recent years to produce composites in an attempt to improve its resistance to catastrophic brittle fracture. Stabilized zirconia (ZrO_2) was introduced in the mid-1980s in response to concerns about Al_2O_3 femoral head fractures in THA (Christel, 1989; Piconi and Maccauro, 1999). Silicon nitride (Si_3N_4) bearings are currently undergoing clinical trials for application in THA and TKA (Bal *et al.*, 2008, 2009a). A list of ceramics currently used or under development for bearings in total joint replacement is given in Table 7.1.

Ceramic bearings significantly reduce wear in THA and TKA articulations (Skinner, 1999), thereby contributing to the longevity of THA and TKA, and reducing the likelihood of repeat hip and knee joint surgery (Harris, 1995; Kurtz *et al.*, 2005; Lavernia *et al.*, 1995). Al_2O_3 femoral heads articulating against UHMWPE leads to lower wear than CoCr–UHMWPE articulations (Skinner, 1999). Al_2O_3 heads can also be used with sockets of the same material, with the resulting Al_2O_3–Al_2O_3 articulations having the lowest wear of any THA bearing combination (Bizot *et al.*, 2004; D'Antonio *et al.*, 2002; Hamadouche *et al.*, 2002; Oonishi *et al.*, 2002; Sedel *et al.*, 1998; Urban *et al.*, 2001, Wroblewski *et al.*, 1996). At intermediate follow-up, THA with Al_2O_3–Al_2O_3 articulations is associated with less femoral bone loss than THA with metal-on-polyethylene bearings (D'Antonio *et al.*, 2005).

The limitation of ceramic bearings in total joint replacement is related to their characteristic property of brittleness, which can lead to catastrophic failure *in vivo*. Improvements in material quality, manufacturing methods, and implant design over several years (1980s and 1990s) have resulted in a drastic reduction of the incidence of such failures (Heros and Willmann, 1998; Willman, 2000). The incidence of catastrophic failure of modern Al_2O_3 femoral heads *in vivo* is rare, approximately 1 in 5000–10 000, but this risk has persisted during the last decade or so despite many improvements in Al_2O_3 starting materials, manufacturing, and quality control (Garino *et al.*, 2006). A less serious issue with Al_2O_3–Al_2O_3 THA articulations *in vivo* is 'squeaking' (audible noise), which has been recognized within the last 5 years or so (Capello *et al.*, 2008; Walter *et al.*, 2008). The overall occurrence of this 'squeaking' phenomenon is in the range 0.5–10% (Walter *et al.*, 2008).

While modern Al_2O_3 ceramic bearings are safe and reliable if used with THA and TKA components with proven design and durability (Bierbaum *et al.*, 2002;

Table 7.1 Ceramic materials currently used or under development for bearing applications in total hip arthroplasty (THA) and total knee arthroplasty (TKA)

Material	Articulation	Clinical applications	Representative manufacturers	Trade name	Availability
Al_2O_3	Ceramic–ceramic; ceramic–poly	THA; TKA	CeramTec, Metoxit, Kyocera, Ceraver, Morgan Matroc	Biolox; Biolox *forte*	Yes
Y-TZP	Ceramic–poly	THA; TKA	Desmarquest, Kyocera, Metoxit, Morgan Matroc	–	No[a]
Mg-PSZ	Ceramic–poly	THA; TKA	Xylon, Signal, Biopro	Ziralloy	Yes
ZTA	Ceramic–ceramic; ceramic–poly	THA; TKA	CeramTec	Biolox *delta*	Yes
Si_3N_4	Ceramic–ceramic; ceramic–poly; ceramic–metal	THA; TKA	Amedica	MC[2]	No[b]
Oxidized zirconium	Ceramic–poly	THA; TKA	Smith & Nephew	Oxinium	Yes
Diamond-like coating	Ceramic–ceramic	THA	Diamicron	–	No[c]

Material: Al_2O_3 = alumina; Y-TZP = yttria-stabilized tetragonal zirconia polycrystals; Mg-PSZ = magnesia partially stabilized zirconia; ZTA = zirconia toughened alumina.
Articulation: poly = ultra-high molecular weight polyethylene (UHMWPE), or crosslinked polyethylene.
Availability: [a]Withdrawn from US market. Y-TZP containing small quantities of oxides such as Al_2O_3 is available in Japan and in Europe; [b]in process of approval for clinical applications; [c]in development for clinical applications.

D'Antonio *et al.*, 2003; Garino, 2000), the risk of catastrophic failure of Al_2O_3 bearings *in vivo*, while rare, is still unacceptably high. Even a small risk of unexpected brittle failure *in vivo* discourages the widespread adoption of ceramic bearings, given the prospect of expensive litigation and complex repeat surgery. The development of alternative ceramics and ceramic composites, deposition of ceramic coatings on metals, and surface modification of metals to produce ceramic surfaces, are the main approaches that have been investigated to achieve the low wear of ceramic articulating surfaces with reduced risk of catastrophic failure.

7.2 Ceramics for bearing applications

Bearings for total joint replacement must remain mechanically and chemically stable *in vivo* for greater than 10 years, while enduring 2 million or more gait-related cycles of loading each year. The loads vary from three times the body weight (3 kN) for normal walking, to eight times the body weight (8 kN) for jogging or stumbling (Bergmann *et al.*, 1993). High elastic modulus is required to resist deformation and to maintain shape, whereas high strength, high resistance to fracture, and high resistance to mechanical fatigue are required to minimize the risk of failure. For bioinertness and biocompatibility, the material should have high corrosion resistance in the body fluids. High hardness and the ability to be polished to a smooth surface finish are required for long-term wear resistance and low friction. Good wetting (low contact angle) between the bearing surface and the synovial fluids of the joint is necessary for good lubrication.

The strong bonding of the atoms by ionic and covalent bonds, and the crystalline structure are responsible for the desirable mechanical properties (high compressive strength, elastic modulus, and hardness), and chemical inertness *in vivo* of ceramic bearing materials such as Al_2O_3, ZrO_2, and Si_3N_4. The biocompatibility of these materials is related to the high chemical stability of these materials, which confers resistance to corrosion and reliable *in vivo* behavior over time. The surfaces of these ceramics have polar hydroxyl (–OH) groups that promote interaction with the aqueous body fluids to provide a lubricating layer.

7.2.1 Physical and mechanical properties

Table 7.2 compares the several physical and mechanical properties of Al_2O_3, ZrO_2, and Si_3N_4 ceramics with those for CoCr alloys and for bone. Modern Al_2O_3 bearings, fabricated by sintering and hot isostatic pressing, have a dense, fine-grained microstructure, providing a flexural strength >400 MPa, and an elastic modulus of >450 GPa. Al_2O_3 has a Vickers hardness number of more than 14–16 GPa, compared with a value of less than 3–4 GPa for common orthopedic metals such as CoCr and Ti alloys. On the other hand the low fracture

Table 7.2 Material properties (at room temperature) of dense ceramics, currently used or in process of approval for total joint replacement, compared with those for CoCr alloy and cortical bone

Property	Al_2O_3	Mg-PSZ	Y-TZP	ZTA	Si_3N_4	CoCr	Cortical bone
Density (g/cm^3)	>3.97	5.75	6.05	4.40	3.15–3.20	8–9	1.7–2.0
Grain size (μm)	1–5	50	0.1–1.0	1–2	Elongated[a]	–	
Strength (MPa)							
Tensile	250–300	300–400	–	–	–	600–1800	–
Compressive	2000–3000	2000–3000	3000–4000	–	–		130–180
Flexural	300–400	600–700	1000–1500	700–1000	800–1200		60–160
Fracture toughness, K_{IC} ($MPa\,m^{1/2}$)	4–5	6–10	6–12	6–10	8–12	50–100	2–12
Elastic modulus (GPa)	400–450	200–250	200–250	300–350	300–320	210–250	10–20
Hardness (Vickers) (GPa)	14–16	10–12	12–14	12–15	14–16	3–4	
Thermal expansion coefficient ($10^{-6}\,K^{-1}$)	8	7–10	11	8.5	3.0–3.5	$\sim$14.0	
Thermal conductivity ($W\,m^{-1}\,K^{-1}$)	30	2	2	17	20–30	$\sim$100	

Al_2O_3 = alumina (›99.9% purity); Mg-PSZ = magnesia partially stabilized zirconia (8 mol% MgO); Y-TZP = yttria-stabilized tetragonal zirconia polycrystals (3 mol% Y_2O_3); ZTA = zirconia toughened alumina (20 vol% ZrO_2); Si_3N_4 = *in situ* toughened silicon nitride.
[a]Typically 1–3 μm in diameter $\times$ 5–20 μm long.

toughness of Al_2O_3 (4 MPa $m^{1/2}$), compared with a value of 50–100 MPa $m^{1/2}$ for CoCr alloys, is a limitation.

ZrO_2 stabilized in the tetragonal phase with Y_2O_3, referred to as yttria-stabilized tetragonal zirconia polycrystals, Y-TZP, has flexural strength and fracture toughness values that are almost twice those for Al_2O_3. However, use of Y-TZP in THA and TKA has severe limitations, due to degradation in a moist atmosphere which leads to microcracking and loss of strength. Following an unusually high rate of clinical failures which resulted from alteration of the manufacturing variables, Y-TZP was withdrawn from clinical use (Masonis *et al.*, 2004). Si_3N_4 bearings are currently undergoing clinical trials for applications in THA. Control of the manufacturing variables can lead to the production of Si_3N_4 with a dense microstructure of elongated grains, referred to as '*in situ* toughened' Si_3N_4, with a flexural strength as high as 1 GPa and a fracture toughness of 10–12 MPa $m^{1/2}$.

7.2.2 Wear of ceramic bearings

Al_2O_3 femoral heads articulating against UHMWPE reduce wear by at least a factor of 2 when compared to the standard CoCr femoral head, and Al_2O_3–Al_2O_3 bearing couples provide the least wear rate, with a value that is often more than 50–100 times lower than that of the standard CoCr–UHMWPE couple (Table 7.3) (Willmann *et al.*, 1996). Si_3N_4–Si_3N_4 and Si_3N_4–CoCr bearing couples have shown wear rates that are comparable to those of Al_2O_3–Al_2O_3 bearings (Bal *et al.*, 2008, 2009a; Clarke *et al.*, 2000).

Since the 1970s, the standard bearing couple has consisted of a CoCr femoral head articulating against a UHMWPE liner. In some countries, the femoral head consists of stainless steel. The CoCr–UHMWPE couple has the advantage of low cost. However, the wear rate is relatively high and depends on the activity of the patient and on the diameter of the femoral head. The lifetime is typically not more than 10 years, so this implant is often recommended for elderly or inactive patients. Because of their low wear rates and low prevalence of osteolysis,

Table 7.3 Volumetric wear at 10×10^6 cycles for bearing couples in identical hip simulators and testing protocols

Bearing couple	Volumetric wear (mm^3)
CoCr–UHMWPE	62
Al_2O_3–UHMWPE	<30
CoCr–CoCr	6.5
Al_2O_3–Al_2O_3	0.35–0.6
Si_3N_4–Si_3N_4	0.65
Si_3N_4–CoCr	0.47

From Bal *et al.* (2008, 2009a); Clarke *et al.* (2000).

Al_2O_3–Al_2O_3 bearings provide an attractive option, particularly for younger patients.

In addition to the normal (low) wear associated with the articulating surfaces, observations of unbroken Al_2O_3–Al_2O_3 bearing couples retrieved from patients showed that some bearing couples had an unusual wear pattern, described as 'stripe wear' (Nevelos *et al.*, 1993, 1999, 2001; Shishido *et al.*, 2003; Walter *et al.*, 2004; Yamamoto *et al.*, 2005). This stripe wear pattern consists of a long narrow area of damage on the femoral head and a matching area of wear near the rim of the acetabular liner (Fig. 7.2), resulting from contact between the femoral head and the rim of the acetabular liner. Stripe wear has been associated with steep acetabular cup angles, young patients, and revision surgery (Nevelos *et al.*, 2001). Observations with well-fixed and well-positioned acetabular components indicated that another phenomenon, microseparation of the femoral head and acetabular liner during the swing phase of walking, could also contribute to stripe wear (Lombardi *et al.*, 2000; Nevelos *et al.*, 2000; Walter *et al.*, 2004; Yamamoto *et al.*, 2005). Hip simulator studies have shown that stripe wear leads to higher wear rates, depending on the severity of the microseparation. However, even for bearings with stripe wear, the wear rate and volume of wear debris are so small that the incidence of osteolysis (implant loosening) for Al_2O_3–Al_2O_3 bearings should be far lower than for bearing couples with UHMWPE acetabular liners. Further studies are necessary to understand and reduce the occurrence of stripe wear, particularly under conditions corresponding to severe microseparation conditions found in hip simulator experiments.

7.3 Limitations of ceramics for bearing applications

7.3.1 Failure of ceramic bearings

As in most load-bearing applications, particularly those subjected to a tensile (or hoop stress), the inherent brittleness of ceramics is a major concern. Catastrophic failure of ceramic bearings *in vivo* (Fig. 7.3), while rare, is a serious complication, with profound consequences for the patient, surgeon, and orthopedic bearing manufacturer. Failure of ceramic bearings *in vivo* commonly results from slow crack growth under the static or repetitive loading experienced in the body. Under an applied tensile stress σ, the stress at the tip of a crack can be described by the stress intensity K_I given by

$$K_I = \sigma \sqrt{\pi a} \qquad 7.1$$

where πa is the length of the crack (Lawn, 1993). It is generally assumed that fast failure occurs in brittle solids if the stress intensity at the crack tip, represented by K_I in Equation 7.1, becomes equal to, or greater than, the critical stress intensity factor, K_{IC}, more commonly called the fracture toughness. The fracture strength σ_f of a brittle material can be written as

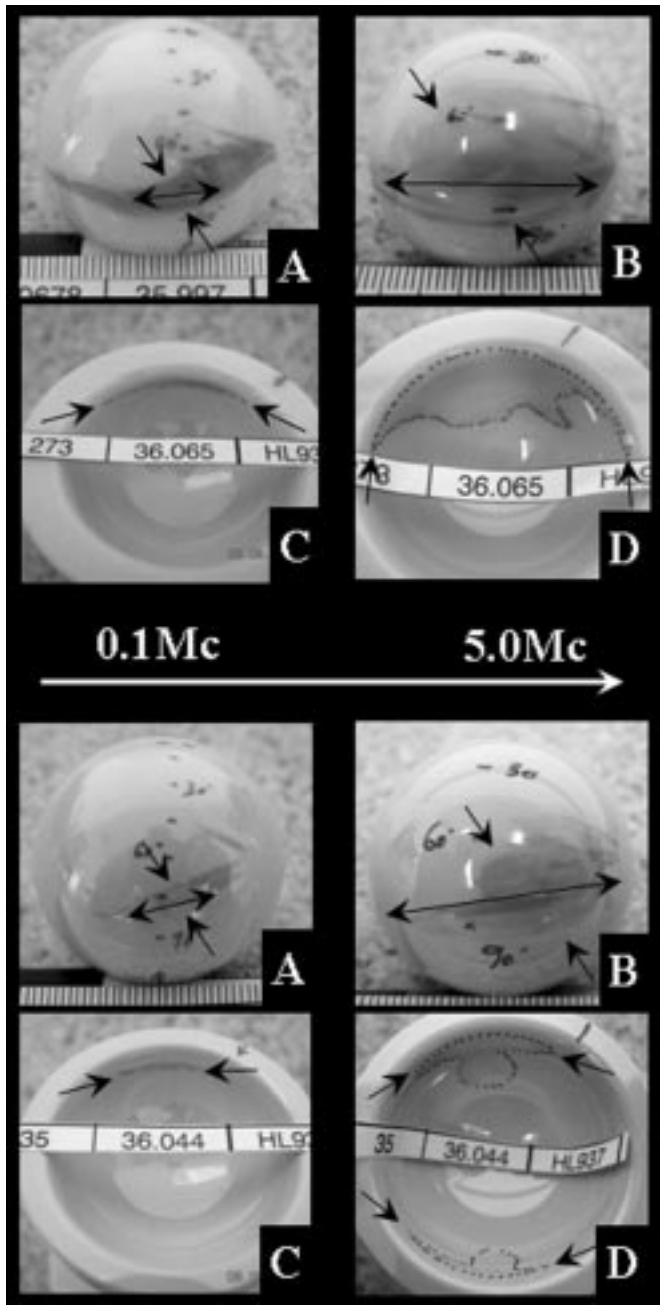

7.2 Typical stripe wear formation in a hip simulator over the initial 10^5 cycles (0.1 Mc) and for the duration of the study (5×10^6 cycles) (5.0 Mc) for an Al_2O_3–Al_2O_3 bearing couple (top: A–D) and an AMC–AMC bearing couple (bottom: A–D). (AMC is Al_2O_3 matrix composite.) (Courtesy of I.C. Clarke.)

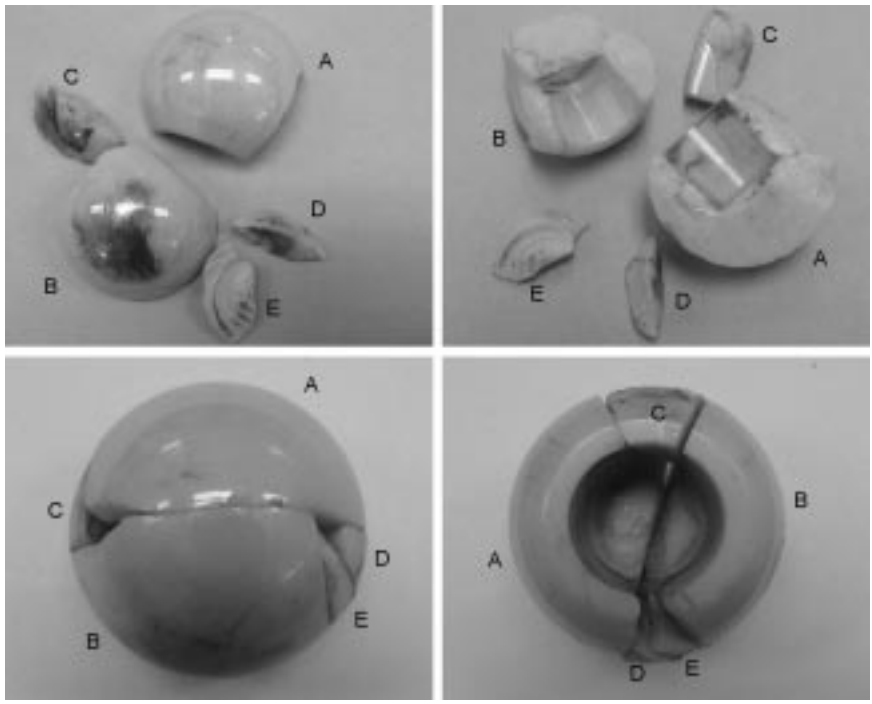

7.3 Example of *in vivo* failure of a ceramic (Y_2O_3-stabilized ZrO_2) femoral head, showing the parts retrieved from the patient and their reassembly. A–E refer to the corresponding parts of the broken and re-assembled femoral head.

$$\sigma_f = \frac{K_{IC}}{\sqrt{\pi a}} \qquad 7.2$$

According to Equation 7.2, the fracture strength of a brittle material is determined by its fracture toughness and flaw size.

Equation 7.2 represents a critical value for *fast crack growth*. It is now well recognized that brittle materials are susceptible to *slow crack growth* at values well below σ_f (or K_{IC}) (Lawn, 1993). The phenomenon is often referred to as *subcritical crack growth*, and it is notable for its sensitivity to applied stress, as well as to environmental factors such as water, water vapor, and temperature. The crack keeps growing, and when it has grown to the critical length for failure at that stress level (Equation 7.2), the material fails suddenly by fast fracture, without warning, often after a long time.

Slow crack growth in bioceramics is attributed to stress-assisted corrosion at the crack tip or at any pre-existing flaw in the material. It results from the combined effect of high stresses at the crack tip and reaction of water (or body fluid) molecules with the molecules at the crack tip (reducing the surface energy at the crack tip), inducing crack propagation in a subcritical manner. A threshold (K_{I0}) in the stress intensity factor, below which no crack propagation occurs, has

been the subject of theoretical and experimental investigations (Chevalier *et al.*, 1999; Wan *et al.*, 1990). The K_{I0} corresponds to crack equilibrium with zero crack velocity, so crack propagation does not occur. It determines the safe range for using ceramics in total joint replacement. A higher K_{I0} value is indicative of a higher reliability and, hence, a longer lifetime of the material. The K_{I0} value represents a more intrinsic property for a material when compared with the fracture toughness K_{IC}, which applies to fast crack growth.

Failure of ceramic bearings can originate from flaws introduced into the bearing during fabrication or post-fabrication surface finishing, or flaws produced as a result of *in vivo* corrosion or degradation. Flaws due to inadequate fabrication or surface finishing include porosity, large grains, and microcracks. Observations of bearings retrieved from patients often show a variety of flaws on the articulating surface resulting from corrosion or degradation, due to a dislocated bearing rubbing against the acetabular component (Bal *et al.*, 2007). These flaws include enhanced porosity, metal staining from a metallic acetabular component, scratches, pits, or grooves. Clinically, ceramic bearing failures have been found to occur in the absence of any identifiable risk factor or explanation (Barrack *et al.*, 2004; Hannouche *et al.*, 2003), which is symptomatic of failure caused by slow crack growth. Patient obesity and strenuous activity may not contribute significantly to the catastrophic failure (fast fracture) of ceramic bearings because the loads applied are well below the fracture strength of the material, but they may contribute to failure by slow crack growth.

Tensile (or hoop) stresses, such as those generated when a ceramic femoral head is impacted on the metal taper of a femoral implant or during impaction of an eccentrically seated ceramic acetabular insert in a metal shell, are relevant to the risk of bearing failure. Until the mid-1970s ceramic femoral heads were attached to femoral stems with suboptimal methods such as gluing, screwing, and brazing. Introduction and optimization of the Morse taper design for ceramic bearings led to a decline in the incidence of ceramic femoral head failures (Hannouche *et al.*, 2003). Finite element analysis of the stress distribution in ceramic femoral heads subjected to a standard rupture test (ISO 7206-10) shows that the areas of maximum tensile (or hoop) stress occur in the contact area to the metal taper and at the bottom of the taper bore (Fig. 7.4a) (Affolter *et al.*, 2009). As ceramic taper bores can have large and numerous surface flaws from drilling, slow crack growth of these surface flaws, particularly in the areas of maximum tensile stress, can provide an important failure mechanism.

According to Equation 7.2, two ways of improving the strength of ceramics are: (1) decreasing the presence of flaws, as well as the size a of the flaws, by careful processing and quality control, and (2) increasing K_{IC}, by alloying or by forming the ceramic into a composite. Advances in materials processing, quality control, and implant design in the 1980s and 1990s have markedly improved the reliability and lifetime of ceramic bearings. The use of tightly controlled ceramic

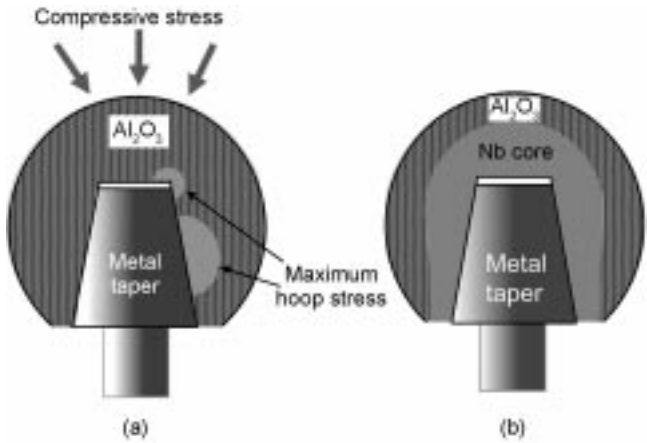

7.4 (a) Schematic diagram of Al_2O_3 femoral head on a metal taper. Finite element model predictions (Affolter *et al.,* 2009) of the regions of maximum tensile (hoop) stress in a ceramic femoral head loaded in compression on a metal taper are indicated (on one half of the symmetrical system). (b) Schematic of Al_2O_3–Nb composite femoral head on a metal taper.

processing procedures, clean-room facilities, optimized sintering and hot isostatic pressing, and rigorous proof testing has resulted in the production of modern Al_2O_3 bearings with improved mechanical reliability and wear (Willmann, 2000). Coupled with these processing and quality control procedures, the use of alternative ceramics, such as Si_3N_4, and ceramic composites, such as ZrO_2-toughened Al_2O_3 (ZTA) can lead to an increase in both K_{I0} and K_{IC} (De Aza *et al.*, 2002). For the same pre-existing defect size, these composites can be stressed to higher loads than the corresponding monolithic ceramics and not suffer delayed failure.

7.3.2 Squeaking of ceramic bearings

A less serious concern with Al_2O_3–Al_2O_3 THA articulations *in vivo* is the risk of 'squeaking' (audible noise) which has been recognized within the last 5 years or so. Squeaking occurs during activities such as walking, bending, and stair climbing, and it is more common in younger, heavier, and taller patients. Several suggestions have been put forward to explain this phenomenon, including mismatched bearing diameters, edge loading due to acetabular component malpositioning or to microseparation of the femoral head and acetabular liner, and disruption of fluid film lubrication leading to enhanced friction between the hard-on-hard bearings (Capello *et al.*, 2008; Walter *et al.*, 2008). While the causes of Al_2O_3–Al_2O_3 hip bearing noise are unclear, it appears that bearing noise is multifactorial in origin, and is related to a combination of implant, patient, and surgical factors.

7.4 Development of ceramics for bearing applications

7.4.1 'Single-phase' ceramics

Following the pioneering work of Boutin (1971) on the use of ceramic bearings for THA, the first generation Al_2O_3 bearings suffered unacceptably high fracture rates *in vivo*. However, advances in materials processing, quality control, and implant design in the 1980s and 1990s resulted in a marked improvement in the strength and reliability Al_2O_3 bearings. Modern Al_2O_3 bearings, such as femoral heads manufactured by CeramTec and sold under the trade name Biolox *forte*, have a failure rate reported to the manufacturer of 0.02% (Garino *et al.*, 2006). Whereas Al_2O_3 bearings are by far the most widely used ceramic bearings, the low fracture toughness (or low resistance to brittle fracture) of Al_2O_3 remains a concern.

Zirconia-based femoral heads were introduced in the 1980s in response to concerns about Al_2O_3 femoral head fractures in THA (Christel, 1989; Piconi and Maccauro, 1999). Zirconia stabilized in the tetragonal phase with yttria (Y_2O_3), referred to as yttria stabilized tetragonal zirconia polycrystals (Y-TZP), has a flexural strength and fracture toughness that are 2–3 times the values for Al_2O_3 (Table 7.2), making it one of the most fracture-resistant ceramics. It was anticipated that ZrO_2 would reduce the risk of femoral head fracture while retaining the excellent wear performance of smaller diameter heads against UHMWPE. However, the degradation of Y-TZP in a moist atmosphere leads to microcracking and loss of strength. Following an unusually high rate of clinical failures which resulted from alteration of the manufacturing variables, Y-TZP was withdrawn from clinical use (Masonis *et al.*, 2004). The addition of small quantities of Al_2O_3 (0.15–3 wt%) to Y-TZP reduces the degradation. The stabilization of ZrO_2 with ceria (CeO_2), to form Ce-TZP, has lower mechanical properties than Y-TZP, but the resistance to degradation is superior. Zirconia partially stabilized with magnesia, referred to as Mg-PSZ, has superior smoothness and fracture toughness than Al_2O_3, but its strength and fracture toughness are inferior to those for Y-TZP. Mg-PSZ does not suffer from the degradation problems of Y-TZP in a moist atmosphere. Mg-PSZ femoral heads are presently available for use in ceramic–UHMWPE articulations in THA, and Mg-PSZ femoral bearings are currently undergoing clinical trials for use in ceramic–UHMWPE articulations in TKA. Zirconia-based bearings articulating against UHMWPE have a similar wear rate to that of Al_2O_3–UHMWPE bearings, but they are not approved for use in ceramic-on-ceramic bearing couples.

Si_3N_4 bearings, manufactured by Amedica Corp., Salt Lake City, UT, under the trade name MC^2, are currently undergoing trials for THA and TKA applications (Fig. 7.5). Si_3N_4 has been the subject of considerable research and development for decades, for high temperature structural applications such as

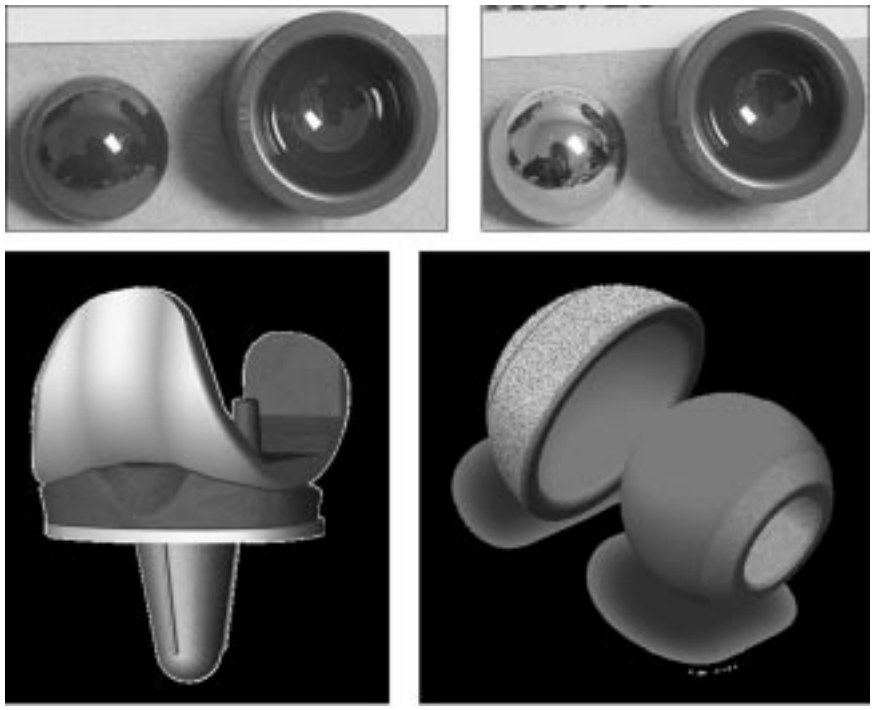

7.5 Examples of Si_3N_3–Si_3N_4 and Si_3N_4–CoCr bearing couples under development or in process of approval for applications in total hip arthroplasty and total knee arthroplasty. (Courtesy of Amedica Corp., Salt Lake City, UT.)

engines (Riley, 2000). This extensive research and development work has resulted in the ability to produce Si_3N_4 with attractive mechanical properties and high reliability. Dense Si_3N_4 produced by optimized methods with an elongated grain microstructure, referred to as '*in situ* toughened' Si_3N_4, can have a flexural strength of 1 GPa and a fracture toughness of 10–12 MPa $m^{1/2}$, values that are far superior to those of Al_2O_3. Testing of Si_3N_4–Si_3N_4 and Si_3N_4–CoCr bearings has shown wear rates that are comparable to those of Al_2O_3–Al_2O_3 bearings (Bal *et al.*, 2008, 2009a). Si_3N_4 is biocompatible, and elicits no adverse biological response *in vivo* (Howlett *et al.*, 1989; Kue *et al.*, 1999). These properties may allow the use of Si_3N_4 bearing couples in THA and TKA which retain the advantages of CoCr, but with the low wear rates associated with ceramic-on-ceramic bearings.

7.4.2 Ceramic composites

Al_2O_3-based composites have been developed in an attempt to retain the high hardness and low wear of Al_2O_3, but to improve the fracture toughness and strength. ZrO_2-toughened Al_2O_3 (ZTA) is a composite material consisting of 20

vol% fine ZrO_2 particles of size 1 μm or smaller, in a dense, fine-grained Al_2O_3 matrix. While data in the literature are limited, hip simulator tests indicate that the wear rate of ZTA–ZTA bearing couples is lower than that for Al_2O_3–Al_2O_3.

An Al_2O_3-matrix composite (AMC), manufactured by Ceram Tec, and available under the trade name Biolox *delta*, has been reported to have a flexural strength >1.2 GPa (3 times the value for Al_2O_3), and a fracture toughness of 6.5 MPa $m^{1/2}$ (1.5 times the value for Al_2O_3), as well as a wear rate even lower than the values for Al_2O_3-on-Al_2O_3 or ZTA-on-ZTA (Willmann, 2001). This AMC material is based on the ZTA composition, but also includes small amounts of SrO and Cr_2O_3 as additives, which react with the Al_2O_3 matrix to produce a small fraction of plate-like Al_2O_3 grains during the high temperature fabrication process. These plate-like grains provide an additional mechanism (crack deflection at the boundaries of the plate-like grains) for enhancing the toughness of Al_2O_3.

7.4.3 Hard ceramic coatings on metals

The bearing surfaces control the wear behavior, so it is not necessary to use a monolithic bearing composed of the same material. Surface treatments such as ion implantation and deposition of hard ceramic coatings have been widely investigated for improving the surface hardness and, hence, the wear and corrosion resistance of metal implants (Lappalainen and Santavirta, 2005). Many of these treatments have not proved to be successful in clinical applications, because of problems such as delamination of the coating, corrosion, poor interfacial bonding, and porosity (Harman *et al.*, 1997; Raimondi and Pietrabissa, 2000). For example, titanium nitride (TiN) coating can improve the hardness and wear of metal (CoCr) bearings, but a key problem is that the TiN coating can fracture and chip off when subjected to a stress concentration caused by wear debris between the articulating surfaces, or by inadvertent contact with hard components such as the metal rim of the acetabular cup, leading to catastrophic third-body wear (Goldberg and Gilbert, 2004; Raimondi and Pietrabissa, 2000; Williams *et al.*, 2003).

Diamond-like coatings (DLCs) may represent a promising way to improve the wear resistance of metal bearings such as CoCr. DLCs have desirable properties, such as low friction, high wear and corrosion resistance, good surface-to-bone bonding, and excellent resistance to surface abrasion (Lappalainen *et al.*, 1998, 2003). Thin film diamond-coated CoCr femoral heads for use in THA are under development by Diamicron Inc., Orem, UT.

7.4.4 Surface modification of metals

Because of the persistent concern of ceramic bearing failure *in vivo*, and the unpredictable behavior of hard coatings on metals, an approach based on

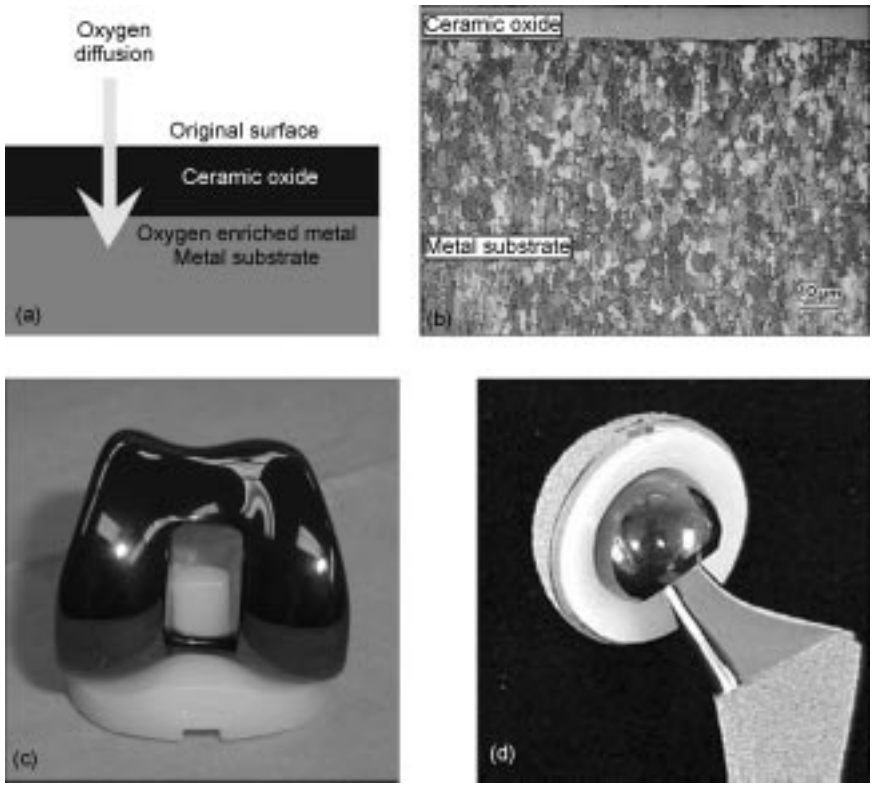

7.6 (a) Schematic of the surface modification of Zr alloy to produce Oxinium bearing surface; (b) microstructure of Oxinium bearing; (c) Oxinium bearings for total knee arthroplasty; (d) Oxinium femoral head for total hip arthroplasty. (Courtesy of Smith & Nephew, Memphis, TN.)

modification of the surface of a metal to form a ceramic has been successfully used in the manufacture of THA and TKA bearings. In this approach, a zirconium alloy (Zr–2.5%Nb) is oxidized by thermal diffusion to create a 5–10 μm oxidized zirconium layer (Laskin, 2003). The ZrO_2-based ceramic surface forms the articulating surface of the femoral head, whereas the metal substrate provides the strength and ductility to resist fracture (Fig. 7.6). Oxidized zirconium, manufactured by Smith & Nephew, Memphis, TN, under the trade name Oxinium, has had a successful clinical experience when used as an articulating bearing against UHMWPE, providing favorable reduction in wear when compared with CoCr (Good *et al.*, 2003; Spector *et al.*, 2001). However, oxidized zirconium is not intended for use in hard-on-hard bearing applications. Furthermore, recent reports (Evangelista *et al.*, 2007; Kop *et al.*, 2007) have expressed concerns about surface damage or breakdown of the ZrO_2-based surface on Oxinium femoral heads, particularly subsequent to dislocation. Damage features included general scratching, indentation, and large gouges,

with significant deformation of the zirconium substrate and associated cracking of the ZrO_2-based surface layer.

7.5 Future developments in ceramic bearing materials

The ideal orthopedic bearing material in THA and TKA must be able to withstand high cyclic loads for a few decades, without major corrosion or fretting at modular connections to metal implants, with reliable biocompatibility and material stability *in vivo*, and with low wear rates. In addition to the experimental validation of these characteristics, clinical studies are necessary to determine how the bearing performs in the *in vivo* environment, where multiple unpredictable variables can affect material behavior.

Modern bioceramics meet or exceed many of the requirements of the ideal orthopedic bearing material, but catastrophic failure *in vivo*, while rare, is a persistent concern. Future developments in ceramics for THA and TKA are aimed at maintaining the low wear of the articulating surfaces but providing the safety associated with ductile metal bearings. Systems under development include ceramic–metal composite bearings, nanoceramics, and ceramic nanocomposites.

7.5.1 Ceramic–metal composite bearings

As described earlier (Fig. 7.4a), when a compressive stress is applied to the femoral head during physiological activity, it gives rise to a tensile (or hoop) stress component in the taper bore which is concentrated at the contact area to the metal taper and at the bottom of the taper bore. Ceramic–metal composite femoral heads (Fig. 7.4b) are under development by Columbia Biomaterials LLC, Columbia, MO, in which the articulating surface of the femoral head is dense, fine-grained Al_2O_3, whereas the taper bore is a biocompatible metal (Nb or Ta) (Huang *et al.*, 2009; Rahaman *et al.*, 2010). In this design, tensile stresses in the taper bore are dissipated by plastic deformation of the ductile metal phase, so they cannot lead to catastrophic failure by slow crack growth as would occur in monolithic ceramic femoral heads. This design differs from that of oxidized zirconium in that the ceramic surface layer is considerably thicker (2–3 mm), and has a dense, fine-grained microstructure, similar to that of modern Al_2O_3 femoral heads. The composite femoral head is intended to provide an alternative to Al_2O_3 articulating against UHMWPE, as well as Al_2O_3–Al_2O_3 (hard-on-hard) bearings.

7.5.2 Nanoceramics and ceramic nanocomposites

The mechanical properties of ceramics for bearing applications, in particular wear, can be further improved by using ceramics with ultrafine or nanoscale

grain sizes, or better still, by using ceramic nanocomposites (Bal *et al.*, 2009b; Rahaman *et al.*, 2007). In the present context, nanoscale ceramics are defined as ceramics with grain sizes smaller than 50–100 nm. Ceramic nanocomposites are defined as ceramic composites with more than one solid phase, in which at least one of the phases has dimensions in the nanoscale range (<50–100 nm).

Because of the widespread use of Al_2O_3 in orthopedic and engineering applications, Al_2O_3-based nanocomposites have been the subject of considerable research and development. Al_2O_3 nanocomposites for potential bearing applications are typically dense two-phase materials, consisting of nanosize particles of a hard ceramic phase (such as SiC or ZrO_2), often 5–10 vol%, dispersed in a fine-grained Al_2O_3 matrix. While improvements in strength and fracture toughness over the unreinforced ceramic (without nanoparticles) can be modest, the improvement in the wear resistance can often be significant. For an equivalent Al_2O_3 grain size (2–3 μm), the wear rate of Al_2O_3/SiC nanocomposites (5 vol% SiC) was lower than that of Al_2O_3 by a factor of 3–5 at high contact loads (Rodríguez *et al.*, 1999). ZTA nanocomposites containing up to 10 vol% ZrO_2 nanoparticles were found to have a substantially higher fracture toughness (10 MPa $m^{1/2}$) than Al_2O_3 (4 MPa $m^{1/2}$), but the their wear resistance was not significantly different from that for Al_2O_3 (Taddei *et al.*, 2006).

ZrO_2/Al_2O_3 nanocomposites, consisting of a ZrO_2 matrix stabilized with 10 mol% CeO_2, and doped with 0.05 mol% TiO_2, referred to as Ce-TZP, and 30 vol% of Al_2O_3 as a second phase were reported to have a fracture toughness that is 4–5 times that of Al_2O_3, and a flexural strength that is ~2 times the value for Al_2O_3 (Nawa *et al.*, 1998; Tanaka *et al.*, 2002).

7.6 Future trends

Promising new technologies based on non-oxide ceramics, composites of existing ceramics, bearing surface modifications, and ceramic nanocomposites can provide improved bioceramics for use in total hip and knee joint replacement, and contribute to the longevity of these commonly performed surgical procedures. As the number of prosthetic hip and knee joint surgery performed in the US and overseas keeps increasing, the result will be a significant reduction in healthcare costs, as well as a reduction in pain and suffering to patients, owing to a reduction in the number of revision surgery.

Superior wear properties and reliability of ceramic bearing materials will also contribute to newer designs of total hip and knee replacement implants that are bone-conserving, allow greater function, and can be implanted with less invasive surgical techniques. Improved wear resistance has already allowed the use of large diameter femoral heads in total hip replacement, leading to increased arc of movement and less risk of prosthesis dislocation. Newer designs will enable ceramic bearings to be implanted into a wider range of patients, and to be used in a wider range of repeat surgery resulting from failed metal bearings. Previous

experience shows that each new material technology should be approached with caution, and adopted only after carefully controlled clinical series can validate the basic engineering and material science principles associated with its manufacture.

7.7 References

Affolter C, Weisse B, Stutz A, Köbel S, and Terrasi GP (2009), 'Optimization of the stress distribution in ceramic femoral heads by means of finite element analysis', *Proc Inst Mech Eng H*, **223**, 237–48.

Bal BS, Rahaman MN, Aleto T, Miller FS, Traina F, and Toni A (2007), 'The significance of metal staining on alumina femoral heads in total hip arthroplasty', *J Arthroplasty*, **22**, 14–19.

Bal BS, Khandkar A, Lakshminarayanan R, Clarke IC, Hoffman AA, and Rahaman MN (2008), 'Testing of silicon nitride bearings for total hip arthroplasty', *J Biomed Mater Res Part B*, **87B**, 447–54.

Bal BS, Khandkar A, Lakshminarayanan R, Clarke IC, Hoffman AA, and Rahaman MN (2009a), '*In vitro* performance of silicon nitride ceramic in total hip bearings', *J Arthroplasty*, **24**, 110–16.

Bal BS, Rahaman MN, Fu Q, Khanna S, Tinunagari P, and Ellingsen MD (2009b), 'Nanoceramics and ceramic nanocomposites in prosthetic hip and knee joints', in *Handbook of Nanoceramics and Their Based Nanodevices*, Volume 5, Chapter 8, edited by Tseng T-Y and Nalwa HS, American Scientific Publishers, Valencia, CA, pp. 187–202.

Barrack RL, Burak C, and Skinner HB (2004), 'Concerns about ceramics in THA', *Clin Orthop Rel Res*, **429**, 73–9.

Bergmann G, Graichen F, and Rohlmann A (1993), 'Hip joint loading during walking and running, measured in two patients', *J Biomech*, **26**, 969–90.

Bierbaum BE, Nairus J, Kuesis D, Morrison JC, and Ward D (2002), 'Ceramic-on-ceramic bearings in total hip arthroplasty', *Clin Orthop Rel Res*, **405**, 158–63.

Bizot P, Hannouche D, Nizard R, Witvoet J, and Sedel L (2004). 'Hybrid alumina total hip arthroplasty using a press-fit metal-backed socket in patients younger than 55 years. A six- to 11-year evaluation', *J Bone Joint Surg Br*, **86**, 190–4.

Boutin P (1971), 'Alumina and its use in surgery of the hip', *Presse Med*, **79**, 639–40.

Capello WN, D'Antonio JA, Feinberg JR, Manley MT, and Naughton M (2008), 'Ceramic-on-ceramic total hip arthroplasty: update', *J Arthroplasty*, **23**, 39–43.

Charnley J (1961), 'Arthroplasty of the hip: a new operation', *Lancet*, **1**, 1129–32.

Chevalier J, Olagnon C, and Fantozzi G (1999), 'Subcritical crack growth in 3Y-TZP ceramics: static and cyclic fatigue', *J Am Ceram Soc*, **82**, 3129–38.

Christel PS (1989), 'Zirconia: the second generation of ceramics for total hip replacement', *Bull Hosp Joint Dis Orthop Inst*, **49**, 170–7.

Clarke IC, Good V, Williams P, Schroeder D, Anissian L, Stark A, Oonishi H, Schuldies J, and Gustafson G (2000), 'Ultra-low wear rates for rigid-on-rigid bearings in total hip replacements', *Proc Inst Mech Eng H*, **214**, 331–47.

Crowninshield R, Rosenberg A, and Sporer S (2006), 'Changing demographics of patients with total joint replacement', *Clin Orthop Rel Res*, **443**, 266–72.

D'Antonio J, Capello W, Manley M, and Bierbaum B (2002), 'New experience with alumina-on-alumina ceramic bearings for total hip arthroplasty', *J Arthroplasty*, **17**, 390–7.

D'Antonio J, Capello W, and Manley M (2003), 'Alumina ceramic bearings for total hip arthroplasty,' *Orthopedics*, **26**, 39–46.

D'Antonio J, Capello W, Manley M, Naughton M, and Sutton K (2005), 'Alumina ceramic bearings for total hip arthroplasty: five-year results of a prospective randomized study', *Clin Orthop Rel Res*, **436**, 164–71.

De Aza AH, Chevalier J, Fantozzi G, Schehl M, and Torrecillas R (2002), 'Slow crack growth of alumina, zirconia and zirconia toughened alumina ceramics for joint prostheses', *Biomaterials*, **23**, 937–45.

Emery DFG, Clarke HJ, and Grover ML (1997), 'Stanmore total hip replacement in younger patients: review of a group of patients under 50 years of age', *J Bone Joint Surg*, **79**, 240–6.

Evangelista GT, Fulkerson E, Kummer F, and Di Cesare PE (2007), 'Surface damage to an oxinium femoral prosthesis after dislocation', *J Bone Joint Surg Br*, **89B**, 535–7.

Garino JP (2000), 'Modern ceramic-on-ceramic total hip systems in the United States: early results,' *Clin Orthop Rel Res*, **379**, 41–7.

Garino JP, Rahaman MN, and Bal BS (2006), 'The reliability of modern alumina bearings in total hip arthroplasty', *Semin Arthroplasty*, **17**, 113–19.

Goldberg JR and Gilbert JL (2004), 'The electrochemical and mechanical behavior of passivated and TiN/AlN-coated CoCrMo and Ti6Al4V alloys,' *Biomaterials*, **25**, 851–64.

Good V, Ries MD, Barrack RL, Widding K, Hunter G, and Heuer D (2003), 'Reduced wear with oxidized zirconium femoral heads', *J Bone Joint Surg Am*, **85**, 105–10.

Hamadouche M, Boutin P, Daussange J, Bolander ME, and Sedel L (2002), 'Alumina-on-alumina total hip arthroplasty: a minimum 18.5-year follow-up study', *J Bone Joint Surg Am*, **84**, 69–77.

Hannouche D, Nich C, Bizot P, Meunier A, Nizard R, and Sedel L (2003), 'Fractures of ceramic bearings: history and present status', *Clin Orthop Rel Res*, **417**, 19–26.

Harman MK, Banks, SA, and Hodge WA (1997), 'Wear analysis of a retrieved hip implant with titanium nitride coating', *J Arthroplasty*, **12**, 938–45.

Harris WH (1995), 'The problem is osteolysis', *Clin Orthop Rel Res*, **311**, 46–53.

Heros RJ and Willmann G (1998), 'Ceramic in total hip arthroplasty: history, mechanical properties, clinical results, and current manufacturing state of the art', *Semin Arthroplasty*, **9**, 114–22.

Howlett CR, McCartney E, and Ching W (1989), 'The effect of silicon nitride ceramic on rabbit skeletal cells and tissue. An *in vitro* and *in vivo* investigation', *Clin Orthop Relat Res*, **244**, 293–304.

Huang TS, Rahaman MN, and Bal BS (2009), 'Alumina–tantalum composite for femoral head applications in total hip arthroplasty', *Mater Sci Eng C*, **29**, 1935–41.

Kop AM, Whitewood C, and Johnston DJL (2007), 'Damage to Oxinium femoral heads subsequent to hip arthroplasty dislocation', *J Arthroplasty*, **22**, 775–9.

Kue R, Sohrabi A, Nagle D, Frondoza C, and Hungerford D (1999), 'Enhanced proliferation and osteocalcin production by human osteoblast-like MG63 cells on silicon nitride ceramic discs', *Biomaterials*, **20**, 1195–201.

Kurtz S, Mowat F, Ong K, Chan N, Lau E, and Halpern M (2005), 'Prevalence of primary and revision total hip and knee arthroplasty in the United States from 1990 through 2002', *J Bone Joint Surg Am*, **87**, 1487–97.

Lappalainen R and Santavirta SS (2005), 'Potential coatings in total hip replacement', *Clin Orthop Rel Res*, **430**, 72–9.

Lappalainen R, Anttila A, and Heinonen H (1998), 'Diamond coated total hip replacements,' *Clin Orthop Rel Res*, **352**, 118–27.

Lappalainen R, Selenius M, Anttila A, Konttinen YT, and Santavirta SS (2003), 'Reduction of wear in total hip replacement prostheses by amorphous diamond coatings,' *J Biomed Mater Res Part B: Appl Biomater*, **66**, 410–13.

Laskin RS (2003), 'An oxidized Zr ceramic surfaced femoral component for total knee arthroplasty', *Clin Orthop Rel Res*, **416**, 191–96.

Lavernia CJ, Drakeford MK, Tsao AK, Gittelsohn A, Krackow KA, and Hungerford DS (1995), 'Revision and primary hip and knee arthroplasty: a cost analysis', *Clin Orthop Rel Res*, **311**, 136–41.

Lawn BR (1993), *Fracture of Brittle Solids*, 2nd edn, New York, Cambridge University Press.

Lombardi AV, Mallory TH, Dennis DA, Comistek RD, Fada RA, and Northcut EJ (2000), 'An *in vivo* determination of total hip arthroplasty pistoning during activity', *J Arthroplasty*, **15**, 702–9.

Masonis JL, Bourne RB, Ries MD, McCalden RW, Salehi A, and Kelman DC (2004), 'Zirconia femoral head fractures: a clinical and retrieval analysis', *J Arthroplasty*, **19**, 898–905.

Nawa M, Nakamoto S, Sekino T, and Niihara K (1998), 'Tough and strong Ce-TZP/alumina nanocomposites doped with titania', *Ceram International*, **24**, 497–506.

Nevelos AB, Evans PA, Harrison P, and Rainforth M (1993), 'Examination of alumina ceramic components from total hip arthroplasties', *Proc Inst Mech Eng H*, **207**, 155–62.

Nevelos JE, Ingham E, Doyle C, Fisher J, and Nevelos AB (1999), 'Analysis of retrieved alumina ceramic components from mittelmeier total hip prosthesis', *Biomaterials*, **20**, 1833–40.

Nevelos JE, Ingham E, Doyle C, Streicher R, Nevelos AB, Walter W, and Fisher J (2000), 'Microseparation of the centers of alumina–alumina artificial hip joints during simulator testing produces clinically relevant wear rates and patterns', *J Arthroplasty*, **15**, 793–5.

Nevelos JE, Prudhommeaux F, Hamadouche M, Doyle C, Ingham E, Meunier A, Nevelos AB, Sedel L, and Fisher J (2001), 'Comparative analysis of two different types of alumina–alumina hip prosthesis retrieved for aseptic loosening', *J Bone Joint Surg Br*, **83B**, 598–603.

Oonishi H, Clarke IC, Williams PA, Shishido T, and Gustafson A (2002), 'Characterization of steady-state wear in all-alumina THR to 20 mc', *Key Eng Mater*, **218–220**, 587–90.

Piconi C and Maccauro G (1999), 'Zirconia as a ceramic biomaterial,' *Biomaterials*, **20**, 1–25.

Rahaman MN, Bal BS, Garino JP, Ries MD, and Yao A (2007), 'Ceramics for prosthetic hip and knee joint replacement,' *J Am Ceram Soc*, **90**, 1965–88.

Rahaman MN, Huang T, Bal BS, and Li Y (2010), '*In vitro* testing of Al_2O_3–Nb composite for femoral head applications in total hip arthroplasty', *Acta Biomater*, **6**, 708–14.

Raimondi MT and Pietrabissa R (2000), 'The *in vivo* wear performance of prosthetic femoral heads with titanium nitride coating,' *Biomaterials*, **21**, 907–13.

Riley FL (2000), 'Silicon nitride and related materials', *J Am Ceram Soc*, **83**, 245–65.

Rodríguez J, Martín A, Pastor JY, LLorca J, Bartolomé JF, and Moya JS (1999), 'Sliding wear of alumina/silicon carbide nanocomposites', *J Am Ceram Soc*, **82**, 2252–4.

Sedel L, Nizard R, Bizot P, and Meunier A (1998), 'Perspective on a 20 year experience with ceramic-on-ceramic articulation in total hip replacement', *Semin Arthroplasty*, **9**, 123–34.

Shishido T, Clarke IC, Williams P, Boehler M, Asano T, Shoji H, Masaoka T, Yamamoto K, and Imakiire A (2003), 'Clinical and simulator wear study of alumina ceramic THR to 17 years and beyond', *J Biomed Mater Res Part B: Appl Biomater*, **67B**, 638–47.

Skinner HB (1999), 'Ceramic bearing surfaces,' *Clin Orthop Rel Res*, **369**, 83–91.

Spector BM, Ries MD, Bourne RB, Sauer WS, Long M, and Hunter G (2001), 'Wear performance of ultra-high molecular weight polyethylene on oxidized zirconium total knee femoral components', *J Bone Joint Sur Am*, **83**, 80–6.

Taddei P, Affatato S, Torrecillas R, Fagnano C, Ferrieri P, and Toni A (2006), 'Wear behavior, fluorescence and SEM investigations on nanocomposite zirconia-toughened alumina', *J Mater Sci*, **41**, 5310–16.

Tanaka K, Tamura J, Kawanabe K, Nawa M, Oka M, Uchida M, Kokubo T, and Nakamura T (2002), 'Ce-TZP/Al_2O_3 nanocomposite as a bearing material in total joint replacement', *J Biomed Mater Res Part B: Appl Biomater*, **63**, 262–70.

Urban JA, Garvin KL, Boese CK, Bryson L, Pedersen DR, Callaghan JJ, and Miller RK (2001), 'Ceramic-on-polyethylene bearing surfaces in total hip arthroplasty. Seventeen to twenty-one-year results', *J Bone Joint Surg Am*, **83**, 1688–94.

Walter WL, Insley GM, Walter WK, and Tuke MA (2004), 'Edge loading in third generation alumina ceramic-on-ceramic bearings', *J Arthroplasty*, **19**, 402–13.

Walter WL, Waters TS, Gillies M, Donohoo S, Kurtz SM, Ranawat AS, Hozack WJ, and Tuke MA (2008), 'Squeaking hips', *J Bone Joint Surg Am*, **90**, 102–11.

Wan K, Lahtabai S, and Lawn BR (1990), 'Crack velocity functions and thresholds in brittle solids', *J Europ Ceram Soc*, **6**, 259–68.

Williams S, Tipper JL, Ingham E, Stone MH, and Fisher J (2003), '*In vitro* analysis of the wear, wear debris and biological activity of surface-engineered coatings for use in metal-on-metal total hip replacements,' *Proc Inst Mech Eng H*, **217**, 155–63.

Willmann G (2000), 'The evolution of ceramics in total hip replacement', *Hip International*, **10**, 193–203.

Willmann G (2001), 'Ceramics for joint replacement: what are the options for this millennium?', *Key Eng Mater*, **192–195**, 565–8.

Willmann G, Früh HJ, and Pfaff HG (1996), 'Wear characteristics of sliding pairs of zirconia (Y-TZP) for hip endoprostheses', *Biomaterials*, **17**, 2157–62.

Wroblewski BM, Siney PD, Dowson D, and Collins SN (1996), 'Prospective clinical and joint simulator studies of a new total hip arthroplasty using alumina ceramic heads and cross-linked polyethylene cups', *J Bone Joint Surg Br*, **78**, 280–5.

Yamamoto T, Masanobu S, Ueno M, Hananouchi T, Tokugawa Y, and Yonenobu K (2005), 'Wear analysis of retrieved ceramic-on-ceramic articulations in total hip arthroplasty: femoral head makes contact with the rim of the socket outside the bearing surface', J *Biomed Mater Res Part B: Appl Biomater*, **73B**, 301–7.

8

Biomaterials for improving the blood and tissue compatibility of total artificial hearts (TAH) and ventricular assist devices (VAD)

D. UFUK ERBULUT and I. LAZOGLU,
Koc University, Turkey

Abstract: This chapter reviews biomaterials used for artificial hearts and ventricular assist devices. The chapter identifies some of the commercially available cardiac devices and the materials used within, stretching the most important polymers, metals and ceramics. It then discusses the interaction between blood/tissue and biomaterials and subsequently the way of refinement of biomaterials in order to achieve optimum performance. The chapter includes also the evaluation of biomaterials in terms of their blood and tissue compatibility and related international standards.

Key words: biomaterials, cardiac devices, biocompatibility, LVAD, total artificial heart.

8.1 Introduction

What are the initial requirements for biomaterials of cardiovascular assist devices? The first problem that researchers had to face during early development was to find an appropriate material that can offer both drive and flexion capabilities as well as compatibility with the human body. Perhaps the most scientific problem was to overcome the issue related to the interaction between biomaterial surface and human body. In addition, biomaterial must not produce blood clots (thrombi), which cause strokes. To overcome the above problems, materials have to be specifically considered for medical devices and their components for use within the human body.

In this chapter, early attempts and recent advances in the field of biomaterials of artificial hearts are demonstrated, in particular the interaction of the heart with blood and tissue. Section 8.2 reviews the chronological background of ventricular assist devices and total artificial heart evolution. Section 8.3 establishes an appropriate background indicating critical biocompatible (polymers, metals, ceramics, etc.) in a specified device, including explanation of utilization of each materials and why the different materials are used for the same application. Section 8.4 outlines the mechanical and physical requirements of

biomaterials used for VADs and TAHs and their surface requirements for minimal generation of thrombosis. Section 8.5 reviews the refinement methods of biomaterial surfaces (polymers, metals, ceramics, etc.) and the correlation between their interface performances and haemocompatibility. Finally, the methods of blood and tissue compatibility measurement for biomaterials used for cardiac devices and their international standards are described.

8.2 Historical background of cardiac assist devices

Mechanical hearts are used to assist in cases of congestive heart failure, which basically decreases the ability to pump blood. There are mainly three possible scenarios after the surgery of a heart: when the heart becomes too weak to meet the blood pumping requirements and needs a time of load reduction to recover, the heart never functions (Frazier *et al.*, 2001) or the heart cannot be fixed (Rose *et al.*, 2001). If the heart cannot be recovered with surgery, then the best option to cure the disease would be a heart transplant. Unfortunately, even though there are insufficient numbers of heart donations, a transplant has to be applicable to a patient in terms of blood and tissue type. The second best option is then to assist the heart with mechanical devices while the donor heart becomes available. These mechanical devices are called ventricular assist devices (VADs). They are termed left ventricular, right ventricular or biventricular assist device, depending on which part of the heart is being supported.

These mechanical devices can also be employed for a longer period until heart transplantation, when patients do not recover successfully from heart surgery. In this case, the VADs are described as a bridge to transplant. There is another type of artificial heart, the total artificial heart (TAH), which is applied for end-stage heart failure. The TAH basically is a replacement for a complete failing heart.

The early evolution of artificial hearts occurred during 1812–1957. Since then, there has been rapid development on mechanical heart design and implementation. In 1812, the pumping blood hypothesis was made by French physiologist Le Gallois, which proposed that assisting organs might help retain life. The records show us a number of experimental works related to an organ perfusion with pumps in 1828–1868 (Ratner *et al.*, 2004). In 1881, Étienne-Jules Marey published a photograph to demonstrate a blood circulation device, although it is believed that this was never tried out (Ratner, 2000).

However, it has been only five decades that scientists have been investigating mechanical cardiac devices and their components. In 1957, the artificial heart was examined in animals by Dr William Kolff (Ratner *et al.*, 2004). The heart was made of poly(vinyl chloride). Dr Paul Winchell patented the first artificial heart in 1963.

8.2.1 Total artificial heart (TAH)

About 12 years later, in 1969, the first pneumatically actuated TAH was implemented clinically by Cooley and Akutsu (Frazier and Macris, 1994). In 1972, Jarvik introduced first artificial heart out of aluminium, polyester and a plastic named Jarvik-3 (Hajar, 2005). In 1982, the first permanent TAH, the Jarvik-7, a two-chamber device made of polyethylene, was implemented (Joyce *et al.*, 2004). It was used as a bridge to transplantation. Between 1985 and 1992, eight different brands of TAH as a bridge to transplantation were implemented: Phoenix, Berlin, Pennsylvania State, Brno, Vienna, Unger, Poisk and Cardiowest (Frazier and Macris, 1994).

8.2.2 Ventricular assist devices (VADs)

Ventricular support devices, including counterpulsation (Papaioannou and Stefanadis, 2005), centrifugal (Iijima *et al.*, 1997; Curtis *et al.*, 1999), and axial (Nosé *et al.*, 2000), aimed to offer a short-term support to recovery or long-term bridge to transplant. In 1961, Dennis *et al.* initiated roller pump to assist the left ventricle (Frazier and Macris, 1994). Moulopoulos *et al.* (1962) introduced the intraaortic balloon pump (IABP) in 1962. Kantrowitz *et al.* (1968) announced the first clinical application of an IABP in 1968. Currently IABPs are widely used as a cardiac assist device (Frazier *et al.*, 2008). In 1990s, the records indicate several successful VAD implementations that enabled patients to recover from heart failure. In 1993, US Food and Drug Administration (FDA) approved the first VAD, the Abiomed BVS 5000, for commercial use (Frazier and Macris, 1994), which will be described in detail in the following sections.

8.3 Characterization of biomaterials: interaction with blood and tissue surface

A biomaterial is implemented and used to assist human health. Therefore, it must be sufficiently safe. Identification of fundamental biological requirements and characterization of biomaterials are explained and the complications are then reported.

Investigation of mechanical and functional properties of a biomaterial is important in order to meet the requirements of a successful cardiac device. For example, it has to be mechanically strong to withstand the flex-time of 42 million flexes per year and be capable of interacting with blood as well as tissue cells without any damage.

Another important criterion for material choice is the intended clinical application of the biomaterial. The requirements of the same material would be different for different medical applications. For example, the material perform-

ance expected when the same biomaterial is used for low flow rate circulatory device is different from that for a high flow rate device. The FDA regulates and approves the medical devices only within certain clinical applications instead of a biomaterial itself for biocompatibility. More details related to the preparation and testing of biomaterials are given in Section 8.6.

In order to investigate the biomaterial used for artificial hearts, one must define the blood–material interaction phenomena and its complications accordingly.

8.3.1 Complications of VADs

Protein adsorption

Plasma protein adsorption is the first reaction when blood interfaces with an artificial surface. It usually starts in a few seconds after blood–surface interaction. It simply means that the dissolved matters in a solution, especially proteins, adsorb on to the surface of the foreign substance. Primarily, protein deposition to the surface does not always indicate body's response to the material but rather large amount of proteins simply cause adhesion to the surface (LeDuc and Wang, 2006). The influence on the blood cells by adhesive protein has been a matter of concern. This problem has made a direct challenge to developers to modify artificial surfaces in order to reduce protein adsorption, and hence prevent damaging blood cells. However, controlled protein adsorption can be usefull due to the formation of a thin natural surface to interact with blood. Studies of protein absorption to different materials are mentioned in the next subsections.

Thromboembolism

One of the complications of cardiac devices is thrombosis, to be considered during cardiac device *in vivo* testing (see Section 8.7). Thrombosis is the formation of thrombus in a vessel, which can cause death. Platelet adhesion and aggregation cause thrombus formation on artificial surfaces and this formation contains aggregated platelets, red cells, fibrins and other cellular elements.

Platelets

Platelets are blood cells, approximately 2–4 μm in diameter, which are responsible for blood clotting during bleeding. Adhesion, release and aggregation are the main reactions of platelets to vessel wall damages. One way of reducing platelet adhesion is the reduction of surface energy which can be controlled by a surface of hydrophilic and/or hydrophobic domains (Klee and Höker, 1999).

Toxicity

Obviously, biomaterials must not be toxic as they are used inside the human body. Several tests (see Section 8.7) should be carried out before initiation of a biomaterial in order to prevent negative effects. Toxicity studies are aimed at understanding the degree of toxic substances from biomaterial to its environment. Therefore, chemical and biochemical degradation can be prevented.

8.4 Biomaterials of current cardiac devices

In 1953, the first biomaterial, silicon rubber, was introduced for medical purposes. Even though it can be used as biomaterial, different types of silicon rubbers, polydimethyl-siloxane derivatives, were found to be in appropriate for pump bladders (Poirier, 1997b) because of their weak mechanical properties.

Biocompatible material can be considered in terms of its blood compatibility (haemocompatible) and tissue compatibility (histocompatible). Haemocompatible material should not develop a blood clot (thrombosis), damage blood cells and activate proteins. Histocompatible material should not be toxic and allergenic (Lamba *et al.*, 1998). On the other hand, the term 'biocompatible' does not always indicate haemocompatibility of the bulk material.

There are a few criteria which need to be understood about biomaterial. First of all it is doubtful that one biomaterial can meet all the mechanical and functional requirements for a blood circuitry device.

Substrate materials may require modification in order to provide the desired properties for clinical applications. In the early 1990s, researchers tried to improve the haemocompatibility of bulk materials such as new innovations in polyurethane material (Szycher and Lee, 1993). For example, although polyurethane was a potential polymer as a biocompatible material along with its excellent mechanical properties, it may not offer the required adequate functional properties for a medical device. In addition, titanium and its alloys were commonly used for cardiovascular support devices without surface modification, yet they have a limitation on haemocompatibility (Sin *et al.*, 2009). Montiès *et al.* (1997) investigated titanium alloy (Ti_6Al_4V) and alumina ceramic (Al_2O_3) for short and middle-term assistance, titanium nitride (TiN), borum carbide (B_4C) and diamond-like carbon (DLC) coatings on different kinds of graphite for long-term and permanent assistance with regard to physiochemistry, mechanics and tribology. The study shows that a composite material, a substrate and a coating, is the most appropriate. Aluminium alloy can also be used, although it is incapable of withstanding corrosion.

In fact, material surface interactions with blood and tissue can lead to serious complications such as thromboembolism, bleeding and infection. In order to eliminate these complications, part of the material development research has shifted to surface modification fields. Therefore, material and its surface

modification (see Section 8.5) is now a crucial factor for blood contacting applications in the market.

Secondly, as mentioned before, different requirements are usually assigned to the same biomaterial depending on the clinical applications and the required mechanical/biomedical functionality of the mechanical device. For example, ISO 10993 – Part 4 (ISO, 2002) is a guide for the development of biomaterials into a specific mechanical device. FDA approval is also only for the medical device, not for the biomaterial used.

Table 8.1 shows selected commercially available TAHs and VADs as well as corresponding materials and surface coatings. Table 8.2 shows some of the third generation blood pumps and corresponding materials and surface coatings. As seen on the list, titanium, titanium alloys and polycarbonate are the most used materials for housing blood pumps. Different components of artificial hearts and VADs are made of polyurethane. These components include mostly housing, chambers and diaphragms. Bioactive surface coatings are noticeably dominant over others as a blood-contacting surface for both second and third generation blood pumps.

Table 8.1 Some cardiac devices and corresponding materials and surface coatings

VAD	
Continuous flow	
Centrifugal pumps	
Biomedicus Bio-Pump (Medtronic BioMedicus, Inc.)	
Housing	Polycarbonate
Optional coating	Carmeda BioActive Surface or Trillium Biosurface
Sarns centrifugal pump (3-M Health Care, Ann Arbor, MI)	
Blood contact materials	Acrylic, silicone rubber, silicone lubricant, nylon, aluminium oxide
Housing	Durable polycarbonate
Optional coating	X Coating™
Evaheart (Eveheart Medical USA, Inc.) (long-term support)	
Pump	Pure titanium
Entire blood-containing surfaces	Coated with MPC (commercially developed coating by NOF Corp. of Japan) or DLC
Inflow and outflow cannula	Expanded polytetrafluoroethylene (ePTFE) or polyester vascular graft
Seat ring	Silicon carbide (SiC)
Seal ring	Carbon graphite
Gyro Centrifugal	
Prototype pump housing	Polycarbonate, titanium
The male pivot bearing	Stainless steel, alumina ceramic
The female pivot bearing	Ultra-high molecular weight polyethylene (UHMWPE), gamma ray irradiated high molecular weight polyethylene (GIHMWPE), polyethylene
Impeller	Polycarbonate, polyurethane
The shaft of the impeller	Alumina ceramic
Reservoir bag	Polyvinyl
Tubing	Polyvinylchloride

Table 8.1 Continued

Axial flow pumps	
MicroMed DeBakey VAD (MicroMed Cardiovascular Inc., Houston, TX) (can be used as bridge to transplant)	
Pump unit	Polished titanium
Inflow cannula	Polished titanium
Outflow graft	Dacron
Jarvik-2000 (Jarvik Heart Inc., New York, NY) (electromagnetically actuated) (neodymium–iron–born magnet)	
Pump and impeller	Titanium
Bearings	Ceramic
Blood-contacting surfaces	Highly polished titanium
Thoratec HeartMate II LVAS (Thoratec Corp., Pleasanton, CA)	
The internal pump surfaces, inlet outlet elbows, cannula	Textured with titanium microsphere coatings
Axial-flow rotary pump	Titanium
Inlet and outlet cannula	Woven Dacron (C.R. Bard, Haverhill, PA)
Outlet graft sheath for bend relief	Polypropylene
Pulsatile flow	
Pulsatile-paracorporeal devices	
Abiomed BVS 5000i (Abiomed Cardiovascular, Inc., Danvers, MA)	
Dual chamber	Polyurethane
Thoratec (Thoratec Corporation, Pleasanton, CA) (paracorporeal VAD)	
Pumping chamber (blood sac)	Thoralon polyurethane
Housing	Polycarbonate
Percutaneous cannula	Thoralon polyurethane with reinforcement and polyester velour covering
Valve housing	Stainless steel
Disk valves	Occluder material (pyrolytic carbon and Delrin)
Berlin Heart (German Heart Institute, Berlin)	
Housing	Semi rigid polyurethane
Blood chamber/internal	Polyurethane/extremely smooth polyurethane
Inner surface	Heparin coated (Carmada method)
Cannula	Silicon rubber (no need heparin coating)
Outflow graft	Dacron-velour covered sewing rim
Pulsatile-intracorporeal devices	
Thoratec HeartMate XVE LVAS (Thoratec Corp., Pleasanton, CA)	
Pump chamber	Titanium alloy
Inflow and outflow conduit	Titanium cage that contains 25 mm porcine xenograft valve within a woven Dacron™-fabric graft
Diaphragm	A flexible polyurethane (separates the blood chamber and the air chamber)
Blood chamber	Textured surfaces (chamber promotes the development of a cellular lining) (sintered titanium and textured polyurethane)
Novacor (LVAS) (World Heart Corp., Oakland, CA)	
Blood sac	Polyurethane
Inflow cannula	Low-porosity polyester
Integral wall	Gelatin-sealed polyester graft or Vascutek graft
Inflow conduit	PTFE

Table 8.1 Continued

Thoratec (bridge to transplantation)	
Housing	Smooth-surfaced polished titanium alloy
Pumping chamber (blood sac)	Thoralon polyurethane
Percutaneous cannula	Thoralon polyurethane with reinforcement and polyester velour covering
Disk valves	Occluder material (pyrolytic carbon and Delrin)
TAH	
CardioWest (SynCardia Systems Inc., Tucson, AZ)	
Internal surface	Lined with polyurethane
Diaphragm	Four layer segmented polyurethane
Valves in the conduits	Medtronic-Hall (Medtronic, Inc., Minneapolis, MN)
AbioCor (Abiomed Cardiovascular Inc., Danvers, MA)	
All blood-contacting surfaces (the two blood pumps, four trileaflet valves)	Smooth polyurethane
Inflow cuff to the outflow graft	Textured surface Dacron atrial cuffs
Pump domes are reinforced	Stycast epoxy (most common used, highly versatile)

Table 8.2 Materials of third generation blood pumps

Axial flow rotor	
Incor (BerlinHeart (German Heart Institute, Berlin)	
Pump	Titanium alloy
Blood contacting surfaces	Heparin coated (Carmeda process)
Inflow and outflow cannula	Medical grade silicon
Centrifugal rotor	
Ventrassist (Ventrassist Division, Ventracor Ltd, Chatswood, NSW, Australia) (long-term ventricular support)	
Pump	Titanium, aluminium, vanadium alloy
Blood-contacting surfaces	Carbon coating
Inflow cannula	10 mm internal diameter silicone
Outflow cannula	10 mm gelatin-impregnated woven polyester graft
HeartMate III (Thermo Cardiosystems Inc.) (long-term ventricular support) (magnetic levitation) (bearingless)	
Pump	Titanium
Blood-contacting surfaces	Sintered titanium
Impeller	Smooth titanium
Outflow cannula	Woven polyester graft

8.4.1 Polymers

Polyurethane

Synthetic biomaterials include silicon rubber, polyvinylchloride (PVC), nylon, polytetrafluoroethylene (PTFE), polyethylene teraphthalate (PET) and poly-

urethane. Polyurethane is one of the most used polymer elastomer for cardiac devices. Its excellent properties, such as inherent blood compatibility, flexure endurance and abrasion resistance, made it the most favoured synthetic polymer for successful cardiac devices (Szycher and Poirier, 1983; Zdrahala and Zdrahala, 1999). Polyurethanes have been used for over 20 years in medicine and no records have been found related to its degradation (Pinchuk, 1994).

There are over 30 commercially available biomedical polyurethanes (Lamba *et al.*, 1998). However, only a few of them have been used for artificial medical devices, i.e. Biomer (Ethicon, Inc., Somervilee, NJ), Cardiothane (Kontron, Inc., Everett, MA), Pellethane (Upjohn Chemical, North Haven, CT) and Tecoflex (Thermedics Inc., Walthan, MA). Biomer is one of the first biomedical grade polyurethane which has been used for artificial hearts (Guelcher, 2006).

To test for advantages of Biomer, Poirier (1997a) investigated flexure endurance evaluation of materials for artificial heart diaphragms. Among seven different materials, SRI (linear segmented, ether-type urethane), Silastic (silicone rubber), TecothaneB (2-component polyester, cross-link urethane), Tecoflex HR (aliphatic, polyether-based, linear-segmented elastomer containing 100% linkage), Hexsyn (polyolefin rubber), Pellethane (thermoplastic polymer) and Biomer (segmented polyether urethane), Biomer performed longer, implying suitability for long-term cardiac assist devices.

However, a few drawbacks have been reported related to its functionality within the artificial hearts and VADs. One of the limitations of polyurethane is its water permeablility, which may affect the functionality of electrically actuated blood pumps due to water transfer into the system (Lamba *et al.*, 1998). A composite of butyl rubber and Biomer has been used as a diaphragm in an intra-abdominally positioned blood pump (E type ALVAD) by McGee *et al.* (1980) in order to prevent water interaction with actuator. Biomer (0.020 inches; 0.5 mm)/butyl rubber (0.010 inches; 0.25 mm)/Biomer (0.010 inches; 0.25 mm) composites provide a sufficient barrier to fluid and provide a flexible blood interface.

The deposition of calcium minerals onto polyurethane is considered to be another limitation. Calcification is a process of building up calcium minerals on a material or soft tissue. Pierce *et al.* (1980) have shown that polyurethane is often affected by calcification in which calcium phosphate deposits mostly on the flexion surface, resulting in flexure failure. Perforations and stiffening of polyurethanes are other effects of these deposits.

Dacron and expanded polytetrafluoroethylene (ePTFE)

Dacron graft, a synthetic material, and expanded polytetrafluoroethylene (ePTFE) are used for manufacturing inlet and outlet cannula of blood circulatory devices. Dacron graft and ePTFE cannula have been used in a few devices such as EvaHeart, ThoratecHeartMate II LVAS, ThoratecHeartMate XVE LVAS,

BerlinHeart and Novacor as listed in Tables 8.1 and 8.2. High crystallinity and hydrophobicity are the advantages of both materials. These two characteristics of ePTFE and Dacron ensure the prevention of hydrolysis (Xue and Greisler, 2003). Diameters of more than 6 mm of both materials provide optimum functional performance. Clinical grade Decron is usually available in woven or knitted form. Outflow graft bend relief is a polyester graft to avoid twisting and abrasion and its life cycle is about 10 years without corrosion.

HeartMate VE LVAS, a commercially available assist device includes Decron for its inflow and outflow conduits. Improvements on reliability and durability have been achieved by changing the materials of percutaneous-lead connection of external controller to internal pump, of the HeartMate VE LVAS (Dowling *et al.*, 2004). Materials with improved percutaneous-lead include high flex cadmium–copper alloy, high strength silicone, hardenable stainless steel, fibres, and polycarbonate-based polyurethane and two independent coil springs. Vent adapter is made of acetal.

Ultrahigh molecular weight polyethylene (UHMWPE)

Ultrahigh molecular weight polyethylene (UHMWPE) is used as a female pivot for pivot-bearing system of centrifugal pump (Takami *et al.*, 1997). The male pivot of the system is high grade alumina (Al_2O_3) ceramic with a purity of 99.7%. Even though a combination of these two materials is usually used for joint implants for long-term biomedical devices, they have proven useful as a blood-contacting surface for centrifugal pumps as well. Al_2O_3 ceramic counter bearing male-pivot decreases wear of UHMWPE.

Synthetic materials have a propensity of increasing the possibility of stroke in humans (Lamba *et al.*, 1998). For example, polyurethane has a limitation due to occlusion of a blood vessel as mentioned below.

8.4.2 Metals

Titanium

Titanium has been widely used as a material for implant devices since the late 1930s. It has been a preferred metallic biomaterial for the investigation of human tissue–biomaterial interactions (Kasemo, 1983). Mechanochemical properties of titanium such as lightness, corrosion resistance by the oxide layer, strength and inertness and that it is not magnetic made it the mostly used metal for cardiac devices. There are four grades of titanium, which are graded based on the percentage of impurities such as nitrogen, carbon, hydrogen, iron, oxygen (Park and Lakes, 1992). For medical implants especially for VADs, extra low interstitial alloy is generally used (i.e. Ti6-Al4-V ELI) and the main elements of the alloy are aluminium (5.5 to 6.75% (m/m)) and vanadium (3.5 to 4.5% (m/m)).

Table 8.3 Mechanical properties of wrought titanium 6-aluminium 4-vanadium alloy in annealed condition (ISO, 1996)

Form of alloy	Tensile strength R_m min (MPa)	Proof stress of nonproportional elongation $R_{\rho 0.2}$ min (MPa)	Percentage elongation after fracture[a] A min	Mandrel diameter for bend test
Sheet and strip	860	780	8	10τ[b]
Bar[c]	860	780	10	Not applicable

[a] Gauge length $= 5.65\sqrt{S_0}$ or 50 mm, where S_0 is the original cross-sectional area, in square millimeters.
[b] τ = thickness of the sheet or strip.
[c] Maximum diameter or thickness = 75 mm.

ISO 5832 Implants for surgery – Metallic materials, Part 3: Wrought titanium 6-aluminium 4-vanadium alloy (ISO, 1996) provides details of the mechanical properties and corresponding test methods for Ti-6Al-4V. The ISO standard for Ti-6Al-4V is depicted in Tables 8.3 and 8.4 (ISO, 1996) in terms of mechanical properties and test methods in annealed condition respectively.

Dion *et al.* (1993a) evaluated *in vitro* haemocompatibility tests for surface portion of Ti-6Al-4V and compared with Scurasil, silicone elastomer. Scanning electron microscopy (SEM) observations and R_a roughness criterion indicated that titanium alloy is a suitable biocompatible material for orthopaedic and cardiovascular medical devices. In addition, Grade 4, CP Ti, is also used as an implant biomaterial (Brunski, 2004).

Shape memory nickel–titanium (nitinol) has also been considered for intravascular devices. For example, it is the most common material used for stents

Table 8.4 Test methods (ISO, 1996)

Parameter	Relevant part	Test methods
Chemical composition	3	Recognized analytical procedures (ISO methods where these exist)
Microstructure	4	ETTC 2
Mechanical properties	5	
Tensile strength		ISO 6892
Proof stress of nonproportional elongation		ISO6892
Percentage elongation		ISO 6892
Bending		ISO 7438 Bend the sheet or strip through an angle of 105° around a mandrel of the diameter specified in Table 8.3

because of its shape memory effects (Biehl *et al.*, 2002; Liu *et al.*, 2004). With respect to its unique properties (Duerig *et al.*, 1999), nickel–titanium is recommended as a potential biomaterial for VADs by Levi *et al.* (2008). The report demonstrated that fluid pumps manufactured from thin film NiTi showed higher power production per unit volume when compared with other small-scale pumps. NiTi performed better than AISI 316 LVM stainless steel in terms of resistance to chemical breakdown of passivity (Wever *et al.*, 1998).

Even though titanium and its alloys have excellent biocompatibility, there is an absolute need for the evaluation of haemocompatibility based on stringent clinical requirements. Improvement of titanium and its alloys with respect to haemocompatibility can be successfully achieved with surface coatings (see Section 8.5) in order to reduce the complications outlined in Section 8.3 (Ebel *et al.*, 2005).

Reaction of titanium and oxygen is immediate when titanium contacts with air (Ellingsen and Lyngstadaas, 2003). This reaction forms a 5–6 nm oxide layer, which is mostly TiO_2 and Ti_2O_3 on the surface (Kasemo, 1983). Consequently, tissues interface mainly with TiO_2 for titanium implantation and TiO_2 properties are different from pure Ti as TiO_2 behaves like ceramics (Ellingsen, 1991). In addition, studies showed that the mole ratio of fibrinogen/albumin adsorption to oxide layer is very low, which leads to higher haemocompatibility (Sunny and Sharma, 1991) since thromboses are mainly related to fibrinogen adsorption (Dion *et al.*, 1993c). Ellingsen (1991) reported that TiO_2 has a possible biocompatibility because same proteins, e.g. albumin, prealbumin and IgG, are adsorbed from human serum to TiO_2 as they absorbed to hydroxyapatite. The albumin proteins binds Ca^{2+} ions which behave as a joint between the negatively charged albumin and TiO_2 surface (Klinger *et al.*, 1997). Sunny and Sharma (1991) also reported that blood compatibility of titanium depends slightly on the stable oxide layer on it. Different thickness of oxide layers (26, 40.8, 126.8 nm) were investigated and the results showed that oxide layer could increase hydrophobicity of titanium, which causes greater adsorption of protein (Ellingsen, 1991). Several other authors also indicate an increase of blood compatibility of titanium with oxide layer (Huang *et al.*, 1997, 2003).

8.4.3 Ceramics

Ceramics which have been utilized to repair or replace body parts, especially bone, are usually called bioceramics (Hench, 1991). They are inorganic, chemically inert, thermodynamically stable hydrophilic, highly wettable, hard and tribologically excellent (Christel, 1992). Owing to these properties, bioceramics are widely used for many orthopaedic procedures, especially articulating components of total joint prosthesis and dental applications. In addition, they have been considered as a biomaterial for blood-contacting applications.

Blood haemolysis of various ceramic powders, alumina, i.e. Al_3O_2, zirconium oxide/yttrium oxide ZrO_2/Y_2O_3, silicon carbide SiC, aluminum nitride AIN, boron carbide B_4C, boron nitride BN, titanium diboride TiB_2, titanium carbide TiC, titanium nitride TiN was investigated according to ISO/TR 7405-1984 (F) by Dion *et al.* (1993b). Test results indicated that most of the ceramic powders produced almost no haemolytic activity.

Alumina is the most used bioceramic in orthopaedics because of its mechanical (high hardness, low friction and wear) and biological (inertness to the *in vivo*) properties. Polycrystalline Al_3O_2 with an UHMWPE is accepted as the best combination of biomaterials for total hip prosthesis (Kumta, 2006). This combination has also been used for double-pivot bearings of centrifugal blood pump (Takami *et al.*, 1997, 1998). The study analysed the materials *in vitro* and *in vivo* (systemic toxicity, sensitization, cytotoxicity, mutagenicity, direct contact haemolysis and thrombogenicity). The results indicated that both Al_3O_2 and UHMWPE are suitable for bearings of blood pumps.

8.5 Modifications of biomaterials to enhance haemocompatibility and biocompatibility

Any implanted biomaterial cardiac device is a foreign material for human body and it can cause complications such as thrombosis and infections (see Section 8.3). Biomaterials trigger the defence mechanism of the body when the material comes into contact with tissue and blood. Therefore, surface modification of any biomaterial is considered to be inevitable for cardiac devices. Different methods have been investigated for modifying blood-contacting surfaces in order to reduce these complications (Klee and Höker, 1999). These methods are either forming a biological layer or coating of organic/inorganic material on biomaterial surface without changing the mechanical properties.

Current blood contacting surfaces are categorized into three sections as smooth surfaces, textured surfaces and biolized surfaces (Nosé *et al.*, 1996). This section draws heavily on the most used surface coatings with respect to commercial cardiac devices. These coatings include titanium nitride (TiN) (inorganic), DLC (inorganic), 2-methacryloyloxyethyl phosphorylcholine (MPC) (organic), heparin (bioactive) and textured (bioactive).

TiN coatings (inorganic)

TiN, which is a refractory ceramic coating and corrosion resistant, has been used in many left VADs (LVAD) because of its mechanical characteristics (Sin *et al.*, 2009). Its mechanical properties make it an excellent tribological coating. Physical or chemical vapour deposition methods are used for TiN coating on a bulk material. Its blood compatibility behaviour makes it a preferred coating for heart valves and heart assist devices (Dion *et al.*, 1992). Dion *et al.* (1993d)

investigated TiN coating based on the principle of the Maillard-Wankel rotary pump. The report indicates that TiN coating performed well with respect to blood interaction. However, SEM observations showed irregularities on its surface. Montiès *et al.* (1997) investigated TiN coating on graphite substrate for long-term and permanent implantable LVAD. They reported a low roughness and good blood compatibility on its surface.

On the other hand, the enormous use of DLC coatings for VADs eliminates the use of TiN coatings due to advances on haemocompatibility of DLC coatings.

DLC coatings (inorganic)

DLC, known as amorphous hydrogenated carbon (a-C:H), consists of 50–70% carbon and 50–30% hydrogen. DLC can be deposited easily by several methods, including chemical vapour deposition, cathodic arc deposition, pulsed laser deposition, direct ion beam deposition, ion beam conversion of condensed precursor, magnetron sputtering, plasma source ion deposition and direct current/radiofrequency sputtering (Dearnaley and Arps, 2005). A wide range of substance materials, e.g. Ti (Krishnan *et al.*, 2002), NiTi (Sui and Cai, 2006; Sui *et al.*, 2007), Ti-6Al-4V (Dion *et al.*, 1993c), polymeric materials (Alanazi *et al.*, 2000; Ohgoe *et al.*, 2004; Igarashi *et al.*, 2006) are suitable for DLC coating. It has received considerable attention as a coating material due to its advantages such as very smooth surface state, good wear resistance, low frictional coefficient, inertness, excellent biocompatibility and haemocompatibility over other coatings. Several studies of DLC coating with respect to blood compatibility indicated a considerable reduction of platelet adhesion to titanium (Jones *et al.*, 2000; Krishnan *et al.*, 2002).

Comparison of platelet attachment on Ti substrate and DLC coating is depicted in Fig. 8.1. In the case of DLC coating, disk-shaped platelets at the end of incubation period of 15 min remain the same for 60 min. This indicates that the DLC coatings prevent activation of platelets. However, morphology of the widely spread platelets is different after 60 min on Ti substrate without any coatings.

The clear thrombus formation on TiN coating can be seen in Fig. 8.2(a). The same results were reported for titanium and TiC surfaces. However, no thrombus was observed on the SEM micrograph of the DLC surface as depicted in Fig. 8.2(b).

Despite the fact that the DLC coating provides excellent haemocompatibility and biocompatibility, DLC coating on Ti-6Al-4V presented double the platelet retention than on silicon elastomer (Dion *et al.*, 1993c). One of the other disadvantages of this coating is the chance of micro-cracks on the surface. In fact, this can cause serious problems after implantation of a DLC-coated device (Sin *et al.*, 2009). Therefore, this limitation deserves serious attention that the

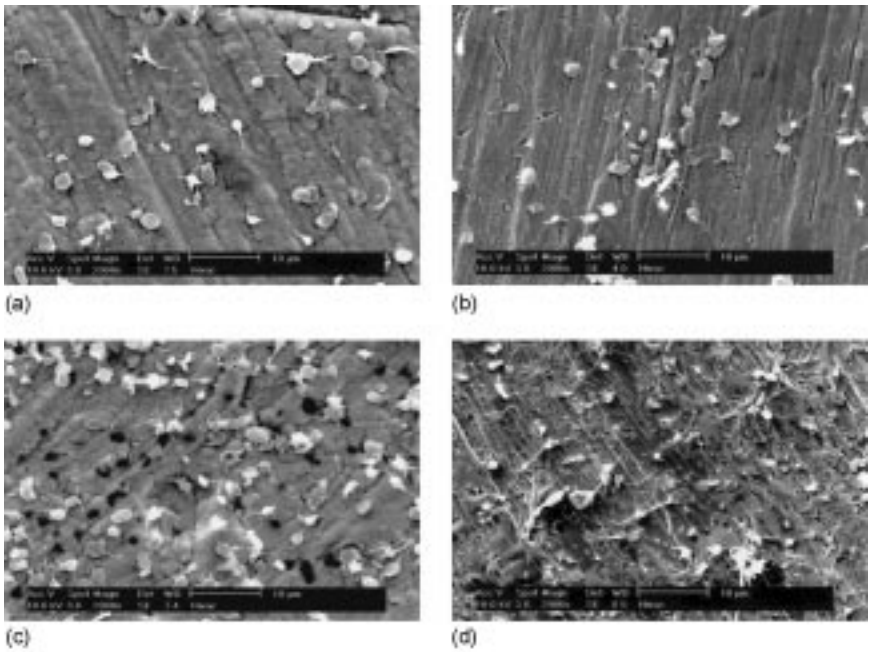

8.1 Platelets adsorption to DLC coatings and titanium substrate for incubation period of 15 min (a, b) and 60 min (c, d) respectively (Jones *et al.,* 2000). (Reprinted with permission of John Wiley & Sons, Inc.).

deposition process, forming the substrate surface (Dearnaley and Arps, 2005) and alloying DLC with different elements (e.g. Si, F, N, O, W, V, Co, Mo, Ti) (Hauert, 2003) must be effectively optimized to eliminate the failure and to enhance tribological properties.

Commercially, EVAHEART (second generation LVAD) and VentrAssist (third generation LVAD) utilize DLC coatings on their titanium and titanium alloy substrates respectively.

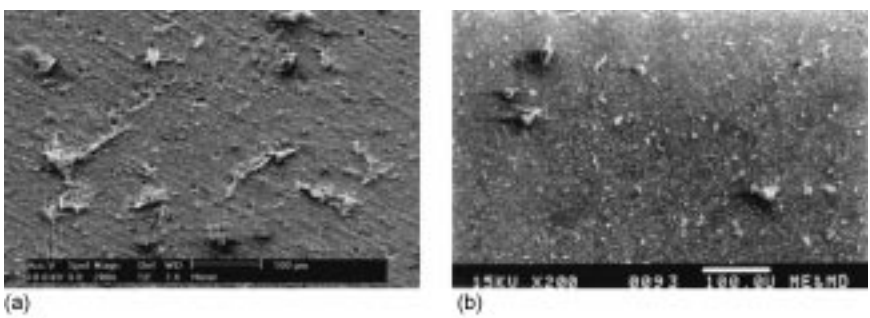

8.2 (a) Platelet activation on TiN surface; (b) platelet activation on DLC coating (Jones *et al.,* 2000). (Reprinted with permission of John Wiley & Sons, Inc.)

2-methacryloyloxyethyl phosphorylcholine (MPC) polymer coatings (organic)

Copolymer MPC coatings are also used for VADs owing to their excellent haemocompatibility. MPC coatings offer the elimination of thrombus deposition. They were designed as a non-thrombogenic surface approximately 20 years ago. The idea was to create a non-thrombogenic surface by having phospholipid membranes, which are accumulated from the bloodstream on the blood-contacting surface. In other words, the non-thrombogenic surface is achieved by the reduction of protein adsorption as a consequence of accumulation of free water in the MPC hydrogels (Nakabayashi and Iwasaki, 2004; Sin *et al.*, 2009).

The relative amount of protein adsorption depends on the MPC units in the polymer (Trevor *et al.*, 2007). The intensity of protein adsorption can be decreased by increasing MPC units which also leads to an increase in surface phospholipid levels (Nakabayashi and Williams, 2003).

It has been reported that MPC surface coatings can suppress platelet adhesion, complement activation and protein adsorption. They offer minimum thrombus formation without anticoagulants (Ishihara, 2000).

Comparison of thrombogenicity and biocompatibility of MPC and DLC coatings was conducted on pure titanium substance by Kihara *et al.* (2003). In this, blood compatibility of the SunMedical EVAHEART LVAS (SunMedical Technology Research Corporation, Nagano, Japan) system was evaluated with the coatings. There were no major differences between MPC and DLC surface coatings in terms of thrombogenicity and biocompatibility. On the other hand, MPC polymer surface coating offers reduction of anticoagulation in the acute postoperative period. It is also less expensive and easy to apply over DLC surface coatings. On the other hand, DLC coating is an expensive technology and hard to deposit on a complex featured surfaces. However, the study showed that low thrombogenicity occurred after around one month without anticoagulation. This indicates that MPC coatings may not offer the above advantages over a long period.

One of the major drawbacks of MPC surface coatings is that they last for a limited period of time because of their biodegradability (Yamazaki *et al.*, 2002). This characteristic of MPC leads to the use of anticoagulants after the coating diminishes (Sin *et al.*, 2009). In addition, compared to other coatings for blood circulatory devices (i.e. TiN and DLC), MPC coating seems weak and not stable on polymeric and metallic bulk materials.

Heparin coatings (bioactive)

Biological active coatings are used to improve haemocompatibility of the device. Heparin is one of the agents used to create bioactive surface. The most important characteristic of heparin coatings is the effective inhibition of thrombus over other repellent surface coatings. There are two different hypotheses on how heparin coating leads to reduction in thrombogenicity: (1) by the inhibition of

thrombin by catalyzing the inactivation of enzymes i.e. thrombin and Factor X_a, and (2) reducing/selective plasma protein adsorption (Oeveren, 2005).

Roller and centrifugal pumps with and without heparin coating were compared *in vivo* in order to measure blood activation potentials (Moen *et al.*, 1996). The results showed that the heparin-coated surface performed well in terms of reduction of blood activation compared with non-coated surfaces. In addition, less haemolysis was observed with heparin-coated centrifugal pump over axial pump.

BerlinHeart is another commercial application which utilizes heparin coating. Even though cannulas of BerlinHeart are made of silicon rubber (high flow rate on extreme smooth surface) which does not need any coating, the inner blood contact surfaces are completely deposited with heparin. Carmeda BioActive Surface (Carmeda AB) technology was used for coating in which heparin is attached by covalent bonding (Drews *et al.*, 2000). Evaluation of heparin effects on occurrence of heparin/platelet factor 4 antibodies (HPF4/A) was studied by Koster *et al.* (2001). No effect of heparin coating was observed on incidence of HPF4/A which is associated with thromboembolic complications.

In another study, heparin coating was investigated in a blood pump made of polycarbonate substrate (Muramatsu *et al.*, 2001). *In vitro* observation showed that heparin coatings show anticoagulant activity. Christensen *et al.* (2001) performed an investigation on platelet and coagulation activation within the heparin-coated stent StentGraft™ (JomedImplantate GmbH, Germany). The experiments indicated the occurrence of significant activation of platelets and coagulation without coatings. However, heparin-coated stent grafts functioned well in terms of blood compatibility as proved by SEM.

Reduction of fibrinogen adsorption was reported when the heparin coating present on the polymer substrate for particular situations (Vroman and Adams, 1969). Heparin coating has been used for extracorporeal systems as well. Wendel and Ziemer (1999) investigated a heparin-coated surface in order to decrease the intensity of unspecific post-perfusion syndrome. A comparison study of coated and non-coated surfaces showed that heparin coating performed well in terms of reduction of humoral and cellular activation, platelet protection and total cost savings.

Owing to the above properties of heparin, titanium alloy blood-contacting surfaces of the magnetically suspended third generation blood pump, Incor (BerlinHeart, Germany), are coated with heparin (Hetzer *et al.*, 2004). The Carmeda process, covalent binding of heparin, is used for titanium alloy surface.

Other commercial methods for heparin coatings are Duraflo technology (Baxter International, Inc., Deerfield, IL) and PhotoLink photo heparin coatings (SurModics) and Medi-Coat hydrogels (STS). The implications of these coating methods are out of the scope of the chapter.

On the other hand, as a disadvantage, it is important to consider the lifetime of heparin coatings, which is limited due to its biodegradable nature. The

selection of coatings, TiN, DLC or heparin, should be carefully decided in relation to the duration of clinical application. In addition, as mentioned, mostly used covalent binding technology of heparin to the substance surface is rather chemically complex (Sin *et al.*, 2009).

Textured surface (bioactive)

Another bioactive surface coating is the textured surface coating. The first application of textured surface was conducted by Bernhard *et al.* (1968). Decron fibrils were applied with polyurethane adhesive to a silastic bladder of an LVAD.

Whalen (1988) developed and examined two different textured surfaces (polyurethane fibrils woven into a fabric and an integrally textured silicone rubber surface with nonfibril geometry to silicone rubber substrates) as alternatives to the polyester velour surface (Hall *et al.*, 1967, 1968; Liotta *et al.*, 1996; Reichenbach *et al.*, 2001) for chambers of artificial hearts. The study showed that tissue fixation depended on the textured surface morphology. In comparison with smooth surface silicone rubber, formation of tissue capsules was thinner for both examined textured surfaces.

Synthetic polymer has been known as potential cause for thromboembolism. Polyurethane vascular patches with textured luminal surface were produced to diminish this problem and compared with non-textured polyurethane surface for period of 1–3 weeks post-implantation (Fujisawa *et al.*, 1999). The study investigated the effect of controlled surface texture on the formation of blood-compatible pseudo-neointima. The major finding of the study is that the formation of a stabilized thrombus layer can be achieved only by having textured surface on a substance. Another study suggested that the thickness of pseudo-neointima can be handled by the ability to control the surface texturing (Fujisawa *et al.*, 2000). Three different lengths of microfibers, 25, 50 and 100 μm were produced on a polyurethane as shown in Fig. 8.3.

As an example of commercial use, the polyurethane diaphragm is textured with integral fibrillar texture in HeartMate LVAD. This textured surface allows a thin coagulum to be built, which leads to a neo-intimal surface. This neo-intimal surface consists of acellular elements and progenitor cells that differentiate into fibroblasts, myotibroblast, monocytes and endothelial cells. Stable, thin layer biological neo-intimal remains without a large hanging flap of tissue on the surface (Long, 2001). It prevents the connection of blood and the material surface once it is formed. Therefore, this cellular matrix derived from the blood offers remarkable thrombosis reduction and minimizes the need for anticoagulants such as warfarin (Poirier, 1997a; Frazier *et al.*, 2001).

Many methods are used to create a textured surface on a substrate, such as the formation of sintered titanium microspheres on a titanium substrate (Dasse *et al.*, 1987; Graham *et al.*, 1990). Excimer laser micromachining is utilized in order to

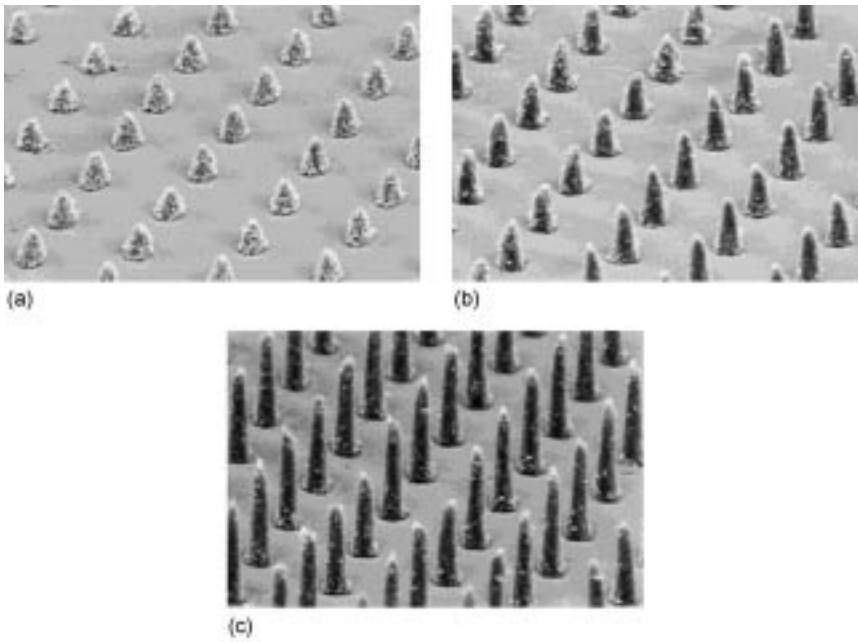

8.3 Polyurethane textured surface with different length of fibres: (a) 25, (b) 50, (c) 100 μm (Fujisawa *et al.*, 2000). (Reprinted with permission of John Wiley & Sons, Inc.)

create a master negative mould of patterned cavities, to fabricate a polyurethane textured surface (Zapanta *et al.*, 2006). Argon plasma etching is also used to manufacture micropatterns on titanium oxide films, which is accomplished by plasma immersion and deposition (Jing *et al.*, 2007).

For excellent biocompatibility, smooth titanium surfaces are textured with titanium microsphere coatings (smooth surface) and the Dacron portions of the inlet and outlet cannulas are rough flocked surfaces in HeartMate II. Having both smooth and rough surfaces in a same device is considered to be beneficial (Griffith *et al.*, 2001).

However, there are a couple of drawbacks for the textured-surface method. The textured surface does not work properly in terms of biological requirements for the small opening areas in VADs such as conduits (Fig. 8.4). For instance, serious thrombosis has been reported for HeartMate II axial flow pumps (Farrar *et al.*, 2007).

8.6 Preparation and testing for biocompatibility and haemocompatibility

There is no generalized test for the evaluation of biological response to artificial material due to the complexity of the reaction mechanisms of blood and tissue.

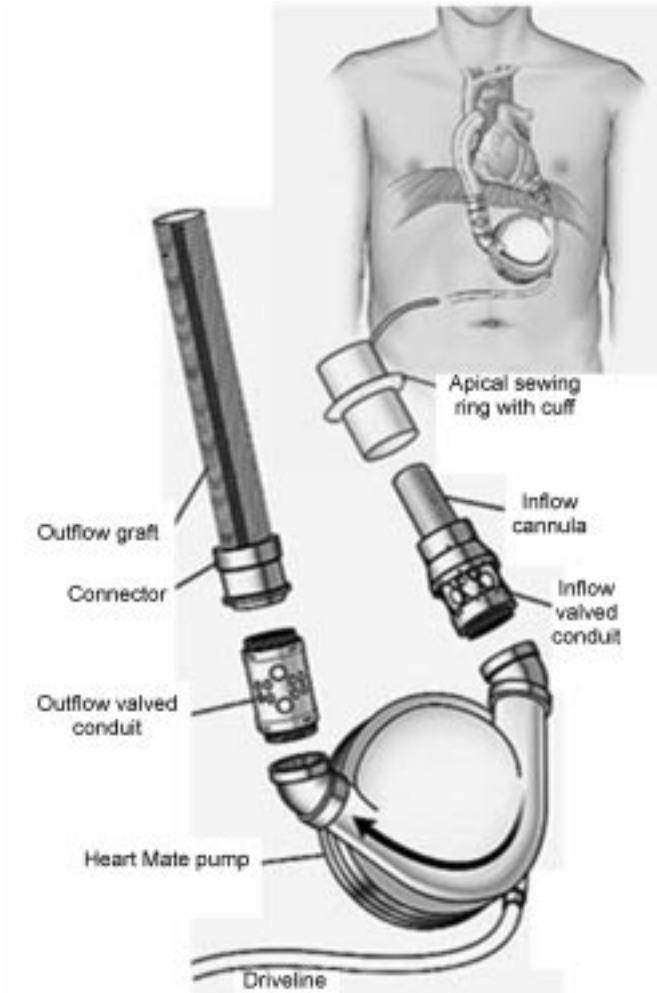

8.4 Conduit and cannula component placement in Thoratec extracorporeal biventricular (Thoratec, 2009).

A few tests have been developed by researchers to determine the human body's reaction to foreign materials, i.e. *in vitro*, *ex vivo* and clinical. This section consequently will provide information on preparation and testing of biomaterial for cardiac devices and the related standards applied to them.

In vitro is an initiation for development steps of biomaterials, which can be of great help in understanding biological response to biomaterial and vice versa. Cell adhesion or activation and cytotoxicity are identified with fundamental biocompatibility cell culture assays for *in vitro* test (Anderson, 2006). It is an important step since performing an *in vitro* test helps cut down development expenses and time of biological evaluation of medical devices and its com-

ponents. The reason is that *in vitro* apparatus has an advantage as it allows the user to control parameters such as time and temperature in a laboratory environment. There are standardizations such as ASTM, BSI and ISO related to *in vitro* cell culture cytotoxicity assays (Winn *et al.*, 2006).

ISO 10993, Biological Evaluation of Medical Device – Part 5: Test for *in vitro* Toxicity, has been reviewed for a systematic look at the *in vitro* assessment. The test is to be assessed with one or more of three tests, namely the extract test, direct contact test and indirect contact test which is decided based on the nature of part, potential portion of use and nature of use (ISO, 2009). Both direct and indirect contact methods should be applied for adequate evaluation of cell response because indirect contact methods pose the risk of providing results that lead to misjudging the cytotoxicity test for implant material. Different results of cytotoxicity from direct and indirect methods have been reported for the same implant biomaterial (Muller, 2008).

Subsequently, these will lead to the preparation of the material and the cell culture, and the manner of their interaction. Primarily, it is inevitable that two parts of ISO 10993, Part 1: Evaluation and testing within a risk management system (ISO, 2003) and Part 12: Sample preparation and reference material (ISO, 2007), are to be carried out before implementation of Part 5. ISO 10993, Part 5 is investigated after certain duration of the test and the results in toxicity determination can be accordingly explored in four sections, i.e. cell morphology damage, cell damage, cell growth and specific aspect of cellular metabolism. ISO 10993 Part 12 is for the preparation of samples and selection of reference material for medical device testing in accordance with one or more parts of the ISO 10993 series (ISO, 2007).

ISO 10993 Part 4: Selection of tests for interaction with blood (ISO, 2002) also offers advantages as the test can be conducted in the early development phase of biomaterials. Part 4 investigates biomaterials in terms of their interaction with blood and its effects on the blood/tissue/organ or device. ISO 10993-4 (ISO, 2002) provides a list of blood-circulating medical devices and the tests (i.e. thrombosis, coagulation, platelets, haematology and complement system) accordingly. The choice of one or more of these tests depends upon the system conditions such as duration of blood–device contact, temperature, sterility, flow conditions and the device characteristics in contact with blood as categorized in ISO 10993-1 (ISO, 2003) (i.e. non-contact, external connecting and implant devices).

Haemocompatibility tests can be applied to a single component of a device for screening purposes. However, as mentioned before, it cannot provide sufficient information of haemocompatibility of the complete device. Another area of caution is the type of blood being used for the tests. The standard suggests that human blood differs among individuals. If it is not absolutely necessary, species of animal blood should be investigated according to ISO 10993-2.

On the other hand, as advised, the haemolysis test alone is not good enough to determine the blood responses such as coagulation activation (Muller, 2008). Therefore, other methods such as blood count and SEM are recommended for comprehensive evaluation.

Sterilization of the test sample is a previous requirement of the assessment and if the sample cannot be sterilized due to a change on its properties, bacterial contamination should be investigated. On the other hand, if the product is supplied without sterilization, the correct method must be considered. A method such as plasma sterilization should not be applied on polymers as it poses serious problems to the biomaterial structure (Muller, 2008).

Repetition of cell and blood testing is a stringent requirement *in vitro*. For this perspective, to delve into blood–device complex interplay and adequate evaluation, for example, tested biomaterial inherently induces different responses from different blood donors, and a combination of investigations with different blood donors is necessary.

Ex vivo testing is a dynamic, one-pass and continued flow test. The device is located outside of the living body and attached to the circulatory system. *Ex vivo* is mainly applied to evaluate the coagulation effects of biomaterials on blood. However, *in vitro* and *ex vitro* must be followed up by *in vivo* testing since it is a clinical and final evolution of mechanical cardiac devices.

In vivo testing is necessary for successful cardiac devices. It is performed after the medical device is implemented within an animal and then investigated for a period of time. In other words, *in vivo* assessment is a simulation of intended clinical application. In general, the assessment is carried out to investigate the biocompatibility of the medical device and biomaterials to ensure that the expected functionality of device meets optimum clinical requirements. One of the specific purposes of *in vivo* tests is to determine whether the material used for medical device is blood compatible or not, which is based on the thrombus formation. International standards organizations such as ASTM and ISO provide standards and comprehensive guidelines to evaluate interface in between blood and cardiac devices.

8.7 Future trends

Cardiac devices have been in great development process and recent enhancements tend to eliminate thromboembolic complications and extend the durability. For example, third-generation blood pumps, magnetically or hydraulically suspended, are bearing-less which offers enhanced durability. A few of third-generation devices are listed in Table 8.2. Only some of them are in clinical use (VentrAssist and Incor, etc.) and the rest are still under investigation. Advances in power systems and reduction in size also provide less surgical trauma due to easier implantation and better patient mobility.

Principally, blood-contacting surfaces of the cardiac devices are also of great

research interest. Although DLC and heparin coatings are utilized for some of the third generation commercial cardiac devices due to their excellent haemocompatibility, bioactive coatings on blood-contacting surfaces have been a topic of intense research.

Endothelial cell (EC) lining on biomaterials is suggested for long-term cardiac devices due to its antithrombotic properties (Scott-Burden *et al.*, 1998). A few attempts on the use of an EC lining to enhance the blood compatibility can be seen in the literature (Wang *et al.*, 2002; Sreerekha and Krishnan, 2006). EC lining can be created on different materials with textured surface using *in vitro* cell culture. Even though biological surface coatings seem to be promising as a future technology compared with the current technology, they need further development and investigation due to their possible lasting limitations.

8.8 References

Alanazi, A., Nojiri, C., Noguchi, T., Kido, T., Komatsu, Y., Hirakuri, K., Funakubo, A., Sakai, K. & Fukui, Y. (2000) Improved blood compatibility of DLC coated polymeric material. *ASAIO Journal*, **46**, 440–443.

Anderson, J. M. (2006) Fundamental biological requirements of a biomaterial. In Guelcher, S. A. & Hollinger, J. O. (Eds) *An Introduction to Biomaterials.* Boca Raton, FL, Taylor & Francis Group.

Bernhard, W. F., Lafarge, C. G., Robinson, T., Yun, I., Shirahige, K. & Kitrilakis, S. (1968) An improved blood–pump interface for left-ventricular bypass. *Annals of Surgery*, **168**, 750–763.

Biehl, V., Wack, T., Winter, S., Seyfert, U. T. & Breme, J. (2002) Evaluation of the haemocompatibility of titanium based biomaterials. *Biomolecular Engineering*, **19**, 97–101.

Brunski, J. B. (2004) Metals. In Ratner, B. D., Hoffman, A. S., Schoen, F. J. & Lemons, J. E. (Eds) *Biomaterials Science: An Introduction to Materials in Medicine*, 2nd edn. London, Elsevier.

Christel, P. S. (1992) Biocompatibility of surgical-grade dense polycrystalline alumina. *Clinical Orthopaedics & Related Research*, **282**, 10–18.

Christensen, K., Larsson, R., Emanuelsson, H., Elgue, G. & Larsson, A. (2001) Heparin coating of the stent graft – effects on platelets, coagulation and complement activation. *Biomaterials*, **22**, 349–355.

Curtis, J. J., Walls, J. T., Wagner-Mann, C. C., Schmaltz, R. A., Demmy, T. L., McKenney, C. A. & Mann, F. A. (1999) Centrifugal pumps: description of devices and surgical techniques. *Annals of Thoracic Surgery*, **68**, 666–671.

Dasse, K. A., Chipman, S. D., Sherman, C. N., Levine, A. H. & Frazier, O. H. (1987) Clinical experience with textured blood contacting surfaces in ventricular assist devices. *ASAIO Journal*, **33**, 418–425.

Dearnaley, G. & Arps, J. H. (2005) Biomedical applications of diamond-like carbon (DLC) coatings: a review. *Surface and Coatings Technology*, **200**, 2518–2524.

Dion, I., Baquey, C., Candelon, B. & Montiès, J. R. (1992) Hemocompatibility of titanium nitride. *Biomaterials*, **15**, 617–621.

Dion, I., Baquey, C., Montiès, J. R. & Havlik, P. (1993a) Haemocompatibility of Ti6Al4V alloy. *Biomaterials*, **14**, 122–126.

Dion, I., Lahaye, M., Salmon, R., Baquey, C., Montiès, J. R. & Havlik, P. (1993b) Blood haemolysis by ceramics. *Biomaterials*, **14**, 107–110.

Dion, I., Roques, X., Baquey, C., Baudet, E., Cathalinat, B. B. & More, N. (1993c) Hemocompatibility of diamond-like carbon coating. *Bio-Medical Materials and Engineering*, **3**, 51–55.

Dion, I., Rouais, F., Trut, L., Baquey, C., Montiès, J. R. & Havlic, P. (1993d) Tin coating: surface characterization and haemocompatibility. *Biomaterials*, **14**, 169–176.

Dowling, R. D., Park, S. J., Pagani, F. D., Tector, A. J., Naka, Y., Icenogle, T. B., Poirier, V. L. & Frazier, O. H. (2004) Heartmate® VE LVAS design enhancements and its impact on device reliability. *European Journal of Cardio-Thoracic Surgery*, **25**, 958–963.

Drews, T., Loebe, M., Hennig, E., Kaufmann, F., Müller, J. & Hetzer, R. (2000) The 'Berlin heart' assist device. *Perfusion*, **15**, 387–396.

Duerig, T., Pelton, A. & Stöckel, D. (1999) An overview of nitinol medical applications. *Materials Science and Engineering A*, **273–275**, 149–160.

Ebel, T., Gerling, R. & Otto, K. H. (2005) Surface modifications for improved hemocompatibility and wear resistance of titanium alloys used in artificial heart valves. In Stallforth, H. & Revell, P. (Eds) *Materials for Medical Engineering*, Weinheim, Wiley.

Ellingsen, J. E. (1991) A study on the mechanism of protein adsorption to TiO_2. *Biomaterials*, **12**, 593–596.

Ellingsen, J. E. & Lyngstadaas, S. P. (2003) Increasing biocompatibility by chemical modification of titanium surfaces. In Ellingsen, J. E. & Lyngstadaas, S. P. (Eds) *Bio-implant Interface – Improving Biomaterials and Tissue Reactions.* Boca Raton, FL, CRC Press.

Farrar, D. J., Bourque, K., Dague, C. P., Cotter, C. J. & Poirier, V. L. (2007) Design features, developmental status, and experimental results with the Heartmate III centrifugal left ventricular assist system with a magnetically levitated rotor. *ASAIO Journal*, **53**, 310–315.

Frazier, O. H. & Macris, M. P. (1994) Current methods for circulatory support. *Texas Heart Institute Journal*, **21**, 288–295.

Frazier, O. H., Rose, E. A., Oz, M. C., Dembitsky, W., McCarthy, P., Radovancevic, B., Poirier, V. L. & Dasse, K. A. (2001) Multicenter clinical evaluation of the heartmate vented electric left ventricular assist system in patients awaiting heart transplantation. *Thoracic and Cardiovascular Surgery*, **122**, 1186–1195.

Frazier, O. H., Myers, T. J. & Gregoric, I. (2008) Total artificial heart. In Cohn, L. (Ed.) *Cardiac Surgery in the Adult.* New York, McGraw-Hill.

Fujisawa, N., Poole-Warren, L. A., Woodard, J. C., Bertram, C. D. & Schindhelm, K. (1999) A novel textured surface for blood-contact. *Biomaterials*, **20**, 955–962.

Fujisawa, N., Odell, R. A., Poole-Warren, L. A., Bertram, C. D., Woodard, J. C. & Schindhelm, K. (2000) Acute cellular interaction with textured surfaces in blood contact. *Journal of Biomedical Materials Research*, **52**, 517–527.

Graham, T. R., Dasse, K., Coumbe, A., Salih, V., Marrinan, M. T., Frazier, O. H. & Lewis, C. T. (1990) Neo-intimal development on textured biomaterial surfaces during clinical use of an implantable left ventricular assist device. *European Journal of Cardiothoracic Surgery*, **4**, 182–190.

Griffith, B. P., Kormos, R. L., Borovetz, H. S., Litwak, K., Antaki, J. F., Poirier, V. L. & Butler, K. C. (2001) Heartmate ii left ventricular assist system: From concept to first clinical use. *Annals of Thoracic Surgery*, **71**, S116–120.

Guelcher, S. A. (2006) Polyurethanes. In Guelcher, S. A. & Hollinger, J. O. (Eds) *An*

Introduction to Biomaterials. Boca Raton, FL, Taylor & Francis Group.
Hajar, R. (2005) The artificial heart. *Heart Views*, **8**, 70–76.
Hall, C. W., Liotta, D., Ghidoni, J. J., Debakey, M. E. & Dressler, D. P. (1967) Velour fabrics applied to medicine. *Journal of Biomedical Materials Research*, **1**, 179–196.
Hall, C. W., Liotta, D., O'Neal, R. M., Adams, J. G. & Debakey, M. E. (1968) Medical application of the velour fabrics. *Annals of the New York Academy of Sciences*, **146**, 314–324.
Hauert, R. (2003) A review of modified DLC coatings for biological applications. *Diamond and Related Materials*, **12**, 583–589.
Hench, L. L. (1991) Bioceramics: from concept to clinic. *Journal of the American Ceramic Society*, **74**, 1487–1510.
Hetzer, R., Weng, Y., Potapov, E. V., Pasic, M., Drews, T., Jurmann, M., Hennig, E. & Muller, J. (2004) First experiences with a novel magnetically suspended axial flow left ventricular assist device. *European Journal of Cardiothoracic Surgery*, **25**, 964–970.
Huang, N., Yang, P., Cheng, X., Leng, Y., Zheng, X., Cai, G., Zhen, Z., Zhang, F., Chen, Y., Liu, X. & Xi T. (1997) Blood compatibility of amorphous titanium oxide films synthesized by ion beam enhanced deposition. *Biomaterials*, **19**, 771–776.
Huang, N., Yang, P., Leng, Y. X., Chen, J. Y., Suna, H., Wang, J., Wang, G. J., Ding, P. D., Xi, T. F. & Leng, Y. (2003) Hemocompatiblility of titanium oxide films. *Biomaterials*, **24**, 2177–2187.
Igarashi, A., Hayashi, H., Yamanobe, T. & Komoto, T. (2006) Structure and morphology of diamond-like carbon coated on nylon 66/poly(phenylene ether) alloy. *Journal of Molecular Structure*, **788**, 238–245.
Iijima, T., Inamoto, T., Nogawa, M. & Takatani, S. (1997) Control of centrifugal blood pump based on the motor current. *Artificial Organs*, **21**, 655–660.
Ishihara, K. (2000) New polymeric biomaterials – phospholipid polymers with a bio-compatible surface. *Frontiers of Medical and Biological Engineering*, **10**, 83–95.
ISO (1996) 'Implants for surgery – metallic materials – part 3: Wrought titanium 6-aluminium 4-vanadium alloy', International Organization for Standardization 5832–3:1996(E).
ISO (2002) 'Biological evaluation of medical devices – part 4: Selection of tests for interaction with blood', International Organization for Standardization 10993–4:2002(E).
ISO (2003) 'Biological evaluation of medical devices – part 1: Evaluation and testing within a risk management system', International Organization for Standardization 10993-1:2003(E).
ISO (2007) 'Biological evaluation of medical devices – part 12: Sample preparation and reference materials', International Organization for Standardization 10993-12:2007(E).
ISO (2009) 'Biological evaluation of medical devices – part 5: Tests for *in vitro* cytotoxicity', International Organization for Standardization 10993-5:2009(E).
Jing, F. J., Wang, L., Fu, R. K. Y., Leng, Y. X., Chen, J. Y., Huang, N. & Chua, P. K. (2007) Behavior of endothelial cells on micro-patterned titanium oxide fabricated by plasma immersion ion implantation and deposition and plasma etching. *Surface and Coatings Technology*, **201**, 6874–6877.
Jones, M. I., McColl, I. R., Grant, D. M., Parker, K. G. & Parker, T. L. (2000) Protein adsorption and platelet attachment and activation, on tin, TiC, and DLC coatings on titanium for cardiovascular applications. *Journal of Biomedical Materials Research*, **52**, 413–421.

Joyce, L. D., Noon, G. P., Joyce, D. L. & Debakey, M. E. (2004) Mechanical circulatory support – a historical review. *ASAIO Journal*, **50**, x–xii.

Kantrowitz, A., Tjonneland, S., Freed, P. S., Phillips, S. J., Butner, A. N. & Sherman, J. L., Jr. (1968) Initial clinical experience with intraaortic balloon pumping in cardiogenic shock. *Journal of the American Medical Association*, **203**, 113–118.

Kasemo, B. (1983) Biocompatibility of titanium implants: surface aspects. *Journal of Prosthetic Dentistry*, **49**, 835–837.

Kihara, S., Yamazaki, K., Litwak, K. N., Litwak, P., Kameneva, M. V., Ushiyama, H., Tokuno, T., Borzelleca, D. C., Umezu, M., Tomioka, J., Tagusari, O., Akimoto, T., Koyanagi, H., Kurosawa, H., Kormos, R. L. & Griffith, B. P. (2003) *In vivo* evaluation of a MPC polymer coated continuous flow left ventricular assist system. *Artificial Organs*, **27**, 188–192.

Klee, D. & Höker, H. (1999) Polymers for biomedical applications: improvement of the interface compatibility. *Advances in Polymer Science – Biomedical Applications/ Polymer Blends.* Berlin, Springer.

Klinger, A., Steinberg, D., Kohavi, D. & Sela, M. N. (1997) Mechanism of adsorption of human albumin to titanium *in vitro*. *Journal of Biomedical Materials Research*, **36**, 387–392.

Koster, A., Loebe, M., Sodian, R., Potapov, E. V., Hansen, R., Muller, J., Mertzlufft, F., Crystal, G. J., Kuppe, H. & Hetzer, R. (2001) Heparin antibodies and thromboembolism in heparin-coated and noncoated ventricular assist devices. *Journal of Thoracic Cardiovascular Surgery*, **121**, 331–335.

Krishnan, L. K., Varghese, N., Muraleedharan, C. V., Bhuvaneshwar, G. S., Derangère, F., Sampeur, Y. & Suryanarayanan, R. (2002) Quantitation of platelet adhesion to Ti and DLC-coated Ti *in vitro* using 125I-labeled platelets. *Biomolecular Engineering*, **19**, 251–253.

Kumta, P. N. (2006) Ceramic biomaterials. In Guelcher, S. A. & Hollinger, J. O. (Eds) *An Introduction to Biomaterials.* Boca Raton, FL, Taylor & Francis Group.

Lamba, N. M. K., Woodhouse, K. A. & Cooper, S. L. (1998) *Polyurethanes in Biomedical Applications*. New York, CRC Press.

Leduc, P. & Wang, U. (2006) Protein adsorption at the biomaterial/tissue interface. In Guelcher, S. A. & Hollinger, J. O. (Eds) *An Introduction to Biomaterials.* Boca Raton, FL, Taylor & Francis Group.

Levi, D. S., Kusnezov, N. & Carman, G. P. (2008) Smart materials applications for pediatric cardiovascular devices. *Pediatric Research*, **63**, 552–558.

Liotta, D., Hall, C. W., Villanueva, A., O'Neal, R. M. & Debakey, M. E. (1996) A permanent autologous lining for implantable blood pumps: a pseudoendocardium. *Cardiovascular Research Center Bulletin*, **4**, 69–80.

Liu, X., Chu, P. K. & Ding, C. (2004) Surface modification of titanium, titanium alloys, and related materials for biomedical applications. *Materials Science and Engineering: R: Reports*, **47**, 49–121.

Long, J. W. (2001) Advanced mechanical circulatory support with the Heartmate left ventricular assist device in the year 2000. *Annals of Thoracic Surgeons*, **71**, 176–182.

McGee, M. G., Szycher, M., Turner, S. A., Clay, W., Trono, J. M., Fuqua, J. & Norman, J. C. (1980) Use of a composite biomer-butyl rubber/biomer material to prevent transdiaphragmatic water permeation during long-term, electrically-actuated left ventricular assist device (LVAD) pumping. *Cardiovascular Diseases*, **7**, 278–287.

Moen, O., Fosse, E., Dregelid, E., Brockmeier, V., Andersson, C., Hogasen, K., Venge, P., Mollnes, T. E. & Kierulf, P. (1996) Centrifugal pump and heparin coating

improves cardiopulmonary bypass biocompatibility. *Annals of Thoracic Surgery*, **62**, 1134–1140.

Montiès, J. R., Dion, I., Havlik, P., Rouais, F., Trinkl, J. & Baquey, C. (1997) Cora rotary pump for implantable left ventricular assist device: biomaterial aspects. *Artificial Organs*, **21**, 730–734.

Moulopoulos, S. D., Topaz, S. R. & Kolff, W. J. (1962) Extracorporeal assistance to the circulation and intraaortic balloon pumping. *Transactions – American Society for Artificial Internal Organs*, **8**, 85–89.

Muller, U. (2008) *In vitro* biocompatibility testing of biomaterials and medical devices Medical Device Link. Available from: http://www.devicelink.com/mdt/archive/08/03/006.html [Accessed 30 June 2009].

Muramatsu, K., Masuoka, T. & Fujisawa, A. (2001) *In vitro* evaluation of the heparin-coated Gyro c1e3 blood pump. *Artificial Organs*, **25**, 585–590.

Nakabayashi, N. & Iwasaki, Y. (2004) Copolymers of 2-methacryloyloxyethyl phosphorylcholine (MPC) as biomaterials. *Bio-Medical Materials and Engineering*, **14**, 345–354.

Nakabayashi, N. & Williams, D. F. (2003) Preparation of non-thrombogenic materials using 2-methacryloyloxyethyl phosphorylcholine. *Biomaterials*, **24**, 2431–2435.

Nosé, Y., Ohashi, Y., Tasai, K. & Debakey, M. E. (1996) Biomaterial considerations for cardiac prostheses. In Wise, D. L., Trantolo, D. J., Altobelli, D. E., Yaszemski, M. J. & Grasser, J. D. (Eds) *Human Biomaterials Applications.* Totowa, NJ, Humana Press.

Nosé, Y., Yoshikawa, M., Murabayashi, S. & Takano, T. (2000) Development of rotary blood pump technology: past, present, and future. *Artificial Organs*, **24**, 412–420.

Oeveren, W. V. (2005) Blood flow dnamics and surface interactions. In Vadgama, P. (Ed.) *Surfaces and Interfaces for Biomaterials.* Cambridge, Woodhead Publishing.

Ohgoe, Y., Hirakuri, K. K., Tsuchimoto, K., Friedbacher, G. & Miyashita, O. (2004) Uniform deposition of diamond-like carbon films on polymeric materials for biomedical applications. *Surface and Coatings Technology*, **184**, 263–269.

Papaioannou, T. G. & Stefanadis, C. (2005) Basic principles of the intraaortic balloon pump and mechanisms affecting its performance. *ASAIO Journal*, **51**, 296–300.

Park, J. B. & Lakes, R. S. (1992) *Biomaterials: An Introduction*, New York, Plenum Press.

Pierce, W., Donachy, J., Rosenberg, G. & Baier, R. (1980) Calcification inside artificial hearts: inhibition by warfarin-sodium. *Science*, **208**, 601–603.

Pinchuk, L. (1994) A review of the biostability and carcinogenicity of polyurethanes in medicine and the new generation of 'biostable' polyurethanes. *Journal of Biomaterials Science*, *Polymer Edition*, **6**, 225–267.

Poirier, V. L. (1997a) The heartmate left ventricular assist system: worldwide clinical results. *European Journal of Cardio-Thoracic Surgery*, **11**, S39–S44.

Poirier, V. L. (1997b) The LVAD: a case study. National Academy of Engineering (NAE). Available from: http://www.nae.edu/cms/Publications/TheBridge/Archives/7342/ 7484.aspx [Accessed 14 May 2009].

Ratner, B. D. (2000) Blood compatibility – a perspective. *Journal of Biomaterials Science, Polymer Edition*, **11**, 1107–1119.

Ratner, B. D., Hoffman, A. S., Schoen, F. J. & Lemons, J. E. (2004) *Biomaterials Science: An Introduction to Materials in Medicine*, London, Elsevier.

Reichenbach, S. H., Farrar, D. J. & Hill, J. D. (2001) A versatile intracorporeal ventricular assist device based on the Thoratec VAD system. *Annals of Thoracic Surgeons*, **71**, 171–175.

Rose, E. A., Gelijns, A. C., Moskowitz, A. J., Heitjan, D. F., Stevenson, L. W., Dembitsky, W., Long, J. W., Ascheim, D. D., Tierney, A. R., Levitan, R. G., Watson, J. T., Ronan, N. S., Shapiro, P. A., Lazar, R. M., Miller, L. W., Gupta, L., Frazier, O. H., Desvigne-Nickens, P., Oz, M. C., Poirier, V. L. & Meier, P. (2001) Long-term use of a left ventricular assist device for end-stage heart failure. *New England Journal of Medicine*, **345**, 1435–1443.

Scott-Burden, T., Tock, C. L., Bosely, J. P., Clubb, F. J., S.M. Jr, P. S. M., Schwarz, J. J., Engler, D. A., Frazier, O. H. & Casscells, S. W. 3rd (1998) Nonthrombogenic, adhesive cellular lining for left ventricular assist devices. *Circulation*, **10**, II339–II345.

Sin, D. C., Kei, H. L. & Miao, X. (2009) Surface coatings for ventricular assist devices. *Expert Reviews of Medical Devices*, **6**, 51–60.

Sreerekha, P. R. & Krishnan, L. K. (2006) Cultivation of endothelial progenitor cells on fibrin matrix and layering on dacron/polytetrafluoroethylene vascular grafts. *Artificial Organs*, **30**, 242–249.

Sui, J. H. & Cai, W. (2006) Effect of diamond-like carbon (DLC) on the properties of the NiTi alloys. *Diamond and Related Materials*, **15**, 1720–1726.

Sui, J. H., Gao, Z. Y., Cai, W. & Zhang, Z. G. (2007) DLC films fabricated by plasma immersion ion implantation and deposition on the NiTi alloys for improving their corrosion resistance and biocompatibility. *Materials Science and Engineering: A*, **454–455**, 472–476.

Sunny, M. C. & Sharma, C. P. (1991) Titanium-protein interaction: changes with oxide layer thickness. *Journal of Biomaterials Applications*, **6**, 89–98.

Szycher, M. & Lee, S. L. (1993) Cardiovascular devices for the 1990s. *Journal of Biomaterials Applications*, **8**, 31–63.

Szycher, M. & Poirier, V. L. (1983) Synthetic polymers in artificial hearts: a progress report. *Industrial & Engineering Chemistry Product Research and Development*, **22**, 588–593.

Takami, Y., Nakazawa, T., Makinouchi, K., Glueck, J. & Nosé, Y. (1997) Biocompatibility of alumina ceramic and polyethylene as materials for pivot bearings of a centrifugal blood pump. *Journal of Biomedical Materials Research*, **36**, 381–386.

Takami, Y., Yamane, S., Makinouchi, K., Otsuka, G., Glueck, J., Benkowski, R. & Nosé, Y. (1998) Protein adsorption onto ceramic surfaces. *Journal of Biomedical Materials Research*, **40**, 24–30.

Thoratec (2009) Ventricular assist devices (VAD). Thoratec Corporation. Available from: http://my.clevelandclinic.org/heart/disorders/heartfailure/lvad_devices.aspx [Accessed 18 July 2009].

Trevor, A. S., Hiroyuki, T., Shin'ichiro, K., Takehide, A., Kenneth, N. L., Marina, V. K., Kenji, Y. & William, R. W. (2007) Preclinical biocompatibility assessment of the evaheart ventricular assist device: coating comparison and platelet activation. *Journal of Biomedical Materials Research Part A*, **81A**, 85–92.

Vroman, L. & Adams, A. L. (1969) Identification of rapid changes at plasma–solid interfaces. *Journal of Biomedical Materials Research*, **3**, 43–67.

Wang, D.-A., Ji, J., Sun, Y.-H., Shen, J.-C., Feng, L.-X. & Elisseeff, J. H. (2002) In situ immobilization of proteins and RGD peptide on polyurethane surfaces via poly(ethylene oxide) coupling polymers for human endothelial cell growth. *Biomacromolecules*, **3**, 1286–1295.

Wendel, H. P. & Ziemer, G. (1999) Coating-techniques to improve the hemocompatibility of artificial devices used for extracorporeal circulation. *European Journal of Cardio-Thoracic Surgery*, **16**, 342–350.

Wever, D. J., Veldhuizen, A. G., de Vries, J., Busscher, H. J., Uges, D. R. A. & van Horn, J. R. (1998) Electrochemical and surface characterization of a nickel–titanium alloy. *Biomaterials*, **19**, 761–769.

Whalen, R. L. (1988) Improved textured surfaces for implantable prostheses. *ASAIO Journal*, **34**, 887–892.

Winn, S. R., Mitchell, J. & Uludag, H. (2006) *In vitro* testing of biomaterials. In Guelcher, S. A. & Hollinger, J. O. (Eds) *An Introduction to Biomaterials.* Boca Raton, FL, Taylor & Francis Group.

Xue, L. & Greisler, H. P. (2003) Biomaterials in the development and future of vascular grafts. *Journal of Vascular Surgery*, **37**, 472–480.

Yamazaki, K., Kihara, S., Akimoto, T., Tagusari, O., Kawai, A., Umezu, M., Tomioka, J., Kormos, R., Griffith, B. & Kurosawa, H. (2002) Evaheart: an implantable centrifugal blood pump for long-term circulatory support. *Japanese Journal of Thoracic and Cardiovascular Surgery*, **50**, 461–465.

Zapanta, C. M., Griffith, J. W., Hess, G. D., Doxtater, B. J., Khalapyan, T., Pae, W. E. & Rosenberg, G. (2006) Microtextured materials for circulatory support devices: preliminary studies. *ASAIO Journal*, **52**, 17–23.

Zdrahala, R. J. & Zdrahala, I. J. (1999) Biomedical applications of polyurethanes: a review of past promises, present realities, and a vibrant future. *Journal of Biomaterials Applications*, **14**, 67–90.

9

Nanostructured biomaterials for artificial tissues and organs

Y. CHEN and T. J. WEBSTER, Brown University, USA

Abstract: This chapter discusses the rationale and the promise of nanotechnology to create the new generation of biomaterials for tissue engineering. It reviews the morphologies and functions of the nanostructures in natural tissues, introduces the methods to produce biomimetic nanostructured materials and demonstrates the improvement of tissue engineering by utilizing such nanostructured biomaterials.

Key words: nanotechnology, biomaterials, biomimic, tissue engineering.

9.1 Introduction and background of nanostructured biomaterials

Over the past two decades, with the accelerated development of tissue engineering, the demand for a variety of synthetic and natural biomaterials has dramatically increased. Biomaterial sales have already exceeded $240 million per year [1] and due to the rapid development of biomaterials, the market will only increase in the years ahead for tissue engineering and artificial organ materials. Specifically, costs related to organ replacement account for 8% of all global healthcare spending and by 2040 as much as 25% of the US gross domestic product (GDP) is expected to be related to healthcare [2]. Such demands require unique, better performing biomaterials for regenerative medicine. For example, it is necessary to develop better material mechanical properties and biocompatibility properties. Conventional biomaterials (or those materials with constituent dimensions greater than 1 μm) have not satisfactorily met clinical demands. Researchers, clinicians and other investigators are thus seeking better novel materials to serve as the next generation of tissue engineering and artificial organ materials.

Nature has always given people inspiration for innovation, but with caution. For example, caution needs to be taken since clearly some of our best engineering accomplishments do not mimic nature, as easily seen by comparing airplane with bird flight. In this context, nature has designed our tissues to have certain roughness. From a biomaterial point of view, to date, researchers and engineers have considered implant texture and surface features only at the

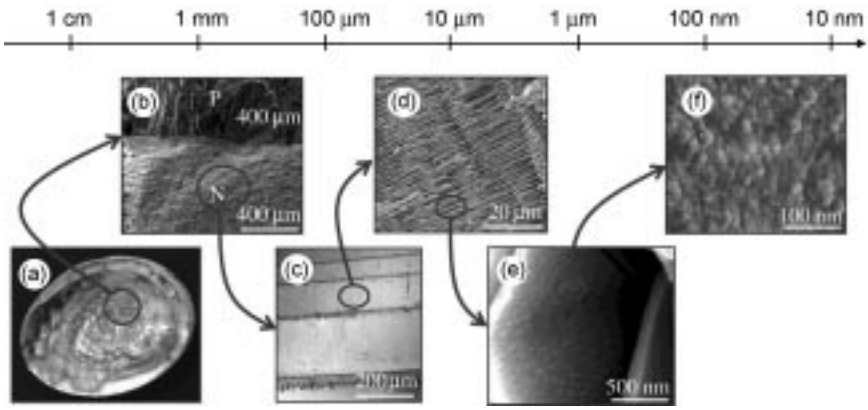

9.1 Hierarchical structures from 'micron' (a) to 'nano' (f) in nacre showing at least six structural levels. (Adapted and redrawn from Luz and Mano [3].)

micron level. While our tissues do have micron-structured features, recently, researchers have emphasized the natural nanostructure of our tissue. Well-organized supramolecules consist of a tiny, finely controlled, functional materials organized at nanometer level (a nanometer is a tenth of a micrometer), just like the nacre shell illustrated in Fig. 9.1. Even though our tissues and organs have nanometer level structures and associated roughness, which are important for various biological functions, nanotechnology has only recently been emphasized in biomaterials. With the growing knowledge of 'nano', researchers have emphasized that nanomaterials, which correlate to materials with at least one dimension less than 100 nm, have unique physical, chemical, mechanical and biological properties, significantly different from corresponding micron structured materials.

The US National Nanotechnology Initiative describes nanotechnology as research and development aimed at understanding and working with (such as observing, measuring and manipulating) matter at the atomic, molecular and supramolecular levels [4]. With the continuous investment and growing demand for innovation (especially in biomaterials), nanotechnology has become an intense area for both industry and academic research. From 2000 to 2007, the US invested around $8.5 billion in nanotechnology and the total sales of nano-technology-related products reached $50 billion. It is estimated that by 2015 the global market for nanotechnology-related products will be $2 trillion [5].

At the core of nanotechnology are nanomaterials and these have attracted much attention. Due to their size, nanomaterials often exhibit unique properties, such as improved magnetic, electrical, structural integrity and optical properties [6]. Thus, they enhance properties of most engineering materials (Table 9.1). Most importantly, previous studies have shown that nanomaterials have great potential for improving tissue/organ implantation and regeneration. Because of the larger surface to volume ratio of nanostructured biomaterials compared with

Table 9.1 Advantages of nanomaterials compared with conventional materials

Small size (for example, penetrating the blood–brain barrier for drug delivery applications) [20,21]
Large surface area (for example, a high density of functional groups can be functionalized with various biological agents) [6–10]
High surface energy (for example, improving certain protein adsorption to enhance tissue cell adhesion and functions) [11–13]
Excellent bio/cytocompatibility and decreased immune responses as well as inhibit bacteria infection [14–19]
Other unique chemical/physical properties (for example, superparamagnetic nanoparticles for enhancing magnetic resonance imaging (MRI)) [6, 22]

traditional micron-structured materials, nanostructured biomaterials are more reactive to bodily fluids (namely ions and proteins) and can be immobilized on a high density of functional groups for specific purposes (such as controlled drug delivery) [6–10]. This is because the larger surface areas and numerous angstrom/nanometer dimensioned defects of nanostructured biomaterials alter surface electron distributions to adsorb particular biological agents [11]. Since proteins are charged, such surface properties of nanostructured biomaterials will change surface energetics to influence protein interactions that subsequently mediate cell functions to regenerate tissues. In addition, hydrophilic nanostructured biomaterials have higher surface energy than corresponding micron-structured materials. For example, decreasing alumina grain size from 167 to 24 nm, alumina surface hydrophilicity was significantly increased to promote the adsorption of hydrophilic proteins that enhance osteoblast (bone forming cells) adhesion [12, 13].

Another novel property of nanostructured biomaterials is that they (in some cases) minimize immune cell recognition. For example, decreased macrophage functions were observed on aligned regions of carbon nanotubes compared with conventional polycarbonate urethane [14]. Thus, implanted nanostructured biomaterials often decrease inflammation allowing for quicker new appropriate tissue growth. Last, but not least, previous studies have demonstrated that nanostructured biomaterials have excellent cytocompatibility properties towards numerous cells (from osteoblasts to endothelial cells). In many cases, they have lower toxicity and integrate better with natural tissue than conventional biomaterials [15–19].

Because of the above, the field of nanostructured biomaterials (also called nanomedicine) has already become a popular field for the synthesis and evalua-

tion of better biomaterials for various academic, clinical and industrial interests. In order to describe the numerous promising applications of nanostructured biomaterials, this chapter will begin by addressing why nanomaterials may be the next generation of improved implants to regenerate tissues and organs. It will cover a variety of medical applications for different tissues and provide some specific examples of recent developments and practical applications of nanomaterials in the clinical and industrial setting. This chapter will finish on how nanostructured biomaterials can be efficiently used to combat current challenges in tissue engineering and artificial organ implantation, pointing out future prospects of nanostructured biomaterials in the medical arena.

9.2 Nanostructured biomaterials for bone applications

9.2.1 Background of orthopedics

Bone tissue engineering is one of the oldest research areas in all of organ replacement. Specifically, in 1923, the first hip replacement surgery was conducted [23, 24]. Clearly, since then, various bone implants (such as for healing bone fractures, repairing defects and reconstructing joints) have been routinely inserted increasing the quality of life for millions of people. The National Center for Health Statistics (NCHS) reported that there were more than 1 039 000 bone fractures in 2004 [25]. Moreover, the American Academy of Orthopedic Surgeons reported that in the US, from 1999 to 2003, there was a 19.7% increase in hip replacement surgeries up from about 274 000 procedures (including 168 000 total hip replacements and 106 000 partial hip replacements) to more than 328 000 procedures (including 220 000 total hip replacements and 108 000 partial hip replacements) [26].

Although bone implants have improved the quality of life for numerous patients, it is important to note that conventional bone implant materials, such as titanium and titanium alloys used for fixation devices for repairing bone fractures and artificial joint replacements to treat osteoarthritis, still have many shortcomings. For example, in just the US, nearly 11% of all hip replacements (36 000 revisions out of 328 000 replacements) and 8% of all knee replacements (33 000 revisions out of 418 000 replacements) failed in 2003 [26]. The number of revisions is increasing steadily. From October 1, 2005 to December 31, 2006, 51 345 total hip replacement revisions were conducted and the most common causes of these revisions included: instability/dislocation, mechanical loosening, infection, etc., as shown in Fig. 9.2 [27]. In addition, the lifetime of current artificial joint implants is only about 10–15 years on average [28], so younger and more active patients (such as those men under 60 and women under 55 years) who receive artificial joint replacements will inevitably need more than one revision surgery in their lifetime.

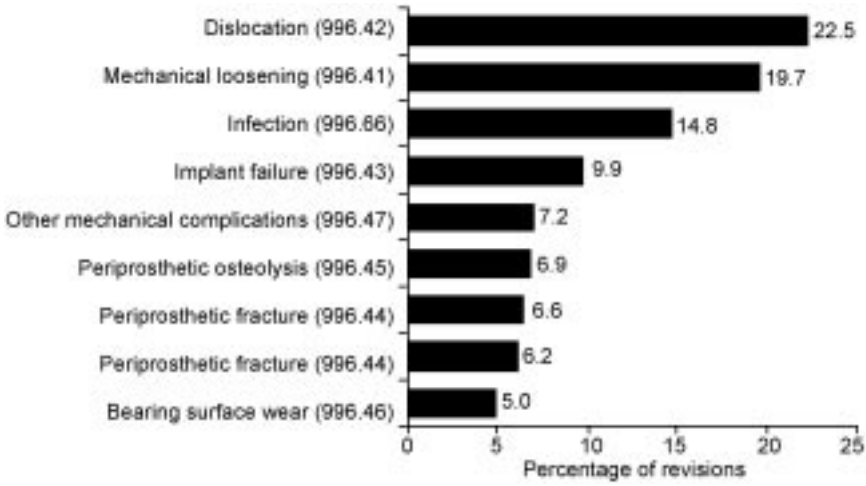

9.2 The most common causes for total hip replacement revisions in the US from 2005 to 2006. (Adapted from Bozic *et al.* [27].)

An ideal bone implant should not only temporarily replace missing bone, but also provide a framework to regenerate and heal host bone and orthopedic soft tissue around it. On the one hand, bone implants should have sufficient mechanical strength to connect severed/fractured bone segments, blood vessels, nerves and other soft tissue and support physiological loads. On the other hand, bone implants should have suitable surface chemistry to successfully integrate into the host tissue. In other words, they should be bio/cyto-compatible, not stimulate foreign body reactions or inflammation, and encourage new tissue growth (not just bone, but also blood vessels, nerves, etc., as such tissues are crucial for the maintenance of healthy bone throughout a person's life). However, current conventional implants display continual problems in these areas leading to implant failure [29, 30]. Of paramount importance, at some point during failure, a lack or separation of bone from the implant leads to failure, which may be because conventional implants usually have poor initial bone growth on the surface of the implant and/or lead to poor maintenance of healthy juxtaposed bone intended to firmly fix the implant for the patient's lifetime. Secondly, wear debris generated from articulating components of implants becomes lodged between the implant and surrounding tissue, thus leading to bone cell death and bone loss. Thirdly, infection also leads to poor bone regeneration or even death of bone tissue. Last but not least, stress and strain imbalances between an implant and surrounding tissue lead to bone loss, implant loosening, and eventually failure.

One way to overcome many of these shortcomings of current bone implants is to stimulate rapid initial bone regeneration and maintain such healthy juxtaposed bone over long periods of time in order to fix an implant firmly between

adjacent bones. Since these goals are not currently being achieved, it is urgent to develop a new generation of biocompatible and bio-integrated artificial bone implants which can restore and improve bone growth to significantly enhance the lifetime of current bone implants.

9.2.2 The necessity of using nanostructured biomaterials as artificial bone implants

Traditionally, 'trial-and-error' science has been a common method used to create better bone implant materials. Although this approach has increased the lifetime of bone implants as mentioned, today, the trial-and-error approach for bone implant engineering has created biomaterials that do not functionally last the lifetime of the patient. To design improved biomaterials with greater functional lifetimes, researchers have explored the natural chemistry and structure of bone more closely. As shown in Fig. 9.3, the hierarchical structure of human bone has three levels: the first is the macrostructure, including cancellous bone and cortical bone categories; secondly, the microstructure, which ranges from 1 to 500 micrometers and includes lamellae, cells, osteons and Haversian systems; and lastly, the smallest structures in bone are measured at the nanostructure level (from a few nanometers to several hundred nanometers) including such items as non-collagenous proteins, fibrillar collagens and embedded calcium phosphate minerals.

Since studies have shown that the more a biomaterial can mimic natural bone tissue, the higher probability such materials can increase bone regeneration, attention has turned to nanomaterials. Conventional biomaterials (as in micron grain size and micron-rough titanium) usually only mimic the macrostructure or microstructure of bone. Thus, nanotechnology has been used to create

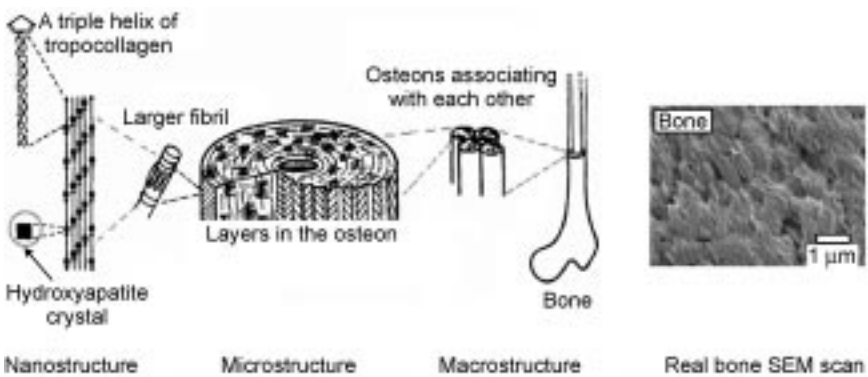

9.3 Schematic structure and a scanning electron microscopy (SEM) image of the human femur highlighting the importance of nanometer surface features. (Adapted and redrawn from Smallman and Bishop [31] and Liu and Webster [32].)

nanostructured features on traditional bone implants to improve bone growth. Since not all 'nano' is created equally, it is important to understand the exact nanostructure of bone which increases bone growth when incorporated onto orthopedic implants.

Natural bone is a composite material, composed of organic compounds (mainly collagen type I) reinforced with inorganic compounds (mainly hydroxyapatite (HA) minerals). The most prominent nanostructures in bone are the collagen fibers surrounded and infiltrated by HA crystals. The linear fibers of collagen (mainly type I collagen) self-assemble into triple helix bundles having a periodicity of 67 nm between the sides of parallel molecules, with 40 nm gaps between the ends of the molecules and pores. HA crystals ($50 \times 25 \times 3\ nm^3$) are located in and between the collagen framework and architecture of bone. This is a highly self-organized system. The entire bone structure consists of a hierarchical architecture from those nano-scaled building blocks, and in general, about 70% of the dry weight of bone is inorganic minerals and the rest is organic matrix [33]. Because of the importance of such nanostructures for the function of bone and bone cells which created the nanostructured extracellular matrix of bone in the first place [29], it is necessary for researchers to create novel biomaterials with nanostructured features on/in bone for orthopedic applications.

9.2.3 Applications of nanostructured biomaterials in orthopedic applications

Nanostructured modified metals and metal alloys

Conventional metals and alloys (like titanium and its alloys as well as CoCrMo alloys) are the most widely used implants for orthopedic applications. However, they do not perform as well as healthy bone and remodel or self-repair with time because they do not exhibit the same physiological, dynamic and mechanical characteristics of natural bone. In the clinic, such metals show insufficient prolonged osseointegration and lack of strong bonding with bone, which may lead to fibrous tissue ingrowth or failure after implantation. However, titanium and titanium-based alloys are highly biocompatible with little toxicity due to the natural formation of an oxide layer. Titanium (or more appropriately, titanium dioxide) was selected as one of the first examples for how nanotechnology can improve bone growth.

The most straightforward method to transform current titanium into that which increases tissue growth by possessing nano-features is via chemical etching as shown in Fig. 9.4. Recently, researchers reported a wet chemistry method to create nano-rough titanium [34]. Specifically, 3D micron porous titanium-based scaffolds were placed in a sodium hydroxide aqueous solution inside a Teflon-lined autoclave. During a heating process (60 ºC), a nano-skeleton layer of titanate formed on the exposed surface in the early stage via the

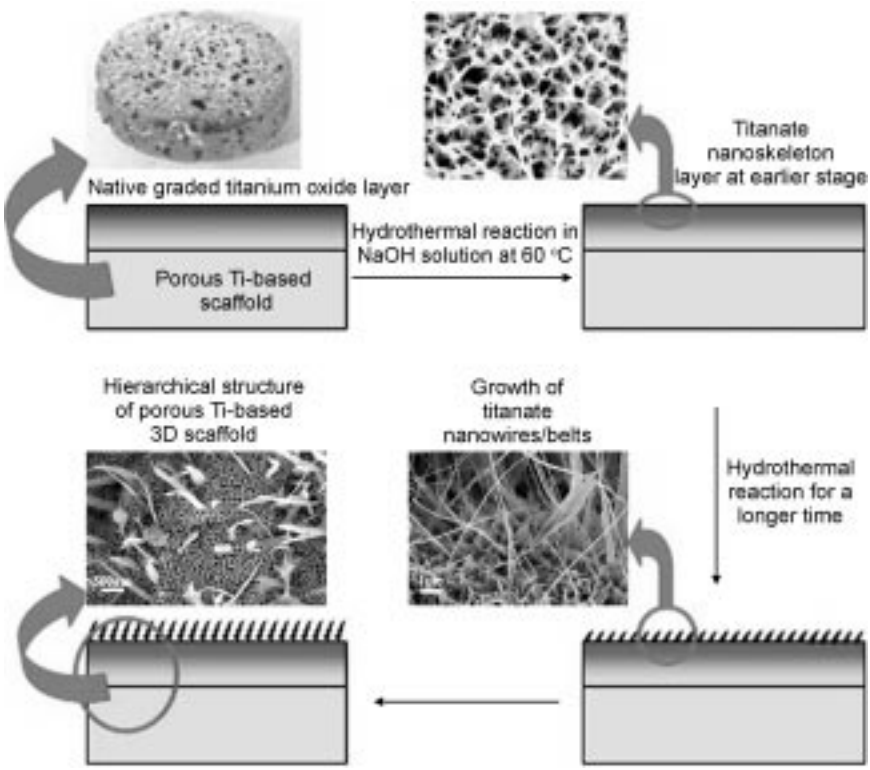

9.4 Schematic diagram of the fabrication process of a hierarchical 3D porous titanium based metal scaffold. (Adapted and redrawn from Wu *et al.* [34].)

reaction between native titanium oxide and sodium hydroxide. As time elapsed, some titanate nano-belts and nano-wires nucleated and grew on the skeleton and, finally, a hierarchical titanium-based metal scaffold was formed. It was found that such surface features on the nanometer scale dramatically improved the bioactivity of typical cell adhesive proteins (such as fibronectin and vitronectin) to accelerate cell attachment and proliferation [34].

Wet chemistry etching of titanium is very efficient to produce nano-rough surface features on titanium at low cost with little equipment required. However, the etching process and resulting surface features are not controllable and are often quite random. In contrast, using a Temescal electron beam evaporator is complex but produces desired thickness and exact nano-roughness morphologies on metals. As shown in Fig. 9.5, during this process, the electron beam is generated by an electron gun that uses the thermo-ionic emission of electrons produced by an incandescent filament. A magnet focuses and bends the electron trajectory so that the beam is accelerated towards a graphite crucible containing the source material. As the beam rotates and hits the surface of the source material, heating and vaporization occur, enabling the atoms and molecules to

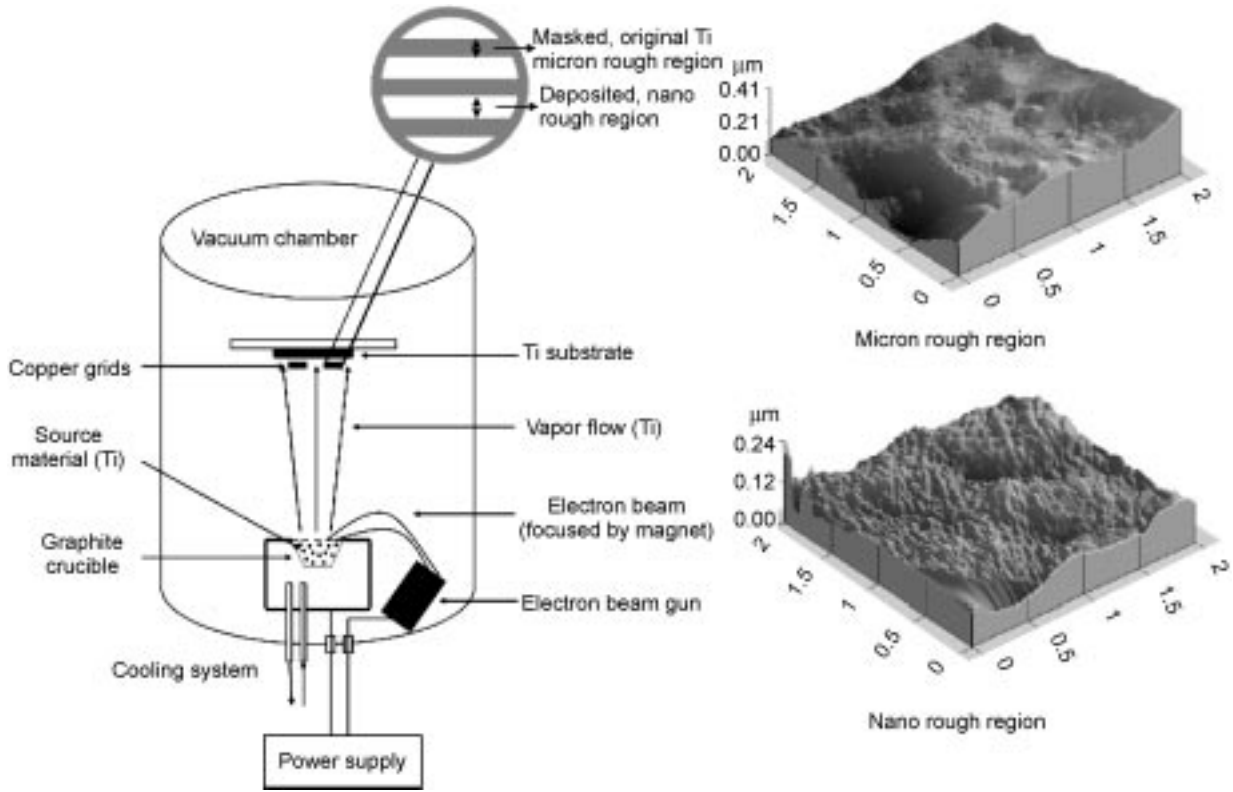

9.5 Schematic diagram of the electron beam evaporation technique used to create novel nano-patterned micron regions on titanium and atomic force microscopy (AFM) scans of micron/nano rough regions. (Adapted and redrawn from Puckett *et al.* [35].)

evaporate freely throughout the vacuum chamber. The atoms and molecules in the vapor flow then condense onto the substrate surface located at the top of the chamber, creating a coating that masks the original surface. It was found that compared with conventional nano-smooth titanium and nano-featured titanium, osteoblasts adhered and aligned on such nanostructured metal features. Such observations confirmed the hypothesis that nano-featured titanium can improve early osteoblast functions (morphology and adhesion), promising for promoting longer-term functions (such as calcium deposition), criteria necessary to improve orthopedic implant efficacy [35–37].

Another promising technique that has recently emerged to create nano-features on titanium is anodization. Anodization is an electrochemical method also known as anodic oxidation and is widely used as a surface modification technique for metals to produce protective oxidative layers [38]. Such anodization processes usually operate in an acidic solution. Anodization will result in the formation of an oxide layer on the anode surface. At the same time, the acid will etch the oxidative layer to cause the initial formation of pores at the weak points on the titanium surface due to localized dissolution. Then, voids will form in these inter-pore regions by field-enhanced oxidation/dissolution [39–42]. After the anodization of titanium, self-ordered nanotubular surface morphologies may be observed, as shown in Fig. 9.6.

An *in vitro* study provided evidence of enhanced calcium deposition by osteoblasts cultured on anodized titanium with nanotube-like structures compared with unanodized titanium and titanium anodized to process nano-particulate structures [43, 44]. A number of *in vivo* studies have also demonstrated the promising future of anodized titanium for orthopedic applications. For example, anodized titanium screws were inserted into rabbit tibia and allowed to penetrate one cortical layer. After 6 weeks, histology stains showed bone tissue formation on the nanostructured titanium implant surfaces that had an oxide thickness of more than 600 nm [45, 46]. Results indicated that the

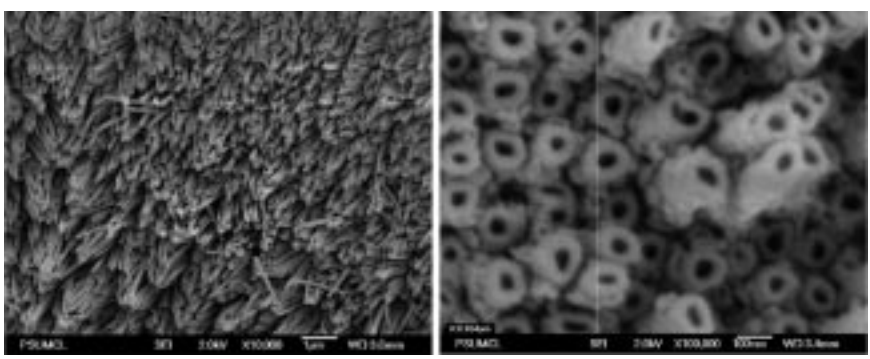

9.6 SEM images of anodized titanium foil samples. (Adapted from Ruan *et al.* [39].)

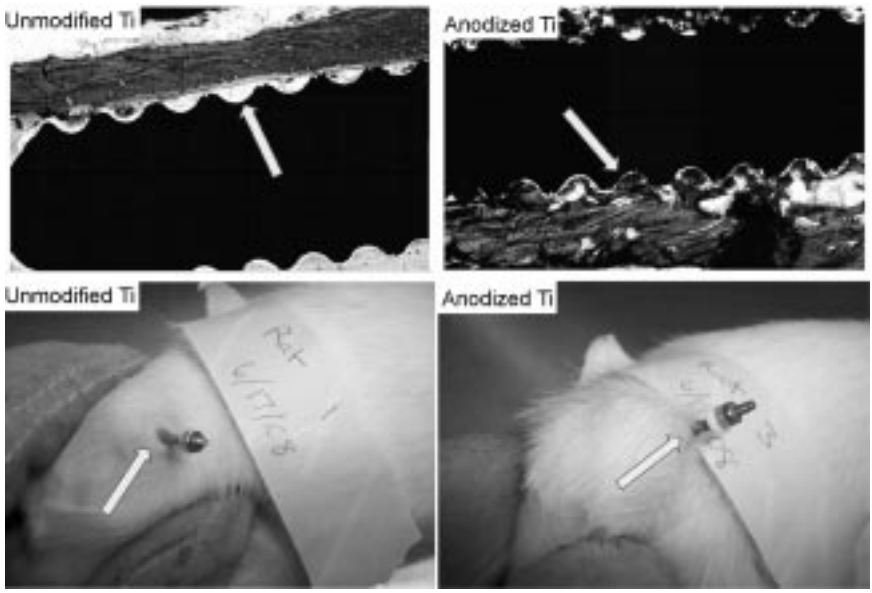

9.7 In vivo comparison of unmodified titanium and anodized titanium. (Arrows point out the comparison of bone growth (top) and inflammatory responses (bone) between unmodified and anodized titanium. Adapted from Puckett *et al.* [47].)

parameters of anodized titanium, like oxide thickness, the pore size distribution, the porosity and the crystallinity of the surface oxides may be factors that influence tissue–material interactions. Similar experiments were also conducted with sheep and rats in which anodized titanium screws or rods were inserted for 4 to 12 weeks. Again, as shown in Fig. 9.7, histological results showed that anodized nanotubular titanium implants have excellent cytocompatibility properties and an ability to quickly grow bone next to the implant [48–50]. Moreover, no infection or inflammatory responses were observed around the anodized nanotubular titanium screws (Fig. 9.7). It is also important to note that anodization is a quick (less than an hour) and inexpensive technique to modify the surfaces of titanium-based implants to improve bone cell functions required for improving orthopedic applications.

As a comparison of all three methods mentioned here for nanostructured metal modification, wet chemistry etching is the easiest approach. It requires little equipment and can react with a large amount of metal samples at the same time. However, the disadvantage of this method is that it is an uncontrollable process creating uneven surface morphologies. In contrast, the Temescal electron beam evaporation technique requires a high vacuum chamber and an extensive energy source supply. In addition, the evaporation and condensation of metal atoms usually take a little bit longer than chemical etching. However, Temescal electron beam evaporation can provide even or patterned nano-surface

morphologies. In particular, it can result in high purity of the substrate surface, superior than the anodization process which has been reported to have excess fluoride on the titanium surface if not carefully cleaned [51]. Unfortunately, to date, there have been no known accurate comparisons of bone growth on these three novel metal nanostructured surfaces, but it is clear that each shows advantages over currently implanted titanium.

Nanostructured ceramics

Ceramics are non-metallic inorganic materials which usually possess excellent biocompatibility properties and in some cases, have a high degree of biodegradability in the physiological environment. For example, HA ($Ca_{10}(PO_4)_6(OH)_2$) is one of the most popular bone graft substitutes and filler materials. As mentioned earlier in this chapter, HA is one of the main components in natural bone, so it should not be surprising that others have reported that HA has good osteoconductive properties to form a tight bond with bone [52]. Although traditional bioceramics have long served as bone substitutes, they have a variety of implant failure modes due to insufficient prolonged osseointegration, poor mechanical properties, osteolysis and detrimental ceramic implant wear debris. Therefore, nanostructured ceramics (as opposed to conventional micron-structured ceramics) which mimic the natural nanostructure of human bone have become novel candidates for improving bone implant performance [53].

With decreased grain size and pore diameters (if porous), surface area, roughness and surface energy of nanostructured ceramics dramatically increase compared with micron-structured ceramics. For instance, nanostructured alumina, HA and titania have improved wettability properties compared with conventional ceramics [54]. As another example, a 23 nm grain size alumina compact prepared by compressing nanoceramic particles had approximately 50% more surface area for cell adhesion than a 177 nm grain size alumina; similarly, a 32 nm grain size titania had about 35% more surface area than that of a 2.12 μm grain size titania [55]. Besides the large surface area of nanoceramics to increase cell adhesion, researchers have also found that the special surface properties (namely, surface energy) of nanomaterials are closely related to their observed excellent biocompatibility and osseointegration properties. An example, nanophase HA with a 67 nm grain size significantly enhanced osteoblast adhesion and inhibited the adhesion of competitive cells that synthesize soft fibrous tissue (fibroblasts) compared to conventional HA [54]. The reason that nano-HA selectively enhanced osteoblast adhesion over fibroblasts could be due to the adsorption of specific proteins necessary for bone cell functions (such as fibronectin) [54, 55]. Some nanoceramics have also demonstrated an antibacterial property even when the respective conventional ceramic is not antibacterial. For instance, nanophase ZnO and TiO_2 inhibited *Staphylococcus epidermidis* (a common bacterium contributing to undesirable biofilm

formation around orthopedic implants) functions, and enhanced bone cell collagen synthesis, alkaline phosphatase activity and calcium mineral deposition [53, 56].

Animal studies have also demonstrated that nanostructured compared with micron-structured ceramics (like the aforementioned nano-HA) accelerated new bone growth. Histology stains from one particular rat calvarial study showed complete osseointegration (after just 4 weeks) of tantalum scaffolds coated with nano-HA compared with uncoated or conventional HA-coated tantalum as shown in Fig. 9.8. Other animal studies revealed that a nano-HA paste appeared to be a suitable bone substitute for bone defects since it showed good tissue incorporation and rapid osseointegration [57]. In yet another study, a bio-resorbable nano-HA was used for acetabular bone grafting. Results showed that nano-HA promoted acetabular cup stability more than pure allografts and at the same time did not cause any adverse biological reactivity [58]. In the industrial world, the promising future of nano-HA in orthopedic applications has sparked lots of attention. For example, FortrOss®, released by Pioneer Surgical Technology, Inc. (www.pioneersurgical.com), is one of the first nano-HA based products currently under clinical trials for bone graft applications.

Although nanostructured ceramics have been widely studied and are on the path for successful commercialization, they still have limited use in large bone defect applications because of their intrinsic brittleness, difficulty in forming specific defect shapes, and poor mechanical properties preventing them from sustaining mechanical loading conditions necessary for replacing large bone defects. Even if such ceramics were applied as coatings on traditional metals, there are many intrinsic problems (such as possible coating delimitations, higher coating stiffness than bone, etc.). Thus, an alternative group of materials, nanostructured composites (polymers/ceramics), have been tested for orthopedic applications.

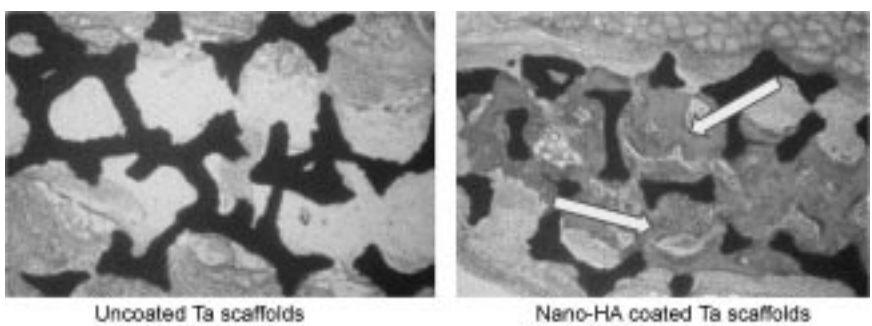

9.8 Histology of rat calvaria after tantalum (Ta) scaffolds coated with either nanostructured or conventional HA were implanted for 2 weeks. (Arrows point out new bone growth. Adapted from Liu and Webster [32].)

Bioactive polymers and nanostructured composites

Natural and synthetic polymers have attracted increasing attention over the past decade for their use as biodegradable scaffold materials [59]. Many have studied such polymers as biodegradable scaffolds because these polymers allow for the precise control of chemical composition, crystallinity, molecular weight, molecular weight distribution, as well as easily controlled microstructure and macrostructure (including porosity) [60–62]. For example, PLGA (poly-lactide-co-glycolide) is one of the most popular US Food and Drug Administration (FDA) approved polymers for orthopedic applications. PLGA was originally developed for use in resorbable surgical sutures and biodegradable drug delivery systems. The first commercial suture, Dexon® (composed of poly-lactide-co-glycolide), was available in 1970 and the first FDA-cleared drug product was the Lupron Depot drug-delivery system (TAP Pharmaceutical Products Inc.; Lake Forest, IL). Since then there has been intensive development of medical devices composed of PGA (polyglycolide), PLA (polylactide), and their copolymers [63]. The use of biodegradable polymers in orthopedic devices for fixation of long bone fractures was first clinically implemented in Finland in 1984 [64, 65]. Since the 1990s, applications of PLA, PGA and PLGAs in tissue engineering have grown considerably [66].

However, owing to the generally weaker mechanical properties of PLGA and its acidic degradation by-products compared with bone, numerous attempts have been made to produce composites of polymers with nanostructured ceramics, optimizing physical, mechanical and biological properties of scaffolds for bone regeneration. For example, Liu *et al.* reported that nanostructured titania/PLGA composites which had the closest surface roughness to natural bone promoted osteoblast adhesion and subsequent calcium containing mineral deposition by osteoblasts the most [67]. For ceramic/metal composites, nanostructured HA has been coated on titanium and then implanted into canine trabecular bone. Results showed a significant advantage for the integration of mineralized bone tissue into HA/titanium composites compared with uncoated titanium [34, 68]. In addition, it was reported that nano-HA/collagen composites synthesized to have a porous microstructure similar to bone promoted the deposition of a new bone matrix more than uncoated collagen. Furthermore, they showed that osteoblasts within this biologically inspired composite eventually acquired a three-dimensional polygonal shape that integrated with juxtaposed bone fragments [69]. A nano-HA/collagen composite product, NanOss® (Pioneer Surgical Technology, Inc. http://www.pioneersurgical.com/), has been released, stated to have superior osteoconduction through a proprietary nanocrystalline HA and collagen formulation designed to mimic bone tissue.

In conclusion, nanostructured biomaterials (including metals/metal alloys, ceramics, polymers and composites thereof) can mimic the natural hierarchical superamolecular organization of bone and, thus, hold great promise for improv-

ing bone implants. Nanotechnology has been shown to be one of the few technologies that can promote the functions of numerous bone implant materials (regardless of chemistry).

9.3 Nanostructured biomaterials for cartilage applications

9.3.1 Cartilage biology, defects and implants

Cartilage is a type of dense connective tissue existing within many joints. It is composed of specialized cells called chondrocytes that produce a large amount of an extracellular matrix composed of collagen fibers (mainly collagen type II), abundant ground substances rich in proteoglycans, and elastin fibers. Chondrogenesis is a natural process in the formation and growth of articular cartilage tissue [70, 71]. The chondrocyte occupies less than 10% of native tissue but is responsible for the creation and maintenance of the extracellular matrix [70, 72, 73]. Chondrocytes have a spherical shape when in the native extracellular matrix [73]. Destruction or removal of the extracellular matrix will result in the loss of differentiated chondrocyte function [74].

Articular cartilage defects are widespread because of intensive sports activities, genetic disorders (like rheumatoid arthritis) and osteoarthritis. Due to cartilage loss, patients usually have significant pain and are limited in joint motion. Today, more than 20 million Americans suffer from arthritis and it is estimated that the worldwide arthritis market will reach nearly $21 billion by 2010 [75]. It is the leading cause of disability in people over the age of 55 in the US [76].

Except for artificial joint replacements (usually including metals as mentioned in the previous section) with their associated short lifespans, there is no appropriate long-lasting treatment for cartilage damage. Currently, many researchers have focused on promoting cartilage tissue growth to repair joints instead of metallic replacement surgeries [77, 78]. To treat cartilage defects, a key step is to repair the damaged extracellular matrix of cartilage.

To successfully repair or replace the cartilage extracellular matrix, it is very important to first understand the structure of cartilage. As shown in Fig. 9.9, just like bone, cartilage also has a self-organized hierarchical structure from macro/micro- to nano-size. Nanotechnology today can help produce nanostructured scaffolds which better mimic the organization of the natural cartilage structure. Tissue-engineered nanostructured scaffolds for cartilage applications need to meet several criteria in order to adequately regenerate cartilage including cell seeding, cell growth and *in vivo* use. The scaffold should be readily processed into 3D structures uniquely designed for their particular use. The scaffold surface and porosity must permit cell adhesion, infiltration, proliferation and differentiation for the synthesis of cartilage tissue. Neither the polymer nor its

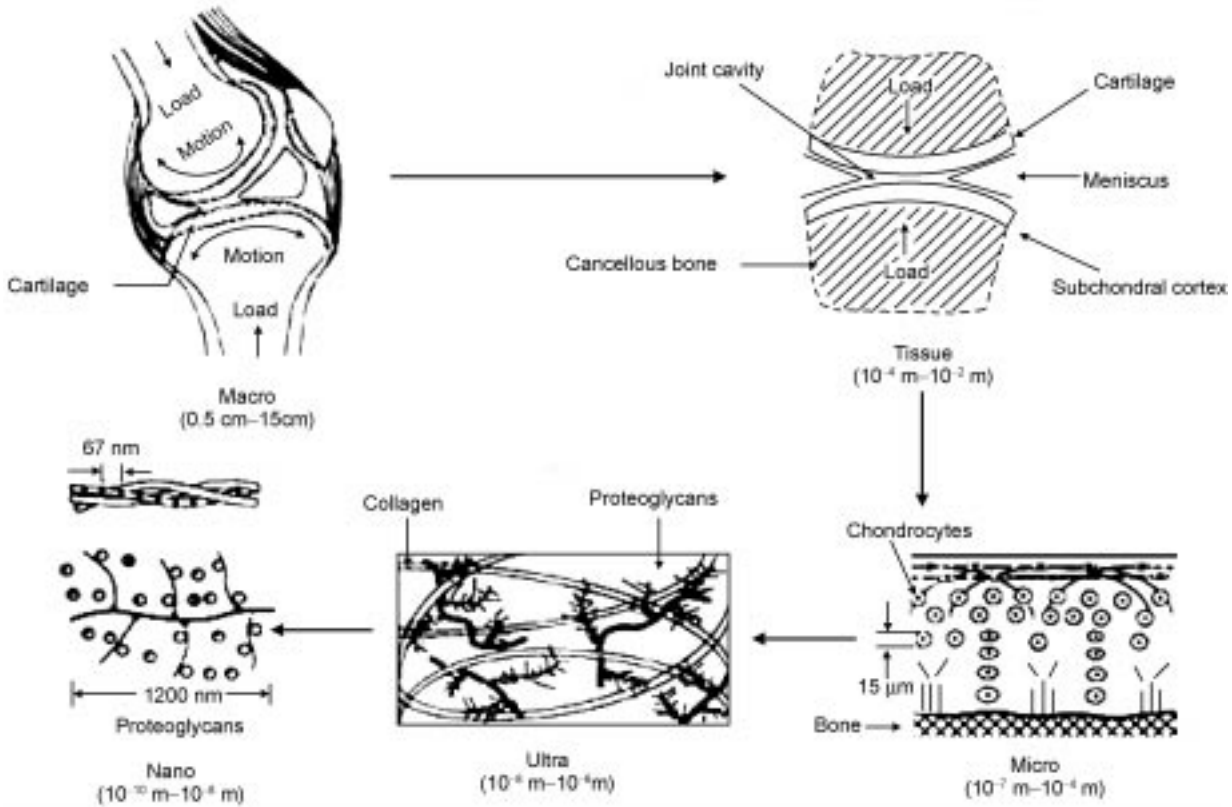

9.9 Schematic structure of articular cartilage. (Adapted from Mow *et al.* [79].)

degradation products should produce chronic inflammatory responses when implanted. The degradation rate of the scaffold should correspond to the rate of new extracellular matrix production [80]. In the following section of this chapter, based on these criteria, nanostructured biomaterial scaffolds and associated nanotechniques have been explored to fabricate the next generation of improved cartilage materials.

9.3.2 Nanostructured biomaterial scaffolds

Synthetic and naturally derived hydrogels

The cartilage extracellular matrix has higher water content, no ceramic component and consequently lower stiffness compared with bone. Therefore, instead of using metals or ceramics, polymers are currently being considered with high water content, i.e. hydrogels, and are one of the most popular materials for regenerating the cartilage extracellular matrix. Hydrogels are a network of polymer chains, sometimes found as a colloidal gel in which water is the dispersion medium. Due to their high water content, hydrogels possess a degree of flexibility very similar to natural tissue. In addition to hydrogels, PCL (polycaprolactone) and PLGA have been widely investigated as cartilage forming materials. PLGA degrades via hydrolysis in which ester bonds are broken in the long polymer chains, gradually degrading in the physiological environment, and eventually cleared by human body (Fig. 9.10) [81, 82]. Polymers that degrade via hydrolysis have a close relationship with molecular weight and degree of polymerization (DP). Generally speaking, lower molecular weight, higher surface area and greater surface energy allow nanostructured hydrogels to have higher hydrolysis rates than conventional hydrogels [82]. Another group of hydrogels tested for cartilage applications belongs to the polysaccharide family, just like glycosaminoglycans (one of the major components in cartilage), alginate, hyaluronic acid and agarose. They do not have ester bonds which undergo hydrolysis and usually require a longer time to degrade.

Just like in orthopedic applications, cartilage applications can benefit from the low-inflammatory response of nanomaterials (especially if blood is exposed in the degraded underlying bone) [14, 83] and the excellent select protein adsorption capability important for mediating chondrocyte adhesion and functions [12]. Moreover, nanofiber hydrogels have been receiving more and

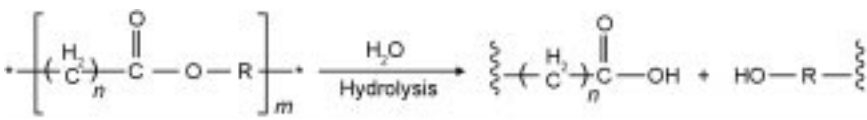

9.10 Mechanisms of the hydrolysis of ester bonds during the degradation of polymers.

more attention for cartilage implant applications since their architecture can be matched to the distinct collagen orientation in cartilage. The alignment and chondrogenic differentiation of bone marrow-derived human mesenchymal stem cells were reported when such cells were cultured on oriented PCL scaffolds [84–86]. For polysaccharide hydrogels, nanotechnology has also been used to produce nanometer surface features to improve the interaction of such materials with natural tissue. Alginate has also been fabricated into nanostructured scaffolds [83]. As in bone tissue engineering, nano-HA and collagen have also served as improved nanostructured hydrogel composites for cartilage applications [87].

Natural collagen

Of course, natural materials have often been investigated for cartilage replacements (such as collagen type II). Collagen (mostly type II) constitutes 50–80% of the dry weight of articular cartilage. There are 29 types of collagen in humans, and most of collagen exists in connective tissue. Collagen (type II) is a fibrous, insoluble, macromolecular protein secreted by chondrocytes, maintains the mechanical integrity of connective tissue, and also provides adhesive qualities towards chondrocytes and other macromolecules (such as proteogylcans) [88–90]. It has high tensile strength, resistance to proteolysis, and weak antigenicity due to the molecular arrangement of its fibrils. Previous studies have demonstrated the ability to fabricate collagen type II into nanostructured fibers with good mechanical properties (with a tangent modulus of 172.5 ± 36.1 MPa and an ultimate tensile strength of 3.3 ± 0.3 MPa compared with a tangent modulus of natural articular cartilage of 5–30 MPa and an ultimate tensile strength of 9–18 MPa) and suitable for chondrocyte seeding and growth [91].

In the clinical and industrial world, collagen is one of the most successful materials used today in regenerative medicine, especially in nanostructured composites. Recently, a case study reported that a 46-year-old athletic patient with a large degenerative chondral lesions of the medial femoral condyle, trochlea and patella, was successfully treated by using a closing-wedge high tibial osteotomy and implanting of a biomimetic nanostructured osteochondral bioactive scaffold (commercialized by Fin-Ceramica SpA in Faenza, Italy). The biomimetic nanostructured scaffold was composed of several layers of nano-HA and collagen type I at different ratios (100% collagen at the top, 60% collagen with 40% HA in the middle and 30% collagen with 70% HA at the bottom) to mimic the transition zone between articular cartilage and subchondral bone (Fig. 9.11). After one year, the patient was pain-free, had full range of knee motion, and had returned to his pre-operation level of athletic activity. Magnetic resonance imaging (MRI) evaluation after 6 months showed a good restoration of the articular surface, with minimal subchondral bone oedema (abnormal

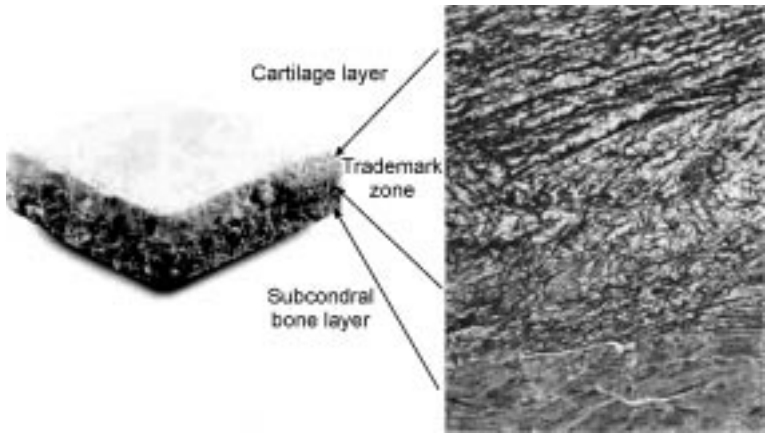

9.11 Macroscopic and histological view of a three-layer nanostructured osteochondral scaffold (Fin-Ceramica SpA, Faenza, Italy).

accumulation of fluid beneath the skin). Subchondral oedema was almost non-visible after 12 months [92]. Genzyme (Cambridge, MA) has also commercialized a collagen type I and autologous chondrocyte composite (MACI®) for cartilage repair, which has successfully treated more than 20 000 patients globally. The Carticel® procedure for MACI® was the first cell therapy ever approved by the FDA.

Bio-inspired self-assembled nanomaterials

Based on nanotechnology, another promising biomaterial for the orthopedic implantation community has emerged recently from bio-inspired self-assembled nanomaterials. For example, rosette nanotubes (RNTs, Fig. 9.12) are novel biomimetic self-assembled supramolecular structures, whose basic building

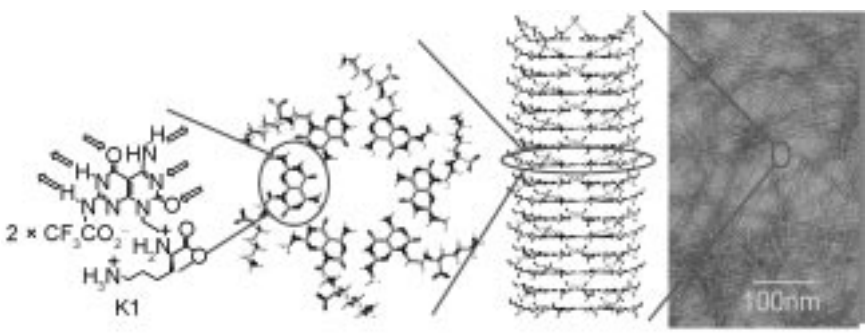

9.12 Rosette nanotubes undergo spontaneous self-assembly under physiological conditions. (Adapted and redrawn from Fenniri *et al.* [93] and Chun *et al.* [94, 95].)

blocks are guanine (G) and cytosine (C) DNA base-pairs [93]. Their units undergo a hierarchical assembly to form a six-membered supermacrocycle by the formation of 18 hydrogen bonds in physiological conditions, then the rosettes form a stable stack with an inner channel 11 Å in diameter based on electrostatic forces, base stacking interactions and hydrophobic effects. It was reported that such nanotubes have a similar size and morphology with collagen, enhance select protein adsorption and consequently a variety of cell functions, and can be functionalized with peptides or drugs tailored for specific applications [94–98]. With the self-assembly of such nanomaterials, they can also increase in viscosity from a solution at room temperature to a gel at body temperature to possess a strong affinity to bond to other components such as nano-HA and hydrogels [98, 99].

A second class of self-assembled orthopedic nanostructured biomaterials has also been inspired from proteins and peptides. These nanostructured biomaterials are genetically selected/designed peptides with specific binding to functional solids, tailoring their binding and self-assembly characteristics, developing bifunctional peptide/protein genetic constructs with both material binding and biological activity, and using these as molecular synthesizers, erectors and assemblers [100]. For example, the PuraMatrix^{TM} hydrogel peptide is a new synthetic 16-amino-acid peptide developed by 3DM (Cambridge, MA). When it is exposed to physiological salt conditions, the peptide forms a hydrogel because of ionic bonds and hydrophobic interactions. It was stated that the nanofiber structure resembled natural collagen with fiber diameters of 5–10 nm and promoted cell (such as osteoblasts and fibroblasts) proliferation greater than any other synthetic scaffold, such as PGA.

9.3.3 Nanotechniques for biomaterial fabrication

As mentioned, in articular cartilage, tissues are organized into three-dimensional functional structures. As shown in Fig. 9.13, cartilage at this level can be divided into four zones: (a) the superficial tangential zone, which comprises 10–20% of cartilage thickness with collagen (mostly type II) fibers oriented parallel to the joint surface to resist shear stress; (b) the middle zone, which comprises 60% of the cartilage thickness, (c) the deep zone, which comprises 30% of the cartilage thickness with collagen (mostly type II) fibers vertically oriented to enhance compression stress, and (d) the calcified cartilage zone where cartilage interfaces with the bone. To engineer such functional extracellular matrices successfully, the scaffolds have to be designed with micron and nanostructures, aligned fiber orientation, controlling material composition, facilitating cell distribution and guiding tissue regeneration in three dimensions.

Because electrospinning can fabricate a variety of organic and inorganic materials, generating different sizes of fibers and controlling fiber orientation in scaffolds, many have studied electrospinning as a very promising technique for

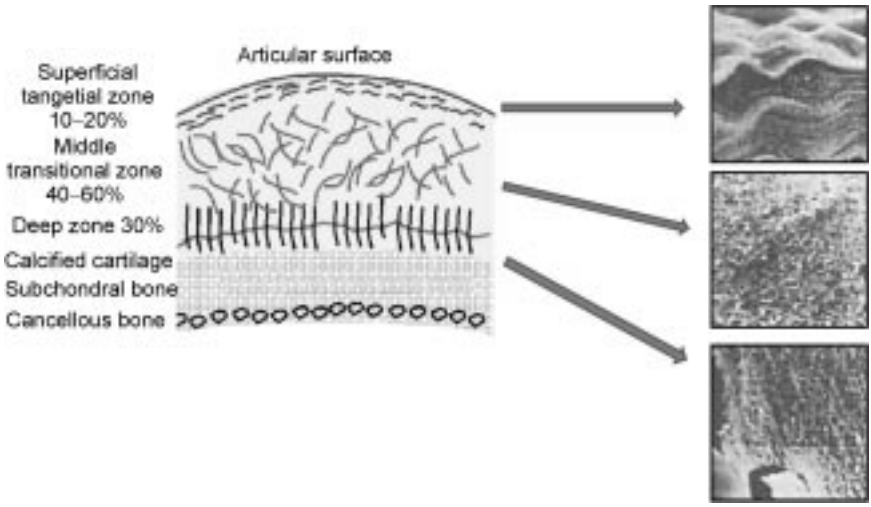

9.13 Schematic of the different functional zones in articular cartilage. (Adapted and redrawn from Mow *et al.* [79] and Cooper *et al.* [82].)

cartilage tissue engineering [101, 102]. For a typical electrospinning set-up (Fig. 9.14), a solution is first fed through a spinneret. A high voltage is then applied to the solution such that at a critical voltage, typically more than 5 kV, the repulsive force within the charged solution is larger than its surface tension and a jet erupts from the tip of the spinneret. Although the jet is stable near the tip of the spinneret, it soon enters a bending instability stage with further stretching of the

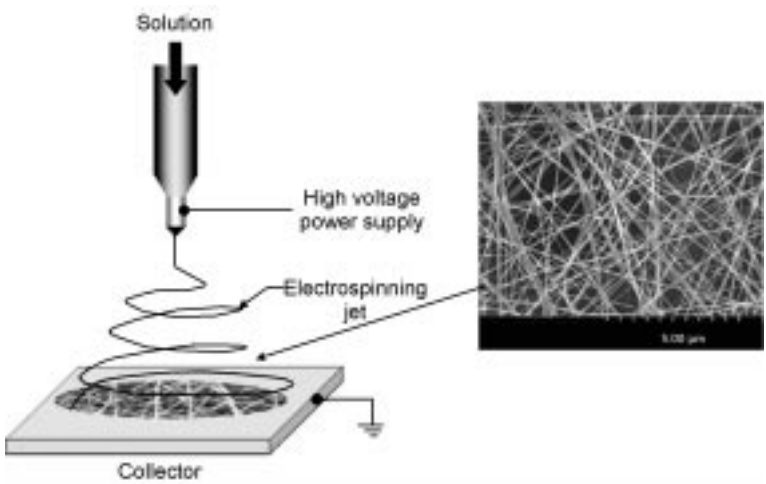

9.14 A typical electrospinning set-up using a grounded static collector and an SEM scan of electrospun collagen type I. (Adapted and redrawn from Teo and Ramakrishna [103] and Shi *et al.* [104].)

solution jet under the electrostatic forces in the solution as the solvent evaporates. In the basic electrospinning set-up, there is no special orientation of the fibers dropping down to the collector. However, by incorporating a rotating device, like rotating drum, rod or plate, electrospinning has been shown to be able to form aligned fiber meshes. In particular, electrospinning is able to fabricate various nanofiber assemblies *in situ*. This gives electrospinning an important edge over other larger-scale nanofiber production methods [103, 105, 106].

To fabricate 3D nanostructured porous polymer scaffolds, solvent-casting/particulate-leaching techniques have also been widely used for nano-engineering tissue [107]. Briefly, this technique involves producing a suspension of polymer composites in a solvent. Salt particles are ground and sieved into small particles and those of the desired size (mostly 100–200 μm range paticles) are transferred into a mold. A polymer suspension is then cast into the salt-filled mold. The solvent is then removed by evaporation in air and/or in vacuum. After evaporation of the solvent, the salt crystals are leached by immersion in water to form a porous structure. Using this technique, the pore size can be controlled by the size of the porogen particles and the porosity can be controlled by the salt/polymer composite ratio. However, this method usually involves organic solvents, which leads to many concerns about the toxicity of the solvent and associated cleaning procedures.

Chemical etching can also be used to fabricate nanostructured polymer scaffolds. For example, sodium hydroxide has been used to etch PLGA three dimensional scaffolds to have nanoscale features within 10 minutes. *In vitro* studies have demonstrated that such NaOH-treated PLGA three-dimensional scaffolds enhanced chondrocyte functions by being more hydrophilic with a greater degree of nano-roughness than non-treated scaffolds [108].

One of the common shortcomings of the fabrication technologies just discussed is the lack of precise control of the three-dimensional porous architecture of the scaffolds. 3D printing has successfully overcome such gaps. This process generates components by ink-jet printing a binder on sequential powder layers. Operation parameters such as the speed, flow rate and drop position can be computer controlled to produce complex 3D polymer scaffolds. The disadvantages of 3D printing techniques are limited material selection and inadequate resolution. The materials must be injectable and the resolution is determined by the size of binder drops, the jet and powder particles, which makes it difficult to design and fabricate scaffolds with fine biological inspired nanostructures.

Besides the techniques mentioned above, many other useful methods are available to fabricate nanostructured scaffolds, such as gas foaming/particulate-leaching, phase separation and emulsion freeze drying, fiber meshes/bonding, etc. In short, nanotechniques have greatly enhanced material fabrication methods, improved the hierarchical structure of tissue scaffolds to mimic those of natural tissue components (from micron to nano level) and provided the possibility to make bio-mimic nanostructured scaffolds to improve cartilage growth.

9.4 Nanostructured biomaterials for nervous system applications

9.4.1 Nervous system facts

Nervous system function has also been restored using nanotechnology. The human nervous system has two components which are the central nervous system and the peripheral nervous system. The central nervous system consists of the brain and spinal cord and the peripheral nervous system consists of nerves outside the brain and spinal cord. It includes both neurons and nerve fibers. The majority of these neurons are located near the spinal cord at ganglia. Nerve fibers extend to sensory structures, glands, blood vessels and muscles. Two major classes of cells, neurons and glia, exist in the nervous system. Glia in the brain is divided into three classes, oligodendrocytes, astrocytes and microglia. They provide structural support for neurons, as well as regulate neuronal activities [109]. The neurons of the nervous systems are interconnected into complex arrangements and use electrochemical signals and neurotransmitters to transmit impulses from one neuron to the next. The nervous system is probably the most complex and mystic system in human beings. In the following section, several common nervous system implants and medical approaches are introduced and how nanotechnology is improving such biomaterials illustrated.

9.4.2 Neutral applications of nanotechnology

For the treatment of brain diseases, current drug delivery systems are far less than satisfactory. The blood–brain barrier (BBB) has at least three resistances, tight junctions, choroid plexus and cerebral capillaries, which can block most drugs except small hydrophobic drugs. One classic example is that dopamine (which was originally chosen to treat Parkinson's disease) cannot pass through the BBB. Lately, nanotechnology has significantly helped drug delivery for brain diseases. For example, iron oxide magnetic nanoparticles consisting of an iron oxide core from several to a few hundred nanometer diameters are coated either with organic (like poly(ethylene glycol)) or inorganic (like silicon) materials to improve biocompatibility and drug delivery [110]. Moreover, one benefit of magnetic nanoparticles is that they can be directed by a magnetic force as well as via surface receptors to control drug delivery. In addition, they are able to pass through artificial and real BBB membranes by endocytosis, due to the small size of nanoparticles [20, 21]. In another study, such magnetic nanoparticles were found not to trigger any inflammatory responses in both *in vitro* and *in vivo* models [111]. In the market today, there are numerous commercialized iron oxide magnetic nanoparticle products, such as SoluLink, TurbeBeads, Bioclone, etc. There are functionalized iron oxide magnetic nanoparticles for either drug delivery or other biomedical applications. Another important application of magnetic nanoparticles is to enhance MRI. For iron

magnetic nanoparticles, when their size is below 30–50 nm, they have superparamagnetism properties (a phenomena when the clusters of magnetic particles are so small that they can randomly flip direction under thermal fluctuations; thus, the material as a whole is not magnetized except in an externally applied magnetic field), which can enhance their sensitivity. Therefore, magnetic nanoparticles are excellent MRI enhancers to identify tumors with higher sensitivity than conventional imaging techniques [22].

Generally speaking, adult nerves are very difficult to self-repair and regenerate, so stem cell therapy has been highly illuminated recently to treat nervous system diseases or damage. For cell therapy, one of the critical concerns is how to promote stem cell differentiation to the desired cell type at the appropriate region for treatment. Nano-based 3D matrices made by various nanotechniques can mimic the natural nervous system extracellular matrices to induce cell differentiation for therapeutic applications (Fig. 9.15). Carbon nanotubes/carbon nanofibers have been found to improve neuron differentiation from human embryonic stem cells to more quickly return motor function

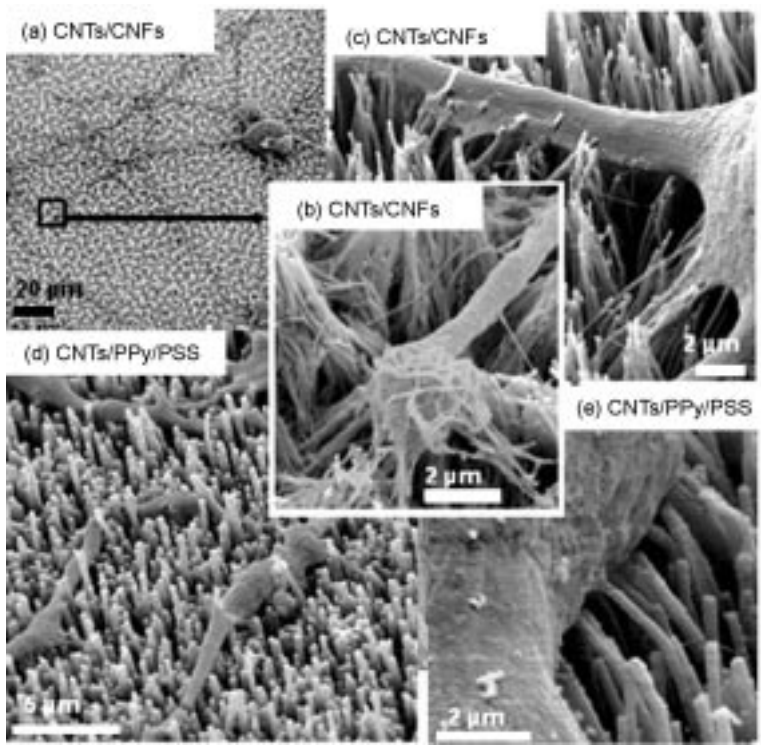

9.15 Neuronal cells grown on polypyrrole (PPy)/polystyrenesulfonate (PSS) coated carbon nanofiber (CNF)/carbon nanotube (CNT) arrays. (Adapted from Andrews [112].)

[113, 114], in a rat stroke model in which carbon nanotubes were implanted [115]. One hypothesis why carbon nanotubes induced neuronal cell differentiation is the conductivity of carbon nanotubes and their ability to adsorb laminin [113]. An *in vitro* brain circuit model has confirmed the relationship between electrical signal transfer and synaptic stimulation of carbon nanotubes and neurons [116]. According to the highly conductive and unique surface energy properties of carbon nanotubes, a novel application of carbon nanotubes is to improve electronic nerve interfaces.

An electronic nerve interface device is an 'artificial nerve' usually employing electrodes to connect with and stimulate host nerves to treat neurological disorders (like chronic spinal cord injury) or improve life quality (like enhancing visual ability or memory). Because electronic tissue interface devices send and receive electrical signals from the nervous tissues via an array of electrodes usually composed of platinum, silicon or silicon rubber, electrode arrays are important to device functions. The lifetime of these devices depend on the stability of the electrode array and the effect and signal quality of such devices depends on the efficiency of single transfer between electrode arrays and host nerves. Electrodes often fail to perform over time due to the accumulation and growth of astrocytes (glial scar tissue forming cells) and neuronal cell death around the electrodes or electrochemical reactions at the interface causing toxicity [117]. A reliable electrode recording requires not only the stability of the electrode itself (reduction of electrochemical degradation and dielectric layer growth) but also favorable cell responses (such as the stimulation of neurons and inhibition of glia) [118]. Again, nanotechnology can help to improve such 'artificial nerve' implant cytocompatibility and electrical functions. Because of their chemical stability, low resistance and high charge capacitance, carbon nanotubes are promising materials for electrodes or as electrode coatings [119, 120]. A study has shown that carbon nanotubes possess excellent cytocompatibility properties and inhibit functions of astrocytes, which could increase the lifetime of electrodes [121]. Nanotechnology also has numerous advantages to allow engineers to design a miniature electrode array with thousands of tiny electrodes to obtain better signal quality and transfer. BrainGate Technology has tried to produce 'tiny' electrode arrays (Fig. 9.16). It produced an electrode array down to micrometer level which was placed on the primary motor surface cortex and penetrated into the intermediate layers for a computer–brain interface to control prosthetic limbs. A more recent report has made the electrode even smaller (nanometer level) to control cell to cell interfaces, as shown in Fig. 9.17. Although the activity recorded so far is only from single cells and only after chemical stimulation (neither spontaneous activity nor signal propagation), it is promising to explore the link between a single cell (even cellular features) and an electrode for highly sensitive interfacing applications [122].

In summary, nanotechnology is able to improve drug delivery through the blood–brain barrier, induce neuron differentiation and function and increase the

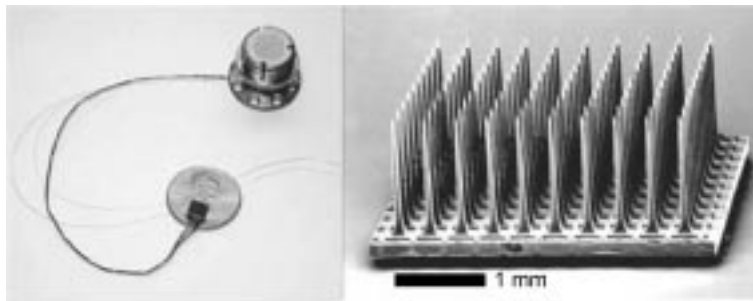

9.16 A brain sensor and an SEM image of electrodes on the sensor. (Adapted from Kennedy and Bakay [123].)

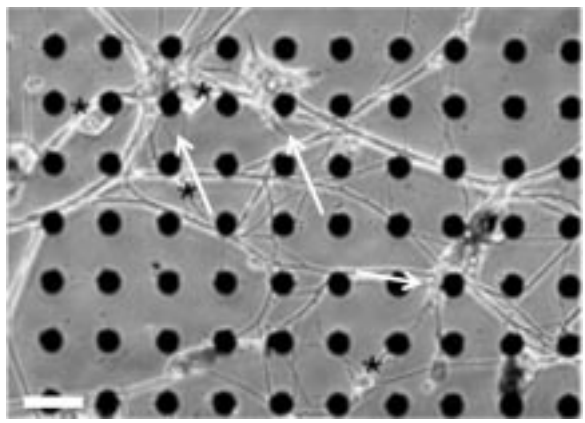

9.17 A network of single cells over carbon nanotube electrodes with single neuronal cells over carbon nanotube electrodes marked with white arrows. Scale bar 80 μm. (Adapted from Greenbaum *et al.* [122].)

lifetime and quality of electronic nerve interface devices. It has a great potential to build 'artificial nerves' or stimulate natural tissue regeneration.

9.5 Nanostructured biomaterial applications for other tissues and organs

Besides the tissues mentioned above, nanostructured biomaterials may also provide for better treatments for many other tissues or organs. For instance, it was reported that superparamagnetic iron nanoparticles under an external magnetic force embedded into the middle ear epithelia of tympanic membranes or ossicles of pigs produced ossicular vibrations in the pig's ear similar to the perception of sound in humans [124]. Thus, magnetic nanoparticles could possibly be implanted to enhance hearing for artificial ear applications. As another example, in the vascular system, 20% of vascular stents suffer from restenosis (a narrowing

of a blood vessel), which contribute to inflammation and neointimal formation [125]. In contrast, nanosurface-modified stents improve endothelial and smooth muscle cell interaction and consequently lower inflammation compared with conventional stents [126, 127]. In short, because of their excellent bio-integration, small particle size, high surface area and energy, and other unique chemical/physical properties, nanomaterials may serve as improved substitutes for artificial tissue/organ implant applications.

9.6 Conclusions and future trends

Because natural tissues/organs have hierarchical structures from the macro- or micro- to nano-level, the introduction of nanostructured biomaterials to the tissue engineering field has greatly enhanced the integration and growth of natural tissue. Combined with the unique chemical and physical properties of nanomaterials, nanotechnology continues to open tremendous opportunities for biomedical applications. However, there are still numerous unresolved problems in this research area, such as nanotube/particle toxicity and long-term influences to the environment and human health. Moreover, extensive research is needed in the continued design, synthesis and evaluation of highly complex or multi-structured nanostructured devices. All in all, nanostructured biomaterials are promising candidates as the next generation of artificial implants for numerous tissue engineering applications.

9.7 References

1. Lysaght MJ, Jaklenec A, Deweerd E. Great expectations: private sector activity in tissue engineering, regenerative medicine, and stem cell therapeutics. *Tissue Eng. Part A* **14**, 305–315, 2008.
2. US Department of Health and Human Services. 2020: A New Vision – A Future for Regenerative Medicine, 2006, available at http://www.hhs.gov/reference/newfuture.shtml.
3. Luz GM, Mano JF. Biomimetic design of materials and biomaterials inspired by the structure of nacre. *Philos Transact A Math Phys Eng Sci* **367**(1893), 1587–1605, 2009.
4. Scott NR. State of the art. *Rev Sci Tech Off Int Epiz* **24**, 425–434, 2005.
5. Denver CO. Nano market to hit 2 trillion dollars by 2015. *Nano Tech* 2008, available at http://www.spacemart.com.
6. Murray CB, Kagan CR, Bawendi MG. Advances in technology. *Science* **287**, 1989–1994, 2000.
7. Zhang J, Li S, Li X. Polymeric nano-assemblies as emerging delivery carriers for therapeutic applications: a review of recent patents. *Recent Pat Nanotechnol* **3**(3), 225–231, 2009.
8. Pickup JC, Zhi ZL, Khan F, Saxl T, Birch DJ. Nanomedicine and its potential in diabetes research and practice. *Diabetes Metab Res Rev* **24**(8), 604–610, 2008.
9. Lu D, Wen X, Liang J, Gu Z, Zhang X, Fan Y. A pH-sensitive nano drug delivery

system derived from pullulan/doxorubicin conjugate. *J Biomed Mater Res B Appl Biomater* **89**(1), 177–183, 2009.
10. Agyare EK, Curran GL, Ramakrishnan M, Yu CC, Poduslo JF, Kandimalla KK. Development of a smart nano-vehicle to target cerebrovascular amyloid deposits and brain parenchymal plaques observed in Alzheimer's disease and cerebral amyloid angiopathy. *Pharm Res* **25**(11), 2674–2684, 2008.
11. Klabunde KJ, Stark J, Koper O. Nanocrystals as stoichiometric reagents with unique surface chemistry. *J Phys Chem* **100**, 121–125, 1996.
12. Thomas CH, McFarland CD, Jenkins MJ, Rezania A, Steele JG, Healy KE. The role of vitronectin in the attachment and spatial distribution of bone-derived cells on materials with patterned surface chemistry. *J Biomed Mater Res* **37**, 81–93, 1997.
13. Webster TJ, Ergun C, Doremus RH, Siegel RW, Bizios R. Enhanced osteoblast functions on nanophase ceramics. *J Biomed Mater Res* **51**, 475–479, 2000.
14. Kim JY, Khang D, Lee JE, Webster TJ. Decreased macrophage density on carbon nanotube patterns on polycarbonate urethane. *J Biomed Mater Res A* **88**(2), 419–426, 2009.
15. Hyde GK, McCullen SD, Jeon S, Stewart SM, Jeon H, Loboa EG, Parsons GN. Atomic layer deposition and biocompatibility of titanium nitride nano-coatings on cellulose fiber substrates. *Biomed Mater* **4**(2), 25001, 2009.
16. Balasundaram G, Sato M, Webster TJ. Using hydroxyapatite nanoparticles and decreased crystallinity to promote osteoblast adhesion similar to functionalizing with RGD. *Biomaterials* **27**(14), 2798–2805, 2006.
17. Heo SJ, Kim SE, Wei J, Kim DH, Hyun YT, Yun HS, Kim HK, Yoon TR, Kim SH, Park SA, Shin JW, Shin JW. *In vitro* and animal study of novel nano-hydroxyapatite/poly(epsilon-caprolactone) composite scaffolds fabricated by layer manufacturing process. *Tissue Eng Part A* **15**(5), 977–989, 2009.
18. Xu FM, Xu JP, Ji J, Shen JC. A novel biomimetic polymer as amphiphilic surfactant for soluble and biocompatible carbon nanotubes (CNTs). *Colloids Surf B Biointerfaces* **67**(1), 67–72, 2008.
19. Huang J, Best SM, Bonfield W, Brooks RA, Rushton N, Jayasinghe SN, Edirisinghe MJ. *In vitro* assessment of the biological response to nano-sized hydroxyapatite. *J Mater Sci Mater Med* **15**(4), 441–445, 2004.
20. Mondalek FG, Zhang YY, Kropp B, Kopke RD, Ge X, Jackson RL, Dormer KJ. The permeability of SPION over an artificial three-layer membrane is enhanced by external magnetic field. *J Nanobiotechnology* **4**, 4, 2006.
21. Peira E, Marzola P, Podio V, Aime S, Sbarbati A, Gasco MR. *In vitro* and *in vivo* study of solid lipid nanoparticles loaded with superparamagnetic iron oxide. *J Drug Target* **11**(1), 19–24, 2003.
22. Neuwelt EA, Varallyay P, Bago AG, Muldoon LL, Nesbit G, Nixon R. Imaging of iron oxide nanoparticles by MR and light microscopy in patients with malignant brain tumours. *Neuropathol Appl Neurobiol* **30**(5), 456–471, 2004.
23. Charnley J. Anchorage of the fermoral head prosthesis to the shaft of the femur. *J Bone Joint Surg* **42B**, 28–30, 1960.
24. Charnley J. Surgery of the hip-joint: present and future developments. *Br Med J* **5176**, 821–826, 1960.
25. National Center for Health Statistics (NCHS), available at: http://www.cdc.gov/nchs/.
26. Frankowski JJ, Watkins-Castillo S. Primary total knee and hip arthroplasty projections for the US population to the year 2030. Rosemont, IL: American Academy of Orthopedic Surgeons, pp. 1–18, 2002.

27. Bozic KJ, Kurtz SM, Lau E, *et al.* The epidemiology of revision total hip arthroplasty in the United States. *J Bone Joint Surg (Am)* **91**, 128–133, 2009.
28. Emery DFG, Clarke HJ, Grover ML. Stanmore total hip replacement in younger patients: review of a group of patients under 50 years of age as operation. *J Bone Joint Surg* **79**, 240–246, 1997.
29. Balasundaram G, Webster TJ. Nanotechnology and biomaterials for orthopedic medical applications. *Nanomed* **1**(2), 169–176, 2006.
30. Balasundaram G, Webster TJ. An overview of nano-polymers for orthopedic applications. *Macromol Biosci* **7**(5), 635–642, 2007.
31. Smallman RE, Bishop RJ. *Modern Physical Metallurgy and Materials Engineering – Science, Process, Applications* (6th Edition). Elsevier, 1998.
32. Liu H, Webster TJ. Nanomedicine for implants: a review of studies and necessary experimental tools. *Biomaterials* **28**(2), 354–369, 2006.
33. Kaplan FS, Hayes WC, Keaveny TM, Boskey A, Einhorn TA, Iannotti J. Form and function of bone. *Orthopedic Basic Science*. Simon SR (ed.). Rosemont, IL: American Academy of Orthopedic Surgeons, pp. 127–185, 1994.
34. Wu S, Liu X, Hu T, Chu PK, Ho JP, Chan YL, Yeung KW, Chu CL, Hung TF, Huo KF, Chung CY, Lu WW, Cheung KM, Luk KD. A biomimetic hierarchical scaffold: natural growth of nanotitanates on three-dimensional microporous Ti-based metals. *Nano Lett* **8**(11), 3803–3808, 2008.
35. Puckett S, Pareta R, Webster TJ. Nano rough micron patterned titanium for directing osteoblast morphology and adhesion. *Int J Nanomedicine* **3**(2), 229–241, 2008.
36. Chiang CY, Chiou SH, Yang WE, Hsu ML, Yung MC, Tsai ML, Chen LK, Huang HH. Formation of TiO_2 nano-network on titanium surface increases the human cell growth. *Dent Mater* **25**(8), 1022–1029, 2009.
37. Ogawa T, Saruwatari L, Takeuchi K, Aita H, Ohno N. Ti nano-nodular structuring for bone integration and regeneration. *J Dent Res* **87**(8), 751–756, 2008.
38. Brunette DM, Tengvall P, Textor M, Thomsen P. Mechanical, thermal, chemical and electrochemical surface treatment of titanium implants: studies on the early tissue response to machined and electropolished implants with different oxide thicknesses. *Biomaterials* **17**, 605, 1996.
39. Ruan C, Paulose M, Varghese OK, Mor GK, Grimes CA. Fabrication of highly ordered TiO_2 nanotube arrays using an organic electrolyte. *J Phys Chem B* **109**(33), 15754–15759, 2005.
40. Allam NK, Grimes CA. Room temperature one-step polyol synthesis of anatase TiO_2 nanotube arrays: photoelectrochemical properties. *Langmuir* **25**(13), 7234–7040, 2009.
41. Alivov Y, Pandikunta M, Nikishin S, Fan ZY. The anodization voltage influence on the properties of TiO_2 nanotubes grown by electrochemical oxidation. *Nanotechnology* **20**(22), 225602, 2009.
42. Berger S, Ghicov A, Nah YC, Schmuki P. Transparent TiO_2 nanotube electrodes via thin layer anodization: fabrication and use in electrochromic devices. *Langmuir* **25**(9), 4841–4844, 2009.
43. Yao C, Slamovich EB, Webster TJ. Enhanced osteoblast functions on anodized titanium with nanotube-like structures. *J Biomed Mater Res A* **85**(1), 157–166, 2008.
44. Burns K, Yao C, Webster TJ. Increased chondrocyte adhesion on nanotubular anodized titanium. *J Biomed Mater Res A* **88**(3), 561–568, 2009.
45. Sul YT, Johansson CB, Röser K, Albrektsson T. Qualitative and quantitative

observations of bone tissue reactions to anodised implants. *Biomaterials* **23**(8), 1809–1817, 2002.
46. Sul YT, Johansson CB, Jeong Y, Wennerberg A, Albrektsson T. Resonance frequency and removal torque analysis of implants with turned and anodized surface oxides. *Clin Oral Implants Res* **13**(3), 252–259, 2002.
47. Puckett S, Lee PP, Ciombor D, Aaron R, Webster T. Nanotextured titanium surfaces for enhancing external fixation device skin growth. Orthopaedic Research Society annual meeting. Poster number 795, 2009.
48. Ishizawa H, Fujino M, Ogino M. Mechanical and histological investigation of hydrothermally treated and untreated anodic titanium oxide films containing Ca and P. *J Biomed Mater Res* **29**(11), 1459–1468, 1995.
49. Giavaresi G, Fini M, Cigada A, Chiesa R, Rondelli G, Rimondini L, Aldini NN, Martini L, Giardino R. Histomorphometric and microhardness assessments of sheep cortical bone surrounding titanium implants with different surface treatments. *J Biomed Mater Res A* **67**(1), 112–120, 2003.
50. Giavaresi G, Fini M, Cigada A, Chiesa R, Rondelli G, Rimondini L, Torricelli P, Aldini NN, Giardino R. Mechanical and histomorphometric evaluations of titanium implants with different surface treatments inserted in sheep cortical bone. *Biomaterials* **24**(9), 1583–1594, 2003.
51. Gong D, Grimes CA, Varghese OK, Hu W, Singh RS, Chen Z, Dickey EC. Titanium oxide nanotube arrays prepared by anodic oxidation. *J Mater Res* **16**, 3331, 2001.
52. Chang CK, Wu JS, Mao DL, Ding CX. Mechanical and histological evaluations of hydroxyapatite-coated and noncoated Ti-6Al-4V implants in tibia bone. *J Biomed Mater Res* **56**, 17–23, 2001.
53. Lemons JE. Bioceramics: is there a difference? *Clin Orthoped Rel Res* **261**, 153–158, 1990.
54. Webster TJ, Ergun C, Doremus RH, Siegel RW, Bizios R. Specific proteins mediate enhanced osteoblast adhesion on naophase ceramics. *J Biomed Mater Res* **78**, 595–604, 2006.
55. Luck M, Paulke BR, Schroder W, Blunk T, Muller RH. Analysis of plasma protein adsorption on polymeric nanoparticles with the different surface characteristics. *J Biomed Mater Res* **39**, 478–485, 1998.
56. Affatato S, Torrecillas R, Taddei P, Rocchi M, Fagnano C, Ciapetti G, Toni A. Advanced nanocomposite materials for orthopedic applications. I. A long-term in vitro wear study of zirconia-toughened alumina. *J Biomed Mater Res B Appl Biomater* **78**(1), 76–82, 2006.
57. Huber FX, Belyaev O, Hillmeier J, Kock HJ, Huber C, Meeder PJ, Berger I. First histological observations on the incorporation of a novel nanocrystalline hydroxyapatite paste OSTIM in human cancellous bone. *BMC Musculoskelet Disord* **7**, 50, 2006.
58. Chris Arts JJ, Verdonschot N, Schreurs BW, Buma P. The use of a bioresorbable nano-crystalline hydroxyapatite paste in acetabular bone impaction grafting. *Biomaterials* **27**(7), 1110–1118, 2006.
59. Agrawal CM, Ray RB. Biodegradable polymeric scaffolds for musculoskeletal tissue engineering. *J Biomed Mater Res* **55**(2), 141–150, 2001.
60. Thomson RC, Mikos AG, Beahm E, Lemon JC, Satterfield WC, Aufdemorte TB, and Miller MJ. Guided tissue fabrication from periosteum using preformed biodegradable polymer scaffolds. *Biomaterials* **20**(21), 2007–2018, 1999.
61. Boccaccini AR, Maquet V. Bioresorbable and bioactive polymer/bioglass®

composites with tailored pore structure for tissue engineering applications. *Composites Sci Technol* **63**(16), 2417–2429, 2003.
62. Liu X, Ma PX. Polymeric scaffolds for bone tissue engineering. *Ann Biomed Eng* **32**(3), 477–486, 2004.
63. Gilding DK, Reed AM. Biodegradable polymers for use in surgery – polyglycolic/poly(lactic acid) homo- and copolymers. *Polymer* **20**(12), 1459–1464, 1979.
64. Rokkanen P, Bostman O, Vainionpaa S, Vihtonen K, Tormala P, Laiho J, Kilpikari J, Tamminmaki M. Biodegradable implants in fracture fixation: early results of treatment of fractures of the ankle. *Lancet* **1**(8443), 1422–1424, 1985.
65. Waris E, Konttinen YT, Ashammakhi N, Suuronen R, Santavirta S. Bioabsorbable fixation devices in trauma and bone surgery: current clinical standing. *Exp Rev Med Devices* **1**(2), 229–240, 2004.
66. Gunatillake PA, Adhikari R. Biodegradable synthetic polymers for tissue engineering. *Europ Cells Mater* **5**, 1–16, 2003.
67. Liu H, Slamovich EB, Webster TJ. Increased osteoblast functions on nanophase titania dispersed in poly-lactic-co-glycolic acid composites. *Nanotechnology* **16**(7), S601–S608, 2005.
68. Wang H, Eliaz N, Xiang Z, Hsu HP, Spector M, Hobbs LW. Early bone apposition *in vivo* on plasma-sprayed and electrochemically deposited hydroxyapatite coatings on titanium alloy. *Biomaterials* **27**(23), 4192–4203, 2006.
69. Du C, Cui FZ, Zhu XD, de Groot K. Three-dimensional nano-HAP/collagen matrix loading with osteogenic cells in organ culture. *J Biomed Mater Res* **44**(4), 407–415, 1999.
70. Freed LE, Hollander AP, Martin I, Barry JR, Langer R, Vunjak-Novakovic G. Chondrogenesis in a cell–polymer–bioreactor system. *Exp Cell Res* **240**, 58, 1998.
71. Freed LE, Martin I, Vunjak-Novakovic G. Frontiers in tissue engineering: *in vitro* modulation of chondrogenesis. *Clin Orthop* **367S**, S46, 1999.
72. Freed LE, Marquis JC, Vunjak-Novakovic G, Emmanual J, Langer R. Composition of cell–polymer cartilage implants. *Biotechnol Bioeng* **43**, 605, 1994.
73. LeBaron RG, Athanasiou KA. *Ex vivo* synthesis of articular cartilage. *Biomaterials* **21**, 2575, 2000.
74. Tuan RS, Boland G, Tuli R. Adult mesenchymal stem cells and cell-based tissue engineering. *Arthritis Res Therapy* **5**, 32–45, 2002.
75. PR Newswire. Milestone Scientific Signs Agreement With Carticept Medical to Collaborate on CompuFlo^{TM} Injection System for Treatment of Arthritic Joints, 2007.
76. Langer R, Vacanti JP. Tissue engineering. *Science* **260**, 920–926, 1993.
77. Temenoff JS, Mikos AG. Review: tissue engineering for regeneration of articular cartilage. *Biomaterials* **21**, 431–440, 2000.
78. Riesle J, Hollander AP, Langer R, Freed LE, Vunjak-Novakovic G. Collagen in tissue-engineered cartilage: types, structure, and crosslinks. *J Cell Biochem* **71**, 313, 1998.
79. Mow VC, Zhu W, Ratcliffe A. Structure and function of articular cartilage and meniscus. *Basic Orthopedic Biomechanics*, London: Lippincott Williams and Wilkins, pp. 114–121, 1991.
80. Shields KJ, Beckman MJ, Bowlin GL, Wayne JS. Mechanical properties and cellular proliferation of electrospun collagen type II. *Tissue Eng* **10**(9–10), 1510–1517, 2004.
81. Kohn J, Abramson S, Langer R. Bioresorbable and bioerodible materials. In *Biomaterials Science: An Introduction to Materials in Medicine*, Ratner BD (ed.),

Boston, MA: Elsevier Academic Press, pp. 115–126, 2004.
82. Cooper SL, Visser SA, Hergenrother RW, Lamba NMK. Polymers. In: *Biomaterials Science: An Introduction to Materials in Medicine*, Ratner BD (ed.), Boston, MA: Elsevier Academic Press, pp. 67–79, 2004.
83. Kim JY, Khang D, Lee JE, Webster TJ. Decreased macrophage density on carbon nanotube patterns on polycarbonate urethane. *J Biomed Mater Res A* **88**(2), 419–426, 2009.
84. Li W-J, Mauck RL, Cooper JA, Yuan X, Tuan RS. Engineering controllable anisotropy in electrospun biodegradable nanofibrous scaffolds for musculoskeletal tissue engineering. *J Biomech* **40**, 1686, 2007.
85. Baker BM, Mauck RL. The effect of nanofiber alignment on the maturation of engineered meniscus constructs. *Biomaterials* **28**, 1967, 2007.
86. Wise JK, Yarin AL, Megaridis CM, Cho M. Chondrogenic differentiation of human mesenchymal stem cells on oriented nanofibrous scaffolds: engineering the superficial zone of articular cartilage. *Tissue Eng Part A* **15**(4), 913–921, 2009.
87. Zhang SM, Cui FZ, Liao SS, Zhu Y, Han L. Synthesis and biocompatibility of porous nano-hydroxyapatite/collagen/alginate composite. *J Mater Sci Mater Med* **14**(7), 641–645, 2003.
88. Butler D, Goldstein S, Guilak F. Functional tissue engineering: the role of biomechanics. *Trans ASME* **122**, 570, 2000.
89. Mow VC, Kuei SC, Lai WM, Armstrong CG. Biphasic creep and stress relaxation of articular cartilage in compression: theory and experiments. *J Biomech Eng* **102**, 73, 1980.
90. Riesle J, Hollander AP, Langer R, Freed LE, Vunjak-Novakovic G. Collagen in tissue-engineered cartilage: types, structure, and crosslinks. *J Cell Biochem* **71**, 313, 1998.
91. Shields KJ, Beckman MJ, Bowlin GL, Wayne JS. Mechanical properties and cellular proliferation of electrospun collagen type II. *Tissue Eng* **10**(9-10), 1510–1517, 2004.
92. Kon E, Delcogliano M, Filardo G, Altadonna G, Marcacci M. Novel nano-composite multi-layered biomaterial for the treatment of multifocal degenerative cartilage lesions. *Knee Surg Sports Traumatol Arthrosc* May, 26, 2009.
93. Fenniri H, Mathivanan P, Vidale KL, Sherman DM, Hallenga K, Wood KV, Stowell JG. Helical rosette nanotubes: design, self-assembly and characterization. *J Am Chem Soc* **123**, 3854–3855, 2001.
94. Chun AL, Moralez JG, Fenniri H, Webster TJ. Helical rosette nanotubes: a biomimetic coating for orthopedics? *Biomaterials* **26**, 7304–7309, 2005.
95. Chun AL, Moralez JG, Fenniri H, Webster TJ. Helical rosette nanotubes: a more effective orthopedic implant material. *Nanotechnology* **15**, s234–s239, 2004.
96. Fine E, Zhang L, Fenniri H, Webster TJ. Enhanced endothelial cell functions on rosette nanotube-coated titanium vascular stents. *Int J Nanomedicine* **4**, 91–97, 2009.
97. Chen Y, Webster TJ. Increased osteoblast functions in the presence of BMP-7 short peptides for nanostructured biomaterial applications. *J Biomed Mater Res A* **91**(1), 296–304, 2009.
98. Zhang L, Rakotondradany F, Myles AJ, Fenniri H, Webster TJ. Arginine-glycine-aspartic acid modified rosette nanotube–hydrogel composites for bone tissue engineering. *Biomaterials* **30**(7), 1309–1320, 2009.
99. Zhang L, Chen Y, Rodriguez J, Fenniri H, Webster TJ. Biomimetic helical rosette nanotubes and nanocrystalline hydroxyapatite coatings on titanium for improving

orthopedic implants. *Int J Nanomedicine* **3**(3), 323–333, 2008.
100. Tamerler C, Sarikaya M. Molecular biomimetics: nanotechnology and bionanotechnology using genetically engineered peptides. *Philos Transact A Math Phys Eng Sci* **367**(1894), 1705–1726, 2009.
101. Wise JK, Yarin AL, Megaridis CM, Cho M. Chondrogenic differentiation of human mesenchymal stem cells on oriented anofibrous scaffolds: engineering the superficial zone of articular cartilage. *Tissue Eng Part A* **15**(4), 913–921, 2008.
102. Jun I, Jeong S, Shin H. The stimulation of myoblast differentiation by electrically conductive sub-micron fibers. *Biomaterials* **30**(11), 2038–2047, 2009.
103. Teo WE, Ramakrishna S. A review on electrospinning design and nanofibre assemblies. *Nanotechnology* **17**, R89–R106, 2006.
104. Shi YV, Chen C, Tsai S, Wang YJ, Lee OK. Growth of mesenchymal stem cells on electrospun type I collagen nanofibers stem cells. *J Biomater Res Part A* **24**(11), 2391–2397, 2006.
105. Yeo LY, Gagnon Z, Chang HC. AC electrospray biomaterials synthesis. *Biomaterials* **26**, 6122–6128, 2005.
106. Pareta R, Brindley A, Edirisinghe MJ, Jayasinghe SN, Luklinska ZB. Electrohydrodynamic atomization of protein (bovine serum albumin). *J Mater Sci Mater Med* **16**(10), 919–925, 2005.
107. Webster TJ. *Nanotechnology for the Regeneration of Hard and Soft Tissues*. Singapore: World Scientific, pp. 30–33, 2007.
108. Park GE, Pattison MA, Park K, Webster TJ. Accelerated chondrocyte functions on NaOH-treated PLGA scaffolds. *Biomaterials* **26**(16), 3075–3082, 2005.
109. Haines DE. *Fundamental Neuroscience*, 2nd Edition, London: Churchill Livingstone, pp. 28–35, 2002.
110. Neuberger T, Schöpf B, Hofmann H, Hofmann M, Rechenberg B. Superparamagnetic nanoparticles for biomedical applications: possibilities and limitations of a new drug delivery system. *J Materials Magnetism* **293**, 483–496, 2005.
111. Cengelli F, Maysinger D, Tschudi-Monnet F, Montet X, Corot C, Petri-Fink A, Hofmann H, Juillerat-Jeanneret L. Interaction of functionalized superparamagnetic iron oxide nanoparticles with brain structures. *J Pharmacol Exp Ther* **318**(1), 108–116, 2006.
112. Andrews RJ. Neuroprotection at the nanolevel – Part II: Nanodevices for neuromodulation – deep brain stimulation and spinal cord injury. *Ann NY Acad Sci* **1122**, 185–196, 2007.
113. Cellot G, Cilia E, Cipollone S, Rancic V, Sucapane A, Giordani S, Gambazzi L, Markram H, Grandolfo M, Scaini D, Gelain F, Casalis L, Prato M, Giugliano M, Ballerini L. Carbon nanotubes might improve neuronal performance by favouring electrical shortcuts. *Nat Nanotechnol* **4**(2), 126–133, 2009.
114. Chao TI, Xiang S, Chen CS, Chin WC, Nelson AJ, Wang C, Lu J. Carbon nanotubes promote neuron differentiation from human embryonic stem cells. *Biochem Biophys Res Commun* **384**(4), 426–430, 2009.
115. Bardi G, Tognini P, Ciofani G, Raffa V, Costa M, Pizzorusso T. Pluronic-coated carbon nanotubes do not induce degeneration of cortical neurons *in vivo* and *in vitro*. *Nanomedicine* **5**(1), 96–104, 2005.
116. Mazzatenta A, Giugliano M, Campidelli S, Gambazzi L, Businaro L, Markram H, Prato M, Ballerini L. Interfacing neurons with carbon nanotubes: electrical signal transfer and synaptic stimulation in cultured brain circuits. *J Neurosci* **27**(26), 6931–6936, 2007.

117. Biran R, Martin DC, Tresco PA. Neuronal cell loss accompanies the brain tissue response to chronically implanted silicon microelectrode arrays. *Exp Neurol* **195**(1), 115–126, 2005.
118. Webster TJ. *Nanotechnology for the Regeneration of Hard and Soft Tissues*. Singapore: World Scientific, pp. 167–168, 2007.
119. An KH, Jeon KK, Kim WS, Park YS, Lim SC, Bae DJ, Lee YH. Characterization of supercapacitors using singlewalled carbon nanotube electrodes. *J Korean Phys Soc* **39**, S511–S517, 2001.
120. Kim YH, Park CJ, Chang KJ. Sub-bands in carbon nanotubes under radial deformation. *J Korean Phys Soc* **37**, 85, 2000.
121. McKenzie JL, Waid MC, Shi R, Webster TJ. Decreased functions of astrocytes on carbon nanofiber materials. *Biomaterials* **25**(7–8), 1309–1317, 2004.
122. Greenbaum A, Anava S, Ayali A, Shein M, David-Pur M, Ben-Jacob E, Hanein Y. One-to-one neuron-electrode interfacing. *J Neurosci Methods* **182**(2), 219–224, 2009.
123. Kennedy PR, Bakay RA. Restoration of neural output from a paralyzed patient by a direct brain connection. *Neuroreport* **9**(8), 1707–1711, 1998.
124. Dormer K, Seeney C, Lewelling K, Lian G, Gibson D, Johnson M. Epithelial internalization of superparamagnetic nanoparticles and response to external magnetic field. *Biomaterials* **26**(14), 2061–2072, 2005.
125. Marschall SR, Patterson C. *Principles of Molecular Cardiology*, Totowa, NJ: Humana Press, 2005.
126. Choudhary S, Berhe M, Haberstroh KM, Webster TJ. Increased vascular cell adhesion on nanostructured metals. *Int J Nanotechnol* **1**(1), 41–49, 2006.
127. Khang D, Liu-Snyder P, Pareta R, Lu J, Webster TJ. Reduced responses of macrophages on nanometer surface features of altered alumina crystalline phases. *Acta Biomater* **5**, 1425–1432, 2009.

10

Matrices for tissue engineering and regenerative medicine

D. GORTH and T. J. WEBSTER, Brown University, USA

Abstract: This chapter provides an overview of the considerations for designing a tissue engineering scaffold and the tools available to create and improve matrices for tissue engineering and regenerative medicine. The chapter begins by discussing the challenges and goals of designing matrices. It then goes on to discuss the strengths and weaknesses of the materials and manufacturing processes available to create matrices.

Key words: extracellular matrix, collagen, biodegradable polymers, electrospinning, self-assembling peptides.

10.1 Introduction

Natural biological systems are composed of an orchestrated chaos of molecular signals, cells and extracellular matrix (ECM) proteins. The human body and its constituent tissues are enormously complex. The goal of tissue engineering is to treat bodily damage and disease by supplementing the function of native damaged tissue and ideally facilitating the complete regeneration of tissue. An ideal tissue engineering construct would result in a final tissue indistinguishable from healthy native tissue.

To meet the challenge of replicating the appropriate biological signals for natural tissue growth, researchers use both cells and three-dimensional matrices. Although stem cells have received a lot of attention for use in tissue engineering and regenerative medicine, the importance of matrices in tissue engineered constructs cannot be overlooked. Not only do matrices provide mechanical support *in vivo*, but they also can promote cell growth and integration once a construct is implanted and begins interacting with native tissue. The use of just cultured cell sheets in tissue engineering applications is not as effective as using the same cell sheets in conjunction with a matrix. Not only do the resulting cell–matrix constructs integrate into living tissue more effectively, but also cell sheets supported by an artificial matrix are easier to handle and store for clinical use (Ng and Hutmacher, 2006).

The field of tissue engineering is constantly evolving, so instead of attempting to just summarize the state of tissue engineering scaffolds, the goal of this

chapter is to provide an overview of the considerations for designing a tissue engineering scaffold and some of the tools available to create improved matrices for tissue engineering and regenerative medicine.

10.2 Design considerations for matrices

The ECM is an intricate meshwork of proteins that supports the growth and stability of the local cells. In many cases it also provides structural support to the entire organism. Consequently, when designing an artificial matrix one must consider both mechanical strength and the construct's ability to provide a local environment that encourages tissue growth and discourages infection and excessive immune responses. To be an effective vehicle for tissue engineering applications, matrices must be more than simply biocompatible. In addition to not triggering an aggressive detrimental immune response leading to fibrous encapsulation, the material used in matrix construction should encourage cell growth.

The engineered matrix must provide a mechanical modulus in the range of 10–1500 MPa for hard tissues such as bone or 0.4–350 MPa for softer tissues in neuronal applications to provide adequate mechanical support until native cells can supplement or replace it with a natural ECM (Hollister, 2005). Not only does this fact illustrate the mechanical aspect of designing matrices, but it also suggests that there must be different materials and processing methods for creating an ECM substitute for different tissues in the body. Mechanical strength seems at the surface to be an easily achieved matrix characteristic when designing a construct using materials with known mechanical properties. However, the mechanical strength of a construct is complicated by the introduction of other design components that make a matrix that provides adequate structural support and that also promotes cellular growth.

One such material property that can significantly alter mechanical properties is porosity. Porosity increases the proliferation of cells into the construct and provides the necessary avenues for cell motion and nutrient diffusion. Like the ideal mechanical modulus for different tissues, optimal pore size is also tissue specific. The optimal pore size for neovascularization is 5 μm, while for fibroblast ingrowth, a pore size of 5–15 μm is optimal. Hepatocyte ingrowth is optimal at a 20 μm pore size. Osteoid, skin regeneration and bone regeneration all have lager optimal construct pore sizes at 40–100 μm, 20–125 μm and 100–350 μm, respectively (Yang *et al.*, 2001). Porosity and mechanical strength are two matrix characteristics that are in conflict. Increased porosity decreases the overall mechanical strength of the construct. This problem can be solved in various ways; one is using two different polymers, a first to meet the mechanical demands of the application and a second to encourage cell growth (Shao *et al.*, 2009).

Another design consideration for optimal tissue engineering matrix design is surface energy. Surface energy is an important component for controlling cell

adhesion and proliferation. This is because cell interactions with biomaterials are heavily dependent on protein adsorption, and surface energy affects protein adsorption onto biomaterials, which in turn affects cell adhesion. Different cell types preferably bind to materials of differing wettability. For instance, most likely due to altered protein adsorption, fibroblasts preferentially bind to surfaces with a contact angle of 70º (Tamada and Ikada, 1994) while endothelial cells bind optimally to surfaces with a contact angle of 40º (van Wachem *et al.*, 1987). Like mechanical strength, wettability is another design consideration that can be optimized for specific tissue engineering applications.

Surface structures are another component that affects tissue growth on engineered matrices. By printing biomimetic features that replicate cell features on polymer conduits, researchers can influence cell growth and migration (Bruder *et al.*, 2007). Nanoscale surface modification can also positively influence cell growth on tissue engineering scaffolds (Miller *et al.*, 2007). The role of nanotechnology will be more thoroughly addressed in a later section in this text.

The interaction between cells and the ECM is bilateral. The ECM is built and continually remolded by surrounding cells, and not only does the ECM provide mechanical support to surrounding cells, but additionally, attributes such as the elasticity of the ECM can affect cell differentiation. The relationship between cells and the ECM has important implications for the design of matrices for tissue engineering and regenerative medicine. Just by altering the mechanical properties of the matrix, mesenchymal stem cells can be directed to differentiate into neuronal, myogenic or osteogenic differentiation (Engler *et al.*, 2006). Unless cells can be incorporated into and remodel the matrix, the engineered construct will not be able to effectively integrate into the surrounding living tissue, and thus it will not be able to grow and develop as a native tissue. Valvular implants in pediatric patients illustrate the importance of designing a tissue engineering matrix that supports cellular ingrowth and remolding. Traditional acelluar constructs are chemically stable, so in pediatric patients they often fail due to their inability to adapt to a growing heart. However, by using a decellularized allograft seeded with autologous cells, it is possible to create a tissue engineered heart valve that develops with the patient (Cebotari *et al.*, 2006).

Except for certain tissues, angiogenesis must also be considered when designing a matrix for tissue engineering and regenerative medicine. Without proper matrix vascularization, the cells in tissue engineered constructs are confined to a 100–200 μm distance from an oxygen and nutrient source. At distances greater than 100–200 μm, the necessary nutrients for maintaining cell viability can no longer reach the cells by simple diffusion. Incorporating vascularization into a tissue engineered matrix will remove the limits of diffusion on tissue development, but this problem is complicated by the fact that endothelial growth is promoted by different surface wettability and porosity properties from other tissue types. Attempts to produce a matrix that promotes vascularization include

seeding the matrix with angiogenic growth factors such as vascular endothelial growth factor (VEGF) and fibroblast growth factor two (FGF2) (Nillesen *et al.*, 2007), gene transfer and seeding endothelial cells into the matrix, but these methods have produced limited success. Neovascularization occurs with a time delay, so promoting vascular growth in a matrix that already is supporting other cell growth does not play a central role in keeping the tissue engineered construct alive; inosculation, the combination growth of existing vasculature, is much more important to blood profusion to implants.

To solve the problem of matrix vascularization, Montano *et al.* (2010) have shown that it is possible to create a prevascularized matrix *in vitro* that then can be implanted and promote cell ingrowth. They accomplished this task by first isolating human microvascular endothelial cells (HuMECs) and growing these isolated cells on a variety of concentrations of fibrin, collagen and fibrin–collagen hybrid hydrogels to optimize three-dimensional organotypic vascular structure formation. Out of these scaffolds, the 10 and 11 mg/mL fibrin-based hydrogels were the only matrices that facilitated three-dimensional luminal structure formation. Fibrin has been previously shown to promote vascular cell growth, but previously fibrin matrices have only facilitated the growth of vascular structures with the additional support of fibroblasts and keratinocytes. The 10 and 11 mg/mL fibrin matrices supported vascular structure formation *in vitro* resembling embryonic development without the addition of other cells in culture. This study showed that engineering pre-vascularized matrices *in vitro* is within reach, but the mechanical properties of fibrin limit its utility in applications requiring structural support.

Another problem that should be considered when designing tissue engineering matrices is innervation. Innervation is particularly important when engineering constructs for muscular applications, because motor and sensory neurons are central to the proper functioning of that implant. In addition to being a consideration when designing tissue constructs for tissue and organ implants, tissue engineering matrices have been employed to solve the problem of axon growth after spinal cord injury. In this scenario, tissue engineered matrices are used to facilitate inosculation of the severed nerves. To the end of creating innervated skin grafts, Schwann cells can be added to the tissue engineered matrix to produce a two-fold increase in the number of sensory neurites migrating into dermal implant (Blais *et al.*, 2009). The development of innervated muscle tissue is more complicated than just including Schwann cells in the matrix. Electrical, chemotropic and mechanical stimulation must all be optimized to manipulate innervation and create a functional matrix for muscular applications. Because of the importance of electrical signals in nerve growth, conducting materials such as polypyrrole, a conductive synthetic polymer, and electrically conductive carbon nanotubes have been integrated into matrices where nerve growth is a consideration. Some similar concepts have been used when designing matrices to foster central nervous system healing. Along with

the use of electrical signals to guide nerve growth, groove patterns and biomimetic features resembling Schwann cells have been used to encourage growth through matrices.

The more one understands the mechanisms of cell–matrix interactions, the more interesting the problem of designing an effective vehicle for tissue growth becomes. The rest of this chapter will examine some of the tools available to researchers and clinicians when designing a proper scaffold for tissue engineering.

10.3 Materials for natural matrices

The use of natural matrices has the intrinsic benefit of already possessing the surface topography of natural tissues. Two common natural matrix sources are porcine urinary bladder and porcine small intestinal submucosa (Mendelson and Schoen, 2006). Before implantation, natural matrices are sterilized and decellularized, leaving only a protein-based, commonly collagen, scaffold. Natural matrices are especially advantageous when the function of the tissue is mechanical, because maintaining the ECM maintains the function of the transplant. An example of a tissue that this is especially true for this is a heart valve. Completely decellularized heart valves perform the same mechanical function as a native cellularized heart valve. However, while natural matrices must be remolded out of their native forms, they are notoriously harder to work with than synthetic thermoplastics such as polylactic acid and polyurethane that can be easily heated and molded. Two other problems facing the use of natural matrices for tissue engineering and regenerative medicine are the poor and static mechanical properties of natural matrices and batch-to-batch variation (Yang *et al.*, 2001).

For the use of natural matrices, the matrices must be processed and stored effectively. Any remaining cell or protein debris can trigger an immune response and lead to failure of the implant, so decellularization is a central component of processing natural matrices. Decellularization can be accomplished using enzymatic treatment, detergent-based methods, freeze-drying or osmotic gradients (Schmidt *et al.*, 2007). Once free of debris, the challenging task becomes finding an effective method to store the matrices before implantation. They can be stored hydrated or dried using vacuum or freeze-drying. If dried, the matrices can simply be rehydrated a few minutes before use. Although both storage methods are currently used, that does not make them equally effective. Procine urinary bladder scaffolds stored in a freeze-dried state can promote more cell growth than the same material stored hydrated (Freytes *et al.*, 2008).

All sources for natural matrices do not create equally effective matrices for tissue engineering. Porcine decellularized scaffolds have a lower propensity to attract cellular ingrowth than those from humans and the porcine scaffolds generate a more severe immune response (Rieder *et al.*, 2005). In addition to the

problem of decreased efficacy of xenogenic scaffolds, there is also a fear of transmitting infectious diseases from the animal to the patient receiving the construct – Creutzfeld–Jakob disease from cattle to humans, or endogenous retroviruses from pigs to humans (Schmidt *et al.*, 2007). Another issue with the use of matrices produced in living organisms is that there is a limited material supply. Allogenic implants perform better, but one of the motivating factors for perusing synthetic tissue engineering matrices is to compensate for the lack of donors of human tissue and organs.

10.4 Materials for synthetic matrices

Synthetically creating scaffolds for tissue engineering is a desirable option considering that the researcher or clinician has almost complete control over the architecture and mechanical properties of their construct. Unlike natural matrices, synthetically fabricated matrices do not have any reliance on a donor population. Despite lacking the native surface topography of natural matrices, synthetic matrices are biocompatible and can perform better in some applications than natural matrices (Ng and Hutmacher, 2006). In the case of biodegradable polymers, both the polymer and its degradation products must be biocompatible. This is the case for biodegradable polymers currently in use, and although biocompatible, the degradation products of some polymers can alter the surrounding chemical environment by lowering the pH (Oh *et al.*, 2006).

By changing the chemistry of the polymer used, the mechanical properties and degradation profile of the polymer scaffold can be controlled. For instance, it is possible to make a matrix for cartilage applications with modulus values comparable to native collagen by altering the molar ratio of poly(glycerol) and sebacate used and by adjusting the time that the polymer cures (Kemppainen and Hollister, 2010). Copolymers are used to fine-tune the properties of a scaffold for tissue engineering (Table 10.1). Polylactic acid and polyglycolic acids are

Table 10.1 Some physical properties of commonly used biopolymers

Polymer[a]	Melting point (°C)	Degradation time (months)[b]	Tensile strength (MPa)	Elongation (%)	Modulus (GPa)
PLGA	Amorphous	Adjustable	41.4–44.2	3–10	1.4–2.8
DL-PLA	Amorphous	12–16	27.6–41.4	3–10	1.4–2.8
L-PLA	173–178	>24	55.2–82.7	5–10	2.8–4.2
PGA	225–230	6–12	68.9	15–20	>6.9
PCL	58–63	>24	20.7–34.4	300–500	0.21–0.34

[a] PLGA, poly(lactic-co-glycolic acid); PLA, polylactic acid; PGA, polyglycolic acid; PCL, poly(ϵ-caprolactone).
[b] Degradation time is also dependent on geometry.
Adapted from Yang *et al.* (2001).

commonly copolymerized into poly(lactic-co-glycolic acid) (PLGA) to obtain a polymer with a specific degradation half-life.

The mechanical properties of a biodegradable polymer are not constant. As a polymer is broken down, it loses some of its mechanical strength (Deng and Ulrich, 2002). As stated in previous sections, one of the goals of including matrices in tissue engineered constructs is to provide mechanical support while the penetrating cells build their own ECM, but because mechanical properties of a matrix are variable, this task is more complex than simply adjusting a polymer to have the appropriate mechanical characteristics upon implantation. To be truly effective, a polymer construct must not only be mechanically adequate upon implantation, but it must also degrade slowly enough to maintain mechanical support while cells build a permanent ECM.

One of the questions pertaining to the design of a synthetic polymer matrix is what material to use. There are a myriad of possibilities, so for the sake of brevity only a few of the most common polymers will be discussed here. Overall, synthetic polymers can be broken up into two major subgroups, biodegradable and non-biodegradable. There is a current research emphasis on the use of biodegradable polymers in tissue engineering and regenerative medicine, because they are susceptible to cellular remolding *in vivo*, and offer the opportunity to create an environment to grow native tissue that can remodel the artificial matrix leaving an *in vivo* produced natural matrix. The polymers listed below are often copolymerized or combined into one construct to achieve mechanical and degradation properties better suited to the intended tissue engineering application (Tessmar and Göpferich, 2007).

10.4.1 Polytetrafluoroethylene (PTFE)

Polytetrafluoroethylene (PTFE) is a non-biodegradable polymer material that has been approved by the US Food and Drug Administration (FDA) for use as an implantable biomaterial for a long time (Shao *et al.*, 2009). It is commonly referred to by its trade name Gore-Tex. One of the advantages of PTFE is its tensile strength, as PTFE prostheses can support 4830 ± 280 N compared to a human anterior cruciate ligament that supports 2195 ± 427 N. Expanded PTFE has been successfully used as a ligament prosthesis in sheep knee joints as an anterior cruciate ligament and as a medial collateral ligament replacement (Dürselen *et al.*, 1996). Although PTFE has good mechanical properties and is not immunoreactive, this polymer does not encourage and support cellular ingrowth. This problem has been addressed by coating PTFE with a bioactive polymer such as polylactic acid, so the PTFE can provide the mechanical support while the bioactive polymer can support cellular ingrowth (Shao *et al.*, 2009).

10.4.2 Polylactic acid (PLA)

Polylactic acid is a commonly used carbon-based biodegradable polymer consisting of lactic acid monomers. Lactic acid is optically active, because it contains an asymmetrical carbon atom. The L-confirmation of lactic acid is a naturally occurring metabolic by-product, but either L- or D-PLA can be used in polymer synthesis to create isotactic L-PLA or D-PLA or syndiotactically alternating D,L-copolymers. The stereochemistry of the polymer monomers affects its ability to crystallize and self-associate, so just by changing the D/L composition of PLA, it is possible to change its mechanical properties. For instance L-PLA is a crystalline polymer with a tensile modulus of 2.23–3.85 kN m/g, but by creating a syndiotactic DL-PLA, the tensile modulus is reduced to 0.80–2.36 kN m/g (van de Velde and Kiekens, 2002). PLA has a typical *in vivo* degradation time of 30 to 50 weeks (Barns *et al.*, 2007).

10.4.3 Polyglycolic acid (PGA)

Polyglycolic acid (PGA) is commonly copolymerized with PLA to form PLGA. Unlike PLA, PGA is not optically active, and when not copolymerized, it is highly crystalline. PGA is more hydrophilic than PLA due to its lack of additional asymmetrical methyl groups. Consequently, increasing the weight percent of PGA in a PLGA copolymer is one method to increase the wettability of a biomaterial made from PLGA. Another consequence of the hydrophilicity of PGA is its comparatively rapid degradation time. *In vivo*, PGA degrades in 2 to 4 weeks, losing 60% of its mass during the first two weeks.

10.4.4 Poly(ϵ-caprolactone) (PCL)

Poly(ϵ-caprolactone) (PCL) is a semicrystalline polymer produced by a catalyzed ring opening of ϵ-caprolactone. The resulting polymer consists of five methylene groups separating a polar ester group. PCL is biocompatible and is currently used as a material for degradable sutures. PCL has a tensile modulus of 0.19–0.38 kN m/g (van de Velde and Kiekens, 2002). PCL has a degradation time of approximately two years, but PCL can be copolymerized with PLGA for a more rapidly degrading polymer (Yang *et al.*, 2001).

10.5 Methods for polymer matrix fabrication

This section will examine some common tissue engineering matrix fabrication methods. The methods included in this section are solvent casting and particulate leaching, melt molding, emulsion freeze-drying, gas foaming, electrospinning and computational techniques. Introducing porosity into a solid polymer is one of the central goals of tissue matrix engineering and this task can

be accomplished in various ways. These processes represent a cross-section of the general principles of matrix fabrication. In the following examples, porosity is introduced by dissolving a dispersed solid particulate, sublimating a frozen solvent, forcing gas into a solid polymer, or laying a polymer in a manner that leaves holes. Slightly more time will be spent describing electrospinning and computational methods of polymer fabrication due to their complexity. Other fabrication techniques that will not be described in more detail include fiber bonding, membrane lamination, extrusion, phase separation and high internal-phase emulsion.

10.5.1 Solvent casting and particulate leaching

Solvent casting and particulate leaching use a solvated liquid polymer combined with a solvated porogen. Particulate leaching is a simple method for introducing porosity into a tissue engineered scaffold. To achieve this goal, the matrix material solution is initially mixed with a suspended porogen. This suspension is then allowed to solidify leaving the porogen dispersed in the solid polymer. The entire construct is then soaked in a solvent specific to the porogen agent used leaving empty space that was previously occupied by the solid porogen. The pore size, geometry and density can be adjusted by altering the size, geometry and concentration of the porogen in the polymer solution (Lee *et al.*, 2003; Mano *et al.*, 2007).

10.5.2 Melt molding

Melt molding is an easy way to adjust the three-dimensional morphology of polymer scaffolds without the use of harsh chemical solvents. Many of the synthetic polymers used are thermoplastics, so they can be easily heated and cooled into various solid forms. For this fabrication technique, the polymers are heated above their glass transition temperature or melting point, so they can assume a liquid form. The resulting polymer is then allowed to cool and solidifies in the form of the mold. Melt molding is used in tandem with particle leaching to introduce porosity into the scaffold. Unlike solvent casting, melt molding does not use polymer solvents, so residual toxic solvents in the matrix are not an issue. Unfortunately, the heat needed to liquefy the polymer restricts the incorporation of active biomolecules.

10.5.3 Emulsion freeze-drying

Freeze-drying is a method of introducing pores into a polymer scaffold without the use of particulate leaching. Emulsion freeze-drying uses a solvated polymer emulsified in a non-miscible liquid. The homogeneous mixture is then poured into a mold and freeze-dried. Varying the weight percentage of the emulsifying

liquid affects the porosity of the final construct. PLGA constructs made using emulsion freeze-drying have average pore sizes between 30 and 50 μm. Using different amounts of emulsifying liquid and using different polymers can manipulate the final polymer structure. Matrices produced using emulsion freeze-drying typically have good connectivity of the internal pores (Baker *et al.*, 2009).

10.5.4 Gas foaming

Gas foaming is a method for creating synthetic matrices that avoids the use of solvents. Consequently, it is a good technique for incorporating sensitive molecules into matrices without drastically reducing their bioactivity (Lee *et al.*, 2008). The first step of gas foaming is high temperature compression molding of the polymer into a solid disc. After the disc is formed, the solid polymer then rests in a high pressure carbon dioxide chamber for several days. During this period, the gas infiltrates the polymer creating pores for tissue ingrowth (Mooney *et al.*, 1996). An advantage of gas foaming is the absence of caustic solvents, so their residual presence is not a factor in the final scaffold and it is possible to incorporate sensitive bioactive molecules.

10.5.5 Electrospinning

In the past five to ten years, electrospinning has emerged as a popular fabrication method for creating synthetic matrices. The appeal of electrospinning rests in its ability to produce an artificial polymer matrix that is reminiscent of the native ECM collagen (Fig. 10.1). Electrospun scaffolds offer a balance between micro and macro characteristics by providing sufficient gross mechanical support for

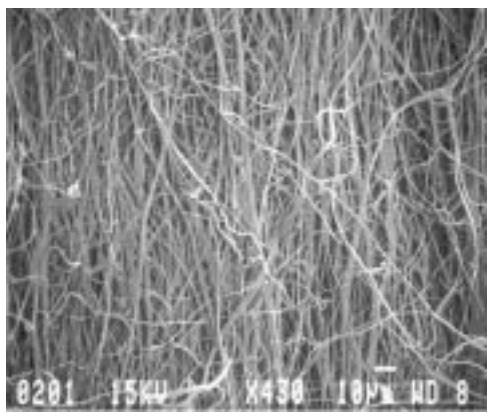

10.1 A scanning electron micrograph of an electrospun type I collagen matrix (Matthews *et al.,* 2002).

the tissue engineered construct and a local nanoscale environment for cell attachment and remolding.

Electrospinning produces an ultrafine meshwork with micron to nanometer scale fibers by manipulating electrostatic and intermolecular forces. During electrospinning a high voltage source charges a solvated polymer. This charged solution accelerates towards a collector of opposite polarity. The repulsive electrostatic forces between the charged polymer molecules and the attractive force between the solution and the collector transform the rounded solution–air interface into a pointed cone. A stream of polymer solution from the cone to the collector forms once the electrostatic forces of the system overcome the surface tension of the liquid. The solvent evaporates as the polymer accelerates towards the collector, leaving a dry polymer mesh on the surface of the collector. The size of the polymer fibers can be manipulated by altering the applied voltage, distance between the capillary and the collector, the polymer concentration, and the solution conductivity. Increasing the distance between the capillary and the collector, increasing the solution conductivity and decreasing the polymer concentration in solution can produce smaller fiber diameter meshes (Sill and von Recum, 2008). Although the harsh fabrication conditions should limit inclusion of the bioactive molecules in electrospun scaffolds, the use of a second spinning channel containing aqueous biological agents can be used to produce a final scaffold seeded with active biological molecules (Zhang *et al.*, 2007).

10.5.6 Computational techniques

Computer-aided design (CAD) has entered the field of tissue engineering. The distinct benefit of CAD techniques is that the designer has full control over the topography of the construct. Consequently, CAD matrix fabrication can address one of the downfalls of the techniques previously mentioned. In the case of a more random matrix fabrication, creating a porous construct does not insure that those pores are interconnected, facilitating diffusion and ingrowth of nutrients and cells throughout the matrix. However, with the use of computer design, the location, interconnectivity and size of pores can all be controlled. This is especially important because two of the primary design considerations for matrices are mechanical strength and creating a hospitable environment for cellular growth. Porosity adversely affects mechanical strength, but aids in cellular ingrowth (Yang *et al.*, 2001). By directly controlling the architecture of the matrix channels, the benefits of internal features can be maximized while minimizing the detrimental side effect of decreased mechanical strength.

One method of converting a computer design into a physical polymer based matrix for tissue engineering is solid free-form fabrication (SFF). SFF is a computer-aided scaffold construction method that builds a three-dimensional

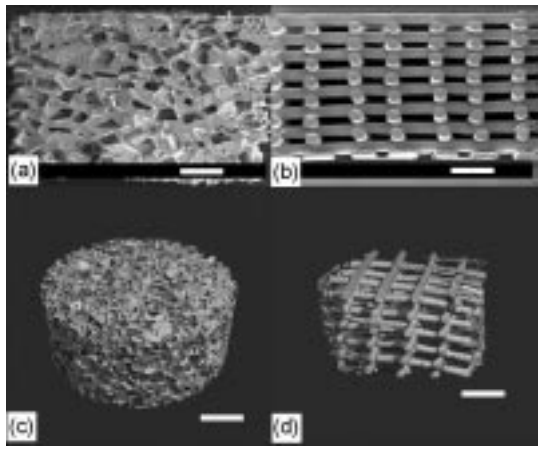

10.2 Electron micrographs and three-dimensional reconstructions of microcomputed tomography (μCT) scans comparing a scaffold made using particulate-leaching techniques (a), (c) and three-dimensional fabrication techniques (b), (d). Scale bar represents 1 mm (Malda *et al.*, 2005).

matrix layer by layer (Fig. 10.2). There are three general categories of SFF devices: laser-based, printing or nozzle-based systems. Regardless of the solidification mechanism, the device contains some type of lift or fabrication piston enabling the SFF setup to work in the *x*–*y* plane in iterative *z*-plane steps. These methods differ in how they accomplish the goal of creating a solid two-dimensional structure in each *z*-plane. Laser methods use electromagnetic energy to selectively polymerize or solidify a monomer solution or powdered material. Printing systems use chemical binders to create structures out of a powder bed or using wax deposition, and nozzle systems extrude a thin chemically or thermally treated material that then solidifies on the collecting base in iterative *z*-planes (Hollister, 2005; Lee *et al.*, 2008).

Computer-aided techniques have shown promise as a method to fabricate matrices for various tissue engineering applications. SFF manufactured matrices have been shown to perform better as vehicles for cartilage growth than matrices created using compression molding and particulate-leaching (Malda *et al.*, 2005). With the use of SFF manufacturing, it is also now possible to create a porated polymer matrix with almost identical stress mechanics as native cartilage (Kemppaien and Hollister, 2010). Currently, the primary drawback of computational matrix fabrication is that the technology does not currently exist to control manufacturing on a submicron scale (Hollister, 2005). The use of nanoscale characteristics has been repeatedly shown to increase the biological activity of matrices and currently SFF scaffolds can only be engineered to have features as small as 100 μm. Until SFF techniques are improved, post-production processing using other methods for surface modifications will have to suffice to create smaller features (Koegler and Griffith, 2004).

10.6 Self-assembling peptide scaffolds

Self-assembling peptide scaffolds (sapeptides) are another class of matrices for tissue engineering applications (Fig. 10.3). Although not yet approved by the FDA, as are other biomaterials mentioned in this chapter, sapeptides are a unique solution to the problem of construction of tissue engineering matrices. Instead of using synthetic polymers or natural decellularized matrices, sapeptides are peptide monomers that spontaneously aggregate into β-sheets due to the arrangement of ionic hydrophobic and hydrophilic amino acids. These β-sheets structures then assemble further to create larger matrix constructs. Sapeptides have similar cellular ingrowth characteristics as other matrices used for tissue engineering (PLLA, PLGA, PCLA, collagen and Matrigel), but they offer the benefit of having no detectable immune response (Dégano *et al.*, 2009) and their degradation products are digestible amino acid monomers that can be reused by the body (Kyle *et al.*, 2009).

Some of the common sequences used for sapeptide scaffolds are named based on their constituent amino acids. For example EAK16-II has the sequence AEAEAKAKAEAEAKAK, and RADA16-I has the sequence AcN-RADARADARADARADA-CNH_2, with the letters referring to the amino acid code A for alanine, E for glutamic acid, K for lysine, R for arginine and D for aspartic acid. Sapeptide monomers can be produced by chemical synthesis or with the use of transgenic organisms. Chemically synthesizing sapetides works in a laboratory setting, but is not suited for scaling up for clinical applications.

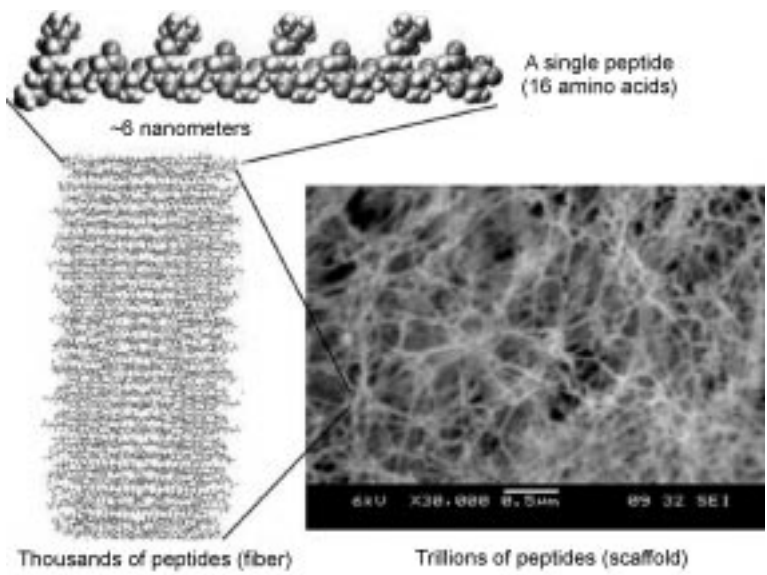

10.3 Example of designer self-assembling peptide nanofiber scaffold (Gelain *et al.,* 2007b).

Polypeptide sequences larger than 35 amino acids stretch the limits of clinical economic viability. Transgenic organisms appear to be the best option for large-scale synthesis of peptides for use in self-assembling peptide scaffolds (Gelain *et al.*, 2007a).

Although sapeptides are amino acid-based, the sequences used to create self-assembling scaffolds are not biologically relevant signaling sequences promoting cell binding and proliferation. That being said, because they are peptide-based, it is especially easy to integrate bioactive sequences into the β-sheet structures. These sapeptide structures that include designer application-dependent bioactive sequences can increase cell proliferation, differentiation and migration into these hybrid scaffolds as compared with those without the integrated bioactive sequences (Horii *et al.*, 2007).

10.7 Future trends

The era when surgeons can take tissue constructs off the shelf, like an automotive mechanic picking through replacement engine pistons, has not arrived. Although many of the methods presented in this chapter have not yet reached clinical viability, the myriad of tools available to engineers to solve the design problems of tissue engineering suggest that a time when off-the-shelf tissue engineered products are commonly used in clinical practice is not far off. Well-designed and easily produced matrices will be a necessary component for making this ideal become a reality.

Despite the promise suggested by the research presented in this chapter, as of the year 2004, the field of tissue engineering had yet to produce a profitable product despite the 4.5 billion dollar research and development investment (Lysaght and Hazlehurst, 2004). In the case of designing matrices for tissue engineering, researchers should turn an eye to the future and consider what will be necessary to convert their research into economically and clinically viable products earlier in the evolution of their research. An increased awareness of process engineering earlier in the product development could lead to the creation of more clinically useful and economically viable tissue engineering products (Archer and Williams, 2005). Tissue engineering research should continue to move away from proof of principle experiments, and focus more closely to explore the clinical efficacy and industrial fabrication processes of concepts.

10.8 References and further reading

Archer R, Williams DJ (2005), 'Why tissue engineering needs process engineering', *Nature Biotechnology*, **23**, 1353–1355.

Baker SC, Rohman G, Southgate J, Cameron NR (2009), 'The relationship between the mechanical properties and cell behavior on PLGA and PCL scaffolds for bladder tissue engineering', *Biomaterials*, **30**, 1321–1328.

Barns CP, Sell SA, Boland ED, Simpson DG, Bowlin GL (2007), 'Nanofiber technology: designing the next generation of tissue engineering scaffolds', *Advanced Drug Delivery Reviews*, **59**, 1413–1433.

Blais M, Grenier M, Berthod F, (2009), 'Improvement of nerve regeneration in tissue-engineered skin enriched with Schwann cells', *Journal of Investigative Dermatology*, **129**, 2895–2900.

Bruder JM, Lee AP, Hoffman-Kim D (2007), 'Biomimetic materials replicating Schwann cell topography enhance neuronal adhesion and neurite alignment *in vitro*', *Journal of Biomaterials Science, Polymer Edition*, **18**, 967–982.

Cebotari S, Lichenberg A, Tudorache I, Hilfiker A, Mertsching H, Leyh R, Breymann T, Kallenbach K, Maniuc L, Batrinac A, Repin O, Maliga O, Ciubotaru A, Haverich A (2006), 'Clinical application of tissue engineered human heart valves using autologous progeitor cells', *Circulation*, **114**, I-132–I-137.

Chun YW, Webster TJ (2009), 'The role of nanomedicine in growing tissues', *Annals of Biomedical Engineering*, **37**, 2034–2047.

Dégano IR, Quintana L, Vilalta M, Horna D, Rubio, Borrós S, Semino C, Blanco J (2009), 'The effect of self-assembling peptide nanofiber scaffolds on mouse fibroblast implantation and proliferation', *Biomaterials*, **30**, 1156–1165.

Eaglstein WH, Alvare OM, Auletta M, Leffel D, Rogers GS, Zitelli JA, Norris JEC, Thomas I, Irondo M, Fewkes J, Hardin-Young J, Duff RG, Sabolinski ML (1999), 'Acute exisional wounds treated with a tissue-engineered skin (Apligraf)', *Dermatology and Surgery*, **25**, 195–201.

Deng M, Ulrich KE (2002), 'Effects of *in vitro* degradation on properties of poly(DL-lactide-co-glycolide) pertinent to its biological performance', *Journal of Materials Science: Materials in Medicine*, **13**, 1091–1096.

Dürselen L, Clases L, Ignatius A, Rübenacker S (1996), 'Comparative animal study of three ligament prostheses for the replacement of the anterior cruciate and medial collateral ligament', *Biomaterials*, **17**, 977–982.

Engler AJ, Sen S, Sweeney HL, Discher DE (2006), 'Matrix elasticity directs stem cell lineage specification', *Cell*, **126**, 677–689.

Even-Ram S, Artym V, Yamada KM (2006), 'Matrix control of stem cell fate', *Cell*, **16**, 645–647.

Freytes DO, Tullius RS, Valentin JE, Stewart-Akers AM, Badlak SF (2008), 'Hydrated versus lyophilized forms of porcine extracellular matrix derived from the urinary bladder', *Journal of Biomedical Materials Research Part A*, **87**, 862–872.

Gelain F (2008), 'Novel opportunities and challenges offered by nanobiomaterials in tissue engineering', *International Journal of Nanomedicine*, **3**, 415–424.

Gelain F, Horri A, Zhang S (2007a), 'Designer self-assembling peptide scaffolds for 3-D tissue cell cultures and regenerative medicine', *Macromolecular Bioscience*, **7**, 544–551.

Gelain F, Lomander A, Vescovi AL, Zhang S (2007b), 'Systematic studies of a self-assembling peptide nanofiber scaffold with other scaffolds', *Journal of Nanoscience and Nanotechnology*, **7**, 424–434.

Hollister SJ (2005), 'Porous scaffold design for tissue engineering', *Nature Materials*, **4**, 518–524.

Horch RE, Kopp J, Kneser U, Beier J, Bach, AD (2005), 'Tissue engineering of cultured skin substitutes', *Journal of Cellular Molecular Medicine*, **9**, 592–608.

Horii A, Wang X, Gelain F, Zhang S (2007), 'Biological designer self-assembling peptide nanofiber scaffolds significantly enhance osteoblast proliferation, differentiation and 3-D migration', *PLoS One*, **2**, e190.

Kang B-C, Kang K-S, Lee, Y-S (2005), 'Biocompatibility and long-term toxicity of InnoPol® implant, a biodegradable polymer scaffold', *Experimental Animals*, **54**, 37–52.

Kemppaien JM, Hollister SJ (2010), 'Tailoring the mechanical properties of 3D-designed poly(glycerol sebacate) scaffolds for cartilage applications', *Journal of Biomedical Materials Research Part A*, **94**, 9–18.

Koegler WS, Griffith LG (2004), 'Osteoblast response to PLGA tissue engineering scaffolds with PEO modified surface chemistries and demonstration of patterned cell response', *Biomaterials*, **25**, 2819–2830.

Kyle S, Aggeli A, Ingham E, McPherson MJ (2009), 'Production of self-assembling biomaterials for tissue engineering', *Trends in Biotechnology*, **27**, 423–433.

Koning M, Harmsen MC, van Luyn MJA, Werker PMN (2009), 'Current opportunities and challenges in skeletal muscle tissue engineering', *Journal of Tissue Engineering and Regenerative Medicine*, **3**, 407–415.

Lee J, Cuddihy MJ, Kotov NA (2008), 'Three-dimensional cell culture matrices: state of the art', *Tissue Engineering: Part B*, **14**, 61–86.

Lee, SH, Kim BS, Kim SH, Choi SW, Jeong Si, Kwon IK, Kang SW, Nikolovski J, Mooney DJ, Han YK, Kim YH (2003), 'Elastic biodegradable poly(glycolde-co-caprolactone) scaffold for tissue engineering', *Journal of Biomedical Materials Research Part A*, **66**, 29–37.

Lysaght MJ and Hazlehurst AL (2004), 'Tissue engineering: the end of the beginning', *Tissue Engineering*, **10**, 309–320.

Madigan NN, McMahon S, O'Brian T, Yaszemski MJ, Windenbank AJ (2009), 'Current tissue engineering and novel therapeutic approaches to axonal regeneration following spinal cord injury using polymer scaffolds', *Respiratory Physiology & Neurobiology*, **169**, 183–199.

Malda J, Woodfield TBF, van der Vloodt F, Wilson C, Martens DE, Tramper J, van Blitterswijk CA, Riesle J (2005), 'The effect of PEGT/PBT scaffold architecture on the composition of tissue engineered cartilage', *Biomaterials*, **26**, 63–72.

Mano JF, Silva GA, Azevedo HS, Malafaya PB, Sousa RA, Silva SS, Boesel LF, Oliveira JM, Santos TC, Marques AP, Neves NM, Reis RL (2007), 'Natural origin biodegradable systems in tissue engineering and regenerative medicine: present status and some moving trends', *Journal of Royal Society Interface*, **4**, 999–1030.

Matthews JA, Wnek GE, Simpson DG, Bowlin GL (2002), 'Electrospinning of Collagen Nanofibers', *Biomacromolecules*, **2**, 232–238.

Mendelson K, Schoen FJ (2006), 'Heart valve tissue engineering: concepts, approaches, progress, and challenges', *Annals of Biomedical Engineering*, **34**, 1799–1819.

Miller DC, Haberstroh KM, Webster TJ (2007), 'PLGA nanometer surface features manipulate fibronectin interactions for improved vascular cell adhesion', *Journal of Biomedical Materials Research Part A*, **81**, 678–684.

Montano I, Schiestl C, Schneider J, Pontigga L, Biedermann T, Bottcher-Haberzeth S, Braziulis E, Meuli M, Reichmann E (2010), 'Formation of human capillaries *in vitro*: the engineering of prevascularized matrices', *Tissue Engineering Part A*, **16**, 269–282.

Mooney DJ, Baldwin DF, Suh NP, Vacanti JP, Langer R (1996), 'Novel approach to fabricate porous sponges of poly(D,L-lactic-co-glycolic acid) without the use of organic solvents', *Biomaterials*, **17**, 1417–1422.

Nillesen ST, Geutjes PJ, Wisamans R, Schalkwijk J, Daamen WF, van Kuppevelt TH (2007), 'Increased angiogenesis and blood vessel maturation in acellular collagen–heparin scaffolds containing both FGF2 and VEGF', *Biomaterials*, **28**, 1123–1131.

Ng KW, Hutmacher DW (2006), 'Reduced contraction of skin equivalent engineered using cell sheets cultured in 3D matrices', *Biomaterials*, **27**, 4591–4598.

Oh SH, Kang SG, Lee JH (2006), 'Degradation behavior of hydrophilized PLGA scaffolds prepared by melt-molding particulate-leaching method: comparison with control hydrophobic one', *Journal of Materials Science: Materials in Medicine*, **17**, 131–137.

Rieder E, Seebacher G, Kasimir M-T, Eichmair E, Winter B, Dekan B, Wolner E, Simon P, Weigel G (2005), 'Tissue engineering of heart valves: decellularized porcine and human valve scaffolds differ importantly in residual potential to attract monocytic cells', *Circulation*, **111**, 2792–2797.

Sato AK, Viswanathan M, Kent RB, Wood CR (2006), 'Therapeutic pepides: technological advances driving peptides into development', *Biomaterials*, **17**, 638–642.

Schmidt D, Stock UA, Hoerstrup SP (2007), 'Tissue engineering of heart valves using decellularized xenogenic or polymeric starter matrices', *Philosophical Transactions of the Royal Society Part B*, **362**, 1505–1512.

Shao H-J, Chen CS, Lee I-C, Wang J-H, Young T-H (2009) 'Designing a three-dimensional expanded polytetrafluoroethylene-poly(lactic-co-glycolic acid) scaffold for tissue engineering', *Artificial Organs*, **33**, 309–317.

Sill TJ, von Recum HA (2008) 'Electrospinning: applications in drug delivery and tissue engineering', *Biomaterials*, **29**, 1989–2006.

Tamada Y and Ikada Y (1994), 'Fibroblast growth on polymer surfaces and biosynthesis of collagen', *Journal of Biomedical Materials Research*, **28**, 783–789.

Tessmar JK and Göpferich AM (2007), 'Customized PEG-derived copolymers for tissue-engineering applications', *Macromolecular Bioscience*, **7**, 23–39.

Van de Velde K, Kiekens P (2002), 'Biopolymers: overview of several properties and consequences on their applications', *Polymer Testing*, **21**, 433–442.

Van Wachem PB, Hogt AH, Beugeling T, Feijen J, Banjes A, Detmers JP, van Aken WG (1987), 'Adhesion of cultured human endothelial cells onto methacrylate polymers with varying surface wetability and charge', *Biomaterials*, **8**, 323–328.

Wan Y, Cao X, Zhang S, Wang S, Wu Q (2008), 'Fibrous poly(chitosan-g-DL-lactic acid) scaffolds prepared via electro-wet-spinning', *Acta Biomaterialia*, **4**, 876–886.

Yang S, Leong KF, Du Z, Chua CK (2001), 'The design of scaffolds for use in tissue engineering. Part I: traditional factors', *Tissue Engineering*, **7**, 679–689.

Zhang YZ, Su B, Venugopal J, Ramakrishna S, Lim CT (2007), 'Biomimetic and bioactive nanofibrous scaffolds from electrospun composite nanofibers', *International Journal of Nanomedicine*, **2**, 623–638.

Index